

Thesis

Ambient air quality and human health in India

Luke Alexander Conibear

Supervisors

Dominick V. Spracklen, Stephen R. Arnold, Christoph Knote (external), Alan Williams

Submitted in accordance with the requirements for the degree of Doctor of Philosophy as part of the integrated PhD/MSc in Bioenergy

Engineering and Physical Sciences Research Council (EPSRC)

Centre for Doctoral Training (CDT) in Bioenergy,

School of Chemical and Process Engineering, Faculty of Engineering, University of Leeds

Institute for Climate and Atmospheric Science,

School of Earth and Environment, Faculty of Environment, University of Leeds

December 2018

Acknowledgements

The candidate confirms that the work submitted is his own, except where work, which has formed part of jointly authored publications, has been included. The contribution of the candidate and the other authors to this work has been explicitly indicated below. The candidate confirms that appropriate credit has been given within the thesis where reference has been made to the work of others. Chapters 4, 5, and 6 are based on work from jointly authored publications. The candidate is the first author of all publications. All publications are published.

Chapter 4

Conibear, L., Butt, E. W., Knote, C., Arnold, S. R., & Spracklen, D. V. (2018). Residential energy use emissions dominate health impacts from exposure to ambient particulate matter in India. *Nature Communications*, 9 (617), 9. <https://doi.org/10.1038/s41467-018-02986-7>

LC, DVS, SRA, and CK designed the research. CK and LC set up the model. LC performed the model simulations, model evaluation, data analysis, derived demographic data, and wrote the manuscript. EB derived the health function. LC, DVS, SRA, and CK evaluated the results and commented on the manuscript.

Chapter 5

Conibear, L., Butt, E. W., Knote, C., Arnold, S. R., & Spracklen, D. V. (2018). Stringent emission control policies can provide large improvements in air quality and public health in India. *GeoHealth*. 2. 196–211. <https://doi.org/10.1029/2018GH000139>

LC, DVS, SRA, and CK designed the research. CK and LC set up the model. LC performed the model simulations, model evaluation, data analysis, and wrote the manuscript. EB derived the health function, population density, population age, and baseline mortality data. LC, DVS, SRA, and CK evaluated the results and commented on the manuscript.

Chapter 6

Conibear, L., Butt, E. W., Knote, C., Spracklen, D. V., & Arnold, S. R. (2018). Current and future disease burden from ambient ozone exposure in India. *GeoHealth*. 2. <https://doi.org/10.1029/2018GH000168>

LC, DVS, SRA, and CK designed the research. CK and LC set up the model. LC performed the model simulations, model evaluation, data analysis, derived the health function, and wrote the manuscript. EB derived the population density, population age, and baseline mortality data. LC, DVS, SRA, and CK evaluated the results and commented on the manuscript.

I am grateful to my supervisors Dominick V. Spracklen, Stephen R. Arnold, Christoph Knote, and Alan Williams. I am especially thankful to Dom, Steve, and Christoph for their guidance, support, and expertise throughout this process. My questions were always answered quickly, cheerfully, and comprehensively. It has been a pleasure working together. I sincerely appreciate the support from the EPSRC CDT in Bioenergy (Grant No.EP/L014912/1). I am very grateful to all in the Bioenergy CDT for the opportunity to have undertaken this PhD.

I acknowledge the use of the many tools and facilities that were fundamental to completing this thesis. The facilities of the N8 High-Performance Computing Centre of Excellence provided and funded by the N8 consortium and EPSRC (Grant No.EP/K000225/1), coordinated by the Universities of Leeds and Manchester. Christoph Knote for helping set up and run the Weather Research and Forecasting model coupled with Chemistry (WRF-Chem) and his WRFotron scripts to automate WRF-Chem runs with re-initialised meteorology. Edward W. Butt for deriving health functions, demographic, and epidemiological data, and the many discussions. The WRF-Chem preprocessor tools (*mozbc*, *fire_emiss*, *anthro_emiss*, and *bio_emiss*) provided by the Atmospheric Chemistry Observations and Modeling (ACOM) laboratory of the National Center for Atmospheric Research (NCAR). The global model output from Model for Ozone and Related Chemical Tracers, version 4 (MOZART-4) (<http://www.acom.ucar.edu/wrf-chem/mozart.shtml>). The post-processing script *wrfout_to_cf.ncl* created by Mark Seefeldt at the University of Colorado (http://foehn.colorado.edu/wrfout_to_cf/). The Aerosol Network (AERONET) staff for establishing and maintaining the observation sites. The Central Pollution Control Board (CPCB), Ministry of Environment and Forests, Government of India for the observational data. The European Centre for Medium-Range Weather Forecasts (ECMWF) for their global reanalyses (<http://apps.ecmwf.int/datasets/>). The International Energy Agency (IEA) for the scenario data from the Energy and Air Pollution, World Energy Outlook Special Report. The boundaries shown on any maps in this work do not imply any judgement concerning the legal status of any territory or the endorsement or acceptance of such boundaries.

This copy has been supplied on the understanding that it is copyright material and that no quotation from the thesis may be published without proper acknowledgement.

Abstract

700 million Indians have used solid fuels in their homes for the last 30 years, contributing substantially to air pollutant emissions. The Indian economy and industrial, power generation, and transport sectors have grown considerably over the last decade, increasing emissions of air pollutants. These air pollutant emissions have caused present-day concentrations of ambient $PM_{2.5}$ and O_3 in India to be amongst the highest in the world. Exposure to this air pollution is the second leading risk factor in India, contributing one-quarter of the global disease burden attributable to air pollution exposure. Air pollutant emissions are predicted to grow extensively over the coming years in India. Despite the importance of air quality in India, it remains relatively understudied, and knowledge of the sources and processes causing air pollution is limited.

This thesis aims to understand the contribution of different pollution sources to the attributable disease burden from ambient air pollution exposure in India and the effects of future air pollution control pathways. The attributable disease burden from ambient $PM_{2.5}$ exposure in India is substantial, where large reductions in emissions will be required to reduce the health burden due to the non-linear exposure-response relationship. The attributable disease burden from ambient O_3 exposure is larger than previously thought and is of similar magnitude to that from $PM_{2.5}$ in the future. Key sources contributing to the present day disease burden from ambient $PM_{2.5}$ and O_3 exposure are the emissions from the residential combustion of solid fuels, land transport, and coal combustion in power plants. The attributable disease burden is estimated to increase in the future due to population ageing and growth. Stringent air pollution control pathways are required to provide critical public health benefits in India in a challenging environment. A key focus should be to reduce the combustion of solid fuels.

Table of Contents

Acknowledgements	2
Abstract	4
Table of Contents	5
List of Tables	8
List of Figures	10
List of Equations	19
1. Ambient air quality and human health in India	20
1.1. Air pollution pathway	20
1.1.1. Fundamentals of ambient air pollution	21
1.1.1.1. Aerosols	21
1.1.1.2. Ozone	23
1.1.2. Air pollution sources.....	25
1.1.2.1. Sectors.....	25
1.1.2.2. Residential emissions and solid fuel use.....	26
1.1.3. Emissions	31
1.1.3.1. Indian emissions.....	31
1.1.3.2. Air pollution control policies in India.....	32
1.1.4. Concentrations	37
1.1.4.1. Present day air pollutant concentrations in India	37
1.1.4.2. Meteorological and geographical impacts on Indian air pollution.....	40
1.1.5. Exposures	42
1.1.5.1. Association and causation.....	42
1.1.5.2. Intake fraction	43
1.1.6. Doses.....	44
1.1.7. Health impacts.....	45
1.1.7.1. Health impacts of PM _{2.5} exposure	46
1.1.7.2. Health impacts of O ₃ exposure.....	51
1.1.7.3. Risk assessments to estimate the burden of disease	53
1.1.7.4. Disease burden from air pollution exposure at the global scale.....	55
1.1.7.5. Disease burden from air pollution exposure within India	61
1.1.7.6. Source contributions to the burden of disease from air pollution	64
1.1.7.7. Future disease burden from air pollution in India	66
1.2. Summary and Aims.....	67
1.3. Outline.....	68
2. Methods	69

2.1.	Air quality modelling.....	69
2.2.	Weather Research and Forecasting Model with Chemistry.....	70
2.2.1.	Model setup	72
2.2.2.	Physics.....	72
2.2.3.	Chemistry.....	75
2.2.4.	Emissions.....	77
2.3.	Exposure-response function for long-term ambient PM _{2.5} exposure	79
2.4.	Exposure-response function for long-term ambient O ₃ exposure.....	84
2.5.	Current and future population of India	86
2.6.	Sector-specific disease burden.....	90
2.7.	Uncertainties.....	90
3.	Model evaluation	92
3.1.	Metrics.....	92
3.2.	Meteorology.....	93
3.3.	Ambient surface PM _{2.5} concentrations	97
3.4.	Aerosol optical depth.....	100
3.5.	Ambient surface O ₃ concentrations	102
4.	Residential energy use emissions dominate health impacts from exposure to ambient particulate matter in India.....	105
4.1.	Abstract.....	105
4.2.	Introduction	105
4.3.	Results	106
4.3.1.	The contribution of emission sectors to ambient PM _{2.5} concentrations.....	106
4.3.2.	Premature mortality due to ambient PM _{2.5} exposure	109
4.3.3.	The contribution of emission sectors to the disease burden	111
4.4.	Conclusion.....	114
5.	Stringent emission control policies can provide large improvements in air quality and public health in India.....	115
5.1.	Abstract.....	115
5.2.	Introduction	115
5.3.	Specific methods.....	117
5.3.1.	Air pollution control pathways	117
5.3.2.	Health impact estimates.....	119
5.4.	Results	119
5.4.1.	Impact of scenarios on ambient PM _{2.5} concentrations in India.....	119
5.4.2.	Indian disease burden under air pollution control pathways	121
5.4.3.	Sensitivities to demography and baseline mortality rates.....	124

5.4.4.	Comparison to previous studies	126
5.5.	Conclusion	130
6.	Current and future disease burden from ambient ozone exposure in India	131
6.1.	Abstract	131
6.2.	Introduction	131
6.3.	Precursor emissions.....	133
6.4.	Results.....	135
6.4.1.	Comparison of disease burden using earlier and updated risks	135
6.4.2.	Reduction in O ₃ concentrations and disease burden per source removal ...	137
6.4.3.	Impact of emission mitigation scenarios on O ₃ and the disease burden	139
6.4.4.	Sensitivities to demography and baseline mortality rates	145
6.5.	Discussion	146
6.6.	Conclusion	150
7.	Discussion and Conclusion	152
7.1.	Summary of work.....	152
7.2.	Critical discussion of work	155
7.3.	Future work.....	158
7.4.	Conclusion	160
	References.....	161
	Appendices.....	202
	Appendix A: Acronyms and Abbreviations	202
	Appendix B: Supplementary information for “Residential energy use emissions dominate health impacts from exposure to ambient particulate matter in India”	209
	Appendix C: Supplementary information for “Stringent emission control policies can provide large improvements in air quality and public health in India”.....	214
	Appendix D: Supplementary information for “Current and future disease burden from ambient ozone exposure in India”	215

List of Tables

Table 1: Recent air pollution related policies in place or discussed within Indian ministries and agencies (Sagar et al 2016, Ministry of Finance 2016, Global Alliance for Clean Cookstoves and Dalberg Global Development Advisors 2013, Ministry of Petroleum and Natural Gas 2018c, Smith 2017b, Ministry of Petroleum and Natural Gas 2018a, Ministry of Environment and Forests 2009, 2018, Forest Survey of India 2017, Nain Gill 2010, Ministry of Environment Forests and Climate Change 2015a, Ministry of Road Transport and Highways 2016a, Government of India 2015, Ministry of Environment Forests and Climate Change 2015b, National Transport Development Policy Committee 2014, National Institution for Transforming India 2015, Ministry of Road Transport and Highways 2016b, Government of India 2014, Ministry of Power 2015, Ministry of New and Renewable Energy 2010, National Institution for Transforming India 2017, Ministry of Environment Forests and Climate Change 2018).....	35
Table 2: Health impacts of PM _{2.5} exposure (U.S. Environmental Protection Agency 2012, 2009b, Brook et al 2010, Newby et al 2015, Loomis et al 2013, Gordon et al 2014, Anderson et al 2012, Pope III and Dockery 2006, Naeher et al 2007, Edwards et al 2014, Bruce et al 2015b, Smith et al 2004, Bruce et al 2015a, Krewski et al 2009, Cohen et al 2017, Pope III 2007, Bell et al 2004, Stieb et al 2003, World Health Organization 2013, World Health Organization Regional Office for Europe 2013, Bell et al 2013, Achilleos et al 2017, Li et al 2016b, Atkinson et al 2012, Héroux et al 2015, Atkinson et al 2014, Levy et al 2012).	48
Table 3: Health impacts of O ₃ exposure (World Health Organization 2013, U.S. Environmental Protection Agency 2013b, Jerrett et al 2009, Zanobetti and Schwartz 2011, Smith et al 2009b, Turner et al 2016, Atkinson et al 2016).....	52
Table 4: Model setup and parameterisation used in the WRF-Chem model.....	72
Table 5: Reduction in population-weighted annual-mean PM _{2.5} concentrations in India caused by removing different emission sectors. Sectors are agriculture (AGR), biomass burning (BBU), dust (DUS), power generation (ENE), industrial non-power (IND), residential energy use (RES), and land transport (TRA).	107
Table 6: Estimated premature mortality associated with ambient PM _{2.5} exposure in India. Results for different emission sectors (both absolute and fractional) for both subtraction and attribution methods. Values in parentheses represent the 95% uncertainty intervals (95UI). Sectors are agriculture (AGR), biomass burning (BBU), dust (DUS), power generation (ENE), industrial non-power (IND), residential energy use (RES), and land transport (TRA).	110
Table 7: Reduction in population-weighted surface O ₃ concentrations in India associated with removing different sources. Two different O ₃ metrics (3mDMA1 and ADM8h) are shown. Sources are biomass burning (BBU), power generation (ENE), industrial non-power (IND), residential energy use (RES), and land transport (TRA). Absolute (ppbv) and relative (%) reductions are shown.....	138

Table 8: Source contributions to the annual premature mortalities associated with ambient O_3 exposure in India in 2015 calculated using Turner et al (2016) risks and LCC_{min} , including source contributions to the annual premature mortalities associated with ambient $PM_{2.5}$ exposure from Conibear et al (2018a) (Chapter 4). The absolute number and percentage of total premature mortalities associated with O_3 exposure in India are shown for two different methods (attribution and subtraction), and for the subtraction method for $PM_{2.5}$ exposure. Sources are biomass burning (BBU), power generation (ENE), industrial non-power (IND), residential energy use (RES), and land transport (TRA). Values in parentheses represent the 95% uncertainty intervals (95UI).....	139
Table 9: Estimated premature mortality associated with ambient $PM_{2.5}$ exposure in India per disease from both subtraction and attribution methods. Values in parentheses represent the 95% uncertainty intervals (95UI). Sectors are agriculture (AGR), biomass burning (BBU), dust (DUS), power generation (ENE), industrial non-power (IND), residential energy use (RES), and land transport (TRA).....	210
Table 10: Estimated years of life lost (YLL) associated with ambient $PM_{2.5}$ exposure in India per sector from both subtraction and attribution methods. Values in parentheses represent the 95% uncertainty intervals (95UI). Sectors are agriculture (AGR), biomass burning (BBU), dust (DUS), power generation (ENE), industrial non-power (IND), residential energy use (RES), and land transport (TRA).....	211
Table 11: Ground measurement air quality stations.....	212
Table 12: AERONET stations.....	213
Table 13: Scaling factors per emission sector and air pollutant in India (International Energy Agency 2016a).	214
Table 14: Ambient surface O_3 observation site details.....	215

List of Figures

Figure 1: Air pollution pathway (Smith 1993, McGranahan and Murray 2003, U.S. Environmental Protection Agency 2009a).	21
Figure 2: The size of particulate matter (Guarnieri and Balmes 2014).	22
Figure 3: The energy ladder (World Health Organization 2006b, Gordon et al 2014).	27
Figure 4: Solid fuel use in India. (a) Primary fuel use in India in 2011 in urban areas, rural areas, and overall. (b) Solid fuel use overall and in the top ten contributing states. (c) Solid fuel use per state as a percentage. (d) Number of households primarily using solid fuels. Change in primary fuel use between 1994 and 2010 in (e) rural areas and (f) urban areas (Energy Sector Management Assistance Program and Global Alliance for Clean Cookstoves 2015, International Energy Agency 2016a, Global Alliance for Clean Cookstoves and Dalberg Global Development Advisors 2013, Jain et al 2015, Government of India 2011).	29
Figure 5: Indian emissions of PM and precursor gases for 2015 by sector ($Mt\ yr^{-1}$) (Venkataraman et al 2018). Emissions of NO_x are NO	31
Figure 6: Annual-mean ambient $PM_{2.5}$ concentrations from the Global Burden of Diseases, Injuries, and Risk Factors Study (GBD) 2016 using the data integration model for air quality (DIMAQ) (Shaddick et al 2018b, Cohen et al 2017, GBD 2016 Risk Factors Collaborators 2017). (a) 2016. (b) 2015. (c) 2014. (d) 2013. (e) 2012. (f) 2011. (g) 2010. (h) 2005. (i) 2000. (j) 1995. (k) 1990.	38
Figure 7: Seasonal ambient O_3 concentrations from the GBD2013 (GBD 2013 Risk Factors Collaborators 2015, Brauer et al 2016). Calculated as the maximum running 3-month average of daily 1-hour maximum values.	38
Figure 8: Size-dependent deposition of particulate matter (Guarnieri and Balmes 2014).	45
Figure 9: Global premature mortalities by major risk factor and cause in 2015. Plot from Landrigan et al (2017) using data from GBD2016 (GBD 2016 Risk Factors Collaborators 2017).	46
Figure 10: Overview of diseases, conditions, and biomarkers affected by ambient air pollution (Thurston et al 2017).	50
Figure 11: The global burden of disease from ambient $PM_{2.5}$ exposure in 2016. (a) Number of premature mortalities per country. (b) Mortality rate per 100,000 population per country (Institute for Health Metrics and Evaluation 2018).	56
Figure 12: Drivers of changes in estimated premature mortality associated with ambient $PM_{2.5}$ exposure by country from 1990 to 2015 (Cohen et al 2017).	57
Figure 13: The global burden of disease from ambient O_3 exposure in 2016. (a) Number of premature mortalities per country. (b) Mortality rate per 100,000 population per country (Institute for Health Metrics and Evaluation 2018).	58

Figure 14: The disease burden from air pollution. (a) Annual premature mortality estimates in 1990. (b) Mortality rate per 100,000 population in 1990. (c) Annual premature mortality estimates in 2016. (d) Mortality rate per 100,000 population in 2016. Data from GBD2016 (Institute for Health Metrics and Evaluation 2018).....	59
Figure 15: Environmental risk transition estimates for India from GBD2016 for ambient $PM_{2.5}$, O_3 , and household solid fuels from 1990–2016 (Institute for Health Metrics and Evaluation 2018). (a) Number of deaths per year. (b) Number of DALYs per year. (c) Mortality rate per 100,000 per year. (d) DALYs rate per 100,000 per year.	60
Figure 16: The Indian burden of disease from ambient $PM_{2.5}$ exposure in 2016. (a) Number of premature mortalities per state. (b) Mortality rate per 100,000 population per state (Indian Council of Medical Research et al 2017a).....	62
Figure 17: The Indian burden of disease from ambient O_3 exposure in 2016. (a) Number of premature mortalities per state. (b) Mortality rate per 100,000 population per state (Indian Council of Medical Research et al 2017a).....	63
Figure 18: Source categories responsible for the largest impact on premature mortality associated with ambient air pollution in 2010 (Lelieveld et al 2015). Source categories are industry (IND), land transport (TRA), residential (RCO), biomass burning (BB), power generation (PG), agriculture (AGR), and natural (NAT). The white areas are where annual-mean $PM_{2.5}$ concentrations are below the theoretical minimum risk exposure level.	65
Figure 19: Increase in premature mortality associated with ambient air pollution exposure from 2010 to 2050 under a business-as-usual scenario (Lelieveld et al 2015).....	66
Figure 20: Model domain used in this thesis. Background colour shows terrain height from WRF-Chem simulated domain on a Lambert conformal conical projection.....	73
Figure 21: International geosphere-biosphere programme (IGBP) modified moderate resolution imaging spectroradiometer (MODIS) based land use classifications in India.....	74
Figure 22: Integrated-exposure response (IER) functions estimating the relative risk (RR) of mortality from ambient $PM_{2.5}$ concentrations from Global Burden of Diseases, Injuries, and Risk Factors Study (GBD) 2015 (GBD 2015 Risk Factors Collaborators 2016b) and GBD2016 (GBD 2016 Risk Factors Collaborators 2017). Mean exposure-response shown in bold line for ischaemic heart disease (IHD), cerebrovascular disease (CEV), chronic obstructive pulmonary disease (COPD), lower respiratory infections (LRI), and lung cancer (LC). IHD and CEV have shaded regions representing the variation between age groups.....	81
Figure 23: Short-term PM and PM_{10} exposure excess risk estimates in India.....	84
Figure 24: Attributable fractions as a function of ambient O_3 concentrations for chronic obstructive pulmonary disease (COPD) from both the earlier American Cancer Society Cancer Prevention Study II (CPS-II) (Jerrett et al 2009) and the updated CPS-II study (Turner et al 2016).	

Mean (solid line) as well as upper and lower 95% confidence intervals (shading) shown for both low-concentration cut-offs (LCC_{min} and LCC_{fifth}). 85

Figure 25: Change in baseline mortality, population age distribution, and population density for India between 2015 and 2050 from the International Futures (IFs) integrated modelling system (Hughes et al 2011) baseline scenario. Baseline mortality rates for (a) lower respiratory infections (LRI), (b) chronic obstructive pulmonary disease (COPD), (c) ischaemic heart disease (IHD), (d) cerebrovascular disease (CEV), and (e) lung cancer (LC) in 2015 and 2050. (f) Population age distribution. (g) Spatial distribution of population density in 2015 for South Asia. (h) Change in population density for South Asia between 2050 and 2015..... 88

Figure 26: Variation in baseline mortality, population age distribution, and population density for India in 2015 between the International Futures (IFs) integrated modelling system (Hughes et al 2011) baseline scenario and data used in GBD2016 (GBD 2016 Risk Factors Collaborators 2017). Baseline mortality rates for (a) lower respiratory infections (LRI), (b) chronic obstructive pulmonary disease (COPD), (c) ischaemic heart disease (IHD), (d) cerebrovascular disease (CEV), and (e) lung cancer (LC) in 2015 from IFs and GBD2016 (Institute for Health Metrics and Evaluation 2018). Note that for LRI, IFs provides age group 0–4 while GBD2016 provides age group 0–5. (f) Population age distribution in 2015 from IFs and GBD2016 (Global Burden of Disease Study 2016 2017a). (g) The difference in population density for South Asia in 2015 from IFs and Gridded Population of the World, Version 4 (GPWv4) (Center for International Earth Science Information Network and NASA Socioeconomic Data and Applications Center 2016b). 89

Figure 27: Spatial distribution of seasonal-mean total precipitation for 2014. (a–d) WRF-Chem. (e–h) ECMWF global reanalyses. (i–l) The difference (WRF-Chem minus ECMWF). Results shown for winter through autumn, see labels at the top of the figure. 94

Figure 28: Spatial distribution of seasonal-mean boundary layer height for 2014. (a–d) WRF-Chem. (e–h) ECMWF global reanalyses. (i–l) The difference (WRF-Chem minus ECMWF). Results shown for winter through autumn, see labels at the top of the figure..... 95

Figure 29: Spatial distribution of seasonal-mean wind speed and direction for 2014. (a–d) WRF-Chem. (e–h) ECMWF global reanalyses. (i–l) The difference (WRF-Chem minus ECMWF). Results shown for winter through autumn, see labels at the top of the figure..... 95

Figure 30: Spatial distribution of seasonal-mean temperature for 2014. (a–d) WRF-Chem. (e–h) ECMWF global reanalyses. (i–l) The difference (WRF-Chem minus ECMWF). Results shown for winter through autumn, see labels at the top of the figure. 96

Figure 31: Annual-mean meteorology correlations between model and ECMWF global reanalyses at each grid cell. (a) Boundary layer height, (b) total precipitation, (c) wind speed, and (d) temperature for 2014. 97

Figure 32: Model domain showing ground measurement sites for $PM_{2.5}$ and AERONET measuring AOD. The Delhi region is expanded in the bottom left.	98
Figure 33: Comparison of observed and simulated $PM_{2.5}$ concentrations. (a) Annual-mean surface $PM_{2.5}$ concentrations. Model results for 2014 (background) are compared with surface measurements from 2016 (filled circles). (b) Comparison of annual and seasonal-mean surface $PM_{2.5}$ concentrations. The best-fit line (green), 1:1, 2:1, and 1:2 lines are shown (black). Annual, winter (DJF), spring (MAM), summer (JJA), and autumn (SON) NMB are -0.10, -0.24, -0.07, 0.69, and -0.10, respectively. The best-fit line for annual data has slope = 0.70 and Pearson's correlation coefficient (r) = 0.19.	99
Figure 34: Seasonal-mean $PM_{2.5}$ concentrations for 2014. (a–d) model results (background) for 2014 for all sources are compared with ground-measurements (filled circles) from 2016, winter to autumn.	100
Figure 35: Evaluation of annual and seasonal-mean model AOD at 550 nm. (a) Comparison of model and satellite (MODIS Aqua C6) at AERONET locations. (b) Comparison of model and measured (AERONET). The best-fit line (green), 1:1, 2:1, and 1:2 lines are shown (black). NMB and slope of the best-fit line are given inset.....	101
Figure 36: Comparison of observed and simulated O_3 concentrations. (a) Annual mean surface O_3 concentrations from the model for 2014 (background) compared with observations (filled circles, with text showing site abbreviation and measured annual mean). (b) Comparison of annual and monthly-mean surface O_3 concentrations (colours of filled circles are grouped per site for annual and monthly values). The overall best-fit line is solid, and the 1:1, 2:1, and 1:2 lines are dashed lines. Comparison of annual mean observed and simulated values: normalised mean bias (NMB) = 0.35; the best-fit line has slope = 1.21, and Pearson's correlation coefficient (r) = 0.55.....	103
Figure 37: Comparison of rural and urban observed and simulated O_3 concentrations. (a) Comparison of annual and monthly-mean ambient surface O_3 concentrations from rural observation sites. The rural site best-fit line (solid), 1:1, 2:1, and 1:2 lines are shown (dashed). Rural site NMB is 0.28, the rural site best-fit line has slope = 1.18, and rural site r = 0.67. (b) Comparison of annual and monthly-mean ambient surface O_3 concentrations from urban observation sites. The urban site best-fit line (solid), 1:1, 2:1, and 1:2 lines are shown (dashed). Urban site NMB is 0.41, the urban site best-fit line has slope = 1.24, and urban site r = 0.47. Colours of filled circles grouped by site.	104
Figure 38: Fractional contribution of residential energy use to annual-mean $PM_{2.5}$. (a) Concentrations. (b) Anthropogenic emissions. Emissions are from EDGAR-HTAP v2.2 (Section 2.2.4).	108

Figure 39: Seasonal-mean anthropogenic $PM_{2.5}$ emissions. Anthropogenic $PM_{2.5}$ emissions in (a) winter and (b) summer. Fractional contributions from the residential sector for (c) winter and (d) summer. Emissions are from EDGAR-HTAP v2.2 (Section 2.2.4). 108

Figure 40: Seasonal-mean $PM_{2.5}$ concentrations for 2014. (a–d) Residential sector $PM_{2.5}$ concentrations, winter to summer. (e–h) The fraction from the residential sector, winter to summer. 109

Figure 41: Disease burden due to exposure to ambient $PM_{2.5}$ across India. (a) Estimate of annual premature mortality due to exposure to $PM_{2.5}$ in India. (b) Attributable fraction of premature mortalities from residential energy use emissions (attribution method). (c) The averted fraction of premature mortalities from removing residential energy use emissions (subtraction method). 110

Figure 42: Comparison of annual premature mortality estimates for India due to exposure to ambient $PM_{2.5}$. (a) Total annual premature mortality from exposure to ambient $PM_{2.5}$ from all emission sources. This study (green) and sensitivity studies (purple) comparing varying model spatial resolution, population year, exposure-response function, baseline mortality rates, and $PM_{2.5}$ concentrations are compared with previous studies (orange). (b) Attributed sector-specific estimates from the attribution method from this study compared to previous studies. (c) Averted sector-specific estimates from the subtraction method from this study compared to previous studies. Error bars for this study and sensitivity analyses represent 95% uncertainty intervals (95UI) calculated by combining fractional errors in quadrature (see Methods). Error bars for previous studies given at the 95% uncertainty level where provided. 113

Figure 43: Cumulative emissions per source within India in 2015 and projected emissions in 2040 under the NPS and CAS (International Energy Agency 2016a). 119

Figure 44: The impact of scenarios on annual-mean ambient $PM_{2.5}$ concentrations in India. (a) Annual-mean ambient $PM_{2.5}$ concentrations in India in 2015 from the control scenario. (b) National-mean changes in 2015 population-weighted annual-mean ambient $PM_{2.5}$ concentrations for each scenario. (c–h) Difference in annual-mean ambient $PM_{2.5}$ concentrations for IEA New Policy Scenario (NPS), IEA Clean Air Scenario (CAS), removal of power generation emissions (ENE 0%), removal of industry emissions (IND 0%), removal of residential energy use emissions (RES 0%), and removal of land transport emissions (TRA 0%) scenarios. 120

Figure 45: The impact of scenarios on air quality metrics in India. (a) Percentage of the population and (b) total population in 2015 (1st bar) and 2050 (2nd bar) exposed to annual-mean ambient $PM_{2.5}$ concentrations exceeding $10 \mu g m^{-3}$ (WHO AQG), $35 \mu g m^{-3}$ (WHO IT-1), and $40 \mu g m^{-3}$ (NAAQS) in each scenario. 121

Figure 46: The impact of scenarios on annual premature mortality from exposure to ambient $PM_{2.5}$ in India. (a) Annual premature mortality from exposure to ambient $PM_{2.5}$ in India in 2015 from the control scenario. (b) National-mean changes in annual premature mortality estimates

from ambient $PM_{2.5}$ exposure per scenario, for both emissions only changes in 2015 and overall changes in 2050. The dashed horizontal line represents the change in annual premature mortality in 2050 if emissions remain at 2015 levels. (c–h) Difference in the annual premature mortality from ambient $PM_{2.5}$ exposure in 2050 for IEA New Policy Scenario (NPS), IEA Clean Air Scenario (CAS), removal of power generation emissions (ENE 0%), removal of industry emissions (IND 0%), removal of residential energy use emissions (RES 0%), and removal of land transport emissions (TRA 0%) scenarios relative to the control scenario in 2015. 122

Figure 47: The impact of scenarios on annual mortality rate per 100,000 population from exposure to ambient $PM_{2.5}$ in India. (a) Annual mortality rate per 100,000 population from exposure to ambient $PM_{2.5}$ in India in 2015 from the control scenario. (b) National-mean changes in annual mortality rate per 100,000 population estimates from ambient $PM_{2.5}$ exposure per scenario, for both emissions only changes in 2015 and overall changes in 2050. The dashed horizontal line represents the change in annual mortality rate per 100,000 population in 2050 if emissions remain at 2015 levels. (c–h) Difference in the annual mortality rate per 100,000 population from ambient $PM_{2.5}$ exposure in 2050 for IEA New Policy Scenario (NPS), IEA Clean Air Scenario (CAS), removal of power generation emissions (ENE 0%), removal of industry emissions (IND 0%), removal of residential energy use emissions (RES 0%), and removal of land transport emissions (TRA 0%) scenarios relative to the control scenario in 2015. 123

Figure 48: (a) The impact of emission scaling on population-weighted annual-mean ambient $PM_{2.5}$ concentrations. (b) The impact of emission scaling on total annual premature mortality from exposure to ambient $PM_{2.5}$ concentrations in India. 124

Figure 49: The impact of scenarios on the disease burden from exposure to ambient $PM_{2.5}$ in India. (a) National-mean annual premature mortality rate per 100,000 population due to ambient exposure to $PM_{2.5}$ in India. (b) Disease breakdown of health burden from ambient $PM_{2.5}$ exposure in India. For each panel, the bars show estimates for 2015, 2050, 2050 with population density from 2015, 2050 with population age grouping from 2015, and 2050 with baseline mortality rates from 2015 (1st to 5th bars per scenario). The vertical error bars show 95% uncertainty intervals (95UI) calculated by combining fractional errors in quadrature (see Methods). 126

Figure 50: Comparison of the impacts of different scenarios on ambient $PM_{2.5}$ concentrations and the associated disease burden in India from this study with previous studies. (a) Comparison of population-weighted annual-mean ambient $PM_{2.5}$ concentrations. (b) Comparison of percentage of the population exposed to various metrics of annual-mean ambient $PM_{2.5}$ concentrations in India. (c) Comparison of total premature mortality estimates due to exposure to ambient $PM_{2.5}$ per year in India from different scenarios. 128

Figure 51: Fractional contribution per sector to total annual anthropogenic emissions. The fractional contribution of land transport (TRA), power generation (ENE), residential energy use

(RES), and industry (IND) to anthropogenic emissions of (a–d) nitrogen oxides (NO_x), (e–h) non-methane volatile organic compounds (NMVOC), and (i–l) carbon monoxide (CO)..... 134

Figure 52: Fractional contribution per season to total anthropogenic emissions. The fractional contribution to total anthropogenic emissions of NO_x from winter (DJF), spring (MAM), summer (JJA), and autumn (SON) to anthropogenic emissions of (a–d) nitrogen oxides (NO_x), (e–h) non-methane volatile organic compounds (NMVOC), and (i–l) carbon monoxide (CO)..... 135

Figure 53: Estimates of (a) premature mortality, (b) mortality rate per 100,000 population, and (c) years of life lost (YLL) in 2015 from ambient O_3 exposure in India using the earlier CPS-II study risks from Jerrett et al (2009) (solid bars) and the updated CPS-II study risks from Turner et al (2016) (dashed bars). Error bars represent 95% uncertainty intervals..... 136

Figure 54: Premature mortality estimates due to O_3 exposure across India in 2015. All calculations for the control scenario. (a, d) Annual mean surface O_3 concentrations. (b, e) Annual premature mortality. (c, f) Annual mortality rate per 100,000 population. (a–c) Calculated following Jerrett et al (2009). (d–f) Calculated following Turner et al (2016). (a) Shows the 3mDMA1 O_3 metric. (d) Shows the ADM8h O_3 metric. See text for details. 137

Figure 55: Impacts of air pollution control pathways on surface O_3 concentrations in India. (a) National-mean relative changes in population-weighted ADM8h surface O_3 concentrations for different emission scenarios relative to the control scenario in 2015. (b–g) Absolute change in ADM8h O_3 concentrations for different emission scenarios relative to the control (CTL) scenario. Emission scenarios are New Policy Scenario (NPS), Clean Air Scenario (CAS), and when individual emission sectors are switched off: power generation (ENE 0%), industrial non-power (IND 0%), residential energy use (RES 0%), and land transport (TRA 0%). 140

Figure 56: Impacts of air pollution control pathways on annual premature mortality from ambient O_3 exposure in India. (a) National-mean changes in annual premature mortality estimates from ambient O_3 exposure per scenario, for both emissions only changes between 2015 and 2050 (solid bars) and overall changes in 2050 including 2015 to 2050 changes in emissions as well as population growth, population ageing, and baseline mortality rates (POP/AGE/BM, dashed bars). The dashed horizontal line represents the change in annual premature mortality in 2050 if emissions remain at 2015 levels. (b–g) Change in annual premature mortality from ambient O_3 exposure in 2050 from different emission scenarios (see Figure 55) relative to the control scenario in 2015 accounting for emission changes and POP/AGE/BM changes. All health impacts are calculated using Turner et al (2016) RR and LCC_{min} 142

Figure 57: Impacts of air pollution control pathways on annual mortality rate per 100,000 population from ambient O_3 exposure in India. (a) National-mean changes in annual mortality rate per 100,000 population estimates from ambient O_3 exposure per scenario, for both emissions only changes between 2015 and 2050 (solid bars) and overall changes in 2050 including 2015 to 2050 changes in emissions as well as population ageing and baseline mortality rates

(POP/AGE/BM, dashed bars). The dashed horizontal line represents the change in annual mortality rate per 100,000 population in 2050 if emissions remain at 2015 levels. (b–g) Annual change in mortality rate per 100,000 population from ambient O_3 exposure in 2050 from different emission scenarios (see Figure 55) relative to the control scenario in 2015 accounting for emission changes and POP/AGE/BM changes. All health impacts are calculated using Turner et al (2016) RR and LCC_{min} 143

Figure 58: The impact of emission scaling on (a) population-weighted ADM8h surface O_3 concentrations, and (b) annual premature mortality estimates from O_3 exposure using Turner et al (2016) risks and LCC_{min} for emissions only changes between 2015 and 2050. For each source sector, a control scenario (CTL, 100%) is compared against scenarios where emission sectors are individually increased by 10% (110% of emissions), decreased by 10% (90% of emissions), and completely removed (0% of emissions). A solid line joins the data points from the idealised simulations (0%, -10%, and +10%) and is added to guide the eye. Linear scaling was applied to the 10% emission reduction scenarios per sector ($10 \times -10\%$, dashed lines) following a similar approach to Wild et al (2012) and Turnock et al (2018). 145

Figure 59: Comparison of premature mortality estimates for India due to ambient O_3 exposure. Estimates are shown using relative risks from either the earlier CPS-II study from Jerrett et al (2009) (solid bars) or the updated CPS-II study from Turner et al (2016) (dashed bars). (a) Total premature mortality from O_3 exposure from all sources. Estimates are shown for both lower concentration cut-offs (LCC_{min} and LCC_{fifth}). This study (green) is compared with previous studies (orange). (b) Estimates of premature mortality from different emission sectors (see key) using either the attribution or the subtraction method. Estimates are shown for LCC_{min} . Error bars represent 95% uncertainty intervals. 148

Figure 60: Comparison of (a) premature mortality and (b) mortality rate estimates for India due to $PM_{2.5}$ and O_3 exposure. Estimates are shown for the 2015 control (CTL) scenario, the New Policy Scenario (NPS) in 2050, and the Clean Air Scenario (CAS) in 2050. Estimates of the disease burden for O_3 exposure (green) are from this study using relative risks from the updated CPS-II study from Turner et al (2016) and LCC_{min} . Estimates of the disease burden for $PM_{2.5}$ exposure (orange) are from Conibear et al (2018b) (Chapter 5) using the IER function (Burnett et al 2014) updated for GBD2016 (GBD 2016 Risk Factors Collaborators 2017). Estimates for O_3 exposure are from COPD only. Estimates for $PM_{2.5}$ exposure are from COPD, LRI, CEV, LC, and IHD combined. Error bars represent 95% uncertainty intervals. 150

Figure 61: Comparison of annual-mean $PM_{2.5}$ concentrations. (a) Model (WRF-Chem). (b) GBD2015 (2016) (Shaddick et al 2018b) DIMAQ. (c) Model minus GBD2015. 209

Figure 62: Premature mortality estimates from exposure to ambient $PM_{2.5}$ in India. (a) Premature mortality rate per 100,000 population. (b) Premature mortality estimate using Indian state-

specific baseline mortality rates (Chowdhury and Dey 2016), where white space represents where there was no state-specific baseline mortality rate data available. 209

Figure 63: Fractional contribution per source to total annual-mean ambient O₃ surface concentrations. (a) Total annual-mean ambient O₃ surface concentrations. (b–f) Fractional contribution from biomass burning (BBU), power generation (ENE), industrial non-power (IND), residential energy use (RES), and land transport (TRA). 216

Figure 64: Dominant source contributions to premature mortality burden due to O₃ exposure across India in 2015. (a) Attributable fraction of premature mortalities from land transport emissions (attribution method). (b) Averted fraction of premature mortalities from removing land transport emissions (subtraction method). (c) Attributable fraction of premature mortalities from energy emissions (attribution method). (d) Averted fraction of premature mortalities from removing energy emissions (subtraction method). All health impacts are calculated using Turner et al (2016) RR and LCC_{min}. 217

Figure 65: The impact of scenarios on O₃ metrics. (a) Percentage of population in 2015 (1st bar) and 2050 (2nd bar) exposed to population-weighted ambient surface O₃ concentrations above 50 ppb (WHO AQG, Indian NAAQS) in each scenario. (b) Absolute population in 2015 (1st bar) and 2050 (2nd bar) exposed to population-weighted ambient surface O₃ concentrations above 50 ppb (WHO AQG, Indian NAAQS) in each scenario. 218

Figure 66: Sensitivities of health impacts due to O₃ exposure in India to demography and baseline mortality rates. (a) Mortality rate per 100,000 population. (b) Total annual premature mortality. Impacts are estimated using either Jerrett et al (2009) (red) and Turner et al (2016) (purple) relative risks with LCC_{min}. For each panel, the control (CTL) scenario is compared against the NPS and CAS scenarios. For each panel, the five bars (left to right) show estimates for 2015 with 2015 population, age, and baseline mortality, 2050 with 2050 population, age, and baseline mortality, and 2050 with population from 2015 (POP2015), population age grouping from 2015 (AGE2015), and baseline mortality rates from 2015 (BM2015). 219

List of Equations

<i>Equation 1: Integrated exposure-response (IER) functions to estimate long-term relative risk from PM_{2.5} exposure (Burnett et al 2014).</i>	80
<i>Equation 2: Long-term premature mortality from PM_{2.5} exposure.</i>	82
<i>Equation 3: Long-term years of life lost from PM_{2.5} exposure.</i>	82
<i>Equation 4: Long-term premature mortality from O₃ exposure.</i>	86
<i>Equation 5: Long-term attributable fraction from O₃ exposure.</i>	86
<i>Equation 6: Long-term hazard ratio from O₃ exposure.</i>	86
<i>Equation 7: Sector-specific premature mortality following the subtraction method.</i>	90
<i>Equation 8: Sector-specific premature mortality following the attribution method.</i>	90
<i>Equation 9: Mean bias.</i>	92
<i>Equation 10: Normalised mean bias.</i>	93
<i>Equation 11: Root mean squared error.</i>	93
<i>Equation 12: Normalised mean absolute error.</i>	93
<i>Equation 13: Pearson's correlation coefficient.</i>	93
<i>Equation 14: The non-linear O₃ response.</i>	144
<i>Equation 15: The percentage contribution of the non-linear O₃ response.</i>	144

1. Ambient air quality and human health in India

Air pollution exposure is a leading global risk factor (Cohen *et al* 2017, GBD 2016 Risk Factors Collaborators 2017, Indian Council of Medical Research *et al* 2017b, India State-Level Disease Burden Initiative Collaborators 2017). Exposure to air pollution is the second leading risk factor in India, contributing one-quarter of the global disease burden attributable to air pollution exposure (Cohen *et al* 2017, GBD 2016 Risk Factors Collaborators 2017, Indian Council of Medical Research *et al* 2017b, India State-Level Disease Burden Initiative Collaborators 2017). The disease burden from air pollution is costly, worsening, and disproportionately falls on susceptible populations (Landrigan *et al* 2017). Despite this importance, research on air pollution in India is limited and little is known about the sources and processes that contribute to air pollution in this region. Understanding the causes and processes behind the health impacts of air pollution exposure across a range of scales is critical to reduce the substantial and growing disease burden in India.

1.1. Air pollution pathway

Exposure to air pollution is a risk factor that causes health impacts (Smith 1993, McGranahan and Murray 2003, U.S. Environmental Protection Agency 2009a). Epidemiological risk is the probability that a disease, injury, or infection will occur. The risk assessment of air pollution follows the air pollution pathway (Figure 1) from sources through emissions, concentrations, exposures, doses, to health impacts (Smith 1993, McGranahan and Murray 2003, U.S. Environmental Protection Agency 2009a). Sources are the origin of the pollutant, generally the quantity and quality of fuel used. Emissions are air pollutants released from the source and are characterised by the environment, transported, and transformed. Concentrations are the amount of an air pollutant in space and time. Exposures are concentrations of air pollutants that are breathed in and depend on pathways, durations, intensities, and frequencies of contact with the pollutant. Doses are how much of the exposure is deposited in the body. Health impacts accrue from doses, can be acute (short-term) or chronic (long-term), and are non-specific in that they have many risk factors. Monitoring and intervention can occur at any stage along this pathway. Health impacts are the primary risk indicators, though control measures at this stage are often too late and complicated due to their non-specific nature. Doses are also too late in the air pollution pathway and are poorly understood for many pollutants. Control measures and standards generally focus on sources, emissions, and concentrations, with recent efforts targeting exposures.

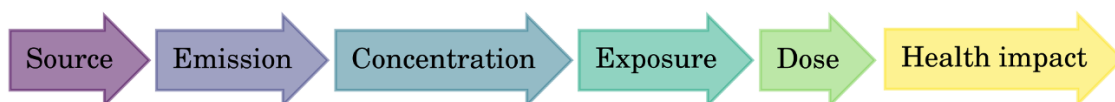


Figure 1: Air pollution pathway (Smith 1993, McGranahan and Murray 2003, U.S. Environmental Protection Agency 2009a).

1.1.1. Fundamentals of ambient air pollution

Ambient air pollution is a complex mixture of many particles and gases. Air quality is generally measured by a small subset of these particles and gases. Fine particles with aerodynamic diameters less than or equal to 2.5 micrometres (PM_{2.5}) and tropospheric ozone (O₃) are two important indicators of air quality. PM_{2.5} is the most consistent and robust predictor of health effects from studies of long-term exposure to air pollution (Health Effects Institute 2018). O₃ has been associated with increased respiratory mortality (Health Effects Institute 2018). This thesis is consistent with the Global Burden of Diseases, Injuries, and Risk Factors Study (GBD) when quantifying exposure to ambient air pollution using PM_{2.5} and O₃ as indicators. The air quality community often refers to aerosol mass as particulate matter (PM).

1.1.1.1. Aerosols

An aerosol is a solid or a liquid suspended in a gas. Aerosol matter are characterised by their size, shape, and composition (Brasseur and Jacob 2016, Seinfeld and Pandis 2016). Aerosols span three orders of magnitude in size, generally categorised into modes. The nucleation mode are particles with a diameter less than 0.01 µm, the Aitken mode are particles sized between 0.01–0.1 µm, the accumulation mode are particles with diameters between 0.1–2.5 µm, and the coarse mode are particles with diameter between 2.5–10 µm. Particles less than 0.1 µm are ultrafine particles, less than 2.5 µm in diameter are fine particulate matter (PM_{2.5}), and particles less than 10 µm (PM₁₀) combine fine and coarse particles. Figure 2 shows the size of fine and coarse PM relative to human hair (Guarnieri and Balme 2014). Fine and coarse particles vary in their origin, transformation, removal, composition, optical properties, and health impacts (Brasseur and Jacob 2016, Seinfeld and Pandis 2016). Aerosols are physically intricate in shape becoming more spherical when dissolved or aged. However, they are often assumed spherical for simplicity (Brasseur and Jacob 2016, Seinfeld and Pandis 2016).

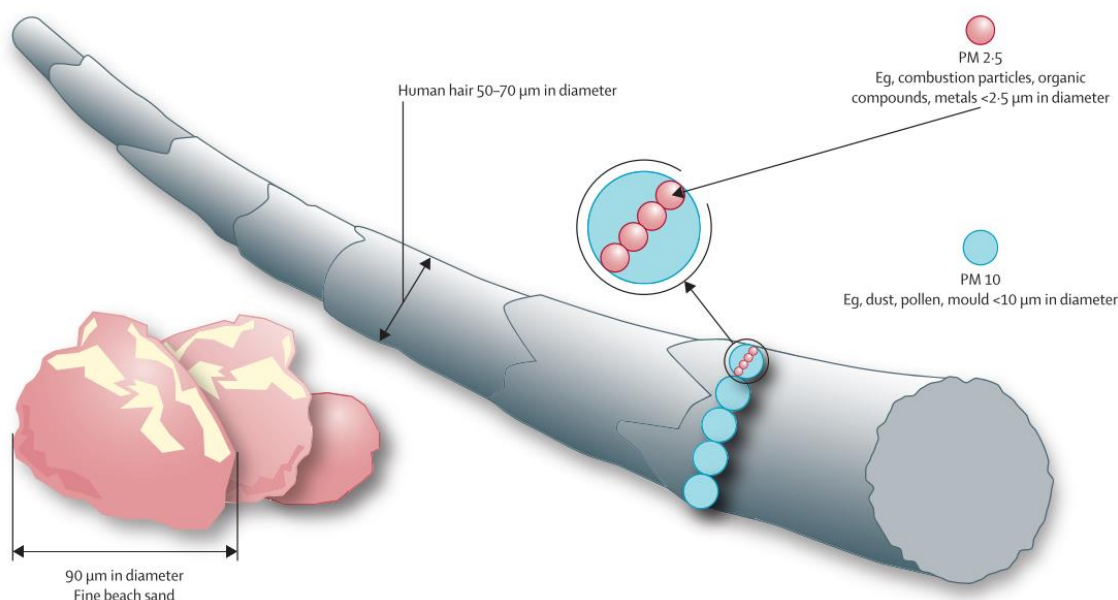


Figure 2: The size of particulate matter (Guarnieri and Balmes 2014).

Aerosols are chemically complex (Brasseur and Jacob 2016, Seinfeld and Pandis 2016). Primary aerosols are directly emitted to the atmosphere, including sea salt (NaCl), mineral dust, sulphate (SO₄), organic carbon (OC), black carbon (BC), metals, and bio-aerosols. Primary SO₄ are from sea spray and fossil fuel combustion. Primary OC and BC are from mobile exhausts, wildfires, agricultural combustion, and solid fuel burning. Primary metals are from volcanoes and industrial processes. Primary bio-aerosols are from viruses and bacteria. Primary organic aerosol (POA) are directly emitted organic matter (OM). Organic aerosol (OA) reacts in the gas, particle, and aqueous phase.

Secondary aerosols are formed in the atmosphere. Secondary inorganic aerosols (SIA) include SO₄, nitrate (NO₃), ammonium (NH₄), ammonium sulphate (NH₄)₂SO₄, and ammonium nitrate (NH₄NO₃). Secondary SO₄ are from the oxidation of sulphur gases, e.g. sulphur dioxide (SO₂) oxidises to sulphuric acid (H₂SO₄) and is neutralised by ammonia (NH₃) to form (NH₄)₂SO₄. Secondary NO₃ are from the oxidation of nitrogen oxides (NO_x) partitioning to the particle phase, forming NH₄NO₃. Secondary NH₄ are from NH₃ emissions from agriculture or industry. Secondary organic aerosols (SOA) are formed from the oxidation of volatile organic compounds (VOC) and semi-volatile and intermediate volatility organic compounds (S/IVOCs) to low-volatility products that condense into the particle phase (Brasseur and Jacob 2016, Seinfeld and Pandis 2016). SOA formation depends on volatility, hygroscopicity, and reactivity of the VOCs and the reacted products. Many different organic species contribute to SOA. POA can dilute and evaporate forming vapours, which can react and recondense to SOA (Brasseur and Jacob 2016, Seinfeld and Pandis 2016).

Important aerosol chemical and microphysical processes include nucleation, coagulation, condensation, gas-phase chemistry, heterogeneous chemistry, cloud interactions, dry deposition,

and wet removal (Brasseur and Jacob 2016, Seinfeld and Pandis 2016). Nucleation describes new aerosol formation from gases. Coagulation is the process by which two particles collide to form one larger particle. Condensation (evaporation) is the mass exchange between gases and particles. Chemistry differs by phase, where heterogeneous chemistry involves the liquid- and solid-phase (Brasseur and Jacob 2016, Seinfeld and Pandis 2016). Cloud interactions depend on aerosol activation forming cloud condensation nuclei in the presence of supersaturated water vapour. Dry deposition is direct exchange with the surface. Wet removal is through washout below clouds and rainout within clouds, where particles that have activated to form cloud condensation nuclei are removed.

Aerosols have a lifetime of minutes to a week, depending on particle size, and is affected by deposition, transport, dispersion, and chemistry. Aerosol hygroscopicity is the uptake of water, is affected by the composition, and has a considerable influence on optical properties (Brasseur and Jacob 2016, Seinfeld and Pandis 2016). Aerosols deliquesce at a relative humidity where particles transition from non-aqueous to aqueous (Brasseur and Jacob 2016, Seinfeld and Pandis 2016).

Nucleation and Aitken mode aerosol are formed from condensed gas and nucleated aerosols, are lost through coagulation, dominate the total aerosol number, and contribute little to the total aerosol mass due to their small size (Brasseur and Jacob 2016, Seinfeld and Pandis 2016). Accumulation mode aerosol are formed from condensation and coagulation, dominating the total aerosol surface area and mass (Brasseur and Jacob 2016, Seinfeld and Pandis 2016). Accumulation aerosols are primarily lost through rainout and dry deposition. Accumulation mode aerosols are largely soluble, hygroscopic, and deliquescent. Accumulation mode aerosols have a longer lifetime and transport further distances, than ultrafine and coarse aerosols. Coarse particles are mainly of primary origin through mechanical or natural processes. Coarse aerosols are lost through dry deposition and washout (Brasseur and Jacob 2016, Seinfeld and Pandis 2016).

Aerosols scatter and absorb radiation, primarily in the visible wavelength range, influenced by their size, chemical composition, and shape (Brasseur and Jacob 2016, Seinfeld and Pandis 2016). This interaction with radiation means aerosols cause visibility impairment and means aerosol can affect the climate through aerosol radiation interactions (ARI) (Intergovernmental Panel on Climate Change 2013). Aerosols also alter the climate indirectly by interacting with clouds, known as aerosol-cloud interactions (ACI) (Intergovernmental Panel on Climate Change 2013). Aerosol radiation interactions can lead to warming through absorption of radiation (e.g. BC) or cooling through scattering (e.g. OC, SO₄) (Intergovernmental Panel on Climate Change 2013).

1.1.1.2. Ozone

O₃ is a secondary gaseous pollutant produced in the atmosphere. O₃ production and loss are controlled by different mechanisms in the stratosphere and troposphere. Photolysis of O₂ controls stratospheric O₃ production following the Chapman mechanism (Brasseur and Jacob 2016,

Seinfeld and Pandis 2016). In the troposphere, where ultra-violet (UV) radiation is not energetic enough to photolyse oxygen (O_2) directly, production of tropospheric O_3 is driven by photochemical oxidation of VOCs and carbon monoxide (CO) in the presence of NO_x . O_3 production is complex and non-linearly dependent on temperature, radiation intensity, spectral distribution, precursor concentrations, among many other factors (Brasseur and Jacob 2016, Seinfeld and Pandis 2016). NO_x is emitted mainly as nitric oxide (NO). NO is oxidised to NO_2 by organic-peroxy (RO_2) or hydro-peroxy (HO_2) radicals released during VOC oxidation. VOC oxidation is initiated mostly by reaction with hydroxyl (OH) radicals. NO_2 photolysis produces NO and a ground-state oxygen atom, $O(^3P)$, which reacts with O_2 to form O_3 . O_3 photolysis produces electronically excited oxygen atoms, $O(^1D)$, which react with water vapour to produce the OH radical, which can then further oxidise VOCs. O_3 can react with NO to produce NO_2 , which is an important O_3 sink in urban areas, where NO concentrations are very high, leading to low O_3 abundances. VOCs are biogenic and anthropogenic, including methane (CH_4), alkanes, alkenes, aromatic hydrocarbons, carbonyl compounds, alcohols, organic peroxides, and halogenated organic compounds. VOC lifetime can vary from an hour to a decade (Brasseur and Jacob 2016, Seinfeld and Pandis 2016).

Chemical production and loss of O_3 show complex dependencies on O_3 precursor concentrations. Isoleths are used to illustrate the dependency of O_3 production on NO_x and VOC concentrations, depicting lines of constant O_3 production rate and regimes where O_3 is insensitive to VOC abundance (NO_x -limited) and relatively insensitive or inversely related to NO_x abundance (VOC-limited) (Brasseur and Jacob 2016, Seinfeld and Pandis 2016). The majority of the troposphere is NO_x -limited. Biogenic and anthropogenic VOCs are important precursors in rural and urban areas, respectively, though O_3 and precursors of O_3 can be transported long distances. Transport of stratospheric O_3 is an additional minor source to tropospheric O_3 . The dominant sinks of tropospheric O_3 are photochemical loss, dry deposition, as well as direct reactions with HO_2 and OH (Brasseur and Jacob 2016, Seinfeld and Pandis 2016).

O_3 lifetime varies with altitude, latitude, and season (Brasseur and Jacob 2016, Seinfeld and Pandis 2016). The global-mean lifetime of O_3 is 19 days, though O_3 lifetime is only a few days at the surface of the boundary layer and a few months in the upper troposphere (Brasseur and Jacob 2016, Seinfeld and Pandis 2016). The gradient of O_3 lifetime with altitude drives increasing O_3 concentrations at higher altitudes. The air quality community is primarily concerned with O_3 at the surface. The diurnal cycles of rural O_3 concentrations are less variable as rural O_3 persists longer than in urban areas due to less chemical scavenging from other primary pollutants. Urban O_3 diurnal cycles have a night-time decrease relative to day-time. O_3 has low aqueous solubility (Brasseur and Jacob 2016, Seinfeld and Pandis 2016).

1.1.2. Air pollution sources

1.1.2.1. Sectors

Throughout the year in India, there are air pollutant emissions from transport (on- and off-road), residential (cooking, lighting, and water heating), industry, power generation, diesel generators (including agricultural pumps and tractors), open waste burning, natural and anthropogenic dust (combustion, industry, and resuspended road). In winter, there are additional emissions from residential heating, commercial heating, and agricultural burning. There are also emissions from informal industrial activities including brick kilns, food operations, and agricultural processing (Venkataraman *et al* 2018).

Residential, industrial, and power generation sectors in India all primarily combust solid fuels (wood, crop residue, dung, and coal). Emission factors from solid fuel use are often three orders of magnitude larger in residential uses relative to those in a large-scale facility, due to advanced combustion control, fuel quality control, post-combustion emission control systems, and legislative and reporting requirements (Shen *et al* 2010, Wang *et al* 2012). Power generation and industrial activities are key in eastern and southern India. The majority (57%) of electricity is produced by coal (Global Alliance for Clean Cookstoves and Dalberg Global Development Advisors 2013). Indian coal has low sulphur contents, high ash and moisture contents, and low net calorific values, with implications for SO₂ and PM emissions. Approximately one-quarter of coal is imported into India (Sahu *et al* 2017). The majority of India's thermal power plants do not adhere to regulations, do not use flue-gas desulphurisation, and have low energy efficiencies, leading to high air pollutant emissions (Venkataraman *et al* 2018). India's brick kilns use predominantly traditional technologies, such as Bull's trench kilns (76%) and clamp kilns (21%), using fired-brick walling materials and coal (Venkataraman *et al* 2018). Agricultural burning of solid fuels is primarily in the northwest (Punjab and Haryana). Natural dust is a strong source of PM in the northwest near the Thar Desert.

The total vehicle fleet in India is currently approximately 150 million, where between 67–82% are two-wheelers including scooters, motorcycles, and mopeds due to their low cost (Pandey and Venkataraman 2014, Guttikunda and Mohan 2014). Approximately one-sixth is from four-wheelers including cars and jeeps, and small shares are from other modes of transport (Pandey and Venkataraman 2014, Guttikunda and Mohan 2014). The vehicle fleet is predominately in urban areas (Pandey and Venkataraman 2014, Guttikunda and Mohan 2014). There is little use of public vehicles, largely due to a lack of infrastructure (Venkataraman *et al* 2018). Between 2000 and 2015, the number of households grew by a 1.39% per year, installed capacity of electricity generation grew by 6.89% per year, industrial cement production grew by 5.06% per year, passenger-kilometres increased by 6.54% per year, and freight-kilometres increased by 3.61% per year (Venkataraman *et al* 2018). The next section focuses on residential emissions and solid fuel use in detail.

1.1.2.2. Residential emissions and solid fuel use

Using solid fuels to create fire is arguably the defining task in human history (Wrangham 2010). Until approximately 1850, everyone used solid fuels for cooking (Smith 2017b). The fraction of the global population using solid fuels decreased to 62% in 1980 and further decreased to 41% in 2010 (Bonjour *et al* 2013). The majority of the global population now use clean fuels, gas and electricity, which is a sign of substantial development (Smith 2017b). However, the absolute number of solid fuel users has remained the same between 1980 and 2010 (approximately 3 billion globally, with 700 million in India) (World Health Organization 2015, Bonjour *et al* 2013). The absolute number of solid fuel users is important when considering absolute emissions. Substantial development between 1990 and 2010 halved the number of extremely poor people (Gapminder 2018) and many in India now have mobile phones and motorbikes (Smith and Sagar 2014). However, most of the Indian population earn between 2 and 8 dollars per day (Gapminder 2018), still using traditional Indian stoves (Chulhas) with solid biomass (primarily brushwood) (Smith and Sagar 2014). Energy consumption per capita in India is 25% of the global average. This poverty is a fundamental reason for solid fuel use.

As the absolute number of solid fuel users has remained the same for the last 30 years, globally and in India, waiting for people to come out of poverty has not solved the issue of solid fuel use. Solid fuel interventions are implemented to address the ongoing issue of solid fuel use. The goal of solid fuel interventions is to either make the *available clean* i.e. to combust biomass cleanly in advanced stoves (move from the bottom left to the top left of the energy ladder, Figure 3), or to make the *clean available* i.e. to make clean fuels affordable (move from the top right to the top left of the energy ladder, Figure 3) (Smith and Sagar 2014). Both types of solid fuel intervention aim to improve population health before they become wealthy.

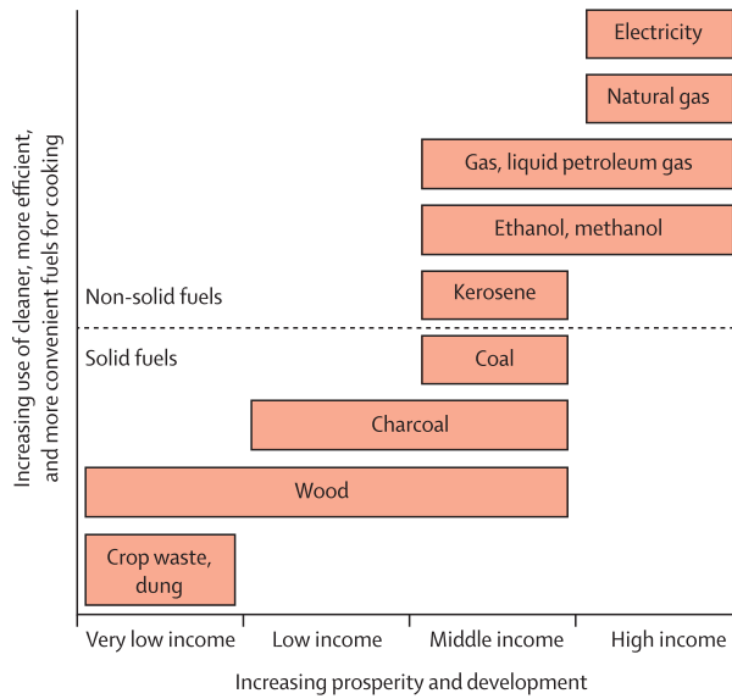


Figure 3: *The energy ladder (World Health Organization 2006b, Gordon et al 2014).*

India’s National Programme on Improved Chulha (NPIC) introduced 32 million improved cookstoves into rural areas between 1984 and 2001, 27% of the programmes aim (Hanbar and Karve 2002, Smith *et al* 1993). The Indian NPIC focused on fuel efficiency, as the benefits of clean combustion were not fully understood, and is cited as failing due to a top-down approach, with little feedback, and poor quality materials (Gifford 2010, Venkataraman *et al* 2010). The NPIC improved cookstoves often had higher air pollutant emissions and similar efficiencies to the traditional stoves they were replacing (Smith 1989).

Two recent cross-sectional studies (defined population at a single point in time) evaluating the health benefits of clean fuels and improved stoves in India found improved respiratory and cardiovascular effects (Lewis *et al* 2017, Sukhsohale *et al* 2013). Randomised control trials (RCT), the gold standard of epidemiological evidence, have been used to study the impacts of solid fuel interventions on reducing air pollutant exposures, mostly the instances of lower respiratory infection (LRI) in young children (Gordon *et al* 2017, Jack *et al* 2015, Chen *et al* 2016, Schilman *et al* 2015, Smith *et al* 2011, Mortimer *et al* 2017, Tielsch *et al* 2016, Hanna *et al* 2016, Alexander *et al* 2017, Aung *et al* 2018). Hanna *et al* (2016) found no effect of improved cookstove use in India on any health indicators measured, due to irregular and inappropriate stove use, failed maintenance, and declined usage over time. Aung *et al* (2018) found improved cookstoves lowered systolic and diastolic blood pressure among exclusive users of the improved cookstove in India, while the confidence intervals included zero. Cookstove stacking (using multiple fuels or stoves at once) worsened systolic and diastolic blood pressure (Aung *et al* 2018). Stove stacking can lead to higher emissions than before the intervention, worsening the health

burden (Pillarisetti *et al* 2014, Masera *et al* 2000, 2007, Ruiz-Mercado *et al* 2011, Pine *et al* 2011, Gordon *et al* 2014).

However, if correctly implemented solid fuel interventions can have large health, climate, and economic co-benefits (Smith *et al* 2014b, Wilkinson *et al* 2009, Smith and Haigler 2008). Wilkinson *et al* (2009) found 150 million advanced cookstoves in India could avoid 2 million premature mortalities, 55 million disability-adjusted life years (DALYs), and emissions of 0.5–1.0 billion tons carbon dioxide (CO₂) equivalent over ten years. Venkataraman *et al* (2010) found clean household fuel in India could avoid 570,000 premature mortalities each year, one-third of national BC emissions, and 4% of all national greenhouse gas emissions.

Figure 4 shows the recent trends in solid fuel use in India (Energy Sector Management Assistance Program and Global Alliance for Clean Cookstoves 2015, International Energy Agency 2016a, Global Alliance for Clean Cookstoves and Dalberg Global Development Advisors 2013, Jain *et al* 2015, Government of India 2011). Two-thirds of Indian households primarily use solid fuels, 26% of urban households compared to 87% of rural households. The rate of solid fuel use has remained high in rural areas since 1990. There has been a substantial conversion from solid fuel use to liquefied petroleum gas (LPG) in urban areas between 1994 and 2010, where LPG use has increased from 30% to 65% (Energy Sector Management Assistance Program and Global Alliance for Clean Cookstoves 2015, International Energy Agency 2016a, Global Alliance for Clean Cookstoves and Dalberg Global Development Advisors 2013, Jain *et al* 2015, Government of India 2011). LPG growth in India is currently 6% per year, and piped natural gas (PNG) (gaseous mixtures of hydrocarbons rich in methane) is growing at 11% annually (Smith 2017b). LPG growth in India has been ongoing for decades, though only enough to cover the growth of the middle class (Smith 2017a). Of India's 700 million solid fuel users, approximately 90% use traditional stoves. Solid fuel use is concentrated in the Indo-Gangetic Plain (IGP), and ten states account for 75% of all solid fuel use in India (Energy Sector Management Assistance Program and Global Alliance for Clean Cookstoves 2015, International Energy Agency 2016a, Global Alliance for Clean Cookstoves and Dalberg Global Development Advisors 2013, Jain *et al* 2015, Government of India 2011). Primary fuel use data does not account for fuel stacking. Other fuels represent electricity and biogas. Two-thirds of the Indian population has electricity access, 55% in rural areas, and 93% in urban areas (Global Alliance for Clean Cookstoves and Dalberg Global Development Advisors 2013). In summary, two-thirds of Indian households primarily use solid fuels, mostly wood in traditional stoves in rural areas within the IGP.

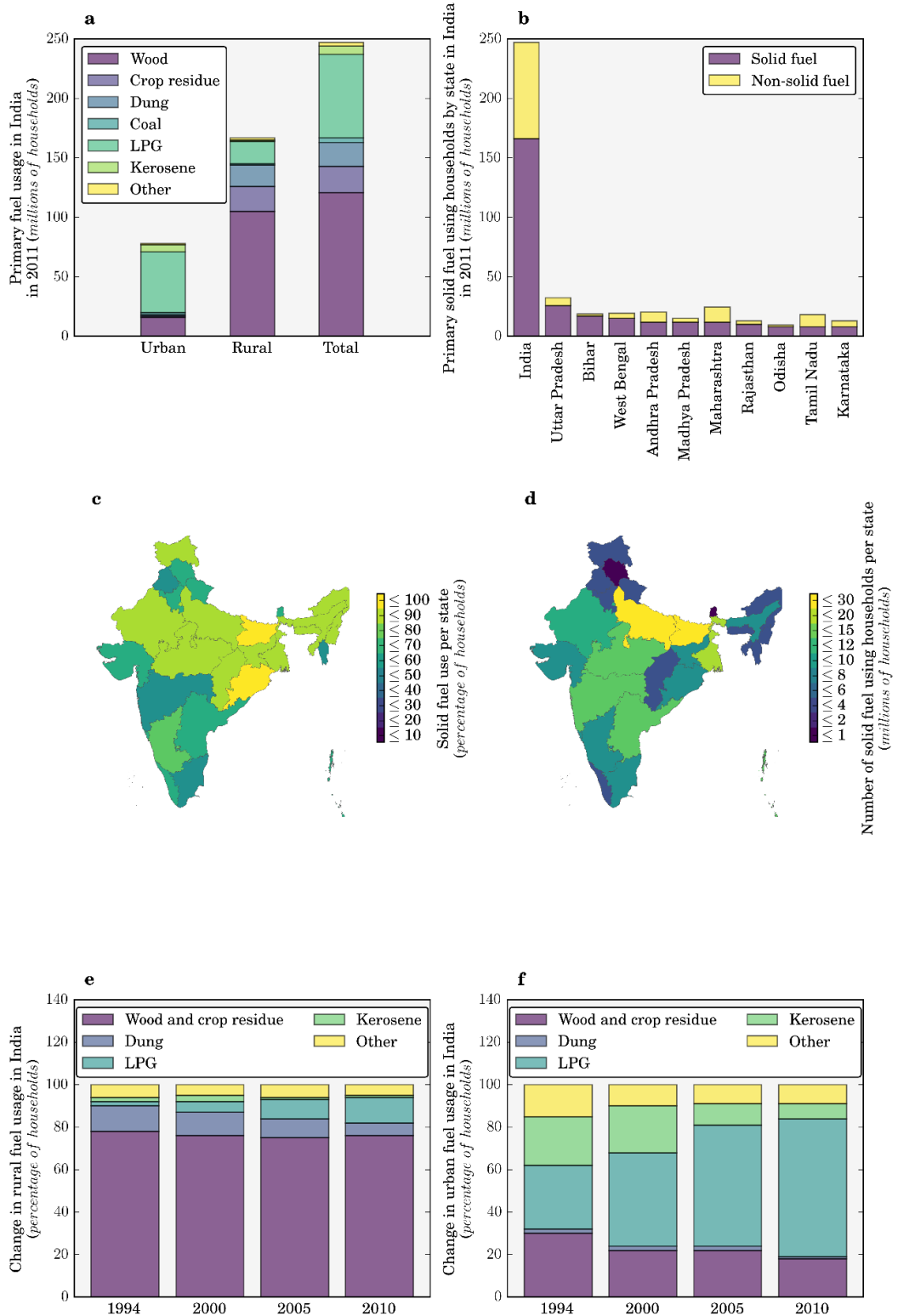


Figure 4: Solid fuel use in India. (a) Primary fuel use in India in 2011 in urban areas, rural areas, and overall. (b) Solid fuel use overall and in the top ten contributing states. (c) Solid fuel use per state as a percentage. (d) Number of households primarily using solid fuels. Change in primary fuel use between 1994 and 2010 in (e) rural areas and (f) urban areas (Energy Sector Management Assistance Program and Global Alliance for Clean Cookstoves 2015, International Energy Agency 2016a, Global Alliance for Clean Cookstoves and Dalberg Global Development Advisors 2013, Jain et al 2015, Government of India 2011).

The combustion of solid fuels is incomplete, leading to substantial emissions of air pollutants (Chafe *et al* 2014a, Lelieveld *et al* 2015, Silva *et al* 2016a, Butt *et al* 2016, Gordon *et al* 2014, Naeher *et al* 2007, Smith *et al* 2000b). The incomplete combustion is due to low combustion efficiencies, low-temperature combustion, and that the combustion gases are not within the combustion chamber long enough for complete combustion to occur (Jetter and Kariher 2009, Jetter *et al* 2012a, Grieshop *et al* 2011, Huang *et al* 2015, Reddy and Venkataraman 2002, Fuzzi *et al* 2015, Fleming *et al* 2018a). These air pollutants impact human health (Edwards *et al* 2014, Smith 2013, Gordon *et al* 2014), climate (Unger *et al* 2010, Butt *et al* 2016, Aunan *et al* 2009, Huang *et al* 2018), environment (Bailis *et al* 2015, Sovacool 2012, Mwampamba 2007), and human well-being (World Health Organization 2016b, Pachauri *et al* 2013, Rosenthal *et al* 2018). Solid fuels mark a fundamental divide on the energy ladder, representing a large difference in emissions of incomplete combustion pollutants (Smith *et al* 2000a, Jetter *et al* 2012a).

Many people use improved cookstoves as opposed, or in addition, to traditional cookstoves. Globally, one-third of solid fuel users have improved cookstoves, with higher use in China (~85%) and lower use in India (~10%) (Energy Sector Management Assistance Program and Global Alliance for Clean Cookstoves 2015). Improved cookstoves encompass a wide variety of physical characteristics and performances, including combustion chamber insulation, chimneys, and fans. Many improved designs were developed before technical standards were in place, leading to high emissions (Hutton *et al* 2006, Energy Sector Management Assistance Program and Global Alliance for Clean Cookstoves 2015, Roden *et al* 2009, Kar *et al* 2012, Jetter and Kariher 2009, Smith *et al* 2000b, Winijkul *et al* 2016). Some improved cookstoves have been found to increase BC emissions relative to traditional stoves (Grieshop *et al* 2017), and these BC differences are not currently accounted for within carbon market accounts (Aung *et al* 2016). The increase in BC could potentially worsen health impacts if BC is found to be more toxic than total PM mass, as suggested by Smith *et al* (2009a) and Baumgartner *et al* (2014), coupled to worsening climate impacts through BC absorbing solar radiation. Chimneys and fans temporarily reduce household exposures by moving air pollutants outside (Sambandam *et al* 2015, Martin *et al* 2013, Venkataraman *et al* 2010). The majority (95%) of improved cookstoves in India are improved chimney Chulha stoves (Energy Sector Management Assistance Program and Global Alliance for Clean Cookstoves 2015). Field studies of improved cookstoves vary considerably to laboratory studies (Edwards *et al* 2014, Smith *et al* 2007, Roden *et al* 2009, Sambandam *et al* 2015, Grieshop *et al* 2017, Kar *et al* 2012, Patange *et al* 2015, Muralidharan *et al* 2015). The variability is due to non-ideal user behaviour, variations in fuel composition, type, size, moisture, and combinations, cooking patterns, situational and measurement variabilities, seasonal patterns, and stove deterioration (Edwards *et al* 2014, Venkataraman *et al* 2010, L'Orange *et al* 2015). It is very difficult to burn biomass in small, low-cost cookstoves cleanly enough to meet the required reductions in emissions to improve health (see non-linear health response to pollution in Section 2.3).

Kerosene, a liquid fuel, is often used in India for lighting by rural populations and those in the lowest socioeconomic decile (Klimont *et al* 2017). Kerosene can increase specific pollutant emissions relative to solid fuels (Bates and Bruce 2014). Gas fuels, in particular LPG, are the primary alternative to traditional solid fuels in India, which improve combustion efficiencies and reduce emissions, though are limited by the high upfront connection cost, high recurring fuel cost, and lack of local fuel distribution (Smith 2015, S. Mehta 2003, Smith *et al* 2000b, Edwards *et al* 2014, Ryu *et al* 2006, Smith *et al* 2000a, Smith and Sagar 2014, Jetter *et al* 2012b, Williams *et al* 2015, Jain *et al* 2015). High fuel costs are often overcome by government subsidies (Venkataraman *et al* 2010), though only 7% of fossil fuel subsidies have been historically distributed to the lowest household income quintile groups (Arze del Granado *et al* 2012, Smith and Sagar 2015). Many people use more than one fuel depending on price, season, and availability (Sinton *et al* 2004). Efficient, cheap, and portable electric induction cookstoves are promoted in India (Smith 2014).

1.1.3. Emissions

1.1.3.1. Indian emissions

Many studies have analysed the sectoral contributions to emissions in India (Venkataraman *et al* 2018, Kumar *et al* 2012b, Sahu *et al* 2017, Saikawa *et al* 2017, Vadrevu *et al* 2017, Mittal *et al* 2015). The most comprehensive emission inventory for India, by Venkataraman *et al* (2018), found present-day PM_{2.5}, BC, OC, and NMVOC emissions are primarily from residential solid fuel, industries, and agricultural burning, while SO₂ and NO_x emissions are primarily from industries and power generation using coal and land transport (Figure 5).

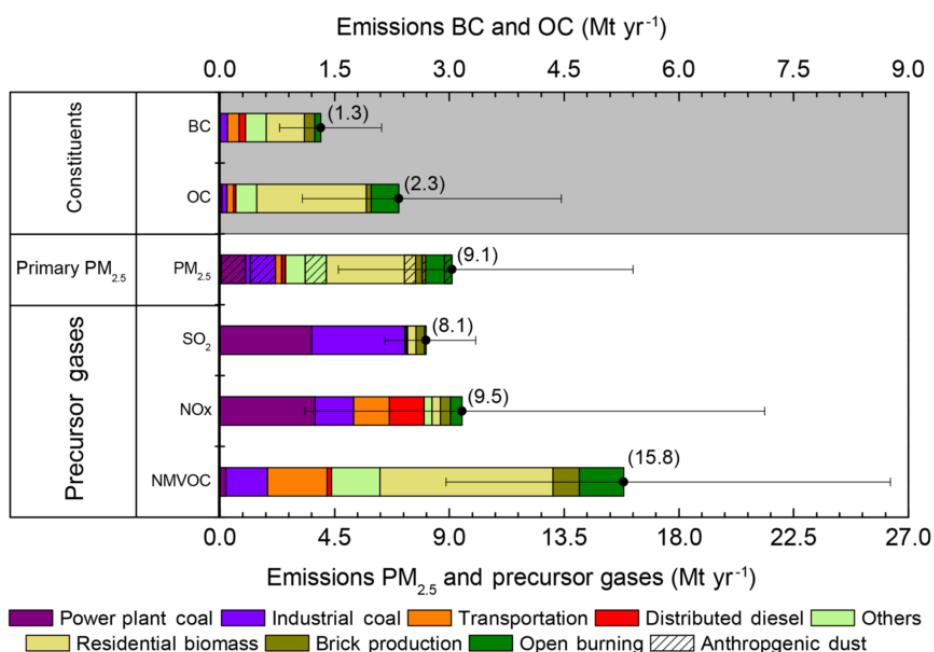


Figure 5: Indian emissions of PM and precursor gases for 2015 by sector (Mt yr⁻¹) (Venkataraman *et al* 2018). Emissions of NO_x are NO.

Residential emissions only account for 10% of global energy use (Chum *et al* 2011) but contribute 25–55% of BC and 72–78% of OC emissions globally (Bond *et al* 2013, Lu *et al* 2011, Huang *et al* 2015). In India, residential emissions account for 45–86% of BC emissions and 68–97% of OC emissions (Bond *et al* 2013, Lu *et al* 2011, Huang *et al* 2015, Paliwal *et al* 2016). All species had increased emissions in India over the last decade (Sahu *et al* 2017, Saikawa *et al* 2017, Sadavarte and Venkataraman 2014, Pandey *et al* 2014). Over the last two decades, anthropogenic emissions of BC and OC in India have been rapidly increasing (Lu *et al* 2011), with emissions factors for BC from residential combustion remaining the same (Masera *et al* 2000, Huang *et al* 2015).

Emissions in India are particularly uncertain (Saikawa *et al* 2017). Residential emissions are generally based on a combination of fuel consumption rates and emissions factors (Butt *et al* 2016, Smith *et al* 2014a), which are uncertain primarily due to emissions factors varying up to three orders of magnitude from fuel type, stove, fuel quality, combustion, and operating conditions (Roden *et al* 2009, Kodros *et al* 2015, Bond *et al* 2004, Jetter *et al* 2012b, Li *et al* 2009, L'Orange *et al* 2012, Junker and Liousse 2008). The fuel type and activity data within residential emission inventories can also vary widely (Tao *et al* 2018). The uncertainty in published estimates for regional scale BC and OC emissions is typically a factor of two to five (Lu *et al* 2011, Kulkarni *et al* 2015, Winijkul *et al* 2016, Li *et al* 2016a). Aerosol optical depth (AOD), BC, and OC are often underestimated by models in regions with high residential emissions, such as India (Bond *et al* 2013, Butt *et al* 2016, Pan *et al* 2015). The uncertainty is potentially due to discrepancies in activity levels, technologies in use, and emission factors (Ramachandran *et al* 2015, Zhong *et al* 2016a). SOA precursor emissions are uncertain in India due to a lack of speciation measurements (Roden *et al* 2006, Martinsson *et al* 2015, Jayarathne *et al* 2018). The emission inventory uncertainty is important considering India is rapidly developing. The large uncertainty in residential emissions, particularly the relative emissions of BC and OC, leads to uncertainty in the net radiative forcing from residential emissions, where the sign of the net forcing is unknown (Butt *et al* 2016, Unger *et al* 2010, Kodros *et al* 2015, Aunan *et al* 2009, Bauer *et al* 2010, Bond *et al* 2013, Jacobson 2010). The uncertainty in sign poses doubt over the extent of climate co-benefits achieved through changes in this sector (Shindell *et al* 2012, Huang *et al* 2015, Fuzzi *et al* 2015, Gao *et al* 2018).

1.1.3.2. Air pollution control policies in India

India has many national and sub-national policies aimed at addressing the health burden from air pollution (Sagar *et al* 2016). Table 1 is a non-exhaustive list of policies in place or being discussed within Indian ministries and agencies relating to air pollution control in India. For the first time, many of these policies are due to be unified within the upcoming National Clean Air Programme (NCAP) (Ministry of Environment Forests and Climate Change 2018). The NCAP provides a framework for air quality management with the aim of attaining Indian air quality

standards throughout the country. The NCAP identifies 100 non-attainment cities that will be required to create their own action plans. The NCAP specifies the need to increase the number of manual and continuous monitoring stations, especially in rural areas, with PM_{2.5} monitoring increasing from 67 to 1,000 stations in 2 years. This thesis will directly compliment the NCAP by providing source-specific estimates of ambient air quality and the exposure-associated health affects at high-resolution in India.

The Ministry of Health and Family Welfare plays a key role with new targets based on the air pollution pathway aimed at providing the most significant exposure reductions, instead of only reducing pollutant concentrations (Ministry of Health and Family Welfare 2015a). The focus on exposures is important as it considers both ambient and household air pollution, and accounts for the large variations in intake fraction (U.S. National Research Council 2012). The Ministry of Finance has committed to provide clean gas for cooking to 50 million households by 2019 (Ministry of Finance 2016). The Ministry of New and Renewable Energy launched the National Biomass Cookstove Initiative (NBCI) in 2009 to promote improved cookstoves utilising carbon-finance to scale (Global Alliance for Clean Cookstoves and Dalberg Global Development Advisors 2013). NBCI aims to provide 10.5 million improved cookstoves by 2022, primarily to rural households. A range of 41 improved cookstoves approved by the Ministry of New and Renewable Energy have been distributed since 2013. However, many homes remain using traditional stoves post-intervention resulting in unrealised air pollutant reductions (Aung *et al* 2016, Pope *et al* 2017). In 2009, the Rajiv Gandhi Gramin LPG Vitran Yojana (RGGLVY) was initiated by the Government of India to increase LPG coverage in rural areas. The RGGLVY scheme commissioned 10,000 connections by late 2014 but was discontinued in 2015 (Tripathi *et al* 2015).

Since 2015, the Ministry of Petroleum and Natural Gas alongside three major oil companies have initiated three programmes to promote LPG to the poor (Mittal *et al* 2017), addressing the 700 million solid fuel users caught in the *Chulha trap* (Smith 2017a). The Pratyaksh Hanstantrit Labh (PAHAL) (Ministry of Petroleum and Natural Gas 2018c) scheme directly pays fuel subsidies into people's bank accounts, meaning that all LPG is now sold at international rates, substantially reducing diversion of LPG to the non-household sector (Smith 2017b). The Pradhan Mantri Ujjwala Yojana (Ujjwala) (Ministry of Petroleum and Natural Gas 2018a) scheme launched in 2016 aims to provide gas connections to 80 million poor households by March 2020 and has already provided 50 million connections as of August 2018 (Dabadge *et al* 2018, Ministry of Petroleum and Natural Gas 2018b). Connections here specifically mean a formal account with a distributor covering a deposit to then access the subsidised LPG (Goldemberg *et al* 2018). There is uncertainty regarding the continued use of LPG post connection due to higher fuel prices (Kishore 2017). The *Give it Up* scheme was designed to persuade middle-class households to give up their fuel subsidies to redirect them to poor households, reaching over 10 million households

by late 2017 (Government of India 2018). The LPG growth rate in India continues to be 6%, though for the poor populations too, which is twice the previous rate (Smith 2017a). The Indian government aims to provide 10 million PNG connections by 2019, to free up LPG connections for the poor (Smith 2017a). India aims to provide clean cooking to 80% of all households by 2019, and 90% by the early 2020's (Goldemberg *et al* 2018). To emphasise, *clean* here refers to exposure-associated health impacts, however, replacing solid fuels with LPG results in minor CO₂ emissions (Haines *et al* 2017, Smith 2014). The Ministry of Power launched the Deen Dayal Upadhyaya Gram Jyoti Yojana (DDUGJY) in 2015 to provide electricity to rural households.

India is involved in many global policies and commitments to reduce the disease burden from air pollution. The main aims of India's Intended Nationally Defined Contribution (INDC) under the United Nations Framework Convention on Climate Change is to achieve a 40% share of electricity generation from renewable sources by 2030, with 175 GW of renewable energy by 2022, and to reduce PM emission intensity by 33–35% by 2030 (Government of India 2015). India's INDCs include stricter emission standards for desulphurisation (Ministry of Environment Forests and Climate Change 2015b), de-NO_x technologies in power generation (Ministry of Environment Forests and Climate Change 2015b), growth in public transport (National Transport Development Policy Committee 2014, National Institution for Transforming India 2015), tighter vehicle emission standards (Ministry of Road Transport and Highways 2016b, Government of India 2014), and improved energy efficiency in industry (Ministry of Environment Forests and Climate Change 2015b) and power generation (Ministry of Power 2015).

Key global policies including India are the air pollution-related sustainable development goals (SDGs) (World Health Organization 2016c), including aiming to eradicate extreme poverty for all people everywhere (target 1.1), to end preventable deaths of children under 5 years of age (targets 1.4 and 3.2), to reduce hunger and increase agricultural productivity (target 2.3), to reduce premature mortality from non-communicable diseases (NCDs) by one third through prevention (target 3.4), to reduce the disease burden from air pollution (target 3.9), to provide universal access to clean household energy (target 7.1), to clean industrial and technological processes (target 9.4), to provide safe, affordable, accessible, and sustainable transport (target 11.2), to improve urban air quality (target 11.6), to provide benefits from reduced climate forcing (goal 13), and reducing deforestation by eliminating domestic solid fuel use (target 15.2) (United Nations 2015, Haines *et al* 2017). India is part of the WHO South-East Asia Region who has the target of a 50% reduction in the proportion of households primarily using solid fuels by 2025 (World Health Organization South East Asia Region 2013).

Table 1: Recent air pollution related policies in place or discussed within Indian ministries and agencies (Sagar et al 2016, Ministry of Finance 2016, Global Alliance for Clean Cookstoves and Dalberg Global Development Advisors 2013, Ministry of Petroleum and Natural Gas 2018c, Smith 2017b, Ministry of Petroleum and Natural Gas 2018a, Ministry of Environment and Forests 2009, 2018, Forest Survey of India 2017, Nain Gill 2010, Ministry of Environment Forests and Climate Change 2015a, Ministry of Road Transport and Highways 2016a, Government of India 2015, Ministry of Environment Forests and Climate Change 2015b, National Transport Development Policy Committee 2014, National Institution for Transforming India 2015, Ministry of Road Transport and Highways 2016b, Government of India 2014, Ministry of Power 2015, Ministry of New and Renewable Energy 2010, National Institution for Transforming India 2017, Ministry of Environment Forests and Climate Change 2018).

Ministry	Air pollution related policy
Ministry of Agriculture	Policies to promote the varied use of crop residue to prevent burning.
Ministry of Earth Sciences	System of Air Quality and Weather Forecasting And Research (SAFAR) to inform, forecast, and increase awareness. National Air Quality Index (NAQI) qualitative scale of six pollutants.
Ministry of Environment, Forest and Climate Change	National Clean Air Programme (NCAP). Increase share of electricity generation from renewable sources. Stricter emission standards for desulphurisation. De-NO _x technologies in power generation. Improved industrial energy efficiency. Reduce PM emission intensity. Measure multiple air pollutants and meteorology through the CPCB. Enforce Indian National Ambient Air Quality Standards (NAAQS). The New Environment Protection Amendment Rules. Continuous emission monitoring systems. Implementation of environment impact assessments on industry. Enforce the banning of agricultural and trash burning through the National Green Tribunal Act. Emission standards for the brick manufacturing industry.
Ministry of Finance	Estimate the cost of health impact from air pollution exposure. Provide clean gas for cooking to 50 million households by 2019.
Ministry of Health and Family Welfare	New targets aimed at the most significant exposure reductions. Tackle total pollution, considering both ambient and household.

Ministry of Heavy Industries and Public Enterprises	Faster adoption and manufacturing of hybrid and electric vehicles.
Ministry of Human Resource Development	Ensure regular check-ups for non-communicable diseases of children. Include the health impacts of air pollution in the school curriculum.
Ministry of Labour and Employment	Ensure regular check-ups for non-communicable diseases of workers. Strengthen hospital capacity to cater for non-communicable diseases.
Ministry of Micro, Small and Medium Enterprises	Zero Effect, Zero Defect campaign to increase efficiency, pollution control, and use of renewable energy.
Ministry of New and Renewable Energy	Launched the NBCI in 2009 to provide 10.5 million improved cookstoves by 2022, primarily to rural households. Increase in solar and electric lighting. Support Integrated Rural Energy Programme on household pollution. Develop a national policy for clean biofuels.
Ministry of Petroleum and Natural Gas	PAHAL scheme directly pays subsidies into people's banks. Ujjwala to provide gas connections. The <i>Give it Up</i> scheme to persuade middle-class households to give up their fuel subsidies to redirect them to poor households. Provide 10 million PNG connections by 2019.
Ministry of Power	National Mission for Enhanced Energy Efficiency. DDUGJY to provide electricity to rural households Improved energy efficiency through Perform, Achieve, and Trade. The Fly Ash Utilisation Policy. Promote improved cookstoves.
Ministry of Road Transport and Highways	Growth in public and electric transport. Tighter vehicle emission standards. Bharat VI standards reducing emissions from buses and trucks.
Ministry of Rural Development	Promote clean air guidelines.
Ministry of Steel	Reduce anthropogenic dust emissions.
Ministry of Urban Development	Disincentives for diesel generators. Enforcement of the ban on trash burning.
Ministry of Women and Child Development	Promote awareness of air pollution from solid fuel use.

1.1.4. Concentrations

1.1.4.1. Present day air pollutant concentrations in India

An increasing share of the global population is exposed to poor air quality, being driven up by increasing ambient PM_{2.5} concentrations rather than changes in population (van Donkelaar *et al* 2015, Brauer *et al* 2016, Shaddick *et al* 2018b, Cohen *et al* 2017, GBD 2016 Risk Factors Collaborators 2017). The Indian population is exposed to very high ambient PM_{2.5} concentrations with annual-mean concentrations of up to 150 µg m⁻³ in the Indo-Gangetic Plain (IGP) (Ministry of Environment and Forests 2018, Conibear *et al* 2018a) and episodic winter concentrations regularly reaching 800 µg m⁻³ (Ministry of Environment and Forests 2018). These concentrations are 15 and 32 times larger than the WHO Air Quality Guideline (AQG), respectively (World Health Organization 2006a). Fourteen of the top fifteen most polluted cities in the world regarding ambient PM_{2.5} concentrations are in India (World Health Organization 2018a). Indian cities entering the most polluted cities list is primarily a consequence of the introduction of air quality monitoring. O₃ concentrations in India often exceed the WHO daily maximum 8-hour mean O₃ concentration of 50 parts per billion (ppb).

Global ambient PM_{2.5} and O₃ concentrations from the GBD are in Figures 6 and 7, respectively. Population-weighted annual ambient PM_{2.5} concentrations in India have increased by 27% from 60 µg m⁻³ in 1990 to 76 µg m⁻³ in 2016 (Figure 6) (Health Effects Institute 2018). Ambient PM_{2.5} concentrations in northern India are amongst the highest in the world (Figure 6a). Daily-mean household PM_{2.5} concentrations in India can exceed 1,500 µg m⁻³, with maximums reaching 5,000 µg m⁻³ (Balakrishnan *et al* 2013, Matawle *et al* 2017, Balakrishnan *et al* 2014b, World Health Organization 2014b, Smith 2013). Population-weighted seasonal ambient O₃ concentrations in India have increased by 27% from 62 ppb in 1990 to 77 ppb in 2016 (Health Effects Institute 2018). The large ambient O₃ concentrations in India are similar to those found in many other countries in the world (Figure 7). For reference, 1 ppb of O₃ is approximately equal to 2 µg m⁻³ (Fleming *et al* 2018b).

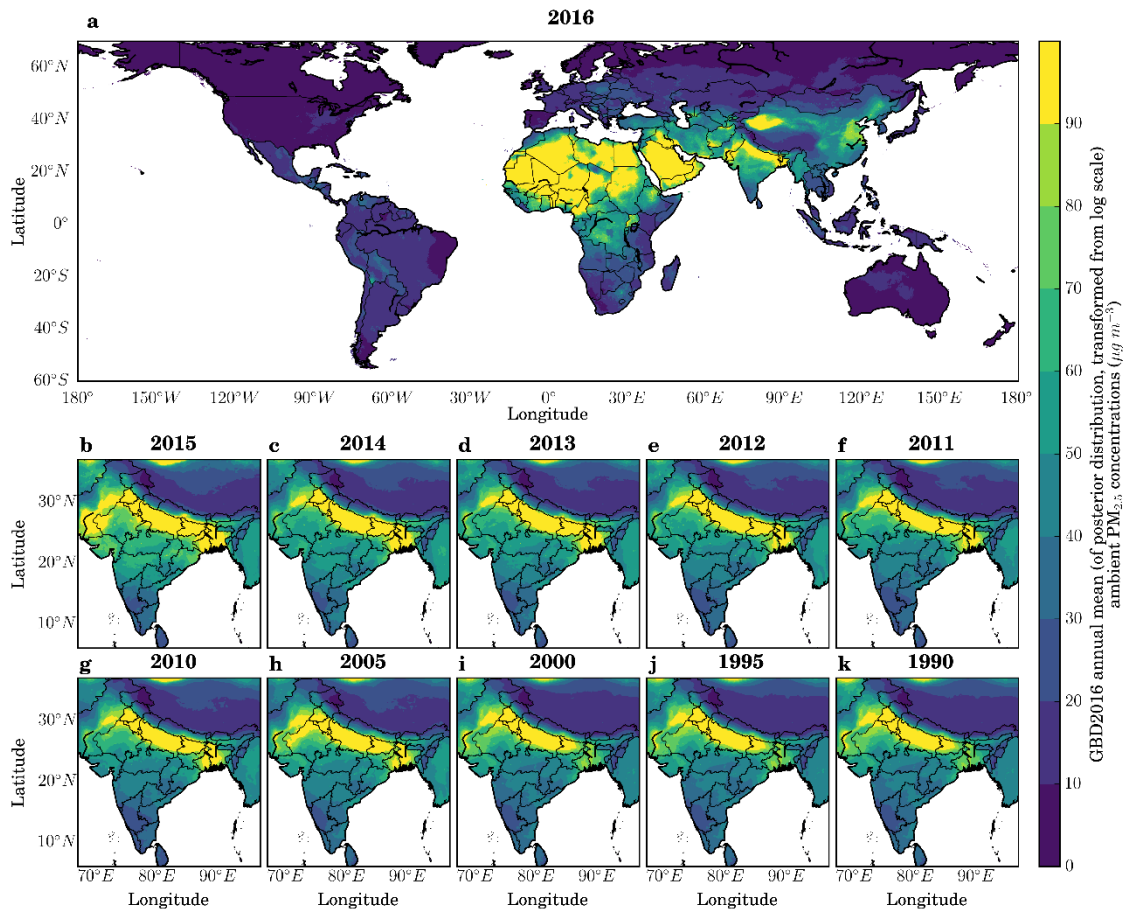


Figure 6: Annual-mean ambient $PM_{2.5}$ concentrations from the Global Burden of Diseases, Injuries, and Risk Factors Study (GBD) 2016 using the data integration model for air quality (DIMAQ) (Shaddick *et al* 2018b, Cohen *et al* 2017, GBD 2016 Risk Factors Collaborators 2017). (a) 2016. (b) 2015. (c) 2014. (d) 2013. (e) 2012. (f) 2011. (g) 2010. (h) 2005. (i) 2000. (j) 1995. (k) 1990.

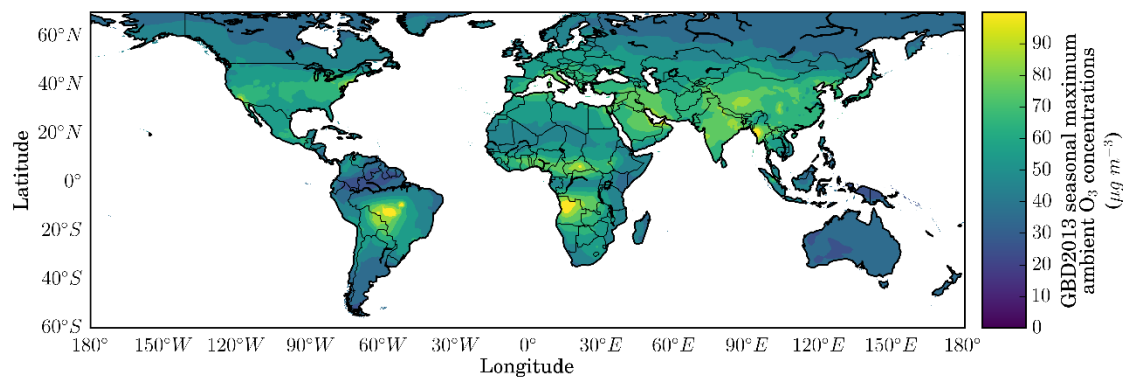


Figure 7: Seasonal ambient O_3 concentrations from the GBD2013 (GBD 2013 Risk Factors Collaborators 2015, Brauer *et al* 2016). Calculated as the maximum running 3-month average of daily 1-hour maximum values.

$PM_{2.5}$ concentrations within India are highest in the IGP (Henriksson *et al* 2011, David *et al* 2018). The IGP, also known as the northern India river plain, is a huge fertile plain encompassing

eastern Pakistan, north and east India, and Bangladesh, via the Indus, Ganges, and Brahmaputra rivers, with the Himalayas to the north. The IGP is home to half of the Indian population, over 700 million people (Tiwari *et al* 2016), mostly combusting solid fuels for their energy needs (Paliwal *et al* 2016). Aerosol loadings in the IGP can be 5–8 times higher than outside the region, with aerosol optical depth (AOD) regularly over 1, and PM_{2.5} concentrations over 140 $\mu\text{g m}^{-3}$ (Nair *et al* 2007, Chowdhury and Dey 2016, Brauer *et al* 2012, Anenberg *et al* 2010, van Donkelaar *et al* 2016, Henriksson *et al* 2011, Kumar *et al* 2014b, Apte *et al* 2015a, Dey and Di Girolamo 2010, Ramachandran and Cherian 2008, Jethva *et al* 2007, Tiwari *et al* 2016). There is an increasing trend in AOD across India, consistent with the trend in PM_{2.5} (Moorthy *et al* 2013a, Moorthy 2016, Satheesh *et al* 2002, 2008).

Natural as well as anthropogenic sources impact aerosol concentrations in India. The major natural aerosol over India is dust from the arid and semi-arid regions of southwest Asia and the Thar Desert in northwest India (David *et al* 2018, Dey *et al* 2004a, Pan *et al* 2015, Govardhan *et al* 2015, Sharma and Dikshit 2016), particularly in the summer (JJA) due to higher wind speeds (Satheesh *et al* 2002, Kaufman *et al* 2002, Satheesh *et al* 2008, Moorthy 2016, Henriksson *et al* 2011, Adhikary *et al* 2007, Ramanathan *et al* 2001, Moorthy *et al* 2013a, Leon *et al* 2001, Cherian *et al* 2013, Chin *et al* 2009, Streets *et al* 2009, Kumar *et al* 2014b, Kharol *et al* 2011, Prasad and Singh 2007b). Pre-monsoon (MAM) dust storms in north India can increase AOD by more than 50%, contributing up to 500 $\mu\text{g m}^{-3}$ to surface PM_{2.5} concentrations (Prasad and Singh 2007a, Dey *et al* 2004b, Kumar *et al* 2014a). Natural aerosols are mostly in areas with low population densities and are coarser in size relative to anthropogenic aerosols, reducing their health impacts (Henriksson *et al* 2011). Anthropogenic aerosol concentrations are maximum in the winter (DJF), due to increased emissions from residential solid fuel use and coal-fired power plants (International Energy Agency 2016a, Choudhry *et al* 2012, Singh *et al* 2004, Karagulian *et al* 2015), less efficient wet removal, and lower boundary layer heights (Moorthy *et al* 2013a, Satheesh *et al* 2002, 2008, Moorthy 2016, Henriksson *et al* 2011, Adhikary *et al* 2007, Ramanathan *et al* 2001, Kaufman *et al* 2002, Leon *et al* 2001).

Agricultural fires are important aerosol source in the spring (MAM) and post-monsoon (ON), especially in the northwest IGP (Sharma and Dikshit 2016, Reddy and Venkataraman 2002, Jena *et al* 2015b, Zhong *et al* 2016b, Vadrevu *et al* 2013, 2011, Badarinath *et al* 2009, Sharma *et al* 2010, Pan *et al* 2015, Rajput *et al* 2014, Jethva *et al* 2018, Mittal *et al* 2009, Mishra and Shibata 2012, Kaskaoutis *et al* 2014, Liu *et al* 2018, Cusworth *et al* 2018). The post-monsoon agricultural burning, although officially banned through the National Green Tribunal Act of 2010 (Nain Gill 2010), generally occurs for a three-week period in late October to early November. This period coincides with weak winds, low boundary layer heights, and stagnation (Mishra and Shibata 2012, Singh and Kaskaoutis 2014), often resulting in serious air pollution episodes. The annual festival of Diwali coincides with the post-monsoon agricultural burning and is known to increase ambient

PM_{2.5} concentrations substantially (Nasir and Brahmaiah 2015, Pal *et al* 2014, Kumar *et al* 2016, Chauhan and Singh 2017).

There has been limited quantifications of secondary PM_{2.5} in India (Pant and Harrison 2012, Pant *et al* 2016). Some studies have focused on specific aerosol components in specific Indian cities, finding 20–68% of PM_{2.5} is attributed to secondary OC (Ram and Sarin 2010, Pant *et al* 2015, Villalobos *et al* 2015, Ram and Sarin 2011). Inorganic aerosols contribute heavily to PM_{2.5} throughout most of India, such as SO₄ in the western IGP and northern India, especially during winter (Venkataraman *et al* 2018, Sadavarte *et al* 2016, David *et al* 2018, Kumar and Sunder Raman 2016, Rastogi *et al* 2016, Ram and Sarin 2011). SOA concentrations are high in the IGP and eastern India, especially during the daytime (David *et al* 2018, Ram and Sarin 2011, Rastogi *et al* 2016). SOA concentrations from biomass burning sources are large in eastern India in the spring and the northwest IGP in autumn (David *et al* 2018). BC and OC concentrations are high over the IGP and northern India, especially in winter and at night (Ram and Sarin 2011, Venkataraman *et al* 2018, Sadavarte *et al* 2016). OC concentrations are often much larger than BC concentrations. NH₄ and NO₃ concentrations are large across the northwest IGP in autumn, and NO₃ concentrations are large in the summer across much of India. Large dust concentrations are found in west and northern India (David *et al* 2018).

1.1.4.2. Meteorological and geographical impacts on Indian air pollution

The complex geography, meteorology, and topography of India influence air quality through changing ventilation, dilution, washout, photochemical reaction rates, dust emissions, biogenic emissions, deposition, atmospheric circulation, stagnation frequency, among other influences (Jacob and Winner 2009, Fiore *et al* 2012, Moorthy 2016, Kumar *et al* 2015a, Guttikunda and Gurjar 2012, West *et al* 2009b, Lawrence and Lelieveld 2010, Kaufman *et al* 2002, Pang *et al* 2009, Zhang *et al* 2015, Han *et al* 2015). Seasons are categorised by winter (DJF), spring (MAM), summer (JJA), and autumn (SON). The summer monsoon season is characterised by the northward migration of the intertropical convergence zone (ITCZ) across the Indian Ocean, where onshore winds provide moisture from the ocean over land, leading to 70–80% of the annual precipitation (Dixit and Tandon 2016, Bollasina *et al* 2011). The winter monsoon season is characterised by offshore winds bringing dry conditions and transporting aerosols from land to ocean (Lawrence and Lelieveld 2010). The climate classifications of India are equatorial in the south, changing to arid, warm temperate, snow, and polar further north (Kottek *et al* 2006). Temperatures are largely high, apart from in the far north (Kottek *et al* 2006).

In summer, large-scale precipitation (washout), strong winds (entrainment), and large boundary layer heights (dilution) lead to aerosol concentration minima (Kumar *et al* 2015c, Tiwari *et al* 2016). In winter, there is little rain, weak winds, low boundary layers, and temperature inversions trapping pollution, leading to aerosol concentration maxima (Joshi *et al* 2016, Singh *et al* 2004, Moorthy *et al* 2005, Subramanian 2016, Yu *et al* 2011). There are stronger seasonal

variations in aerosol concentrations over India than interannual variations (Moorthy *et al* 2001, Joshi *et al* 2016, Henriksson *et al* 2011, Verma 2015, Lodhi *et al* 2013, Ramachandran and Cherian 2008, Kedia *et al* 2014). Air pollution in the IGP is often trapped by shallow atmospheric boundary layers and the topography of the Himalayas and is rarely influenced by marine inflow or the relatively cleaner air in the south (Kar *et al* 2010, David *et al* 2018). The prevailing northwesterly winds transport air pollution from the northwest IGP to the eastern IGP (David *et al* 2018). High O₃ concentrations are often found during summer high-pressure systems when reduced wind speed and cloud cover develop stable conditions and reduce the mixing of O₃ precursors (U.S. Environmental Protection Agency 2013b).

Land use change influences air quality (Vadrevu *et al* 2017, Heald and Spracklen 2015). Substantial areas of India are cropland, with some forest, shrubland, and barren land. The area of harvested agriculture has recently stagnated, while there has been continual large growth in nitrogen fertiliser use across South Asia (Vadrevu *et al* 2017, Xu *et al* 2018). There has been large (and often unplanned) urban growth in India, for example, the population of Delhi has doubled since 2000 to 22 million people, and is projected to further increase by 50% by 2050 (Subramanian 2016).

India has experienced large reductions in forest cover between 1930 and the mid-1990's, mainly attributed to the expansion of agriculture for the growing population (Sudhakar Reddy *et al* 2016). In the 1990's, government initiatives reduced the rates of forest loss, largely because of afforestation, reforestation, and tree plantations (Food and Agriculture Organization of the United Nations 2012). The forest survey of India from the Ministry of Environment and Forest reports recent net gains in forest cover (Forest Survey of India 2017). The net gains in forest cover do not differentiate between natural forests and plantations (Puyravaud *et al* 2010). Since 2000 in India, natural forests have decreased (Gregersen *et al* 2011, Sudhakar Reddy *et al* 2016, Ravindranath *et al* 2012, Hansen *et al* 2013) and plantations have increased (Food and Agriculture Organization of the United Nations 2012). Deforestation is concentrated in the northeast of India (Sudhakar Reddy *et al* 2016). A strong driver for the reduction in natural forests is solid fuel use (Puyravaud *et al* 2010). When biomass is harvested renewably, there is no contribution to CO₂ concentrations. However, a considerable portion of biomass is not harvested renewably, leading to CO₂ emissions and deforestation (Bailis *et al* 2015). The clearing of biomass through fires causes extensive air pollution in India (Mittal *et al* 2009, Mishra and Shibata 2012, Kaskaoutis *et al* 2014, Liu *et al* 2018, Cusworth *et al* 2018, Jethva *et al* 2018). A reduction in forest cover may lead to a reduction in biogenic VOC emissions.

Aerosol in India has been found to influence clouds, radiation, rainfall amount, rainfall onset, Himalayan glaciers, and atmospheric stability, which can all feedback to aerosol loadings (Kedia *et al* 2016, Fosu *et al* 2017, Lau *et al* 2008, Ramanathan *et al* 2005, Bollasina *et al* 2011, Jacobson 2012, Koch and Del Genio 2010, Lohmann and Feichter 2005, Haywood and Boucher 2000, Fiore

et al 2012, Sarkar *et al* 2006, Intergovernmental Panel on Climate Change 2013, Spracklen *et al* 2005, Ramanathan and Carmichael 2008, Jacob and Winner 2009, Reddington *et al* 2015, Dave *et al* 2017). Kedia *et al* (2018) found aerosols and gas chemistry enhanced rainfall by 20% in the Himalayan region. Gao *et al* (2018) found aerosols in India result in an overall negative direct radiative forcing (-3.18 Wm^{-2}) at the top of the atmosphere. Gao *et al* (2018) found strong negative radiative forcing from the power sector offsets the positive radiative forcing from residential emissions in India. Residential cooking and agricultural burning contribute to Atmospheric Brown Clouds (ABCs) (Gustafsson *et al* 2009), which cover much of Asia and the Indian Ocean. ABCs contribute to climate warming through their effects on clouds, precipitation, and water availability (Ramanathan *et al* 2005). ABCs can substantially alter the South Asian monsoon (Bollasina *et al* 2011) and accelerate the melting of the Himalayan-Tibetan glaciers (Ramanathan and Carmichael 2008, Lau *et al* 2008), which are central to Indian meteorology and air pollution removal (Fiore *et al* 2012, Jacob and Winner 2009, Reddington *et al* 2015).

Regional transport of aerosols into and out of India is important. Transport of pollution is highest in northwest India (Venkataraman *et al* 2018), lowest in southern India (Venkataraman *et al* 2018), and there is large aerosol transport from East Asia in the autumn (Sadavarte *et al* 2016). O_3 from East Asian sources affects South Asia in autumn (Chakraborty *et al* 2015).

1.1.5. Exposures

1.1.5.1. Association and causation

Epidemiology is the quantitative study of the distribution, determinants, and control of health, disease, or injury (Glass *et al* 2013). Epidemiology retrospectively observes and detects trends, attributing causes using toxicology to assess biological mechanisms. Epidemiological studies are at the population level, rather than the individual level (Brunekreef *et al* 2007). The *classic approach* of air pollution epidemiology is to question what is the association between pollution and health through a cohort study, and if the association is causal (Zigler and Dominici 2014, Glass *et al* 2013). Causal inferences are derived from observational studies, without the need for RCTs that could be unethical (e.g. smoking), impractical, or too time-consuming for policy-making (Glass *et al* 2013). Various methods are used to judge the causality of health impacts of air pollution exposure. These include the consistency and strength of the observed associations between independent studies in different locations from different researchers. Causality cannot be based solely on a single epidemiologic study. Coherence between epidemiological associations from experimental, cohort (chronic), time-series (acute), controlled human exposure, and toxicological studies are required for causal inference (Ostro and Chestnut 1999, Brunekreef *et al* 2007, Henneman *et al* 2017, U.S. Environmental Protection Agency 2009b). Biologically plausible mechanisms and a well characterised exposure-response (concentration-response) relationship, where health effects increase with exposure and duration, are also needed to infer causality (U.S. Environmental Protection Agency 2009b). The United States Environmental

Protection Agency (EPA) Integrative Science Assessment (U.S. Environmental Protection Agency 2009b, 2013b) is largely based on the classic approach categorising evidence as *not likely*, *inadequate*, *suggestive*, *likely*, and *causal* (Zigler and Dominici 2014, Glass *et al* 2013). The WHO International Agency for Research on Cancer (IARC) is also grounded in the classic approach through its monograph review (Glass *et al* 2013). The classic approach is used to determine the health impacts attributable to air pollution exposure used in this thesis.

Confounding is a key issue for the classic approach, which is commonly mitigated through measurement and statistical adjustment (Glass *et al* 2013, Cole and Hernán 2008). All confounders cannot be known and measured, although no unmeasured confounding is commonly assumed (Cole and Hernán 2008). Confounders can have dynamic feedbacks on the exposure confounding (Glass *et al* 2013). Inferred causality can be later found to be weaker or invalid after additional data, updated methods, and control for further confounders (Dockery *et al* 2013, Henneman *et al* 2017, Moolgavkar 2016, Cox 2017, Cox and Popken 2015, Peel *et al* 2010, Kelly *et al* 2011, van Erp and Cohen 2009). Causation from mechanistic toxicology is different to attributable burden from associational epidemiology.

1.1.5.2. Intake fraction

This thesis, similar to most previous studies, uses pollutant concentrations as surrogates for mean population exposure. The key difference between exposures and concentrations is due to intake fractions (Bennett *et al* 2002). The intake fraction, previously known as exposure effectiveness, is the amount breathed in by the exposed population (Ministry of Health and Family Welfare 2015b, Fantke *et al* 2017). The intake fraction varies by a factor of 100 from power plants to indoor stoves, and the same again to active smoking (Ministry of Health and Family Welfare 2015b, Fantke *et al* 2017, Apte *et al* 2012). Intake fractions are influenced by population, proximity, and persistence. Generally, a small fraction of the total person-hours are spent in areas where ambient levels represent actual exposure (U.S. National Research Council 2012), due to activity level variation, for example, time indoors, in offices, and at school. For ambient air pollution, exposure to household emissions are likely to have a higher intake fraction than many sources of ambient pollution, due to their proximity and duration, and are on similar levels to vehicle emissions (Health Effects Institute International Scientific Oversight Committee 2010). Apte *et al* (2011) studied exposure in Delhi and found on-road commuters are exposed to 1.5 times the concentration of ambient PM_{2.5}. Exposures are also dependent on the escape fraction, which is the extent to which particles are deposited on surfaces before being incorporated into the ambient air (Chafe *et al* 2014b, Lam *et al* 2012). The implication of using concentrations as surrogates for exposures is that local sources are likely to be underestimated and remote sources are likely to be overestimated. This thesis accounts for intake fractions implicitly by accounting for population size, population density, and meteorology.

For household air pollution, exposure levels are mostly lower than household concentrations due to stove location, cooking duration, a division of tasks, the presence of a flue, the ventilation rate, the volume of the home, and the proximity of the home to other households and sources (Balakrishnan *et al* 2014b, Smith *et al* 2014a, Bruce *et al* 2015b, Edwards *et al* 2014, Ruiz-Mercado *et al* 2011). Household air pollutant exposures have been measured in India since 1981 (Smith *et al* 1983). Solid fuel combustion in traditional stoves leads to exposures between that experienced by second-hand smoking and active smoking (Pope III *et al* 2011, Smith and Peel 2010). Traditional cooking with solid fuels is approximately equivalent to 400 cigarettes per hour in terms of PM_{2.5} exposure from second-hand smoke (Smith 1987). Household air pollution is a severe health issue in India (Balakrishnan *et al* 2014a, 2013). Household air pollution is not directly quantified in this thesis, though the contribution from household air pollution (residential emissions) to ambient air pollution is quantified. Ambient and household air pollution interact and exchange (Zhou *et al* 2015, Han *et al* 2015, Gordon *et al* 2014, Rehman *et al* 2011, Balakrishnan *et al* 2011, Chafe *et al* 2014b).

1.1.6. Doses

The dose is the pollutant concentration in body tissues, such as the lung, after repeated exposure. PM dosimetry is the deposition, translocation, clearance, and retention of particles within the respiratory tract (U.S. Environmental Protection Agency 2009b). The dose of PM depends on the concentration, duration, ventilation, and particle characteristics. PM size is a key characteristic controlling deposition, translocation, and clearance of particles after exposure (Figure 8). PM deposition is primarily by diffusion, impaction, and sedimentation. Diffusion is the dominant mechanism for ultrafine PM (0.01–0.1 μm), and sedimentation and impaction dominate coarse PM (2.5–10 μm). Thoracic particles are coarse particles that reach the lung airways past the larynx. Respirable particles are fine particles those that reach the gas-exchange region of the lungs. The IER makes assumptions about the dosing rates between ambient air pollution, household air pollution, second hand smoking, and active smoking. For example, the dose from one cigarette is equivalent to an exposure to 667 $\mu\text{g m}^{-3}$ of ambient PM_{2.5} for 24-hours (Burnett *et al* 2018, 2014).

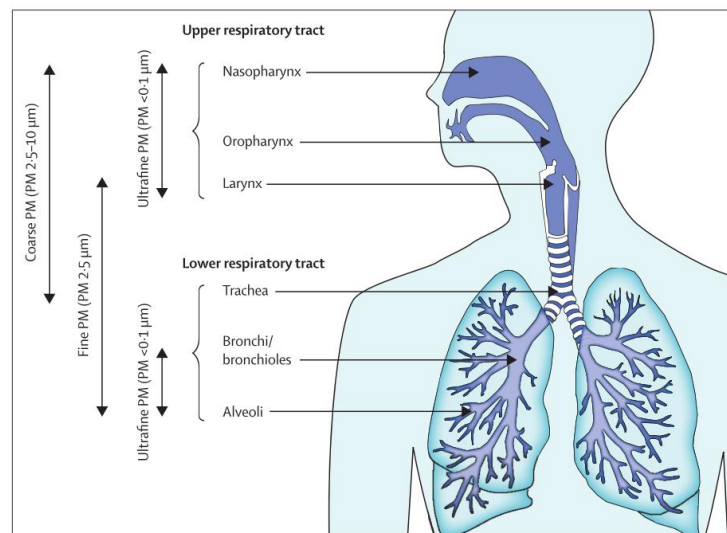


Figure 8: Size-dependent deposition of particulate matter (Guarnieri and Balmes 2014).

O₃ dosimetry within the respiratory tract is affected by concentration, duration, respiratory tract morphology, breathing characteristics, the physicochemical properties of O₃, extracellular lining fluid, and tissue layers (U.S. Environmental Protection Agency 2013b). Approximately 80% of the amount inhaled irreversibly reacts at the airway surface and is deposited (Bromberg 2016).

1.1.7. Health impacts

Exposure to air pollution is a leading risk factor for human health (Cohen *et al* 2017, GBD 2016 Risk Factors Collaborators 2017, Indian Council of Medical Research *et al* 2017b, India State-Level Disease Burden Initiative Collaborators 2017). Figure 9 shows the GBD2016 estimates of global premature mortalities by major risk factor and cause in 2015 (GBD 2016 Risk Factors Collaborators 2017). Total pollution caused 16% of the total global deaths in 2015 (GBD 2016 Risk Factors Collaborators 2017). Air pollution caused 72% of the disease burden from the total of all pollution (GBD 2016 Risk Factors Collaborators 2017). Ambient PM_{2.5} exposure, household air pollution, and ambient O₃ exposure caused approximately 55%, 40%, and 5%, respectively of the disease burden from air pollution (GBD 2016 Risk Factors Collaborators 2017). India contributes approximately 25–30% of the global disease burden from air pollution while having 18% of the population (GBD 2016 Risk Factors Collaborators 2017).

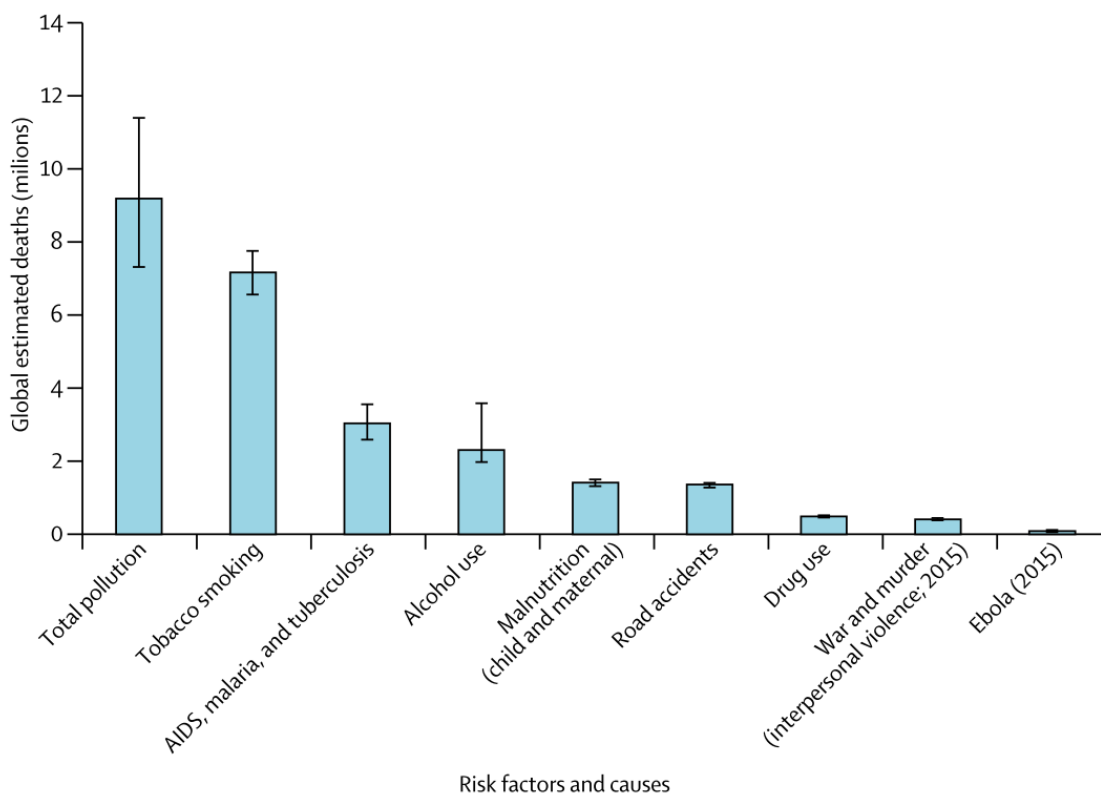


Figure 9: Global premature mortalities by major risk factor and cause in 2015. Plot from Landrigan *et al* (2017) using data from GBD2016 (GBD 2016 Risk Factors Collaborators 2017).

Various other air pollutants are associated with health effects such as CO (U.S. Environmental Protection Agency 2010), lead (U.S. Environmental Protection Agency 2013a), NO_x (U.S. Environmental Protection Agency 2016), sulphur oxides (SO_x) (U.S. Environmental Protection Agency 2017), and polycyclic aromatic hydrocarbons (PAH) (Grosovsky *et al* 1999). This thesis does not explore the health impacts of these other air pollutants.

1.1.7.1. Health impacts of PM_{2.5} exposure

Health effects of ambient PM_{2.5} exposure are non-specific in that the causes have multiple risk factors (Pope III 2007). Health effects depend on concentrations and durations (Pope III 2007). Long-term exposures have larger, more persistent cumulative effects than short-term exposures (Pope III 2007). Observational epidemiological studies for health impacts of PM_{2.5} exposure are primarily based on studies in North America, Europe, and parts of Asia (Apte *et al* 2015a, Pope III *et al* 2009, 2011). Table 2 summarises the health impacts of long- and short-term PM_{2.5} exposure from epidemiological, controlled human exposure, and toxicological studies (U.S. Environmental Protection Agency 2012, 2009b, Brook *et al* 2010, Newby *et al* 2015, Loomis *et al* 2013, Gordon *et al* 2014, Anderson *et al* 2012, Pope III and Dockery 2006, Naeher *et al* 2007, Edwards *et al* 2014, Bruce *et al* 2015b, Smith *et al* 2004, Bruce *et al* 2015a, Krewski *et al* 2009, Cohen *et al* 2017, Pope III 2007, Bell *et al* 2004, Stieb *et al* 2003, World Health Organization 2013, World Health Organization Regional Office for Europe 2013, Bell *et al* 2013, Achilleos *et*

al 2017, Li *et al* 2016b, Atkinson *et al* 2012, Héroux *et al* 2015, Atkinson *et al* 2014, Levy *et al* 2012).

Long-term PM_{2.5} exposure is a cause of all-cause mortality, cardiovascular mortality, and cardiovascular morbidity, a likely cause of respiratory effects, and a suggestive cause of reproductive and developmental outcomes. Short-term PM_{2.5} exposure is a cause of mortality and cardiovascular effects, and a likely cause of respiratory effects. PM is an IARC group 1 carcinogen. The classifications *likely* and *suggestive* causes are due to limited consistency and coherence across studies, and the lack of size-resolved PM exposure cancer studies. Susceptible populations to the health effects of PM exposure are those with underlying cardiovascular and respiratory illnesses, older adults for cardiovascular morbidity, children for respiratory effects, and those with lower socioeconomic status including reduced access to health care, low educational attainment, and residential location (U.S. Environmental Protection Agency 2009b). There is no clear evidence of a low safe threshold or specific lag period from short-term PM_{2.5} exposure for cardiovascular or respiratory effects (U.S. Environmental Protection Agency 2009b).

Table 2: Health impacts of PM_{2.5} exposure (U.S. Environmental Protection Agency 2012, 2009b, Brook et al 2010, Newby et al 2015, Loomis et al 2013, Gordon et al 2014, Anderson et al 2012, Pope III and Dockery 2006, Naeher et al 2007, Edwards et al 2014, Bruce et al 2015b, Smith et al 2004, Bruce et al 2015a, Krewski et al 2009, Cohen et al 2017, Pope III 2007, Bell et al 2004, Stieb et al 2003, World Health Organization 2013, World Health Organization Regional Office for Europe 2013, Bell et al 2013, Achilleos et al 2017, Li et al 2016b, Atkinson et al 2012, Héroux et al 2015, Atkinson et al 2014, Levy et al 2012).

PM_{2.5}			
Duration	Effect	Evidence strength	Mechanism
Long-term, chronic (months to years)	All-cause mortality	Causal	All-cause.
	Cardiovascular morbidity and mortality	Causal	Ischaemic heart disease (IHD), cerebrovascular disease (CEV), atherosclerosis, coagulation, hypertension, and vascular reactivity. Chronic obstructive pulmonary disease (COPD), lower respiratory infection (LRI), impaired lung function, impaired lung growth, increased respiratory symptoms, asthma, altered pulmonary function, mild inflammation, oxidative responses, immune suppression, histopathological changes, and exacerbated allergic responses.
	Respiratory effects	Likely cause	Low birth weight and infant mortality.
	Reproductive and developmental outcomes	Suggestive cause	Lung cancer (LC). Limited evidence for bladder cancer, lung adenoma, enhanced frequencies of chromosome aberrations and micronuclei in lymphocytes, genetic and DNA damage, genetic mutations, altered gene expression, and DNA methylation.
Short-term, acute	Cancer	Causal	
	All-cause mortality	Causal	All-cause.
	Cardiovascular effects	Causal	Hospital admissions from IHD and congestive heart failure, cardiovascular disease, altered

(hours to weeks)	Respiratory effects Likely cause	vasomotor function, altered vessel tone, microvascular reactivity, myocardial ischemia (reduced blood flow), heart rate variability, systemic oxidative stress, altered blood pressure, blood coagulation, and systemic inflammation. Hospital admissions from COPD and respiratory infections, asthma, altered pulmonary function, pulmonary inflammation, oxidative responses, exacerbations of allergic responses, allergic sensitisation, and airway hyper-responsiveness.
-------------------------	-------------------------------------	--

The biological mechanisms of ambient PM_{2.5} exposure are complex, vary with the duration of exposure, and are yet to be fully explained. Further biologically plausible mechanisms have been observed including modulated host defence and immunity, hypoxemia, the sequestration of red blood cells, vascular thrombogenic effects, altered endothelial function, among many others (Seaton *et al* 1999, 1995, U.S. Environmental Protection Agency 2009b, Pope III and Dockery 2006, Health Effects Institute Review Panel on Ultrafine Particles 2013). Multiple mechanisms can overlay the patterns of response and can interact with other risk factors. The health effects of air pollution exposure are considered to be systematic (throughout the whole body) and consistent with accelerated ageing.

New diseases and conditions are continually being associated with exposure to air pollution (Grandjean and Landrigan 2006, Landrigan *et al* 2017). Figure 10 shows the diseases and conditions plausibly affected by air pollution, where the ones in bold type are currently included in GBD categories (Thurston *et al* 2017). The GBD estimates the health impacts PM_{2.5} exposure for four non-communicable diseases (IHD, CEV, COPD, and LC) and one communicable disease (LRI). IHD is associated with a reduction of blood supply to the heart, potentially leading to a heart attack (Global Burden of Disease Collaborative Network 2017, World Health Organization 2018c, Thurston *et al* 2016). CEV is a group of brain dysfunctions related to disease of the blood vessels supplying the brain, including stroke (Global Burden of Disease Collaborative Network 2017, World Health Organization 2018c). COPD is the incompletely reversible obstruction of the airways, defined by three main characteristics; small airways obstruction (thickening cell walls), emphysema (inflammation), and chronic bronchitis (cough and phlegm) (Global Burden of Disease Collaborative Network 2017, World Health Organization 2018c, Postma *et al* 2015). LC is the abnormal change of cells in the lung, categorised as primary or secondary, and non-small cell or small cell (Global Burden of Disease Collaborative Network 2017, World Health Organization 2018c). LRI are a broad group of infections in the airways and lungs, such as pneumonia (Global Burden of Disease Collaborative Network 2017, World Health Organization

2018c). This thesis is consistent with the GBD and estimates health impacts of these five diseases when studying long-term PM_{2.5} exposure.

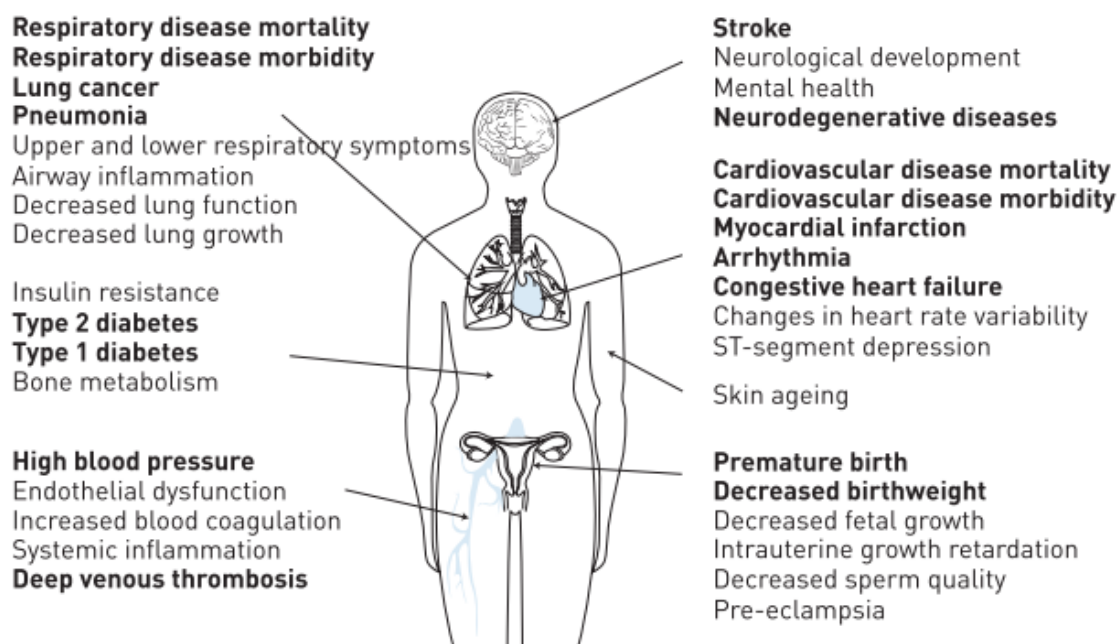


Figure 10: Overview of diseases, conditions, and biomarkers affected by ambient air pollution (Thurston *et al* 2017).

Short-term exposure to coarse PM (2.5–10 µm) has suggestive causality with cardiovascular effects, respiratory effects, and mortality mainly from epidemiological evidence with a limited number of controlled human exposure and toxicological studies (U.S. Environmental Protection Agency 2009b). Short-term exposure to ultrafine PM (0.01–0.1 µm) has suggestive causality for cardiovascular effects from a range of studies and respiratory effects primarily from controlled human exposure studies (U.S. Environmental Protection Agency 2009b). Ultrafine particles can diffuse into the bloodstream and translocate via the circulation. Ultrafine PM are associated with brain inflammation due to translocation to the brain via the olfactory nerve (Health Effects Institute Review Panel on Ultrafine Particles 2013). Research has suggested that the toxicity of PM_{2.5} is more directly related to particle surface area than to mass (Oberdörster *et al* 2005, Maynard and Maynard 2002), suggesting that ultrafine particles would be more damaging to health. However, the current scientific consensus is that the health effects from short-term exposure to ultrafine PM are not dramatically different from those of PM_{2.5} (Health Effects Institute Review Panel on Ultrafine Particles 2013, Atkinson *et al* 2015). There have not been any epidemiologic studies of long-term exposures to ambient ultrafine PM. Ultrafine PM number concentrations are highly variable and are more prone to exposure error than larger particles (Health Effects Institute Review Panel on Ultrafine Particles 2013, Atkinson *et al* 2015). Particle number health studies find positive associations that overlap zero (Atkinson *et al* 2015).

Epidemiological evidence is limited in resolving what specific characteristics, components, and sources of air pollution cause specific health effects (West *et al* 2016). Currently, the scientific consensus treats all fine particles as equally toxic without regard to their source, shape, volatility, and chemical composition (Lelieveld *et al* 2015, World Health Organization 2006a, Burnett *et al* 2014, U.S. Environmental Protection Agency 2009b). Previous studies suggest that carbonaceous aerosol have strong associations with health impacts (Tuomisto *et al* 2008, Atkinson *et al* 2015) and that particles from fossil fuel combustion are more toxic than particles from other sources such as biomass burning (Thurston *et al* 2016). Secondary sulphates, nitrates, and crustal materials have been found to be less toxic than average PM_{2.5} (Tuomisto *et al* 2008, Kelly and Fussell 2012). There is insufficient evidence on the toxicity of metals (Atkinson *et al* 2015). Many previous studies use a single pollutant approach for single diseases, providing limited insight into the toxicity of particle constituents (Levy *et al* 2012, Atkinson *et al* 2015). There are no epidemiological studies that estimate the joint effects of ambient and household air pollution.

1.1.7.2. Health impacts of O₃ exposure

Table 3 summarises the long- and short-term health impacts of O₃ exposure from controlled human exposure, epidemiological, and toxicological studies (World Health Organization 2013, U.S. Environmental Protection Agency 2013b, Jerrett *et al* 2009, Zanobetti and Schwartz 2011, Smith *et al* 2009b, Turner *et al* 2016, Atkinson *et al* 2016). Short-term O₃ exposure is a cause of respiratory effects, a likely cause of cardiovascular effects and all-cause mortality, with suggestive causality for central nervous system effects. Long-term O₃ exposure is a likely cause of respiratory effects, with suggestive causality of cardiovascular, reproductive and developmental effects, central nervous system effects, and all-cause mortality. Previous studies have highlighted the limited and confounded evidence for short-term cardiovascular effects (Goodman *et al* 2014), conflicting evidence for long-term health impacts (Committee on the Medical Effects of Air Pollutants 2015, Atkinson *et al* 2016, U.S. Environmental Protection Agency 2013b), and the limited evidence for use of low concentration thresholds (Committee on the Medical Effects of Air Pollutants 2015). There have been three, recent, major studies of long-term O₃ exposure and human health adding to the original American Cancer Society Cancer Prevention Study II (CPS-II) by Jerrett *et al* (2009); the updated CPS-II study by Turner *et al* (2016), the Harvard Medicare study (Di *et al* 2017), and the Canadian Census Health and Environment Cohort (CanCHEC) study (Crouse *et al* 2015). All studies found O₃ health effects on all-cause mortality, unconfounded by PM_{2.5} or NO₂, with some finding health effects for cardiovascular, diabetes, and respiratory mortality (Jerrett *et al* 2009, Turner *et al* 2016, Di *et al* 2017, Crouse *et al* 2015).

Table 3: Health impacts of O₃ exposure (World Health Organization 2013, U.S. Environmental Protection Agency 2013b, Jerrett et al 2009, Zanobetti and Schwartz 2011, Smith et al 2009b, Turner et al 2016, Atkinson et al 2016).

O₃			
Duration	Effect	Evidence strength	Mechanism
Long-term, chronic (months to years)	Respiratory effects	Likely cause	COPD, respiratory symptoms, new-onset asthma, and respiratory mortality.
	Cardiovascular effects	Suggestive cause	Increased vascular disease.
	Reproductive and developmental effects	Suggestive cause	Decreased sperm concentration, reduced birth weight, and restricted fetal growth.
	Central nervous system effects	Suggestive cause	Alterations in neurotransmitters, motor activity, memory, sleep, and neurodegeneration.
	All-cause mortality	Suggestive cause	All-cause.
Short-term, acute (hours to weeks)	Respiratory effects	Cause	Hospital admissions from respiratory infections, COPD, asthma, respiratory tract inflammation, altered lung function, inflammatory responses, epithelial permeability, airway hyper-responsiveness, and host defence impairment.
	Cardiovascular effects	Likely cause	Autonomic nervous system, oxidative stress, inflammation, decreased cardiac function, altered heart rate, enhanced ischemia injury, and disrupted vascular reactivity.
	All-cause mortality	Likely cause	All-cause.
	Central nervous system effects	Suggestive cause	Alterations in neurotransmitters, motor activity, memory, sleep, and neurodegeneration.

Biologically plausible mechanisms for the adverse health effects of O₃ exposure include pulmonary function decrement, lung permeability, and many others. Susceptible populations to the health effects from O₃ exposure are those with asthma, children, elderly, individuals lacking certain nutrients (e.g. vitamins C and E), outdoor workers, and individuals with gene variations (U.S. Environmental Protection Agency 2013b). The lag of health effects relative to exposure to O₃ is dependent on age and pre-existing conditions and is consistently found to be within the first few days for morbidity and mortality endpoints (U.S. Environmental Protection Agency 2013b). The health effects of O₃ exposure are confounded by temperature (Wilson *et al* 2014, Pattenden *et al* 2010) and other pollutants (Committee on the Medical Effects of Air Pollutants 2015).

1.1.7.3. Risk assessments to estimate the burden of disease

Risk assessments quantify the disease burden of air pollution in terms of mortality and morbidity. This thesis follows the methodology of the comparative risk assessment from the GBD. The first GBD study was in 1993, commissioned by the World Bank (The World Bank 1993). The first comprehensive ambient air pollution study was for 2000 published in 2004 through the WHO and the World Bank (Cohen *et al* 2004, Pandey 2000), which was updated in 2009 by the WHO (World Health Organization 2009). The GBD progressed in 2010 through funding by the Bill & Melinda Gates Foundation and support from the WHO to study a huge scope of risk factors and causes throughout the world. This led to the publications of GBD2010 in 2012 (GBD 2010 Risk Factors Collaborators 2012), GBD2013 in 2015 (GBD 2013 Risk Factors Collaborators 2015), GBD2015 in 2016 (GBD 2015 Risk Factors Collaborators 2016a), and GBD2016 in 2017 (GBD 2016 Risk Factors Collaborators 2017).

There are five key inputs to risk assessments to estimate the burden of disease from air pollution exposure: pollutant concentrations, the counterfactual level, the population exposure, baseline mortality rates, and an exposure-response function (Ostro *et al* 2018). The input methods vary with approach, e.g. improvements to the exposure-response function. The input data vary in time, e.g. the age and size of the population exposed or the pollutant concentration.

Accurate representation of air pollution concentrations is critical. The pollutant concentrations are estimated through chemical transport models (Fang *et al* 2013, Lelieveld *et al* 2013, Silva *et al* 2013, Ghude *et al* 2016, Butt *et al* 2016, Chafe *et al* 2014a, Lelieveld *et al* 2015, Anenberg *et al* 2010), satellite observations (Apte *et al* 2015a, Brauer *et al* 2012, van Donkelaar *et al* 2010, 2016, Evans *et al* 2013), and ground measurements (Cohen *et al* 2004, Nagpure *et al* 2014, Guttikunda and Goel 2013, Chate *et al* 2013). Models allow for air pollutant estimations where ground measurements are limited in space and satellite observations are limited in time. Many ground measurements within the WHO ambient air pollution database, used by the GBD, derived PM_{2.5} from PM₁₀ using conversion factors (World Health Organization 2018a). Recent GBD studies (GBD2015 and GBD2016) have combined all the above sources within a Bayesian hierarchical model, the data integration model for air quality (DIMAQ), along with land use

regression models, population, monitor type, PM_{2.5} to PM₁₀ conversion factors, land use elevation, and the concentrations of SO₄, NO₃, OC, and NH₃ (Shaddick *et al* 2018b). The error in predicted PM_{2.5} concentrations was greatly reduced through the addition of the local population as a covariate (Ostro *et al* 2018).

The counterfactual level, also known as the theoretical minimum risk exposure level or the low-concentration cut-off, is a minimum pollutant concentration where no health effects occur. For long-term PM_{2.5} exposure, the disease-specific counterfactual in the GBD2010 and GBD2013 ranged from 5.8–8.9 µg m⁻³, and in the GBD2015 and GBD2016 ranged from 2.4–5.9 µg m⁻³. For long-term O₃ exposure, the counterfactual varied per study and percentile applied between 26.7–41.9 ppb. The population exposure is the specific group exposed to the pollutant concentration. Baseline mortality rates are the occurrence of the cause already present in that specific group. The exposure-response functions use epidemiological data to relate a specific pollutant concentration to a relative risk of disease. A significant advance in exposure-response function was the development of the integrated-exposure response (IER) functions (Burnett *et al* 2014) as part of the GBD2010 project (GBD 2010 Risk Factors Collaborators 2012) for long-term exposure to ambient PM_{2.5} concentrations. The IER functions combine epidemiological evidence from ambient air pollution, household air pollution, second-hand smoking, and active smoking to estimate the health response to exposures across a widened range of pollutant concentrations. Exposures to PM_{2.5} from air pollution and second-hand smoking are substantially smaller than those from active smoking (Pope III *et al* 2018). The IER functions are a pragmatic approach, including additional epidemiological evidence with each GBD study. The IER functions are detailed in Section 2.3 and used in Chapters 4 and 5. The exposure-response functions for long-term O₃ exposure (detailed in Section 2.4 and used in Chapter 6) use risk estimates per increment in pollutant concentration.

Mortality is measured by the number of premature mortalities, which are considered preventable if the risk were to have been eliminated. The estimates are specifically for *premature* mortality, as death is postponed or brought forward rather than avoided (Brunekreef *et al* 2007). Morbidity is measured by years of life lost (YLL) due to the age-specific premature mortality relative to a healthy life expectancy. Years lost due to disability (YLD) account for the incidence and prevalence of disease, which can be added to YLL per cause to give the total disease burden, known as DALYs (World Health Organization 2018b).

The economic impact of air pollution burden is difficult to assess as evaluation methods vary dramatically in the literature, including metrics of a lost healthy life year, willingness to pay, and ones based on income (World Health Organization 2003). A recent study by The World Bank and the Institute for Health Metrics and Evaluation (IHME) estimated the cost of air pollution following a willingness to pay approach and an income-based approach (The World Bank and Institute for Health Metrics and Evaluation 2016). For the willingness to pay approach, total air

pollution cost 7.4% of gross domestic product (GDP) in South Asia, where ambient PM_{2.5}, household PM_{2.5}, and ambient O₃ cost 3.1%, 4.9%, and 0.4%, respectively (The World Bank and Institute for Health Metrics and Evaluation 2016). For the income-based approach, costs were lower than those from the willingness to pay approach, though were still substantial in India (\$66 billion in 2013 \approx 1% of GDP) largely due to the young population (The World Bank and Institute for Health Metrics and Evaluation 2016).

Estimates of the disease burden attributable to air pollution exposure from 1990 to the present day are updated with each GBD study. The global estimate of premature mortality from long-term ambient PM_{2.5} exposure was 3,223,540 (95th uncertainty interval (95UI): 2,828,854–3,619,148) for 2010 in GBD2010 (GBD 2010 Risk Factors Collaborators 2012), 2,926,000 (95UI: 2,777,000–3,066,000) for 2013 in GBD2013 (GBD 2013 Risk Factors Collaborators 2015), 4,241,000 (95UI: 3,698,000–4,777,000) for 2015 in GBD2015 (GBD 2015 Risk Factors Collaborators 2016a), and 4,092,692 (95UI: 3,624,442–4,575,023) for 2016 in GBD2016 (GBD 2016 Risk Factors Collaborators 2017). The inputs used between GBD2010 and GBD2013 are similar, as are those from GBD2015 and GBD2016 (Ostro *et al* 2018). The increase in estimates for GBD2015 and GBD2016 were driven mostly by the exposure-response function (\sim 55%) and the derived PM_{2.5} concentrations from the DIMAQ (\sim 20%), with contributions from changes in demographics and absolute exposure (Ostro *et al* 2018). The GBD2010 estimated the disease burden from LRI in children only, while all subsequent GBD studies estimated the disease burden from LRI in adults as well (Ostro *et al* 2018). Recent GBD studies (2015 and 2016) increased the historical PM_{2.5} concentrations over India (1990–2016) (Ostro *et al* 2018), suggesting that earlier GBD studies (2010 and 2013) underestimated PM_{2.5} concentration in India. Recent IER functions (2015 and 2016) shifted the disease breakdown, reducing the contributions from heart (IHD) and brain (CEV) disease by ten percentage points each, and increasing the contribution from COPD by 20 percentage points relative to earlier IER functions (2013) (Ostro *et al* 2018).

The GBD estimates the joint effects of ambient PM_{2.5}, household air pollution from solid fuel use, and O₃ exposure through a complex combination of their population attributable fractions under an assumption of independence, rather than summing their impacts (Lopez *et al* 2006, Hill *et al* 2017). This assumption of independence is unlikely for India, where there are large interactions and exchanges between ambient and household air pollution (GBD MAPS Working Group 2018).

1.1.7.4. Disease burden from air pollution exposure at the global scale

The most recent estimates of the global burden of disease attributable to ambient PM_{2.5} exposure are from GBD2016 (Figure 11). In 1990, the global estimate of annual premature mortality attributable to ambient PM_{2.5} exposure was 3,317,916 (95UI: 2,913,074–3,750,917), with dominant contributions of 27% by China (901,262, 95UI: 752,834–1,067,969) and 21% by India (698,245, 95UI: 594,235–807,575) (Cohen *et al* 2017, GBD 2016 Risk Factors

Collaborators 2017). In 2016, the estimates of annual premature mortality from exposure to ambient PM_{2.5} increased globally by 23% to 4,092,692 (95UI: 3,624,442–4,575,023), in China by 19% to 1,075,039 (95UI: 940,395–1,221,813), and in India by 48% to 1,034,420 (95UI: 893,676–1,176,954) (Cohen *et al* 2017, GBD 2016 Risk Factors Collaborators 2017). The large increase in the burden of disease in India between 1990 and 2016 means that China and India both dominate the contribution to the global burden, each contributing one-quarter. The large populations of India and China are important factors to their large disease burdens. For the mortality rate per 100,000 population, which is independent of population size, the Eastern European countries of Bulgaria (126) and Ukraine (118) stand out relative to the rates in India (79) and China (79) in 2016 (Cohen *et al* 2017, GBD 2016 Risk Factors Collaborators 2017). The decrement in life expectancy from ambient PM_{2.5} in South Asia is 1.56 years (Apte *et al* 2018).

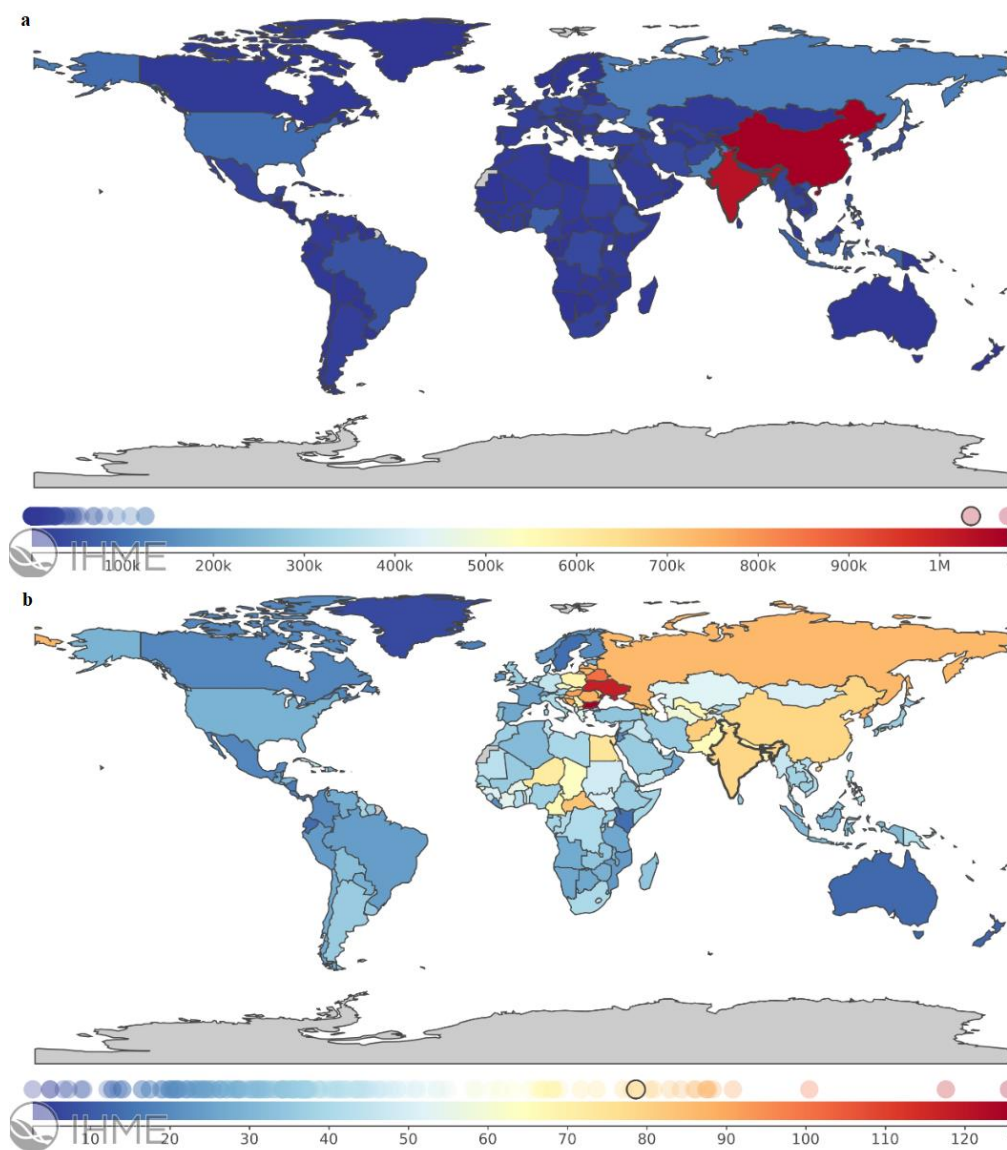


Figure 11: The global burden of disease from ambient PM_{2.5} exposure in 2016. (a) Number of premature mortalities per country. (b) Mortality rate per 100,000 population per country (Institute for Health Metrics and Evaluation 2018).

Figure 12 shows the drivers of the changes in premature mortality attributable to ambient PM_{2.5} exposure by country from 1990 to 2015 (Cohen *et al* 2017). The 23% increase in the global disease burden between 1990 and 2015 was driven by population ageing (+41%) and population growth (+26%), partially offset by improvements in baseline mortality rates (-54%). There are substantial variations in the drivers between countries, where India experienced more substantial impacts of population growth (+50%) and China had strong opposing influences between population ageing (+69%) and improving baseline mortality rates (-79%). The strong roles of the demographic and epidemiological transitions are clear, and often dominate the changes due to variations in exposure.

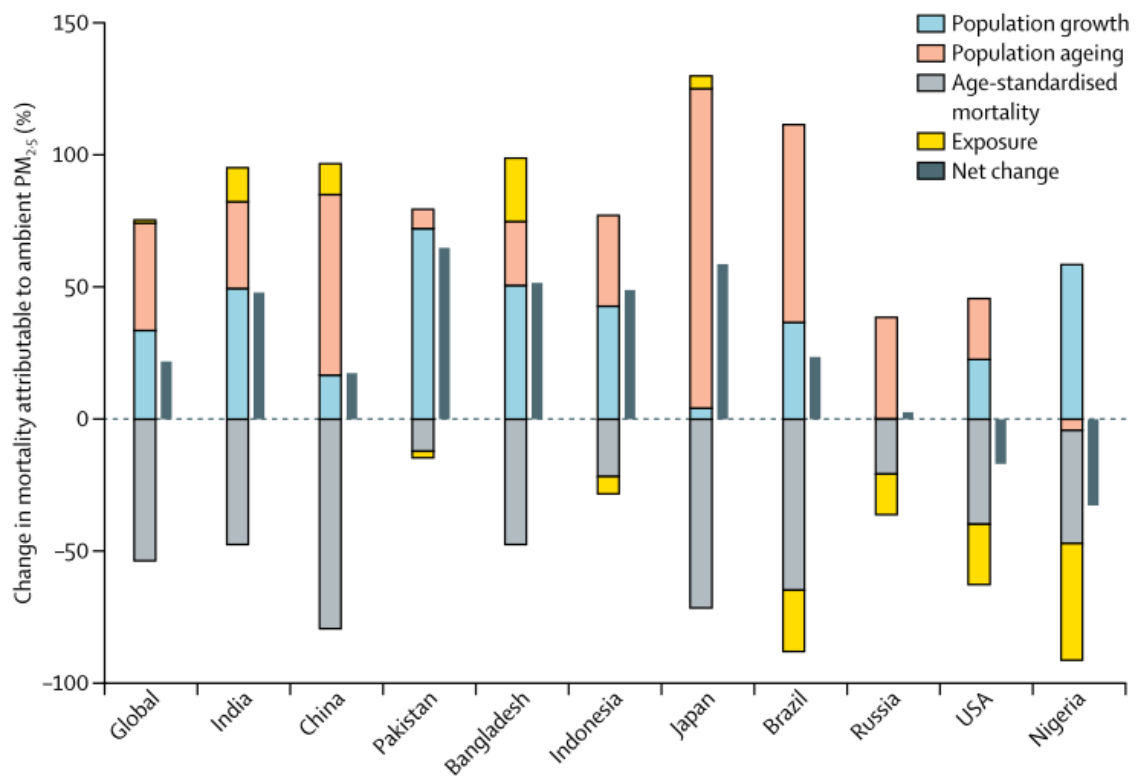


Figure 12: Drivers of changes in estimated premature mortality associated with ambient PM_{2.5} exposure by country from 1990 to 2015 (Cohen *et al* 2017).

Figure 13 shows the global burden of disease from exposure to ambient O₃ in 2016. In 1990, the global estimate of annual premature mortality attributable to ambient O₃ exposure was 153,732 (95UI: 54,522–267,745), with dominant contributions of 44% by China (68,395, 95UI: 24,740–120,304) and 27% by India (41,709, 95UI: 15,172–70,285) (Cohen *et al* 2017, GBD 2016 Risk Factors Collaborators 2017). By 2016, the global estimate of annual premature mortality from exposure to ambient O₃ increased by 52% to 233,628 (95UI: 90,109–385,303), increasing substantially by 116% in India to 90,253 (95UI: 34,556–145,570), while only increasing by 2% in China to 69,707 (95UI: 26,763–115,134) (Cohen *et al* 2017, GBD 2016 Risk Factors Collaborators 2017). The large increase in the disease burden from O₃ exposure in India between 1990 and 2016 means that India dominates the contribution to the global burden (39%). The

mortality rate per 100,000 in India increased by 43% between 1990 and 2016, while there was a 15% reduction in China (Cohen *et al* 2017, GBD 2016 Risk Factors Collaborators 2017). The decrement in life expectancy from ambient O₃ in South Asia is 0.10 years (Apte *et al* 2018).

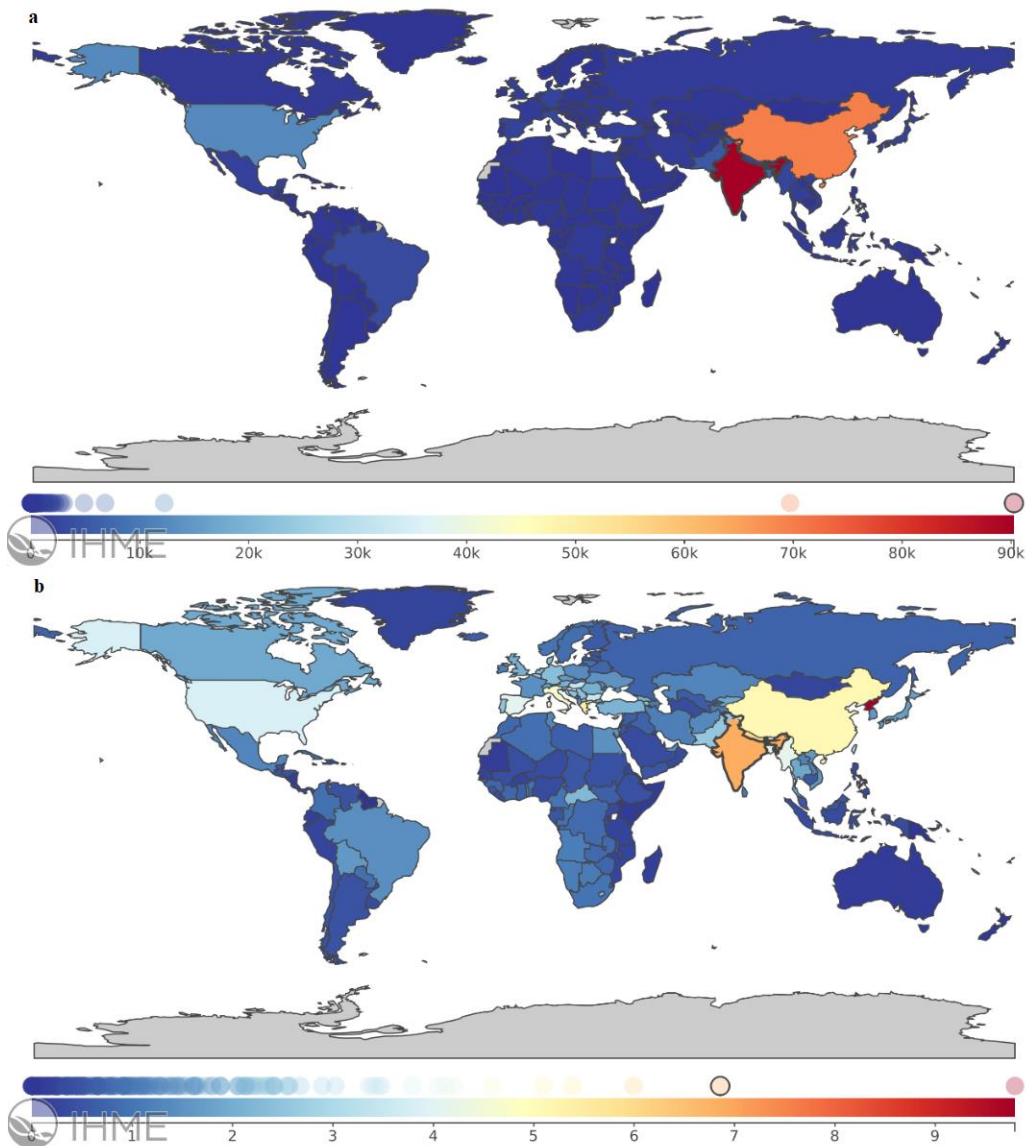


Figure 13: The global burden of disease from ambient O₃ exposure in 2016. (a) Number of premature mortalities per country. (b) Mortality rate per 100,000 population per country (Institute for Health Metrics and Evaluation 2018).

The global burden of disease from household air pollution from solid fuel use in 1990 was 3,738,921 (95UI: 3,255,981–4,301,372) premature mortalities globally, with dominant contributions of 34% by China (1,285,110, 95UI: 1,081,537–1,521,215) and 26% by India (989,826, 95UI: 844,050–1,153,357) (Institute for Health Metrics and Evaluation 2018). In 2016, the global estimate of premature mortality reduced by 31% to 2,576,361 (95UI: 2,215,953–2,968,891), with a substantial reduction of 53% in China (605,098, 95UI: 500,437–735,840) and a smaller reduction in India of 21% (782,905, 95UI: 652,172–941,484) (Institute for Health Metrics and Evaluation 2018). There were large reductions in the mortality rate per 100,000

population of 51% globally, 49% in India, and 61% in China (Institute for Health Metrics and Evaluation 2018). The decrement in life expectancy from household air pollution in South Asia is 1.22 years (Apte *et al* 2018).

Overall, the main trends from 1990 (Figure 14a) to 2016 (Figure 14c) are that the number of premature mortalities from ambient PM_{2.5} exposure increased globally, and especially in India. The mortality rate per 100,000 population for ambient PM_{2.5} exposure remained stable (Figure 14b and 14d), indicating that the growth in the number of premature mortalities was primarily driven by population characteristics. There were large decreases in the number of premature mortalities and the mortality rate from household air pollution from solid fuels, highlighting the important development relating to this issue that has occurred between 1990 and 2016, although a substantial burden remains globally and in India. The burden of disease from exposure to ambient O₃ has remained relatively small compared to exposure to ambient PM_{2.5} and household air pollution.

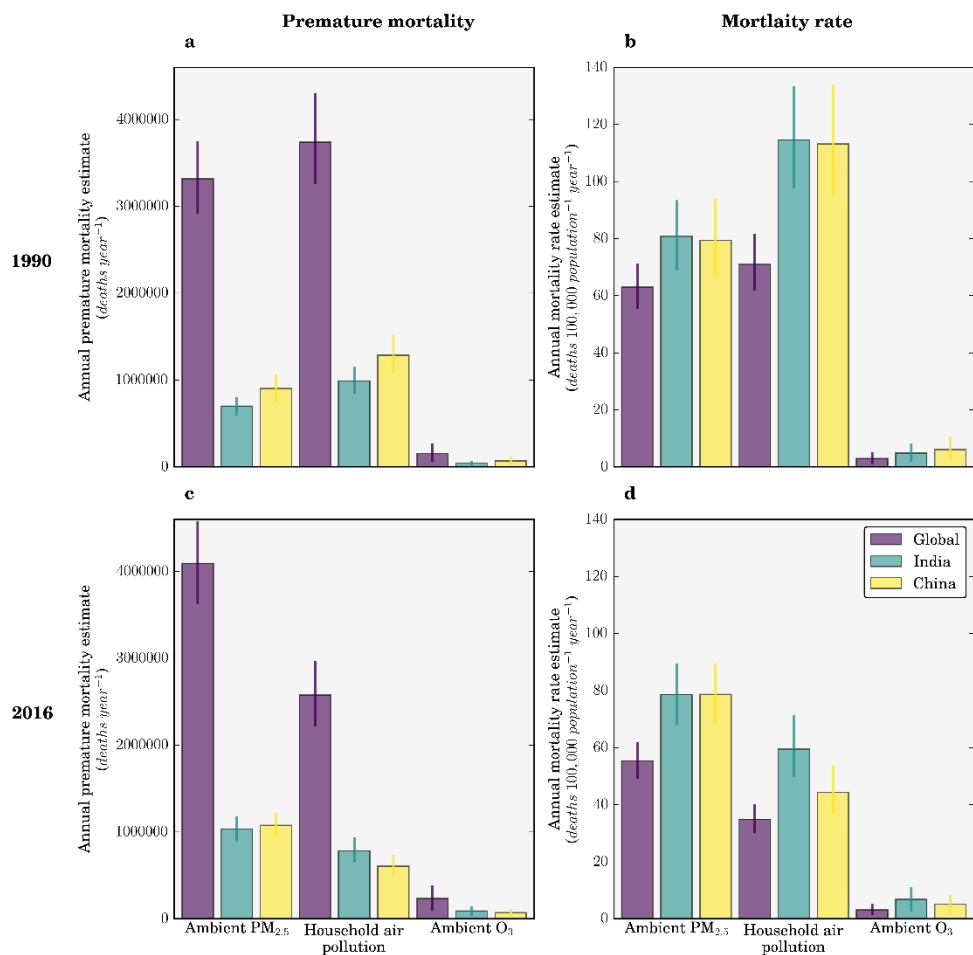


Figure 14: The disease burden from air pollution. (a) Annual premature mortality estimates in 1990. (b) Mortality rate per 100,000 population in 1990. (c) Annual premature mortality estimates in 2016. (d) Mortality rate per 100,000 population in 2016. Data from GBD2016 (Institute for Health Metrics and Evaluation 2018).

Figure 15 shows India is uniquely in the middle of the environmental risk transition (Smith and Ezzati 2005), i.e. the *risk overlap* (Smith 1995), where there are both substantial risks from traditional (household solid fuel) and modern (ambient PM_{2.5}) diseases. Pollutant concentrations have been increasing between 1990 and 2016 for ambient PM_{2.5} and O₃, while solid fuel use (the common surrogate for estimating household air pollution) has remained the same. The reduction in deaths per year for household solid fuel has largely come from improvements in LRI, while the large increase for ambient PM_{2.5} is from IHD in older ages (Figure 15a). The infant (<5 years) YLL in India from LRI due to ambient air pollution exposure decreased by 30% between 2010 and 2015, highlighting the epidemiological improvement (Lelieveld *et al* 2018). The reduction in DALYs per year for both ambient PM_{2.5} and household solid fuel has largely come from improvements in LRI in children (Figure 15b).

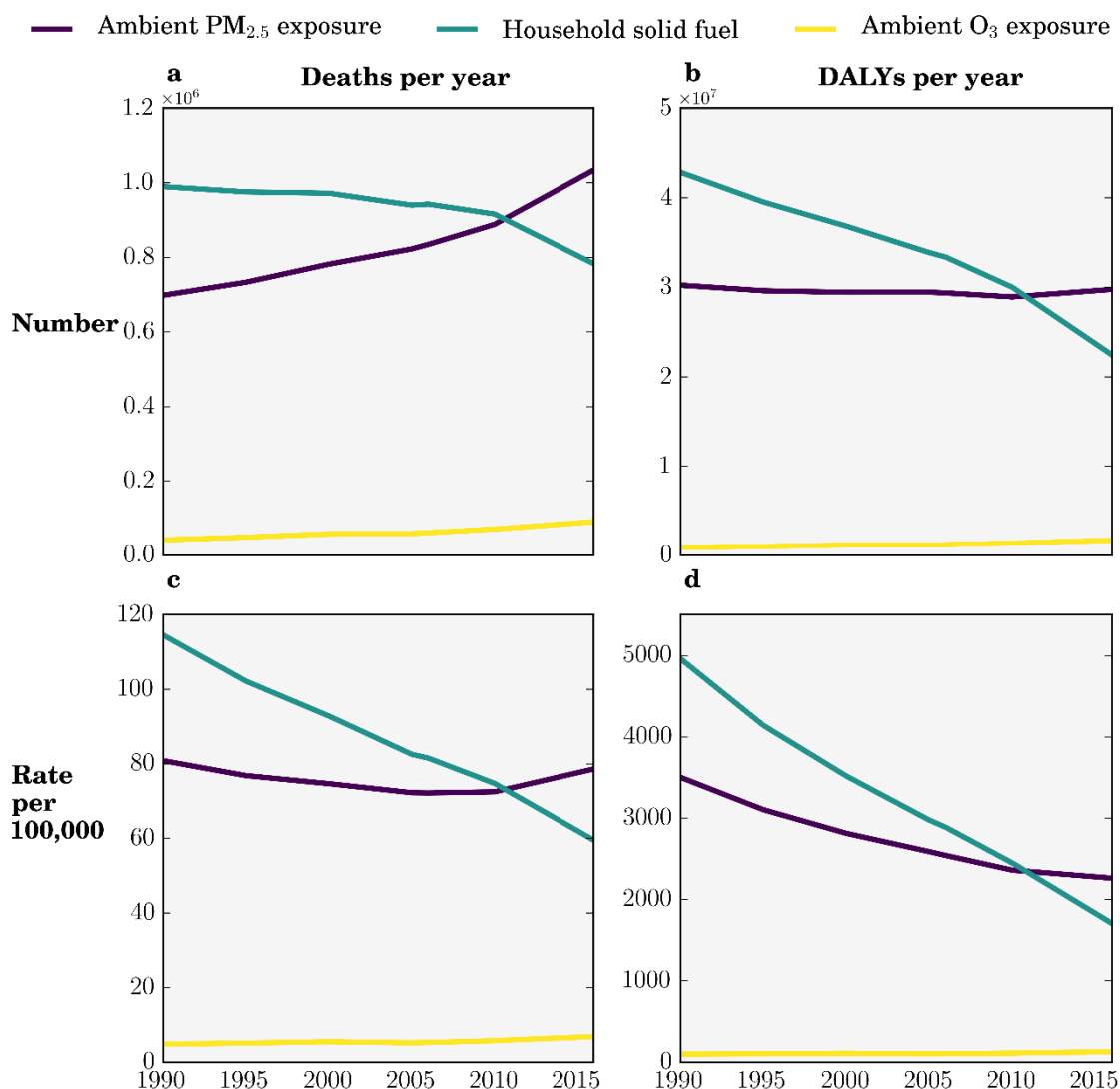


Figure 15: Environmental risk transition estimates for India from GBD2016 for ambient PM_{2.5}, O₃, and household solid fuels from 1990–2016 (Institute for Health Metrics and Evaluation 2018). (a) Number of deaths per year. (b) Number of DALYs per year. (c) Mortality rate per 100,000 per year. (d) DALYs rate per 100,000 per year.

1.1.7.5. Disease burden from air pollution exposure within India

In 2016, air pollution was the second leading risk factor in India, behind child and maternal malnutrition, and up from third in 1990 (India State-Level Disease Burden Initiative Collaborators 2017). Four out of the top five leading causes of disease in India are caused in part by air pollution exposure (India State-Level Disease Burden Initiative Collaborators 2017). Figure 16 shows the Indian burden of disease from exposure to ambient PM_{2.5} in 2016. Within India in 2016, the densely populated state of Uttar Pradesh in the central IGP dominates the contribution (21%) to the national burden of disease from ambient PM_{2.5} exposure, ahead of West Bengal, Maharashtra, and Bihar all contributing 9% each (Indian Council of Medical Research *et al* 2017a). Regarding the mortality rate per 100,000 population, states throughout the IGP have massive burdens, especially Punjab (105), Haryana (103), Uttar Pradesh (99), and West Bengal (95) (Indian Council of Medical Research *et al* 2017a). The disease burden in Delhi from exposure to ambient PM_{2.5} is 11,517 (95UI: 9,757–13,331) premature mortalities per year with a mortality rate of 57 (95UI: 48–66) (Indian Council of Medical Research *et al* 2017a).

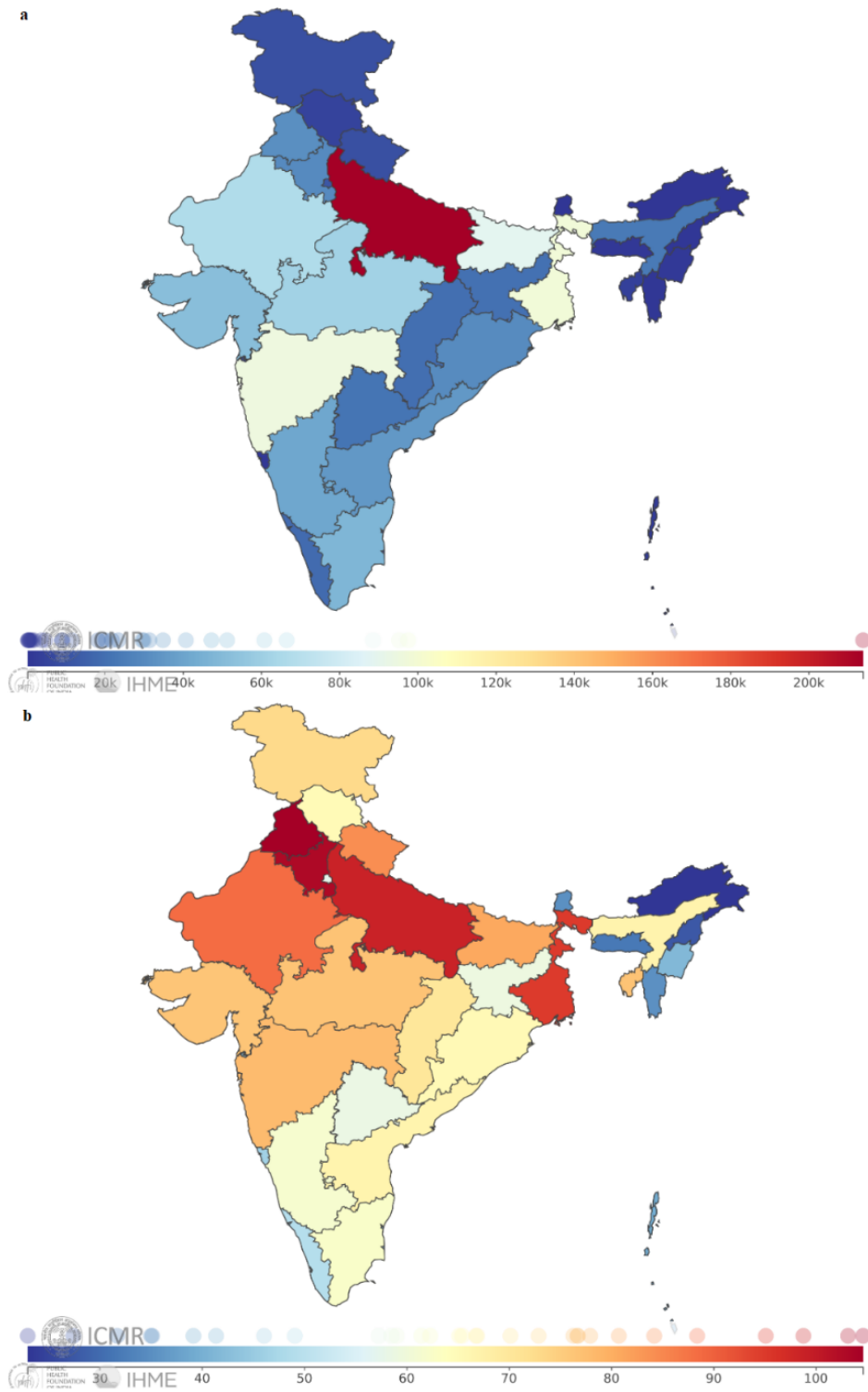


Figure 16: The Indian burden of disease from ambient PM_{2.5} exposure in 2016. (a) Number of premature mortalities per state. (b) Mortality rate per 100,000 population per state (Indian Council of Medical Research *et al* 2017a).

Figure 17 shows the Indian burden of disease from exposure to ambient O₃ in 2016. Uttar Pradesh dominates the contribution to ambient O₃ with 27% of the national burden (Indian Council of Medical Research *et al* 2017a). States in the western IGP have the highest mortality rate per 100,000 population with Uttarakhand (12) and Himachal Pradesh (11), followed by Uttar

Pradesh (11) and Rajasthan (10) (Indian Council of Medical Research *et al* 2017a). Delhi has a mortality rate of 2 per 100,000 (Indian Council of Medical Research *et al* 2017a).

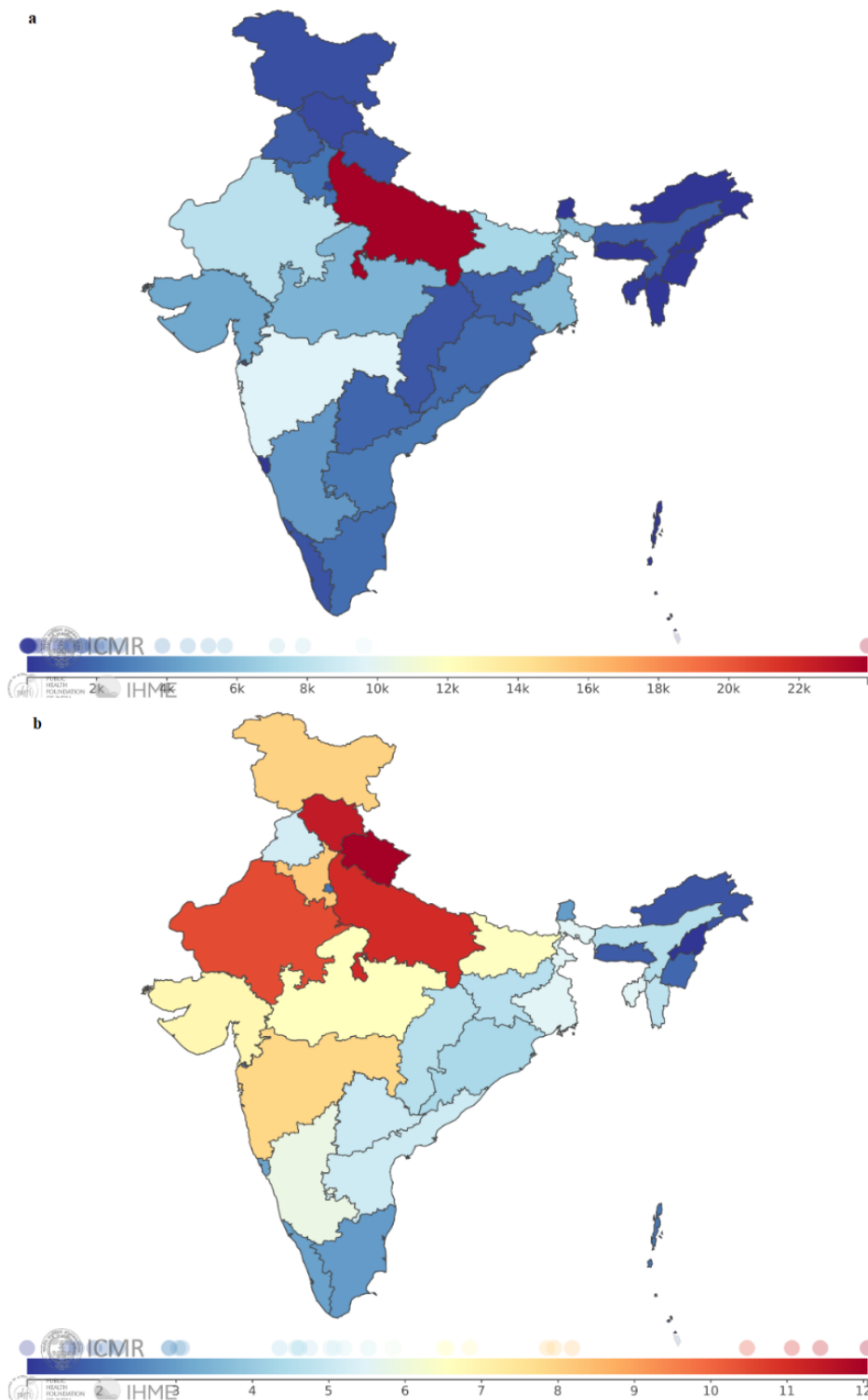


Figure 17: The Indian burden of disease from ambient O₃ exposure in 2016. (a) Number of premature mortalities per state. (b) Mortality rate per 100,000 population per state (Indian Council of Medical Research *et al* 2017a).

In 2016, Uttar Pradesh dominates the contribution (23%) to the national burden of disease from household air pollution from solid fuel use, with Bihar contributing 11% in second (Indian

Council of Medical Research *et al* 2017a). Regarding the mortality rate per 100,000 population, states across northern India have substantial burdens, of 86 in Rajasthan, 82 in Uttar Pradesh, and 76 in Bihar (Indian Council of Medical Research *et al* 2017a). The mortality rate in Delhi from household air pollution from solid fuel use is low (3) (Indian Council of Medical Research *et al* 2017a).

Overall, the disease burden from air pollution in India is highest in states across the IGP. States across the IGP are behind in the epidemiological transition, despite massive progress between 1990 and 2016 (India State-Level Disease Burden Initiative Collaborators 2017). The epidemiological transition is from communicable, maternal, neonatal, and nutritional diseases (CMNNDs) to NCDs (India State-Level Disease Burden Initiative Collaborators 2017). NCDs are not transmittable by infectious agents and are chronic in their development over time (Ezzati *et al* 2018, Health Effects Institute Household Air Pollution Working Group 2018). Major improvement in the epidemiological transition between 1990 and 2016 in India means the disease burden from NCDs in all Indian states now outweighs that from CMNNDs (India State-Level Disease Burden Initiative Collaborators 2017). Cardiovascular (IHD) and chronic respiratory NCDs rates in India are more than double rates in high-income Western countries (Ezzati *et al* 2018).

1.1.7.6. Source contributions to the burden of disease from air pollution

Estimates of premature mortality from exposure to ambient PM_{2.5} in India vary by a factor of three, between 392,000 to 1,090,000 per year (Silva *et al* 2013, Chowdhury and Dey 2016, GBD 2016 Risk Factors Collaborators 2017, Cohen *et al* 2005, Apte *et al* 2015a, Ghude *et al* 2016, Giannadaki *et al* 2016, GBD 2013 Risk Factors Collaborators 2015, Lelieveld *et al* 2015, GBD 2010 Risk Factors Collaborators 2012, Silva *et al* 2016b, GBD 2015 Risk Factors Collaborators 2016a, World Health Organization 2016a, Lelieveld 2017), with differences due to variations in ambient PM_{2.5} estimates, health functions, population datasets, and methodological approaches. Previous global modelling studies find emissions from residential energy use dominate the contribution to PM_{2.5} exposure associated premature mortality in India (Figure 18) (Lelieveld *et al* 2015, Lelieveld 2017, Silva *et al* 2016b). In contrast, air pollutant emissions from energy, industry, agriculture, and land transport dominate in Europe and the USA (Lelieveld *et al* 2015, Lelieveld 2017, Silva *et al* 2016b, Janssens-Maenhout *et al* 2015). Residential combustion has been found to be the dominant source contributor to global premature mortality from ambient PM_{2.5} exposure (Lelieveld *et al* 2015, Lelieveld 2017), with a substantial fraction of the global burden in India (Smith *et al* 2014a). Previous global modelling studies have estimated that emissions from residential energy use cause between 73,000 to 460,500 premature mortalities across India each year (Butt *et al* 2016, Chafe *et al* 2014a, Lelieveld *et al* 2015, Silva *et al* 2016b, Lelieveld 2017).

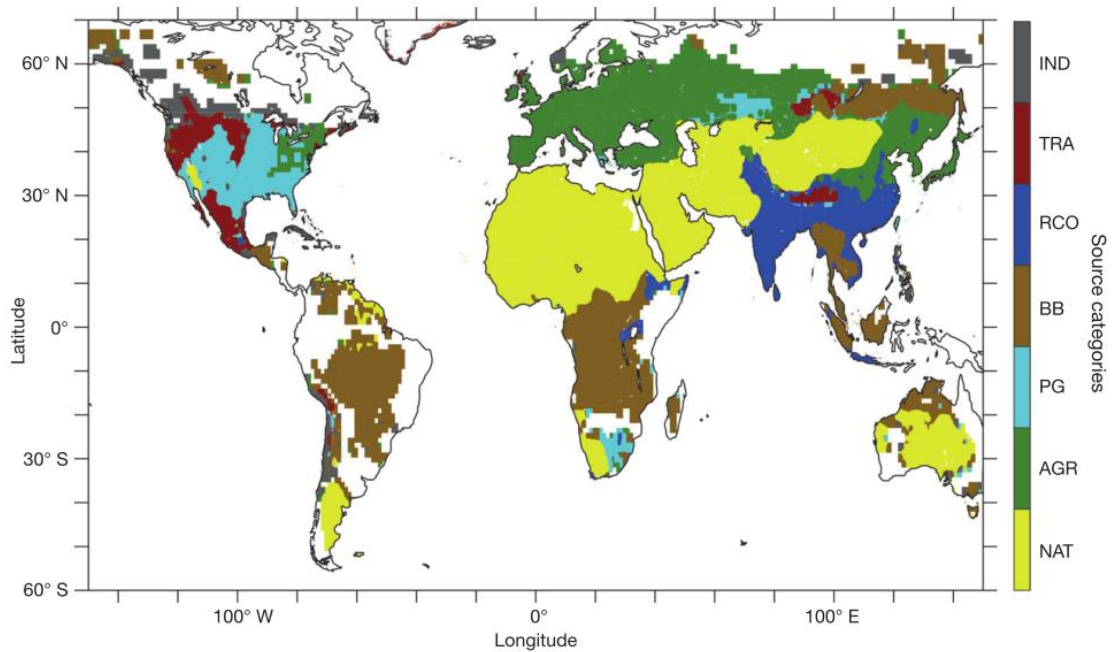


Figure 18: Source categories responsible for the largest impact on premature mortality associated with ambient air pollution in 2010 (Lelieveld *et al* 2015). Source categories are industry (IND), land transport (TRA), residential (RCO), biomass burning (BB), power generation (PG), agriculture (AGR), and natural (NAT). The white areas are where annual-mean $PM_{2.5}$ concentrations are below the theoretical minimum risk exposure level.

All previous global modelling studies estimating the source contributions to the disease burden (Lelieveld *et al* 2015, Lelieveld 2017, Silva *et al* 2016b) used global models with relatively coarse resolution, which may not resolve the high $PM_{2.5}$ concentrations in India, and were limited by lack of ground measurements before 2016. Chapter 4 is the first study to use high-resolution simulations, evaluated by new ground measurements, to estimate the contribution of different emission sectors to ambient $PM_{2.5}$ concentrations and the attributable disease burden from exposure across India.

Previous global modelling studies have estimated the contribution of sources to the disease burden from ambient O_3 exposure in India using the earlier CPS-II risk estimates (Malley *et al* 2017, Silva *et al* 2016b, Lelieveld *et al* 2015). These risk estimates have been recently updated (Turner *et al* 2016). Substantial contributions were found to be from power generation, land transport, and residential emissions (Malley *et al* 2017, Silva *et al* 2016b, Lelieveld *et al* 2015). Previous studies of the total and source-specific disease burden associated with O_3 exposure have used global, offline chemical transport models at relatively coarse spatial resolution (between $0.5^\circ \times 0.67^\circ$ and $2.0^\circ \times 2.5^\circ$) (Malley *et al* 2017, Silva *et al* 2016b, Lelieveld *et al* 2015). Tropospheric O_3 has a non-linear dependence on precursors concentrations, with production on short timescales (Liang and Jacobson 2000, Carey Jang *et al* 1995, Wild and Prather 2006, Sharma *et al* 2017b). Coarse spatial resolution models dilute O_3 precursors, causing simulated concentrations to diverge from observations (Liang and Jacobson 2000, Carey Jang *et al* 1995, Wild and Prather 2006,

Sharma *et al* 2017b). The model resolution also affects estimates of the O₃ exposure relative disease burden (Punger and West 2013, Thompson *et al* 2014, Thompson and Selin 2012). Online-coupled modelling explicitly accounts for feedbacks between chemistry and meteorology (Grell *et al* 2004, Baklanov *et al* 2014), which can be important when considering emission changes through different scenarios. Chapter 6 is the first study to estimate the source-specific disease burden from ambient O₃ exposure in India at high spatial resolution, using the updated CPS-II risk functions (Turner *et al* 2016).

1.1.7.7. *Future disease burden from air pollution in India*

Under a business-as-usual scenario, emissions are predicted to increase in India relative to the present day substantially (GBD MAPS Working Group 2018), with PM_{2.5}, SO₂, and NO_x emissions approximately doubling by 2050 relative to 2015 (Sharma and Kumar 2016, International Energy Agency 2016b), increasing PM_{2.5} concentrations by 67% (Pommier *et al* 2018). This increase in pollutant concentrations, alongside population growth and ageing, increases the disease burden from ambient air pollution exposure (Figure 19) (Lelieveld *et al* 2015, Anenberg *et al* 2012, GBD MAPS Working Group 2018, International Energy Agency 2016a).

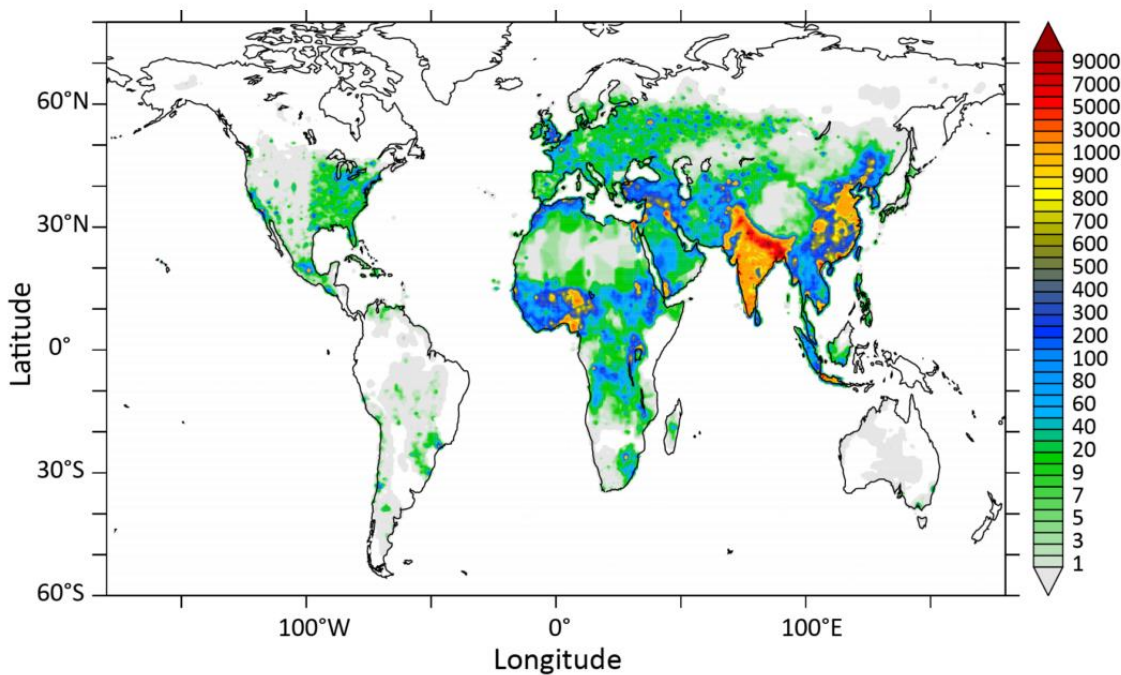


Figure 19: Increase in premature mortality associated with ambient air pollution exposure from 2010 to 2050 under a business-as-usual scenario (Lelieveld *et al* 2015).

Alternative air pollution control pathways (scenarios) for India have been developed and evaluated in previous studies (Sharma and Kumar 2016, International Energy Agency 2016b, Pommier *et al* 2018, International Energy Agency 2016a, GBD MAPS Working Group 2018). The International Energy Agency (IEA) developed the New Policy Scenario (NPS) which

considers all relevant existing and planned policies as of 2016 and the Clean Air Scenario (CAS) which represents aggressive policy action using proven energy policies and technologies tailored to national circumstances (International Energy Agency 2016b, 2016a). Emissions of SO₂, NO_x, and PM_{2.5} under the NPS increased on average by 9% by 2040 relative to 2015, while the premature mortality estimate increased by 53% (International Energy Agency 2016b, 2016a). Emissions of SO₂, NO_x, and PM_{2.5} under the CAS decreased on average by 65% by 2040 relative to 2015, while the premature mortality estimate decreased by 5% (International Energy Agency 2016b, 2016a). The GBD MAPS Working Group studied a business-as-usual reference scenario, an ambitious scenario reflecting stringent emission standards, and an aspirational scenario all through to 2050 (Venkataraman *et al* 2018, GBD MAPS Working Group 2018). Population-weighted ambient PM_{2.5} concentrations across India in 2050 under the reference, ambitious, and aspirational scenarios changed by +43%, +10%, and -35%, respectively relative to the reference scenario in 2015 (Venkataraman *et al* 2018, GBD MAPS Working Group 2018). Premature mortality from ambient PM_{2.5} exposure would increase under the reference, ambitious, and aspirational scenarios by 234%, 194%, and 125% in 2050 relative to 2015 (Venkataraman *et al* 2018, GBD MAPS Working Group 2018). Both the IEA and GBD MAPS Working Group studies highlight the substantial impact of the demographic transition in India.

The previous studies that evaluated Indian scenarios (International Energy Agency 2016b, 2016a, Pommier *et al* 2018, GBD MAPS Working Group 2018) used relatively coarse spatial resolution ($0.5^\circ \times 0.5^\circ$ or $0.5^\circ \times 0.67^\circ$) chemical transport models to estimate the impacts on PM_{2.5} concentrations per scenario, which may not resolve the high PM_{2.5} concentrations in India. No previous studies have analysed the impacts of future air pollution control pathways on ambient O₃ and the associated disease burden.

Chapter 5 and 6 analyse the impacts of multiple air pollution control pathways (scenarios) in India on ambient PM_{2.5} and O₃ concentrations and associated disease burdens, respectively. Both chapters use a higher resolution (30 km, 0.3° horizontal) regional numerical weather prediction model online-coupled with atmospheric chemistry, with the latest exposure-response functions, and disease-specific baseline mortality rates for 2015 and 2050. Both chapters are individually the first high-resolution analyses of the impacts of future scenarios on ambient PM_{2.5} and O₃ concentrations and resulting disease burden in India, respectively.

1.2. Summary and Aims

Two-thirds of Indian households primarily use solid fuels, mostly wood in polluting traditional stoves in rural areas within the IGP. The absolute number of solid fuel users has remained stable for the last 30 years, contributing substantially to air pollutant emissions. India experienced large growth in the economy, industry, power generation, and transport sectors over the last decade leading to a large growth in emissions of air pollutants. Emissions of air pollutants are predicted to grow substantially over the coming years in India. These air pollutant emissions have caused

very high concentrations of ambient $PM_{2.5}$ and O_3 in India. Exposure to these air pollutants is the second leading risk factor in India (GBD 2016 Risk Factors Collaborators 2017, India State-Level Disease Burden Initiative Collaborators 2017). India contributes one-quarter and one-third of the present-day global disease burden attributable to ambient $PM_{2.5}$ and O_3 exposure, respectively (GBD 2016 Risk Factors Collaborators 2017, India State-Level Disease Burden Initiative Collaborators 2017). India is uniquely in the middle of the environmental risk transition, where there is both substantial risk from household air pollution and ambient air pollution (GBD 2016 Risk Factors Collaborators 2017, India State-Level Disease Burden Initiative Collaborators 2017).

Despite the importance of air quality in India, it remains relatively understudied, and knowledge of the sources and processes causing air pollution is limited. It is critical to understand the contribution of different emission sources to ambient air pollution to design effective policies to reduce this substantial disease burden. This thesis aims to understand the source contributions to the attributable disease burden from ambient air pollution exposure in India and the effects of future air pollution control pathways.

The thesis has three main objectives. Firstly, quantify the contributions of different emission sources to ambient $PM_{2.5}$ concentrations and the related disease burden across India in the present day. Secondly, estimate the impact from different future air pollution control pathways on ambient $PM_{2.5}$ concentrations and human health in India. Thirdly, understand the current and future disease burden from ambient O_3 exposure in India, identifying critical contributing emission sources and the impacts of future policy scenarios. These objectives are achieved by combining high-resolution computer simulations, new and extensive observations, and the latest exposure-response relationships. The high-resolution, online-coupled, regional numerical weather prediction (NWP) model, Weather Research and Forecasting Model with Chemistry (WRF-Chem), is used throughout these chapters.

1.3. Outline

Chapter 1 introduces the research topic, aim, objectives, and outline. Chapter 2 discusses the methods. Chapter 3 discusses the model evaluation. Chapter 4 estimates the contribution of different emission sources to ambient $PM_{2.5}$ concentrations and the related disease burden across India. Chapter 5 estimates the impacts of different air pollution control pathways on ambient $PM_{2.5}$ and human health in India. Chapter 6 studies the source contributions of ambient O_3 concentrations in India, the exposure-related disease burden, and the changes under future policy scenarios. Chapter 7 summarises and discusses the work undertaken, highlighting areas of future work.

This chapter describes the methods and models used in this thesis. Section 2.1 summarises the background of air quality modelling. Section 2.2 describes the air quality model used in the thesis. Section 2.3 and 2.4 describe the exposure-response functions for PM_{2.5} and O₃, respectively. Section 2.5 describes the population data used. Section 2.6 explains the methods used to estimate the sector-specific disease burden. Section 2.7 discusses uncertainties in the methods.

2.1. Air quality modelling

Satellite observations are limited in either space or time. Ground measurements are limited in space, especially over India. Models can address these gaps in space and time, giving insight into driving processes and mechanisms of air quality. The main purpose of the model used in this thesis was to simulate total PM_{2.5} and O₃ concentrations accurately and to attribute total concentrations to different emission sectors. There are a wide variety of models. The discussion here, and the term model used subsequently, applies to three-dimensional, mathematical (describing fundamental atmospheric processes), Eulerian (fixed grid), atmospheric models (Seinfeld and Pandis 2016).

The essential components of a model are emissions, transport, and physiochemical transformations (Brasseur and Jacob 2016). Models are based on the non-linear primitive equations including the momentum equation, thermodynamic equation, continuity equation, and the ideal gas law (Brasseur and Jacob 2016). The primitive equations have no analytical solution, and numerical methods are required (Brasseur and Jacob 2016).

Aerosol schemes are required to resolve the large aerosol size range for the chemical and microphysical processes through individual modules (Brasseur and Jacob 2016). Aerosol schemes represent aerosol size, mass, and number (Brasseur and Jacob 2016). Bulk aerosol schemes resolve aerosol mass, assume the size distribution, are numerically efficient, and are useful when focusing on gas-phase chemistry (Brasseur and Jacob 2016). Modal aerosol schemes carry aerosol mass and number, representing aerosol size by overlapping intervals assuming a lognormal distribution (Brasseur and Jacob 2016). Sectional aerosol schemes discretise aerosol size into bins carrying mass and number (Brasseur and Jacob 2016). Aerosol schemes can interact with radiation, photolysis, and clouds (Brasseur and Jacob 2016). The continuity equations solved for aerosol mechanisms are the same as for gas mechanisms (Brasseur and Jacob 2016).

Models use gas-phase mechanisms to simulate chemical production and loss (Brasseur and Jacob 2016, Seinfeld and Pandis 2016). Gas-phase mechanisms use an ensemble of chemical reactions to calculate chemical production and loss using rate laws, aqueous chemistry using cloud type, and phase equilibrium using Henry's law coefficients (Brasseur and Jacob 2016, Seinfeld and Pandis 2016). Gas-phase mechanisms simplify large, complex organic compounds by classifying them by functionality or volatility, which are then represented by a surrogate

species or lumped species (Brasseur and Jacob 2016, Seinfeld and Pandis 2016). More complex gas-phase mechanisms explicitly resolve chemistry (Brasseur and Jacob 2016, Seinfeld and Pandis 2016).

Models include emissions through inventories or calculate them online (Brasseur and Jacob 2016). Bottom-up emissions inventories use knowledge of the underlying processes such as emission factors, activity rate, and scaling factors, with or without top-down constraints from observations (Brasseur and Jacob 2016). Models include emissions from anthropogenic, biogenic, biomass burning, volcanic, and mechanical sources (Brasseur and Jacob 2016). Regional models also require initial and boundary conditions often supplied from a global model (Palmer and Williams 2010). Models are particularly sensitive to the initial conditions (Palmer and Williams 2010).

2.2. Weather Research and Forecasting Model with Chemistry

The simulations performed for this thesis used the Weather Research and Forecasting (WRF) model (Skamarock *et al* 2008). WRF was designed for regional and numerical weather prediction by the National Center for Atmospheric Research (NCAR), the National Oceanic and Atmospheric Administration (NOAA), the National Centre for Environmental Prediction (NCEP), the United States Air Force, the Naval Research Laboratory, the University of Oklahoma, and the Federal Aviation Administration. WRF was publically released in 2000 and has since been extended for many Earth system applications, such as atmospheric chemistry (WRF-Chem), hydrology (WRF-Hydro), fire (WRF-Fire), hurricanes (HWRF), urban meteorology (WRF-Urban), solar and wind energy (WRF-Solar), turbulence (WRF-LES), and polar environments (POLAR WRF) (Powers *et al* 2017). This thesis used WRF-Chem version 3.7.1 (Grell *et al* 2005, Fast *et al* 2006).

The workflow of WRF follows preprocessing, forecast modelling, and postprocessing. Preprocessing input data is performed via the WRF preprocessing system (WPS). WPS first configures the horizontal domain, interpolating static geographical data (geogrid). WPS then reads, reformats, and extracts input data (ungrib, wesely, and exo_coldens). WPS then ingests and interpolates input data creating initial and boundary meteorological conditions (metgrid). Emission inventory variables are mapped onto WRF-Chem variables for biogenic (bio_emiss), anthropogenic (anthro_emiss), and fire (fire_emiss) emissions. The last step of preprocessing is to create initial and boundary chemistry conditions (mozbc). The ACOM laboratory of NCAR provided the preprocessors (bio_emiss, anthro_emiss, fire_emiss, and mozbc).

This thesis used the WRFotron scripts developed by Christoph Knote to automate WRF-Chem simulations with re-initialised meteorology. WRFotron is split into preprocessing (pre.bash), main execution (main.bash), and postprocessing (post.bash). WRFotron allowed WRF-Chem to create optimal initial conditions in the spin-up period using data assimilation, then the model free-

runs for a set period to allow for sophisticated physics without drifting. The input data for nudging has a 3-hour update interval, and values were interpolated in-between. Nudging was only applied to selected variables (horizontal wind, vertical wind, potential temperature, and water vapour mixing ratio) and with a nudging coefficient that still allows for WRF-Chem to create its own dynamic, fine-scale, meteorology.

WRF-Chem is fully online-coupled (Grell *et al* 2005). Online-coupled models account for interactions and feedbacks between air quality and meteorology (Grell *et al* 2005). These interactions can include impacts on radiation, cloud condensation nuclei, removal processes, and transport (Grell *et al* 2005). Offline models treat air quality and meteorology independently using archived meteorology, losing valuable information about atmospheric processes (Grell *et al* 2005). WRF-Chem uses the Advanced Research WRF (ARW) fluid flow solver to calculate air quality and meteorology components using the same transport, grid coordinates, sub-grid scale physics, and timestep (Skamarock and Klemp 2008). ARW is fully compressible, allowing for significant changes in fluid density (Skamarock and Klemp 2008). ARW is non-hydrostatic, calculating the full vertical momentum equation (Skamarock and Klemp 2008). Fully compressible, non-hydrostatic, numerical solvers allow explicit representation of structures previously parameterised (Skamarock and Klemp 2008). ARW has a Eulerian mass conserving dynamical core (Skamarock *et al* 2008). The driving equations of ARW have been derived in full in Skamarock and Klemp (2008). The timestep of ARW is limited by the Courant-Friedrichs-Levy (CFL) stability criterion (Courant *et al* 1928) and is suitable for regional NWP applications not influenced by the pole problem (Brasseur and Jacob 2016). ARW uses terrain-following, hydrostatic, pressure coordinates to account for surface topography (Laprise 1992).

WRF-Chem allows users to select mechanisms, schemes, and parameterisations, including numerous options for physics, chemistry, and dynamics. The application of WRF-Chem over South Asia was first documented in 2012 with two key papers evaluating the model's performance for meteorology (Kumar *et al* 2012a) and chemistry (Kumar *et al* 2012b), establishing its credibility for future use. Since then WRF-Chem has been used extensively over South Asia, including papers using more complex sectional aerosol schemes (Kumar *et al* 2015b), higher resolution simulations (Kumar *et al* 2015c), and exploring the impacts of dust (Kumar *et al* 2014a, 2014b).

2.2.1. Model setup

The setup choices for WRF-Chem implemented in this thesis were initially based on papers using WRF-Chem over South Asia (Kumar *et al* 2012a, 2012b, 2015c, 2014a, 2014b, 2015b). The details of the model setup are summarised in Table 4 and detailed in section 2.2.2, 2.2.3, and 2.2.4.

Table 4: Model setup and parameterisation used in the WRF-Chem model.

Model Setup and Parameterisation	
Process	Method
Domain	60° to 100° East, 0° to 40° North
Timestep	180 seconds
Horizontal	Resolution of 30 km, along a 140 × 140 grid
Vertical	33 vertical and 27 meteorology levels (top at 10 hPa)
Microphysics	Thompson scheme (Thompson <i>et al</i> 2008)
Longwave radiation	RRTM longwave (Mlawer <i>et al</i> 1997) called every 30 mins
Shortwave radiation	RRTM shortwave (Pincus <i>et al</i> 2003) called every 30 mins
Boundary layer physics	Mellor-Yamada Nakanishi and Niino 2.5 (Nakanishi and Niino 2006), called every timestep
Land surface	Noah Land Surface Model (Ek <i>et al</i> 2003)
Convective parameterisation	Grell 3-D ensemble (Grell and Freitas 2014, Grell and Devenyi 2002), called every 60 seconds
Gas-phase chemistry	MOZART-4 (chem_opt = 201) (Emmons <i>et al</i> 2010), every 12 mins
Photolysis scheme	Madronich fTUV (Tie <i>et al</i> 2003) called every 30 mins
Aerosol scheme	MOSAIC 4-bin (chem_opt = 201) (Zaveri <i>et al</i> 2008), using KPP, called every 12 mins
Dust	GOCART with AFWA, dust_opt = 3 (Chin <i>et al</i> 2002, 2000)
Initial and boundary chemistry / aerosol	MOZART-4 / GEOS5 (National Center for Atmospheric Research 2016)
Initial and boundary meteorology	NCEP GFS and NCEP FNL (National Centers for Environmental Prediction <i>et al</i> 2007, 2000)

2.2.2. Physics

Model simulation design considers resolution, complexity, and duration in the context of computational constraints (Brasseur and Jacob 2016). The spatial resolution should reflect the typical scales of the processes of interest (Brasseur and Jacob 2016). Increasing spatial resolution requires shorter timesteps per calculation, substantially increasing the demand on computational memory, storage, and wall clock time (Brasseur and Jacob 2016). Sub-grid scale processes are parameterised using empiricism, rather than deterministic physics (Brasseur and Jacob 2016).

The model domain was a 140×140 cell grid, with a horizontal resolution of 30 km, 33 vertical levels up to 10 hPa, and a timestep of 180 seconds. The resolution of 30 km was chosen as adequate to resolve fine gradients in air pollutant concentrations while remaining computationally feasible to perform 15 years of simulations. The relatively low vertical resolution has been used in previous high horizontal resolution (10 km) simulations for air quality applications due to computational constraints (Kumar *et al* 2015c). The time-step of the model simulation was taken as $6 \times$ grid spacing to ensure that the model does not violate the CFL stability criterion (Courant *et al* 1928). Figure 20 shows the model domain used within all WRF-Chem simulations in this thesis, using a Lambert conformal conical projection, with terrain height displayed.

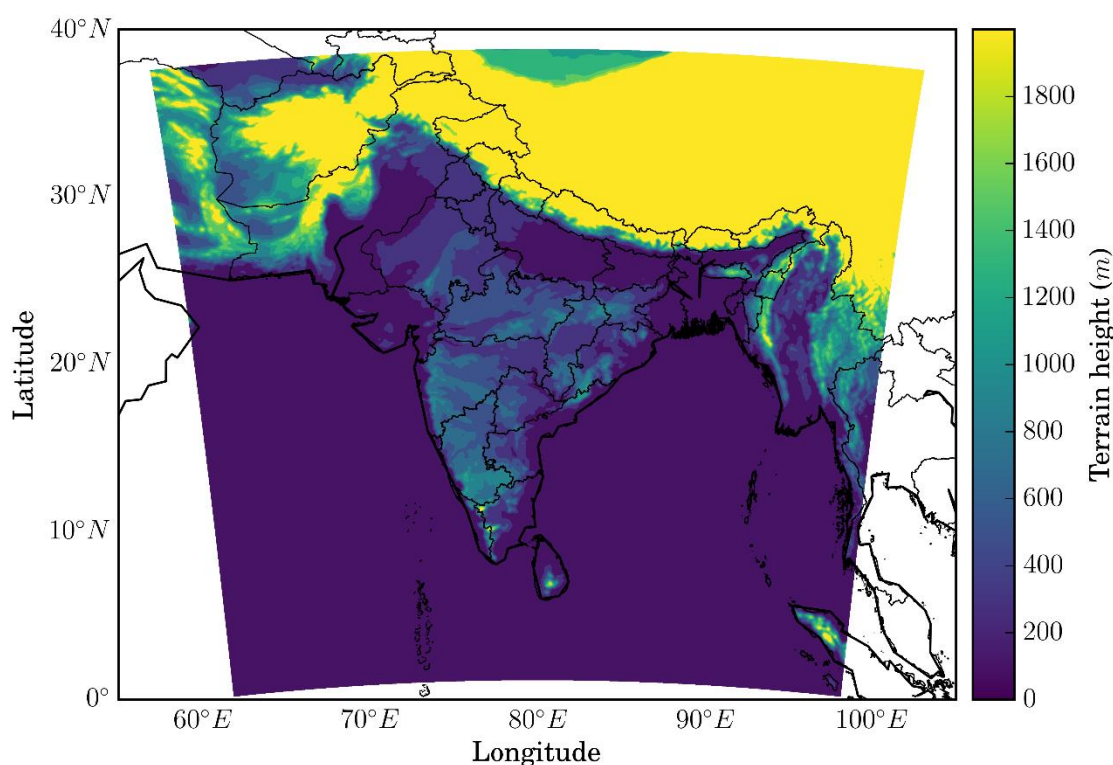


Figure 20: Model domain used in this thesis. Background colour shows terrain height from WRF-Chem simulated domain on a Lambert conformal conical projection.

Static geography fields were interpolated from the 20 category international geosphere-biosphere programme (IGBP) modified moderate resolution imaging spectroradiometer (MODIS) based land use classifications at 30 arc-second resolution by the WPS (Figure 21). Substantial areas of India are cropland, with some forest, shrubland, and barren land. MODIS-based categories should only be used with the Noah Land Surface Model (Ek *et al* 2003), which was used to parameterise heat and moisture fluxes in four soil layers to 2 m. A single layer urban canopy model was implemented with surface effects for roofs, walls, and streets.

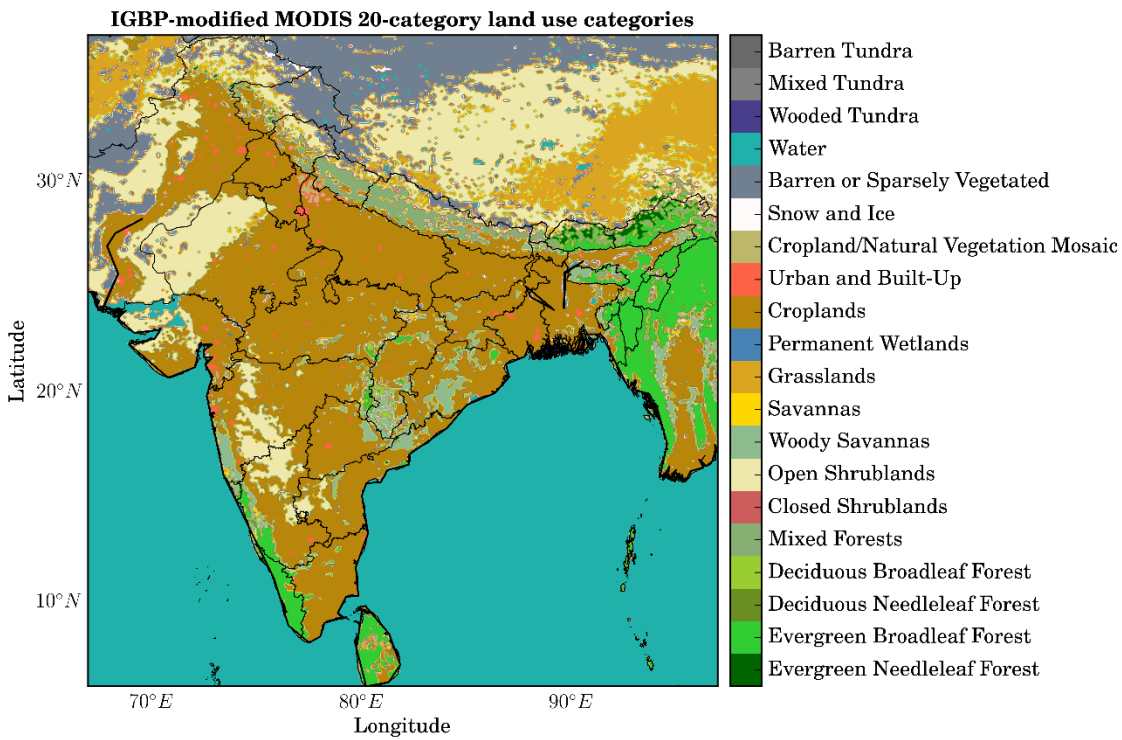


Figure 21: International geosphere-biosphere programme (IGBP) modified moderate resolution imaging spectroradiometer (MODIS) based land use classifications in India.

The Thompson scheme was used for cloud microphysics including cloud formation, phase conversion, and precipitation (Thompson *et al* 2008). The Thompson scheme has been found to accurately simulate Himalayan precipitation (Karki *et al* 2018, Reshmi Mohan *et al* 2018, Rajeevan *et al* 2010). The Grell 3-D scheme (Grell and Freitas 2014) was used for convective parameterisation, which is a development of the Grell-Devenyi scheme (Grell and Devenyi 2002). The Grell scheme has been found to have improved skill at simulating the South Asian monsoon relative to other cumulus schemes (Dash *et al* 2006, Yu *et al* 2011).

The Rapid Radiative Transfer Model (RRTM) option was used for downward and upward fluxes of absorption, scattering, and emission from both shortwave radiation due to solar activity and longwave radiation due to water vapour, clouds, and trace gases (e.g. CO₂ and O₃) (Iacono *et al* 2008). The Mellor-Yamada Nakanishi and Niino 2.5 (Nakanishi and Niino 2006) boundary layer scheme was called every timestep. WRF-Chem has been used to skillfully simulate air pollution episodes over China with the Mellor-Yamada Nakanishi and Niino 2.5 boundary layer scheme and the RRTM radiation schemes (Chen *et al* 2017a).

NCEP Global Forecast System (GFS) 6-hourly analyses initialised meteorological conditions at 0.5° resolution. These, together with GFS 3-hour forecasts in between were also used for boundary conditions and grid analysis nudging (National Centers for Environmental Prediction *et al* 2007, 2000). Simulated mesoscale meteorology was kept in line with analysed meteorology through grid nudging to the NCEP GFS analyses to limit errors in mesoscale transport (National Centers for Environmental Prediction *et al* 2007, 2000). Kumar *et al* (2014b) used WRF-Chem

over South Asia and found nudging improved model skill in simulating meteorology. In this thesis, model meteorology was reinitialised every month to avoid drifting of WRF-Chem, while chemistry and aerosol fields were kept to allow for pollution build up and mesoscale transport phenomena to be captured. During the simulations, horizontal and vertical wind, potential temperature, and water vapour mixing ratio were nudged to GFS analyses in all model layers above the planetary boundary layer using four-dimensional data assimilation (FDDA) (Liu *et al* 2006, 2005). FDDA in WRF-Chem does not use the analyses fields for its values. Instead, it uses them as initial conditions, and then uses the primitive atmospheric equations, affecting chemicals through transport. One-week spin-up was implemented based on previous studies (Berge *et al* 2001, Kumar *et al* 2015c, Knote *et al* 2015). The immediate model results were outputted every hour.

2.2.3. Chemistry

Gas-phase chemical reactions were calculated using the chemical mechanism Model for Ozone and Related Chemical Tracers, version 4 (MOZART-4) (Emmons *et al* 2010). Several updates to photochemistry of aromatics, biogenic hydrocarbons, and other species relevant to regional air quality were applied including a detailed treatment of VOCs (Knote *et al* 2014, Hodzic and Jimenez 2011, Hodzic and Knote 2014). The MOZART-4 scheme has been used in other studies over India using WRF-Chem and captured critical observed features of gas-phase species (Kumar *et al* 2014b, Ghude *et al* 2016). The updated MOZART-4 gas-phase mechanism should be used with either the Tropospheric Ultraviolet-Visible (TUV) (Tie *et al* 2005) or the Fast Tropospheric Ultraviolet-Visible (fTUV) module to calculate photolysis rates (Tie *et al* 2003). The fTUV scheme was implemented as it is a simplified version of the TUV model (Madronich and Weller 1990), reducing computational costs of using the full TUV scheme (Hodzic and Knote 2014). The fTUV code was updated to include aerosol feedbacks on photolysis (Hodzic and Knote 2014). Gas wet deposition was a combination of resolved (Neu and Prather 2012) and convective washout (Grell and Freitas 2014), updated to use Henry's law constants in gas-droplet partitioning (Knote *et al* 2015). Gas dry deposition was based on aerodynamic, transport, and surface resistances (Wesely 1989). The updated version of MOZART-4 has been used in many previous studies (Knote *et al* 2014, 2015, Hodzic *et al* n.d., Campbell *et al* 2015, Im *et al* 2015, Wang *et al* 2015).

Aerosol physics and chemistry were represented by the MOSAIC 4-bin scheme without subgrid convective aqueous chemistry (Hodzic and Knote 2014, Zaveri *et al* 2008). The Kinetic PreProcessor (KPP) (Damian *et al* 2002) was used to convert the underlying chemistry into ordinary differential equations. Four sectional discrete size bins were used within MOSAIC based on dry aerosol diameter; 0.039–0.156 μm , 0.156–0.625 μm , 0.625–2.5 μm , 2.5–10 μm (Hodzic and Knote 2014, Zaveri *et al* 2008). Water uptake and loss do not transfer aerosols between the size bins (Hodzic and Knote 2014, Zaveri *et al* 2008). MOSAIC carries sulphate (SO_4), nitrate

(NO₃), ammonium (NH₄), calcium (Ca), carbonate (CO₃), black carbon (BC), primary organic mass (OM), liquid water (H₂O), sea salt (NaCl), methanesulfonate (CH₃SO₃), and other inorganic mass such as minerals and trace metals (Hodzic and Knote 2014, Zaveri *et al* 2008). The aerosol number was carried separately, and both aerosol mass and number were calculated for each size bin (Hodzic and Knote 2014, Zaveri *et al* 2008). MOSAIC assumes aerosols are spherical, internally mixed within the same size bin and externally mixed with other size bins, implying that per size bin there is no ageing time for emissions to transfer from hydrophobic to hydrophilic (Kumar *et al* 2015c). Wet deposition of aerosols was a mixture of resolved (Neu and Prather 2012) and convective washout (Grell and Freitas 2014). Dry deposition was based on the resistances approach (Wesely 1989) as a function of friction velocity and the boundary layer height (Walcek *et al* 1986). The thermodynamic module in MOSAIC was designed for dynamic gas-particle partitioning, reliably predicting particle deliquescence (moisture absorption until dissolution), water content, and solid-liquid phase equilibrium in multicomponent aerosols, and is computationally efficient (Hodzic and Knote 2014, Zaveri *et al* 2008). MOSAIC removes aerosols via grid-scale precipitation (Chapman *et al* 2009, Easter *et al* 2004).

The SOA formation mechanism varies with or without the use of aqueous chemistry in the MOSAIC aerosol scheme (Hodzic and Knote 2014). For MOSAIC without aqueous chemistry, as used in this thesis, the SOA formation mechanism was from Hodzic and Knote (2014), based work by Hodzic and Jimenez (2011). SOA calculations use a lumped surrogate VOC for anthropogenic (VOC_A) and biomass burning (VOC_{BB}) co-emitted with CO that oxidises with OH and condenses into SOA (Hodzic and Jimenez 2011). The ratio of VOC_A (or VOC_{BB}) to CO emissions was parameterised as being proportional to the ratio of SOA formed to the change in CO in very aged air (Hodzic and Jimenez 2011). CO is typically well produced by models, can be measured by satellites, has similar or collocated emissions sources as anthropogenic SOA precursors, and is approximately inert with regard to SOA timescales (Hodzic and Jimenez 2011). Simulated SOA accuracy from this CO proxy approach is similar to volatility basis set (VBS) parameterisations (Robinson *et al* 2007), while being much less computationally expensive and can be used in regions where the emissions of SOA precursors are not yet available (e.g. India) (Hodzic and Jimenez 2011). Hodzic and Knote (2014) updated the SOA calculations from Hodzic and Jimenez (2011) to use ambient ageing measurements of OA that produce reasonable and efficient simulated SOA precursors. Hodzic and Knote (2014) calculate biogenic SOA via a two-product approach (partitioning coefficient and a proportionality constant for each specie oxidising VOCs) (Odum *et al* 1997, Odum Jay *et al* 1996), with updated yields (Hodzic and Knote 2014). Glyoxal SOA, a product of isoprene oxidation, formation and partitioning were included using a simple surface uptake mechanism (Knote *et al* 2014).

Simulations over India comparing the bulk scheme from Georgia Tech / Goddard Global Ozone Chemistry Aerosol Radiation and Transport (GOCART) (Chin *et al* 2000) and the

MOSAIC 8-bin sectional schemes have shown the MOSAIC scheme more accurately represents aerosol observations (Kumar *et al* 2015b). MOSAIC accounts for many aerosol processes (e.g., aerosol thermodynamics, SOA formation, in-cloud, and impaction scavenging) not included in the GOCART bulk aerosol scheme. The 8-bin MOSAIC sectional aerosol scheme is 1.8 times slower than the 3-mode Modal Aerosol Dynamics Model for Europe (MADE) (Ackermann *et al* 1998) modal aerosol scheme while containing 2.7 times more prognostic chemical species (Fast *et al* 2011). The MOSAIC 4-bin aerosol scheme is less computationally demanding relative to the 8-bin scheme, while still skilfully simulating PM_{2.5} mass over India (Sarangi *et al* 2015, Kumar *et al* 2015b). In this thesis, the MOZART-MOSAIC 4-bin without subgrid convective aqueous chemistry was implemented throughout, due to the balance of detailed aerosol and trace gas processes with computational efficiency. There are uncertainties within MOSAIC, such as aerosol shape and morphology, assumed chemical species density, assumed refractive indices, and the conversion factor between OM and OC (Barnard *et al* 2010).

2.2.4. Emissions

Anthropogenic emissions for 2010 were taken from the Emission Database for Global Atmospheric Research with Task Force on Hemispheric Transport of Air Pollution (EDGAR-HTAP) version 2.2 at $0.1^\circ \times 0.1^\circ$ horizontal resolution (Janssens-Maenhout *et al* 2015). EDGAR-HTAP v2.2 uses the Model Intercomparison Study for Asia Phase III (MIX), which is a mosaic of Asian anthropogenic emission inventory (Li *et al* 2017b). For India, MIX uses the Indian emission inventory provided by the Argonne National Laboratory (Lu *et al* 2011, Lu and Streets 2012) for SO₂, BC, and OC for all sectors, as well as NO_x for power plants, and Regional Emission inventory in Asia (REAS) version 2.1 (Kurokawa *et al* 2013) for other species. The bottom-up global emission inventory EDGAR v4.3 filled gaps in EDGAR-HTAP v2.2 (Janssens-Maenhout *et al* 2015). Emissions include PM_{2.5}, PM₁₀, SO₂, NO_x, CO, NMVOC, NH₃, BC, and OC (Janssens-Maenhout *et al* 2015). Emissions are classified by source sector: aviation, shipping, power generation (ENE), industrial non-power (IND), land transport (TRA), residential energy use (RES), and agriculture (AGR) (Janssens-Maenhout *et al* 2015). Power generation emissions for the energy sector are from electricity and heat production. Industrial non-power emissions include large-scale combustion and industrial processes. Emissions from residential energy use categorised in EDGAR-HTAP v2.2 comprise small-scale combustion devices for heating, cooking, lighting, and cooling in addition to supplementary engines for residential, commercial, agricultural, solid waste, and wastewater treatment (Janssens-Maenhout *et al* 2015). In India, residential emissions are primarily from cooking. Residential energy use emissions of PM_{2.5}, BC, and OC, were qualitatively classified as highly uncertain within EDGAR-HTAP v2.2 (Janssens-Maenhout *et al* 2015). Seasonal cycles were derived from monthly activity data for power generation, industrial non-power, and all transport sectors, while residential energy use depends on regional monthly-mean temperature (Lu *et al* 2011). EDGAR has been found to simulate air

quality well over South Asia using WRF-Chem relative to other anthropogenic emission inventories (Saikawa *et al* 2017). Emissions from EDGAR-HTAP v2.2 were chosen over ECLIPSE due to higher spatial resolution in EDGAR-HTAP v2.2 ($0.1^\circ \times 0.1^\circ$ relative to $0.5^\circ \times 0.5^\circ$), that ECLIPSE underestimated BC and trace gas emission magnitudes and had inaccuracies in their spatial distribution over India (Stohl *et al* 2015, Klimont *et al* 2017), and that simulations using EDGAR emissions estimate PM closer to observations over India (Saikawa *et al* 2017).

Biomass burning emissions were taken from the Fire Inventory from NCAR (FINN) version 1.5 bottom-up inventory using burned area estimates (Wiedinmyer *et al* 2011). Biomass burning emissions are from the open burning of biomass including wildfires, agricultural fires, and prescribed fires, and not biofuel use and trash burning (Wiedinmyer *et al* 2011). FINN uses daily, 1 km resolution, global estimates of gas and aerosol emissions from satellite observations of active fires and land cover with updated emission factors and estimated fuel loadings (Akagi *et al* 2011). FINN fire emissions were used over the Global Fire Emissions Database (GFED) fire emissions as FINN has higher spatial resolution and better captures small fires (Reddington *et al* 2016, Randerson *et al* 2012). However, it is likely that emissions from agricultural fires are still underestimated (Cusworth *et al* 2018).

Biogenic emissions were calculated online by the Model of Emissions of Gases and Aerosol from Nature (MEGAN) (Guenther *et al* 2006) online canopy model. MEGAN is driven by 1 km satellite measurements of land use (Guenther *et al* 2006). MEGAN estimates the net emission of 134 gases and aerosols from terrestrial ecosystems (Guenther *et al* 2006). MEGAN is recommended to be used with the updated gas-phase mechanism of MOZART-4 as it speciates biogenic VOCs online (Hodzic and Knote 2014).

Dust emissions were calculated online through GOCART with Air Force Weather Agency (AFWA) modifications based on wind speed and land surface characteristics (Legrand *et al* 2018, Chin *et al* 2000, Ginoux *et al* 2001, Jones *et al* 2012, 2010, Su and Fung 2015, Kok 2011). The AFWA modifications are based on dust emission parameterisations from Marticorena and Bergametti (1995) with ten saltation size bins and five dust size bins (0–2 μm , 2–3.6 μm , 3.6–6 μm , 6–12 μm , and 12–20 μm) (Legrand *et al* 2018). GOCART AFWA dust emissions were chosen over GOCART dust emissions due to updated physics, over the MOSAIC and MADE/SORGAM dust emissions option due to errors, and over the GOCART dust emissions with University of Cologne (UOC) modifications due to lack of testing (Legrand *et al* 2018).

MOZART-4 / Goddard Earth Observing System Model version 5 (GEOS5) 6-hourly simulation data were used for chemical and aerosol boundary conditions (National Center for Atmospheric Research 2016), which were interpolated onto the WRF-Chem domain using the mozbc preprocessor. The species map within mozbc defines the speciation of initial and boundary

chemistry conditions from MOZART-4 with an assumed size distribution, as MOZART-4 used a bulk scheme for 12 aerosol compounds.

Monthly files were concatenated to annual files for use with the preprocessor `anthro_emiss`. Within `anthro_emiss`, emissions preprocessing was set up for a modal aerosol scheme, MADE (Ackermann *et al* 1998), and mapping splits these to the appropriate size bin. The `anthro_emiss` preprocessor outputs two datasets per domain for 00 and 12 hours Coordinated Universal Time (UTC). Preprocessors map unspiciated $PM_{2.5}$ from emission input files to other inorganics after subtracting all known aerosol. A similar process happens for PM_{10} , where the mass is the difference between PM_{10} and $PM_{2.5}$ only. Within the `fire_emiss` preprocessor, emissions were mapped directly onto WRF-Chem MOSAIC aerosol bins, avoiding double counting, and the size distribution were calculated online.

2.3. Exposure-response function for long-term ambient $PM_{2.5}$ exposure

Long-term (annual) average exposures to ambient $PM_{2.5}$ concentrations were associated with a relative risk of disease estimated through the integrated exposure-response (IER) functions (Burnett *et al* 2014). The IER functions (Burnett *et al* 2014), developed as part of GBD2010 (GBD 2010 Risk Factors Collaborators 2012), represent a significant advance in estimating risk from $PM_{2.5}$ exposure. The IER functions combine epidemiological evidence from ambient air pollution, household air pollution, second-hand smoking, and active smoking to estimate the health response to exposures across a widened range of pollutant concentrations (Burnett *et al* 2014). Exposures to $PM_{2.5}$ increase from ambient air pollution to second-hand smoking, household air pollution from solid fuel combustion, and active smoking (Pope III *et al* 2018). The IER functions enable the estimation of risk factor across the global concentration range of ambient $PM_{2.5}$ (Burnett *et al* 2014). The IER functions assume that $PM_{2.5}$ is an appropriate indicator of risk and that epidemiological data is valid across populations (Ostro *et al* 2018). There are individual IER functions per cause of COPD, IHD, CEV, LRI, and LC. The IER functions primarily use epidemiological data from cohort studies from the United States, Europe, and parts of Asia.

Relative risks (RR) are the ratio of the probability of a health endpoint occurring in a population exposed to a level of pollution, to the probability of that same health endpoint occurring in a population that is not exposed. An RR of one represents no increase in risk. RRs for individual health conditions vary due to differences in approach, exposure estimates, and the mechanisms linking exposures to the health condition (Burnett *et al* 2014, Pope III *et al* 2011). The IER functions use age-specific modifiers for each disease to estimate the RR of mortality associated with ambient $PM_{2.5}$ concentrations (z), as shown in Equation 1. The maximum risk is $1 + \alpha$, the ratio of the IER at low to high concentrations is β , and the power of the $PM_{2.5}$ concentration is γ . Parameter distributions of α , β , and γ were sampled for 1,000 simulations to derive the mean IER function with 95% uncertainty intervals.

$$RR(z) = 1 + \alpha \times \left(1 - \exp\left\{ \beta(z - z_{cf})^\gamma \right\} \right)$$

Equation 1: Integrated exposure-response (IER) functions to estimate long-term relative risk from PM_{2.5} exposure (Burnett *et al* 2014).

IERs are non-linear, especially for cardiovascular diseases (IHD and CEV), where the relative change in RR increases at lower PM_{2.5} concentrations (Burnett *et al* 2014, Bruce *et al* 2014). Consequently, substantial health improvements are only realised at the lowest exposures (Cohen *et al* 2017). The IER functions have large uncertainties within the 30–100 µg m⁻³ PM_{2.5} concentration range, due to limited epidemiological evidence for cardiovascular mortality from ambient PM_{2.5} exposure and a small number of studies of second-hand smoke exposure (Jerrett 2015). The IER functions have been found to underestimate risk over the PM_{2.5} concentration exposure range experienced in China (Yin *et al* 2017) and for infant LRI in Sub-Saharan Africa (Heft-Neal *et al* 2018). IERs are based on the assumptions of equitoxicity of PM_{2.5} from different sources, that PM_{2.5} adequately represents risk from combustion mixtures, and that health outcomes are sufficiently similar across exposure sources and settings (Bruce *et al* 2015b, Burnett *et al* 2014). In contrast to the IERs, there are other exposure-response relationships (e.g. log-linear) that have been used in various studies (Anenberg *et al* 2011, 2010, Cohen *et al* 2005, Apte *et al* 2015b).

The IER functions estimate the age and disease-specific RR for each ambient PM_{2.5} concentration. There are IERs for each health condition (LRI, CEV, COPD, IHD, and LC), where the parameter combinations are updated with additional epidemiological evidence for each release of the GBD project (2010, 2013, 2015, and 2016). The GBD2015 IER (GBD 2015 Risk Factors Collaborators 2016a, Cohen *et al* 2017) was used in Chapter 4, and the GBD2016 IER (GBD 2016 Risk Factors Collaborators 2017) was used in Chapter 5. Both the IER functions from GBD2015 and GBD2016 have uniform theoretical minimum risk exposure levels (z_{cf}) for PM_{2.5} of 2.4 µg m⁻³. However, it is accepted that there is no safe population-level threshold of exposure to PM_{2.5} (World Health Organization 2006a). Figure 22 compares the GBD2015 and GBD2016 IER. The response of RR to PM_{2.5} exposure is very similar between GBD2015 and GBD2016 for the respiratory diseases (COPD and LRI) and LC. For the GBD2016, the RR for cardiovascular diseases (IHD and CEV) reduces relative to the RR in GBD2015. The GBD2015 requires age groupings from LRI for early-, late-, and post-neonatal, and populations between 1 and 80 years upwards in 5-year groupings. The GBD2015 requires age groupings from IHD, CEV, COPD, and LC for adults over 25 years old, split into 5-year age groups. The GBD2016 requires age groupings split into 5-years from 25 to 95 years and upwards for all diseases, in addition to 0 to 25 years for LRI.

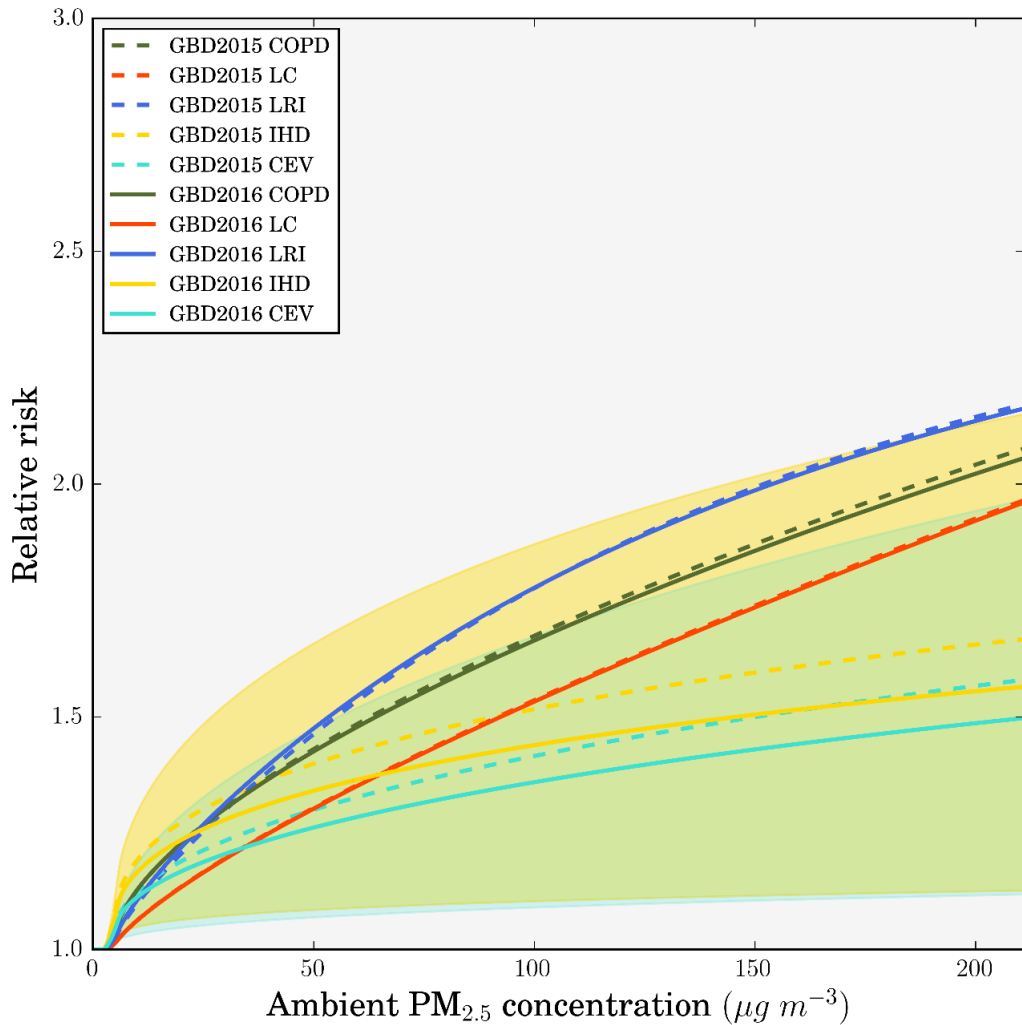


Figure 22: Integrated-exposure response (IER) functions estimating the relative risk (RR) of mortality from ambient $PM_{2.5}$ concentrations from Global Burden of Diseases, Injuries, and Risk Factors Study (GBD) 2015 (GBD 2015 Risk Factors Collaborators 2016b) and GBD2016 (GBD 2016 Risk Factors Collaborators 2017). Mean exposure-response shown in bold line for ischaemic heart disease (IHD), cerebrovascular disease (CEV), chronic obstructive pulmonary disease (COPD), lower respiratory infections (LRI), and lung cancer (LC). IHD and CEV have shaded regions representing the variation between age groups.

Premature mortality (M) was estimated as a function of population (P), baseline mortality rates (I), and the attributable fraction (AF) for a specific RR (Equation 2). The population data used is discussed in Section 2.5. To be consistent with the GBD, country and disease-specific baseline mortality rates from the GBD study (Institute for Health Metrics and Evaluation 2018) in 5-year groupings for both genders combined were used from GBD2015. In Chapters 5 and 6, baseline mortality rates were from the International Futures model as discussed in Section 2.5. A sensitivity study was performed in Chapter 4 using state-specific baseline mortality rates from Chowdhury and Dey (2016) for India accounting for socioeconomic variations across the country through using GDP as a proxy applied to WHO statistics from 2011 (World Health Organization

2011). The sensitivity study applied the state-to-nation ratios from the state-specific baseline mortality rates to the GBD2015 baseline mortalities for COPD, IHD, and CEV. Baseline mortality for LC did not exhibit any relation with GDP, and they did not study LRI. Accordingly, the GBD2015 values were directly used for these diseases. This was done for mean, upper, and lower confidence intervals.

$$M = P \times I \times AF = P \times I \times (RR - 1) / RR$$

Equation 2: Long-term premature mortality from $PM_{2.5}$ exposure.

Years of life lost (YLL) for each age and disease were estimated as a function of premature mortality and age-specific life expectancy (LE) from the standard reference life table from the GBD (Equation 3). The standard reference life table was used from GBD2015 (Global Burden of Disease Study 2015 2016b) in Chapter 4 and GBD2016 in Chapters 5 and 6 (Global Burden of Disease Study 2016 2017b). Applying country-specific life expectancy values (Ministry of Statistics and Programme Implementation 2016) from the Government of India in 2014 reduced YLL by 60% relative to using the GBD2015 LE values. The GBD normative standard life table was used for the main YLL results to be consistent with the extensive work done on this issue by the GBD project. The GBD project in 2010 developed the normative standard life table after consultation with philosophers, ethicists, and economists to compute YLL at each age by identifying the lowest observed death rate for any age group in countries of more than 5 million in population (Murray *et al* 2012). Two principles behind the decision were that the only differences in the rating of death or disability should be due to age and that everyone in the world has the right to best life expectancy in the world. The GBD India-specific study used the same GBD normative standard life table (India State-Level Disease Burden Initiative Collaborators 2017).

$$YLL = M \times LE$$

Equation 3: Long-term years of life lost from $PM_{2.5}$ exposure.

The GBD meta-analyses estimates for $PM_{2.5}$ risks include studies from India for *household* air pollution, but no epidemiologic studies exist for *long-term ambient* $PM_{2.5}$ exposure in India. Recent epidemiological studies in India, supported by the Indian Council of Medical Research (ICMR) and the European Research Council, are underway to analyse the health impacts of long-term exposure to ambient and household air pollution (Tonne *et al* 2017, Balakrishnan *et al* 2015). The IER functions are required for risk assessments in locations where the risk of exposure to air pollution is high, and there are little data on long-term epidemiological studies, such as India. The lack of locally-derived exposure-response functions has impeded previous risk assessment attempts to impact local policy in India (The World Bank 1995, Health Effects Institute Public Health and Air Pollution in Asia Program 2011).

Only a few short-term time-series studies of mortality and air pollution have been conducted in India (Figure 23). The first by Cropper *et al* (1997) for Delhi in 1997 found the excess risk of mortality to be $0.23\% \pm 0.1$ per $10 \mu\text{g m}^{-3}$ increase in total suspended PM concentrations. Nidhi (2008) found risk estimates of 0.6% for hospital admissions per $10 \mu\text{g m}^{-3}$ increase in respiratory suspended particulate matter in Delhi. Two Indian epidemiological studies of short-term PM_{10} exposure exist from the Public Health and Air Pollution in Asia (PAPA) study (Health Effects Institute Public Health and Air Pollution in Asia Program 2011). The Delhi study reported an all-cause risk estimate of 0.15% (95UI: 0.07–0.23) per $10 \mu\text{g m}^{-3}$ increase in PM_{10} concentrations (Health Effects Institute Public Health and Air Pollution in Asia Program 2011). The Chennai study reported an all-cause risk estimate of 0.44% (95UI: 0.17–0.71) per $10 \mu\text{g m}^{-3}$ increase in PM_{10} concentrations (Health Effects Institute Public Health and Air Pollution in Asia Program 2011). Dholakia *et al* (2014) studied five Indian cities for all-cause mortality from PM_{10} exposure and found risk estimates in Shimla of 1.36% (95UI: -0.38–3.1), in Ahmedabad of 0.16% (95UI: -0.31–0.62), in Bangalore of 0.22% (95UI: -0.04–0.49), in Hyderabad of 0.85% (95UI: 0.06%–1.63%), and in Mumbai of 0.2% (95UI: 0.1–0.3). Maji *et al* (2017) estimated risks of 0.14% (95UI: 0.02%–0.26%) for daily all-cause-mortality per $10 \mu\text{g m}^{-3}$ increase in PM_{10} in Delhi. Dholakia *et al* (2014) found more polluted cities had lower relative risks than clean cities, consistent with the non-linear exposure-response function for long-term exposure to $\text{PM}_{2.5}$. Pande *et al* (2018) spatially extrapolated these relative risks for short-term PM_{10} exposure across India. Maji *et al* (2017) also found higher risks at lower PM concentrations, with risk estimates of 0.38% per $10 \mu\text{g m}^{-3}$ increase in PM_{10} concentrations up to $100 \mu\text{g m}^{-3}$, and risk estimates of 0.13% for higher concentrations. Maji *et al* (2018) found hospital admissions increased by 0.47% (95UI: 0.03%–0.91%) per $10 \mu\text{g m}^{-3}$ increase in PM_{10} concentrations in Delhi. The only work analysing $\text{PM}_{2.5}$ was published in 2018 by Balakrishnan *et al* (2018) who studied pregnant mothers in an integrated rural-urban cohort in Tamil Nadu and found a 4 g (95UI: 1.08–6.76) decrease in birth weight and 2% (95UI: 0.5–4.1) increase in the prevalence of low birthweight per $10 \mu\text{g m}^{-3}$ increase in $\text{PM}_{2.5}$ concentrations. Kumar *et al* (2010b) associated air quality indicated through visibility reductions per 1 km to increase mortality by natural causes by 2.4% (95UI: 1.8–3.0).

Overall, the effects of short-term exposure in Indian cities are on a par with those observed in hundreds of studies worldwide (0–2% per $10 \mu\text{g m}^{-3}$ increase in PM concentrations, with excess risk reducing at higher PM concentrations) (Health Effects Institute International Scientific Oversight Committee 2010), which form the basis of the exposure-response functions used by the GBD and this thesis.

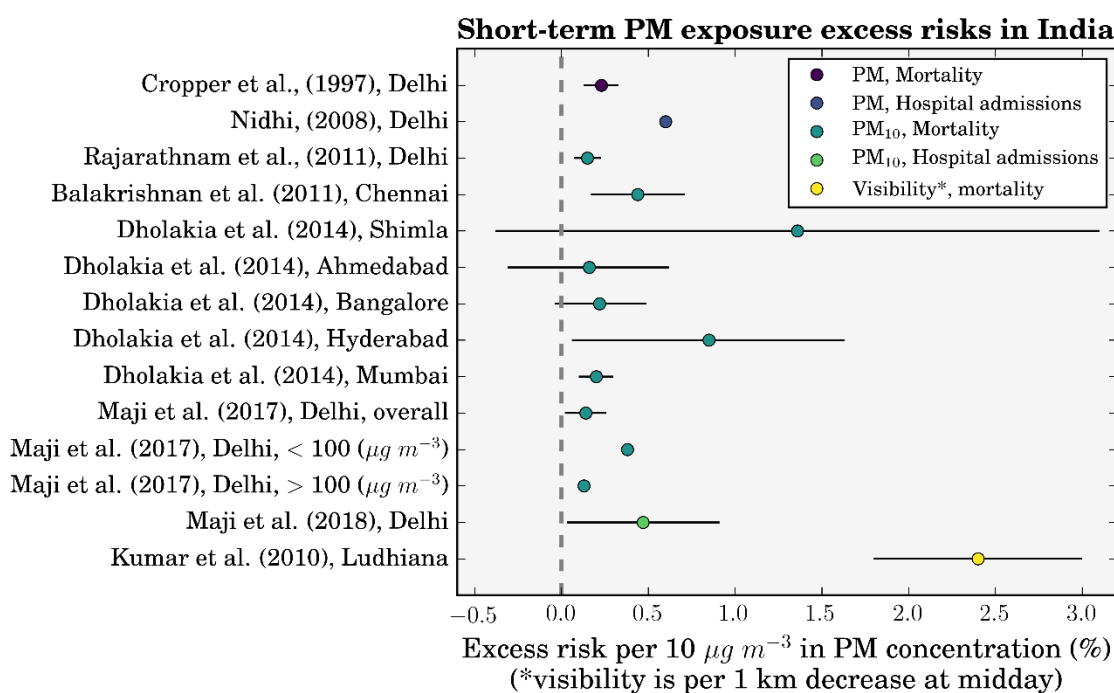


Figure 23: Short-term PM and PM₁₀ exposure excess risk estimates in India.

2.4. Exposure-response function for long-term ambient O₃ exposure

The disease burden associated with COPD from ambient O₃ exposure was estimated using relative risk (RR) estimates from the earlier American Cancer Society Cancer Prevention Study II (CPS-II) study from Jerrett *et al* (2009), in addition to the updated CPS-II study from Turner *et al* (2016). The updated CPS-II study derived RR estimates from a larger study population (+49%), studying twice as many deaths during a longer follow up period (+22%). The updated CPS-II study used improved exposure estimates and found the hazard ratios (HR) for respiratory mortality increased. The earlier CPS-II study found HR per 10 ppb for respiratory mortality after adjusting for PM_{2.5} confounding of 1.04 (95UI: 1.01–1.07), while the updated CPS-II study found HR for COPD mortality after adjusting for PM_{2.5} and NO₂ confounding of 1.14 (95UI: 1.08–1.21). The updated CPS-II study found through sensitivity analyses that the long-term O₃ health impacts are not confounded by socioeconomic status or modelling approach. To be consistent with the GBD, premature mortality was estimated from the risk of ambient O₃ exposure from the cause of COPD only. The GBD used the earlier CPS-II study risks with 3-month average daily maximum 1-hour O₃ concentrations (3mDMA1), while the updated CPS-II study used annual average daily maximum 8-hour O₃ concentrations (ADM8h). Both the earlier (Jerrett *et al* 2009) and updated (Turner *et al* 2016) RR estimates were used, with the corresponding O₃ metric. No epidemiologic studies exist for long-term O₃ exposure in India.

Premature mortality associated with O₃ exposure (M) was estimated for COPD for adults over 25 years of age (as per GBD) following Equation 4. Mortality was a function of the baseline mortality rate (I), attributable fraction (AF), and the exposed population (P) per age group. The

AF was a function of the effect estimate (β) and the change in O_3 concentrations (ΔX) relative to the low-concentration cut-off (LCC), given in Equation 5. Both the earlier and updated CPS-II study AF functions were given in Figure 24, clearly showing the impact of the increased HR for the updated CPS-II study. The exposure-response function for the updated CPS-II is more non-linear, relative to the earlier CPS-II function, where there are larger changes in risk for low concentrations compared with higher concentrations (Pope III *et al* 2015).

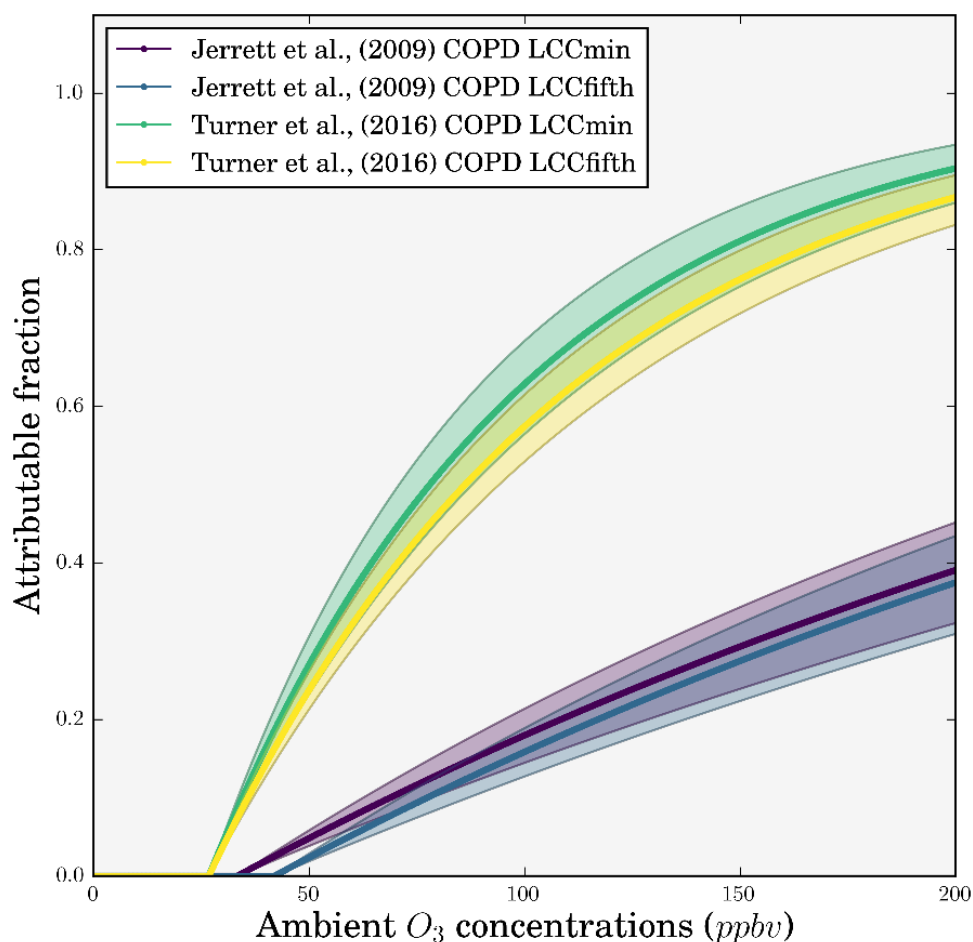


Figure 24: *Attributable fractions as a function of ambient O_3 concentrations for chronic obstructive pulmonary disease (COPD) from both the earlier American Cancer Society Cancer Prevention Study II (CPS-II) (Jerrett *et al* 2009) and the updated CPS-II study (Turner *et al* 2016). Mean (solid line) as well as upper and lower 95% confidence intervals (shading) shown for both low-concentration cut-offs (LCC_{min} and LCC_{fifth}).*

Two LCCs represent uncertainty in the HR as either the minimum exposure (LCC_{min}) or the fifth percentile (LCC_{fifth}), whereby if the O_3 concentration is below the LCC there is no effect of O_3 exposure on mortality and ΔX equals zero. The earlier CPS-II study (Jerrett *et al* 2009) used the minimum and fifth percentile LCCs of 33.3 ppb and 41.9 ppb, respectively, while the updated CPS-II study (Turner *et al* 2016) used the minimum and fifth percentile LCCs of 26.7 ppb and 31.1 ppb, respectively. Epidemiological studies generally find little evidence for low concentration thresholds, and disease burden estimates using thresholds will, therefore, be

conservative (U.S. Environmental Protection Agency 2013b). β is the natural log of the HR for a 10 ppb increase in long-term O₃ exposure (Equation 6). To account for uncertainty in the RR estimates, 1,000 estimates of β were sampled from normal distributions of β using 95% uncertainty intervals to derive a distribution of the AF. YLL were estimated in the same way as detailed in Section 2.3, using the standard reference life table from GBD2016 (Global Burden of Disease Study 2016 2017b).

$$M = I \times AF \times P$$

Equation 4: Long-term premature mortality from O₃ exposure.

$$AF = 1 - e^{-\beta \Delta X}$$

Equation 5: Long-term attributable fraction from O₃ exposure.

$$\beta = \frac{\ln(HR)}{10}$$

Equation 6: Long-term hazard ratio from O₃ exposure.

A couple of previous epidemiological studies have researched the health impacts of short-term O₃ exposure in Delhi, India. Nidhi (2008) and Maji *et al* (2018) found short-term risk estimates of 3.3% and 3.41% (95UI: 0.02%–6.83%), respectively, for hospital admissions per 10 $\mu\text{g m}^{-3}$ increase in O₃ in Delhi. Maji *et al* (2017) estimated risks of 0.31% (95UI: 0.05%–0.57%) for daily all-cause-mortality per 10 $\mu\text{g m}^{-3}$ increase in O₃ concentrations in Delhi. These mortality risks, although for all-cause and Delhi only, are larger than corresponding risks recommended by the WHO (0.29%) (Héroux *et al* 2015) and Turner *et al* (2016) (0.2%) which are in line with the estimates used in this thesis. This suggests the estimates in this thesis are conservative.

2.5. Current and future population of India

For Chapter 4, present-day population density data for 2015 was obtained at $0.25^\circ \times 0.25^\circ$ resolution from the Gridded Population of the World, Version 4 (GPWv4), created by the Centre for International Earth Science Information Network (CIESIN) and accessed from the National Aeronautics and Space Administration (NASA) Socioeconomic Data and Applications Centre (SEDAC) (Center for International Earth Science Information Network and NASA Socioeconomic Data and Applications Center 2016b). The United Nations adjusted version was implemented for 2015 with a total population of 1.302 billion in India. Shapefiles were used to split data per state within India from Spatial Data Repository, The Demographic and Health Surveys Program (ICF International n.d.) and the GADM database of Global Administrative Areas version 2.8 (Hijmans *et al* 2016). Chapter 4 includes rural and urban splits, where urban areas were defined as having a population density of at least 400 persons' km^{-2} , as used in previous studies (Lelieveld *et al* 2015). Population age composition was taken from the GBD2015 population estimates for 2015 for Chapter 4 (Global Burden of Disease Study 2015 2016a). The

GPWv4 national identifier grid (Center for International Earth Science Information Network and NASA Socioeconomic Data and Applications Center 2016a) was used to allocate data by country.

For Chapters 5 and 6, present day (2015) and future (2050) population density, population age structure, and baseline mortality rates for COPD, IHD, CEV, LC, and LRI were obtained from the International Futures (IFs) integrated modelling system (Hughes *et al* 2011) base case scenario (Hughes *et al* 2012). The IFs base case scenario forecasts a range of global transitions in human development including increasing incomes, education, health, infrastructure, governance, and productivity that are continuous with historical patterns, include non-linear relationships, and exclude large disruptive changes (Hughes *et al* 2012). Figure 25 shows the variation in baseline mortality, population age distribution, and population density for India between 2015 and 2050. Baseline mortality rates for all diseases in India show reductions in 2050 relative to 2015, primarily for LRI, CEV, and IHD where there are substantial decreases. The baseline mortality rate for COPD reduces slightly in 2050 relative to 2015 for age groupings 60 years and older. The population age distribution shifts towards older ages (40 years and older), and there is considerable population growth, particularly across the IGP.

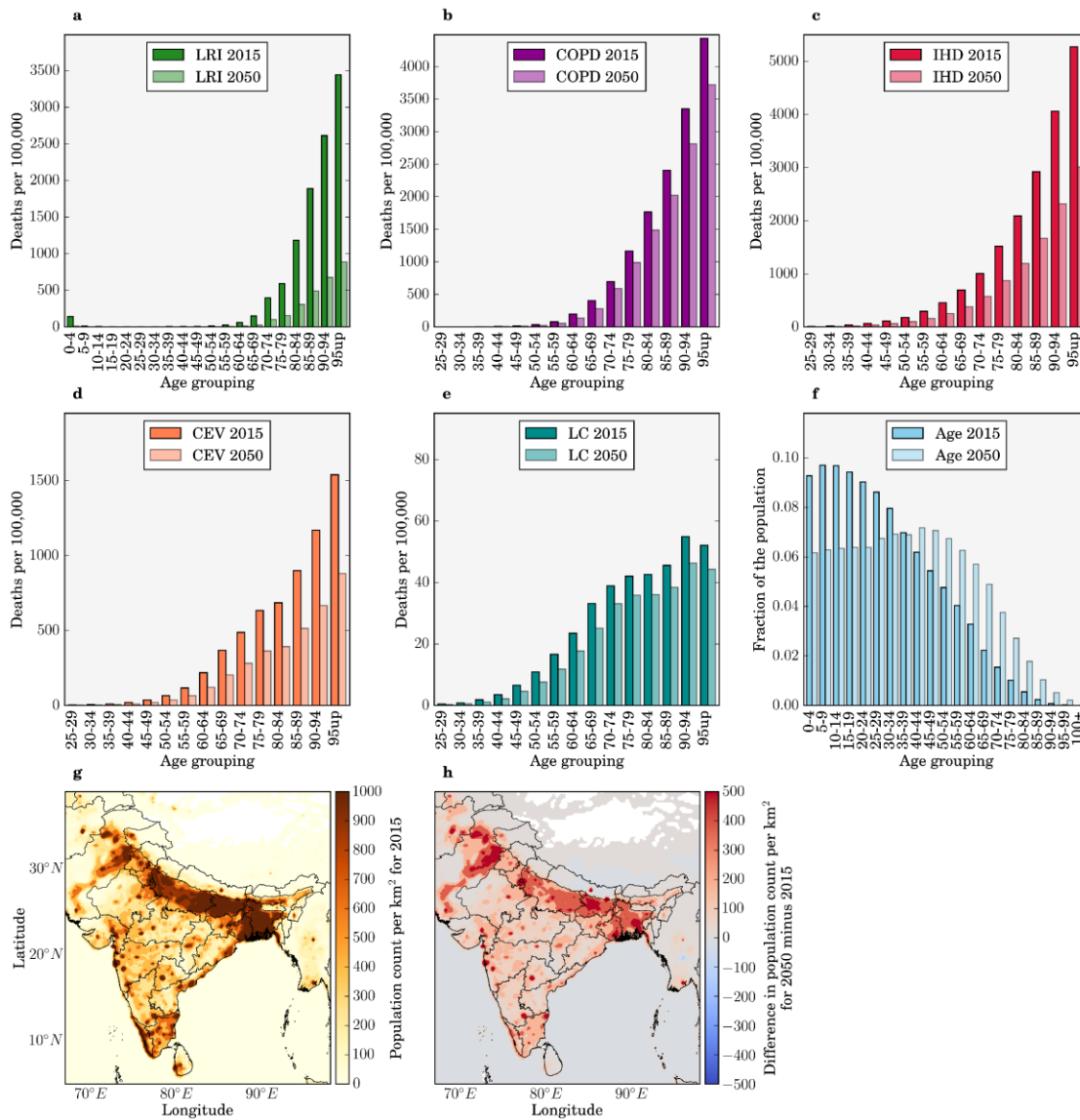


Figure 25: Change in baseline mortality, population age distribution, and population density for India between 2015 and 2050 from the International Futures (IFs) integrated modelling system (Hughes *et al* 2011) baseline scenario. Baseline mortality rates for (a) lower respiratory infections (LRI), (b) chronic obstructive pulmonary disease (COPD), (c) ischaemic heart disease (IHD), (d) cerebrovascular disease (CEV), and (e) lung cancer (LC) in 2015 and 2050. (f) Population age distribution. (g) Spatial distribution of population density in 2015 for South Asia. (h) Change in population density for South Asia between 2050 and 2015.

Figure 26 shows the difference in baseline mortality, population age distribution, and population density for India in 2015 between IFs (Hughes *et al* 2011) and the GBD2016 (GBD 2016 Risk Factors Collaborators 2017). IFs population density for India in 2015 is very similar to the GPWv4 (10,000 smaller population in IFs out of 1.3 billion, primarily across the IGP) (Center for International Earth Science Information Network and NASA Socioeconomic Data and Applications Center 2016b). IFs population age groupings for India is similar to the population age structure used by the GBD2016 (Global Burden of Disease Study 2016 2017a). Baseline

mortality rates below 65 years of age are similar for all diseases between IFs and GBD2016 (Institute for Health Metrics and Evaluation 2018), while above 65 years of age IFs has larger values for respiratory diseases (LRI and COPD) and smaller for cardiovascular diseases (IHD and CEV) and LC relative to the GBD2016. The baseline mortality rate for COPD in 2015 from IFs is slightly larger than the corresponding rate from GBD2016 (Institute for Health Metrics and Evaluation 2018) for age groupings 75 years and older.

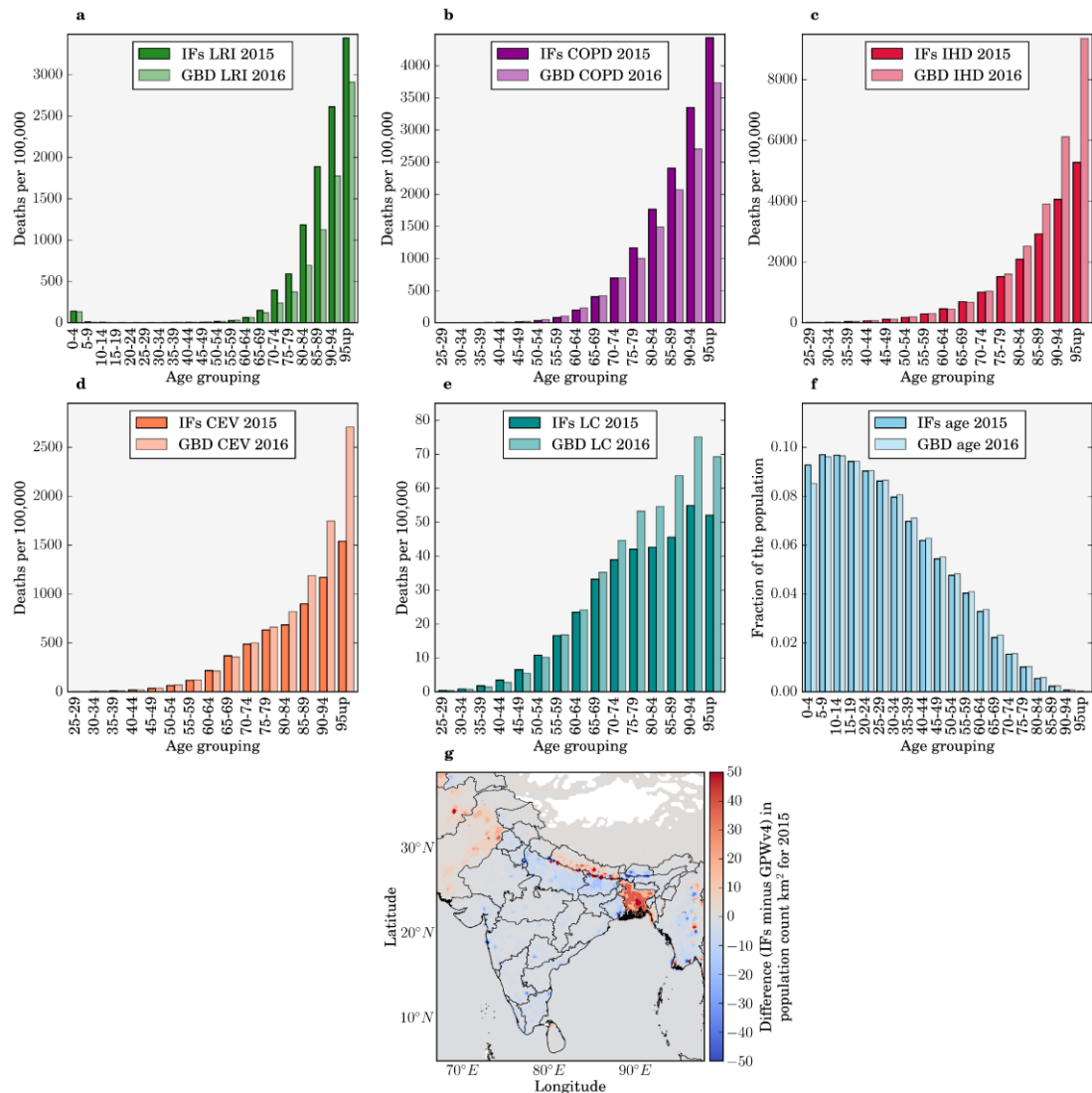


Figure 26: Variation in baseline mortality, population age distribution, and population density for India in 2015 between the International Futures (IFs) integrated modelling system (Hughes et al 2011) baseline scenario and data used in GBD2016 (GBD 2016 Risk Factors Collaborators 2017). Baseline mortality rates for (a) lower respiratory infections (LRI), (b) chronic obstructive pulmonary disease (COPD), (c) ischaemic heart disease (IHD), (d) cerebrovascular disease (CEV), and (e) lung cancer (LC) in 2015 from IFs and GBD2016 (Institute for Health Metrics and Evaluation 2018). Note that for LRI, IFs provides age group 0–4 while GBD2016 provides age group 0–5. (f) Population age distribution in 2015 from IFs and GBD2016 (Global Burden of Disease Study 2016 2017a). (g) The difference in population density

for South Asia in 2015 from IFs and Gridded Population of the World, Version 4 (GPWv4) (Center for International Earth Science Information Network and NASA Socioeconomic Data and Applications Center 2016b).

2.6. Sector-specific disease burden

There are two main methods for estimating the sectoral contributions to premature mortality from ambient air pollution exposure, each giving greatly different results (Kodros *et al* 2016). The subtraction (or zero-out) method calculates the sector-specific mortality (M_{SECTOR}) as the difference between the all-source premature mortality estimate from all sources (M_{ALL}) and the premature mortality estimate based on a model simulation where the emission sector has been removed (M_{SECTOR_OFF}) as in Equation 7 (Silva *et al* 2016b, Kodros *et al* 2016, Chambliss *et al* 2014).

$$M_{SECTOR} = M_{ALL} - M_{SECTOR_OFF}$$

Equation 7: Sector-specific premature mortality following the subtraction method.

Alternatively, the attribution method first calculates the fractional sectoral reduction in $PM_{2.5}$ concentrations from removing an emission sector ($PM_{2.5_SECTOR_OFF}$) and then uses this fraction to scale the total premature mortality estimate (Equation 8) (GBD MAPS Working Group 2016, Lelieveld *et al* 2015, Chafe *et al* 2014a, Kodros *et al* 2016, Archer-Nicholls *et al* 2016, Lelieveld 2017).

$$M_{SECTOR} = M_{ALL} \left(\frac{PM_{2.5_ALL} - PM_{2.5_SECTOR_OFF}}{PM_{2.5_ALL}} \right)$$

Equation 8: Sector-specific premature mortality following the attribution method.

The two methods answer different questions: the attribution method estimates the number of premature mortalities that could be attributed to a sectors' emissions, while the subtraction method estimates the reduction in premature mortalities that could be achieved by removing the sectors' emissions. The non-linear exposure-response relationships mean these two methods give different estimates. Chapters 4 and 6 use and compare both methods when estimating sector-specific disease burdens.

2.7. Uncertainties

Uncertainty intervals at the 95% level (95UI) were estimated through combining fractional errors in quadrature (i.e. square root of the sum of squares) from two standard deviations of weekly $PM_{2.5}$ or daily O_3 concentrations per grid cell, the derived uncertainty intervals for the exposure-response functions, and the provided uncertainties in baseline mortality rates (Institute for Health Metrics and Evaluation 2018). Applying uncertainties in quadrature results in similar uncertainty ranges ($\pm 50\%$) as when using Monte Carlo analysis (Chen *et al* 2017b, Jain *et al* 2017, Silva *et al* 2016b, Liu *et al* 2009). Uncertainty ranges are only noticeably reduced when using

Bayesian Hierarchical modelling as performed by recent updates to the GBD project (GBD 2015 Risk Factors Collaborators 2016a, GBD 2016 Risk Factors Collaborators 2017, Cohen *et al* 2017). However, the relative uncertainty range for India in the GBD is larger than that for many other countries, due to the lack of ground measurements in India (Ostro *et al* 2018).

Model errors arise through limited physical understanding, parameterisations, numerical errors, and model implementation (Brasseur and Jacob 2016). Model uncertainty arises from stochastic, unresolved processes, and parameter uncertainty (Brasseur and Jacob 2016). Emissions inventories for India have significant uncertainties, especially across the IGP (Janssens-Maenhout *et al* 2015, Saikawa *et al* 2017, Monks *et al* 2015, Jena *et al* 2015a, Karambelas *et al* 2018a, 2018b). Monitoring stations are limited in India and are especially scarce in rural areas (Karambelas *et al* 2018b). Consistent with the GBD project, the toxicity of PM_{2.5} were treated as homogenous regarding source, shape, and chemical composition, due to the lack of composition-dependent exposure-response functions. Disease burden estimates do not account for multiple exposure cases or multipollutant scenarios.

Chapter 5 and 6 estimate future air pollution and associated health impacts using the same meteorology inputs and parameterisations, and hence do not include the impacts of climate changes on air quality, although these changes are likely smaller relative to those driven by emission changes for PM_{2.5} (Pommier *et al* 2018, Silva *et al* 2017, Fang *et al* 2013, Jacobson 2008, Kumar *et al* 2018) and O₃ (Pommier *et al* 2018, Kumar *et al* 2018, Silva *et al* 2017). Consequently, the validity of results is limited to the impacts of projected emission changes in India and do not include impacts of future climate change or impacts of emission changes outside India. Reductions in O₃ precursors in India may reduce O₃ concentrations outside of India, providing public health benefits not accounted for (West *et al* 2009a). Reduced O₃ concentrations will also reduce damage to crops and the economic cost associated with premature mortalities (Ghude *et al* 2014, 2016, Sinha *et al* 2015), as well as providing substantial climate co-benefits (Shindell *et al* 2012).

3. Model evaluation

Model evaluation is critical to validate, verify, and estimate model skill in simulating reality (Brasseur and Jacob 2016). Model evaluations use observations as reality (Brasseur and Jacob 2016). Observations are either in-situ or remote, short- or long-term, active or passive, and can be systematically- or randomly-biased relative to reality (Brasseur and Jacob 2016). This section evaluates a WRF-Chem model simulation for 2014. In Section 3.1, the metrics are defined. In Section 3.2, the meteorology is evaluated. In section 3.3, surface PM_{2.5} concentrations are evaluated. In Section 3.4, aerosol optical depth is evaluated. In Section 3.5, surface O₃ concentrations are evaluated.

3.1. Metrics

Statistical metrics recommended for evaluating air quality models (Yu *et al* 2006) include mean bias (MB), normalised mean bias (NMB), root mean square error (RMSE), normalised mean absolute error (NMAE), and Pearson's correlation coefficient (r). These have been used in previous studies for evaluating regional, air quality models (Emery *et al* 2001, Kumar *et al* 2012b, 2012a, Zhang *et al* 2006). The MB indicates the level of overestimation (positive values) or underestimation (negative values) by the model (Equation 9). N represents the total number of model-observation pair values while M_i and O_i represent the ith model and observed values, respectively. The NMB represents the model bias relative to the observations without being overly influenced by small numbers in the denominator (Equation 10). The RMSE captures the average error produced by the model (Equation 11). The NMAE represents the mean absolute difference between the model and observations relative to the observations (Equation 12). The extent of the linear relationship between model and observations is given by the Pearson's correlation coefficient (Equation 13). The over bars represent the respective mean. MB has the same units as the variable being evaluated, while all other metrics are unit-less. The gradient of best fit is determined using least-squares solution to a linear matrix equation. Model performance benchmarks in simulating meteorology for air quality for temperature are < ± 0.5 K for MB and < 2 K for NMAE, while for wind speed are < ± 0.5 m s⁻¹ for MB and < 2 m s⁻¹ for RMSE (Emery *et al* 2001).

$$MB = \frac{1}{N} \sum_{i=0}^N (M_i - O_i)$$

Equation 9: Mean bias.

$$NMB = \frac{\sum_{i=1}^N (M_i - O_i)}{\sum_{i=1}^N O_i}$$

Equation 10: Normalised mean bias.

$$RMSE = \sqrt{\frac{\sum_{i=1}^N (M_i - O_i)^2}{N}}$$

Equation 11: Root mean squared error.

$$NMAE = \frac{\sum_{i=1}^N |M_i - O_i|}{\sum_{i=1}^N O_i}$$

Equation 12: Normalised mean absolute error.

$$r = \frac{\sum_{i=0}^N (M_i - \bar{M})(O_i - \bar{O})}{\sqrt{\sum_{i=1}^N (M_i - \bar{M})^2 \sum_{i=0}^N (O_i - \bar{O})^2}}$$

Equation 13: Pearson's correlation coefficient.

3.2. Meteorology

The meteorological evaluation was undertaken using the ECMWF global reanalysis products (ERA-Interim) of boundary layer height, precipitation, wind speed, wind direction, and temperature (Dee *et al* 2011). For NWP models in general, there is a dry bias over land in India, suggesting parameterisation issues early in the simulations, while there is a wet bias over the Arabian Sea. Overall, WRF-Chem underestimated precipitation (NMB = -0.66, $r = 0.58$), with a dry bias during the summer monsoon especially over Bangladesh and Myanmar. Precipitation on land was better simulated for winter and spring, in contrast to the model underestimation in summer and autumn across southwest India, central India, and the Bay of Bengal (Figure 27). The underestimation of precipitation during the monsoon may underestimate aerosol washout, and lead to overestimated simulated PM_{2.5} concentrations. The Mellor-Yamada Nakanishi and Niino 2.5 boundary layer physics scheme (Nakanishi and Niino 2006) simulated the spatial variability in seasonal South Asian boundary layer height generally well (NMB = 0.38), apart from model overestimation during winter and spring (Figure 28). The overestimation of boundary layer height may lead to excessive dilution of aerosol, reducing simulated surface PM_{2.5} concentrations. Wind speed and direction was well captured by the model (NMB = 0.09, $r = 0.69$) (Figure 29). The MB of 0.14 m s⁻¹ and RMSE of 0.72 m s⁻¹ are within the performance benchmarks of $< \pm 0.5$ m s⁻¹ for MB and < 2 m s⁻¹ for RMSE. The temperature was well simulated by the model for all seasons (NMB = 0.0, $r = 0.94$) (Figure 30). The NMAE of 0.0 K is within the performance benchmark of < 2 K for NMAE, while the MB of -0.99 K is outside the performance benchmark of $< \pm 0.5$ K

for MB. Simulating temperature accurately is key for O₃ studies, as temperature strongly influences O₃ formation rates. Kumar *et al* (2012a) used WRF-Chem over South Asia, with a similar setup to this study (e.g. Thompson microphysics and RRTM long-wave radiation schemes), and found that WRF simulated meteorology is of sufficient quality for use in air quality simulations.

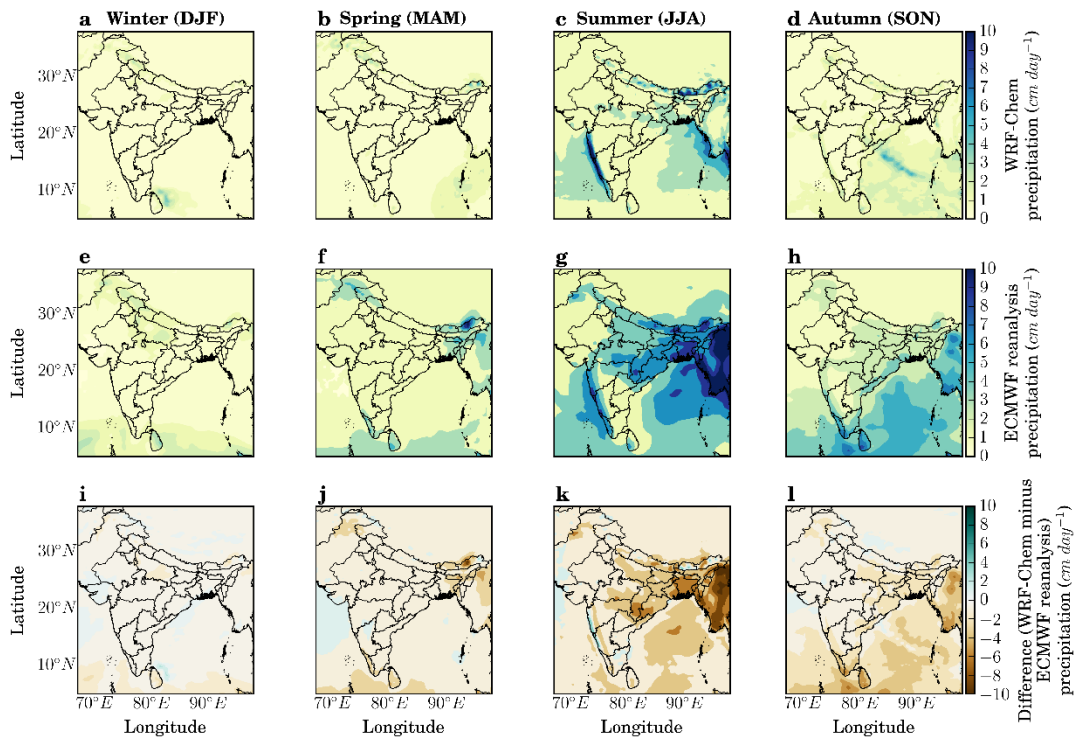


Figure 27: Spatial distribution of seasonal-mean total precipitation for 2014. (a–d) WRF-Chem. (e–h) ECMWF global reanalyses. (i–l) The difference (WRF-Chem minus ECMWF). Results shown for winter through autumn, see labels at the top of the figure.

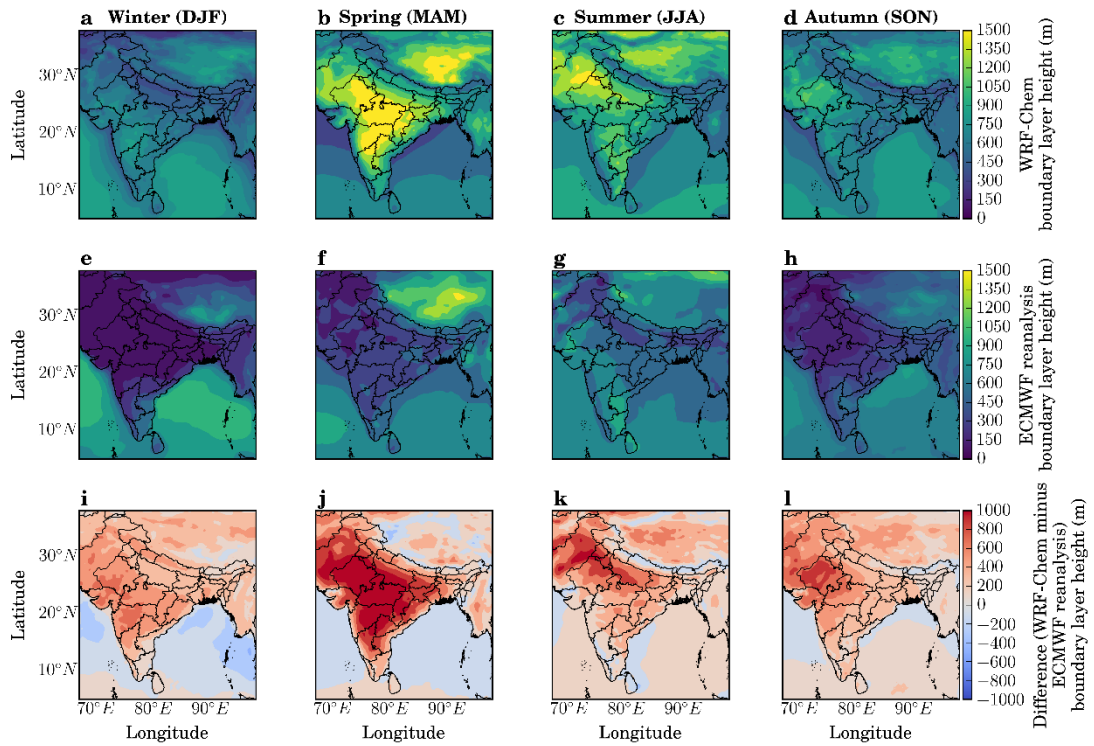


Figure 28: Spatial distribution of seasonal-mean boundary layer height for 2014. (a–d) WRF-Chem. (e–h) ECMWF global reanalyses. (i–l) The difference (WRF-Chem minus ECMWF). Results shown for winter through autumn, see labels at the top of the figure.

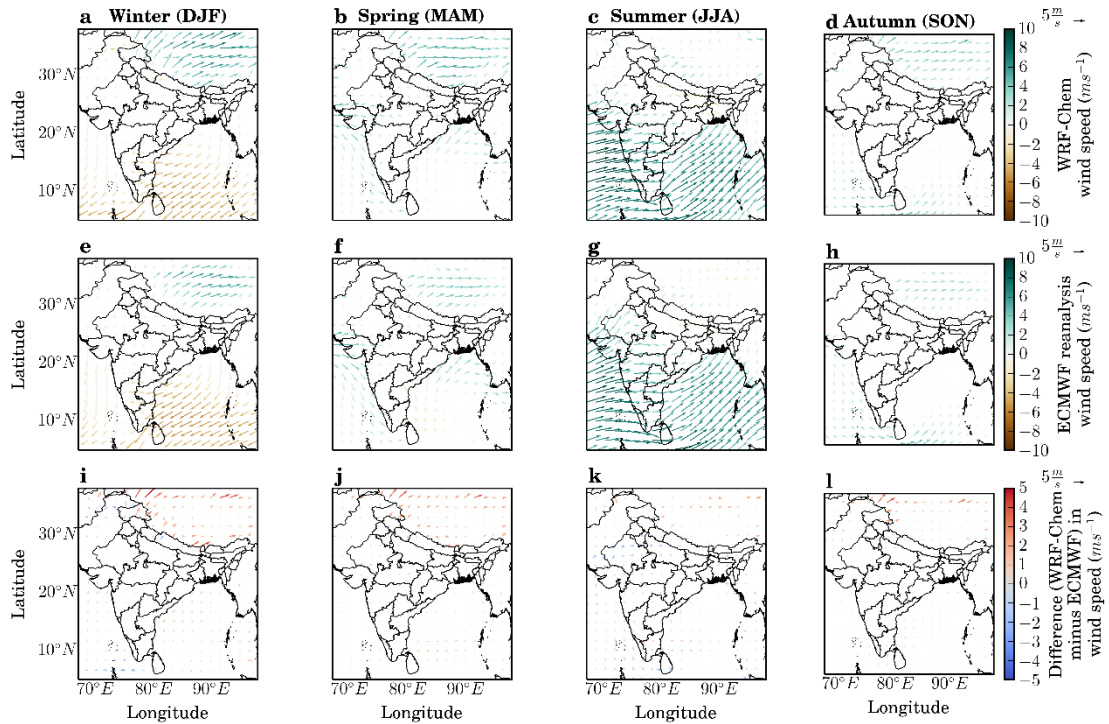


Figure 29: Spatial distribution of seasonal-mean wind speed and direction for 2014. (a–d) WRF-Chem. (e–h) ECMWF global reanalyses. (i–l) The difference (WRF-Chem minus ECMWF). Results shown for winter through autumn, see labels at the top of the figure.

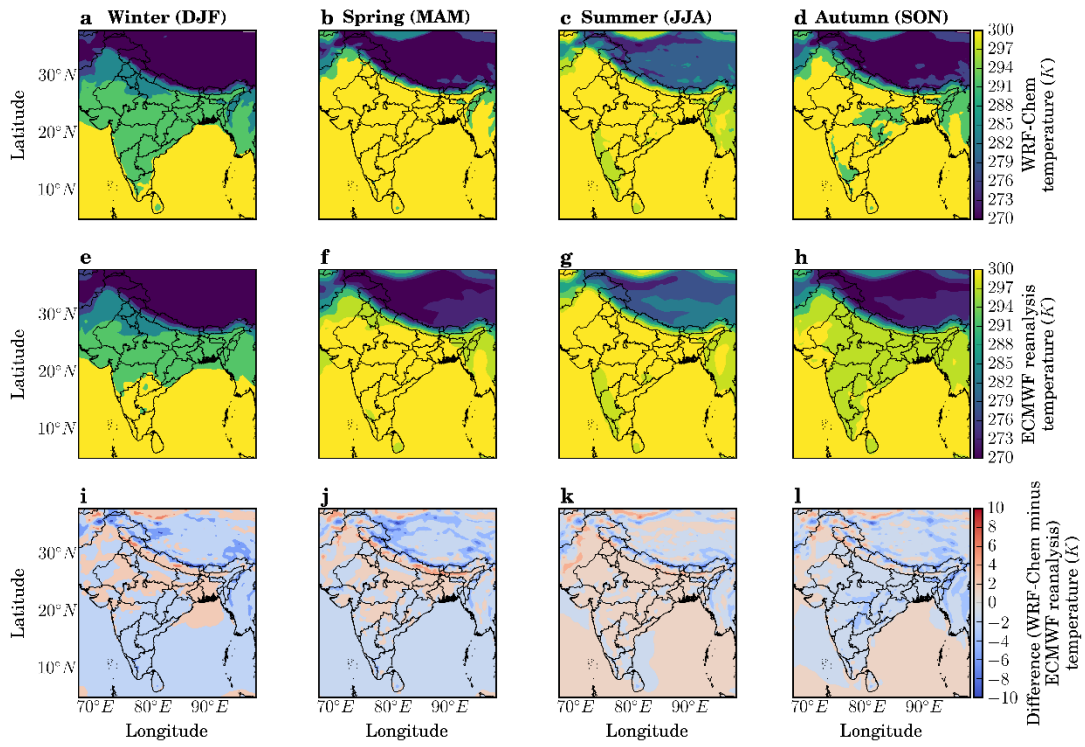


Figure 30: Spatial distribution of seasonal-mean temperature for 2014. (a–d) WRF-Chem. (e–h) ECMWF global reanalyses. (i–l) The difference (WRF-Chem minus ECMWF). Results shown for winter through autumn, see labels at the top of the figure.

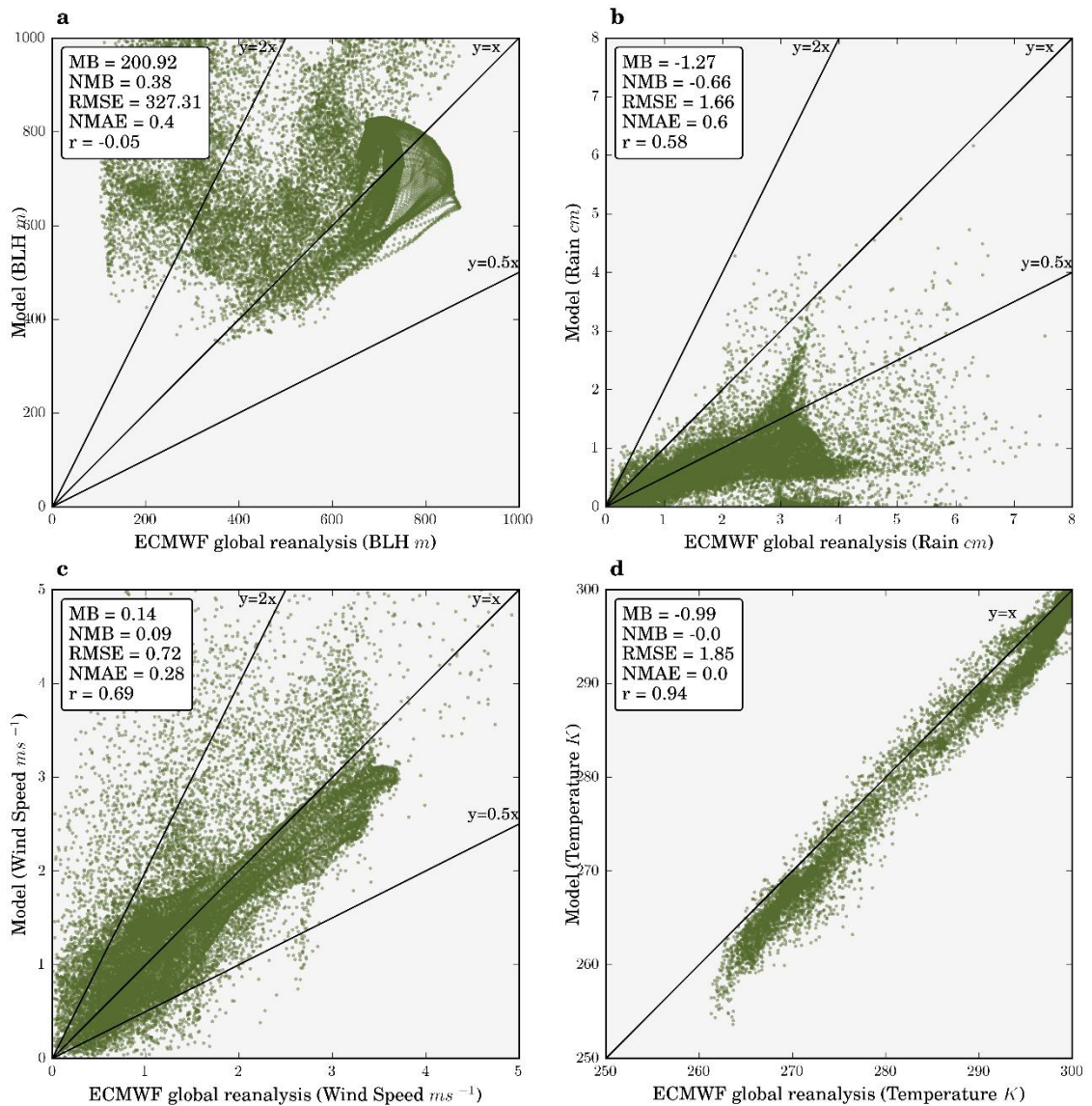


Figure 31: Annual-mean meteorology correlations between model and ECMWF global reanalyses at each grid cell. (a) Boundary layer height, (b) total precipitation, (c) wind speed, and (d) temperature for 2014.

3.3. Ambient surface PM_{2.5} concentrations

Surface measurements of PM_{2.5} were obtained from the National Air Quality Monitoring Program (NAMP) by the Central Pollution Control Board (CPCB), Ministry of Environment and Forests, Government of India (Ministry of Environment and Forests 2018). CPCB measurements used the automatic beta attenuation method (Ministry of Environment and Forests 2013). Environmental data collection in India has primarily been focused on compliance with India's NAAQS (Health Effects Institute Public Health and Air Pollution in Asia Program 2011). Most of the sites are in urban areas. The monitoring sites are shown spatially in Figure 32 and detailed in Table 11 (Appendix B). The network of sites reporting PM_{2.5} has expanded substantially in the last few years, with only four sites reporting in 2014, compared to 45 in 2016. India has strong

seasonal variations in aerosol concentrations, but smaller interannual variability (Moorthy *et al* 2001, Joshi *et al* 2016, Henriksson *et al* 2011, Verma 2015, Lodhi *et al* 2013, Ramachandran and Cherian 2008, Kedia *et al* 2014). PM_{2.5} observations from 2016 are therefore selected to evaluate simulated annual- and seasonal-mean PM_{2.5} from the model for 2014, as the order of magnitude increase in the number of observation sites strengthen the evaluation statistics. India lacks in technical capacity, where the number of monitoring stations is substantially lower than required with few are in rural areas (Indian Institute of Management 2010, Pant *et al* 2018).

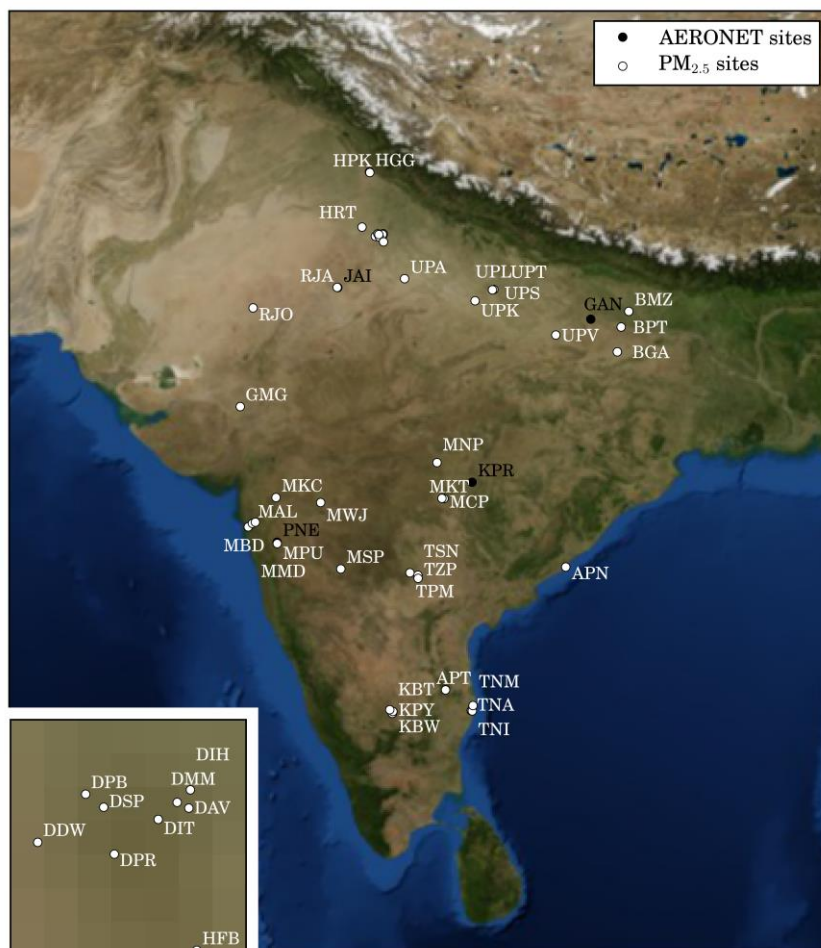


Figure 32: Model domain showing ground measurement sites for PM_{2.5} and AERONET measuring AOD. The Delhi region is expanded in the bottom left.

Figure 33 compares simulated and observed surface PM_{2.5} concentrations over India. The model simulates high annual-mean PM_{2.5} concentrations ($> 100 \mu\text{g m}^{-3}$) over the IGP and lower concentrations over central and southern India, broadly matching observations (Figure 33a). Overall, the model is unbiased against observed annual-mean PM_{2.5} abundances (NMB = -0.10) (Figure 33b). Simulated PM_{2.5} concentrations are closest to observations in spring (NMB = -0.07) and autumn (NMB = -0.10), while the model underestimates in winter (NMB = -0.24) and overestimates in summer (NMB = 0.69). The winter underestimation of surface PM_{2.5} concentrations could be due to the winter boundary layer height overestimation leading to excessive dilution of aerosol. The summer underestimation of surface PM_{2.5} concentrations could

be due to the summer monsoon precipitation dry bias underestimating aerosol washout. The model has limited success in reproducing the spatial variability of $PM_{2.5}$, underestimating near the Thar Desert and in the central IGP. Underestimation of dust in the western IGP has been identified previously (Kumar *et al* 2014b) and likely contributes to model underestimation of $PM_{2.5}$ in this region. Simulated $PM_{2.5}$ concentrations are greatest in winter (DJF) and autumn (SON), and lowest in spring (MAM) and summer (JJA), matching observations (Figure 34a–d).

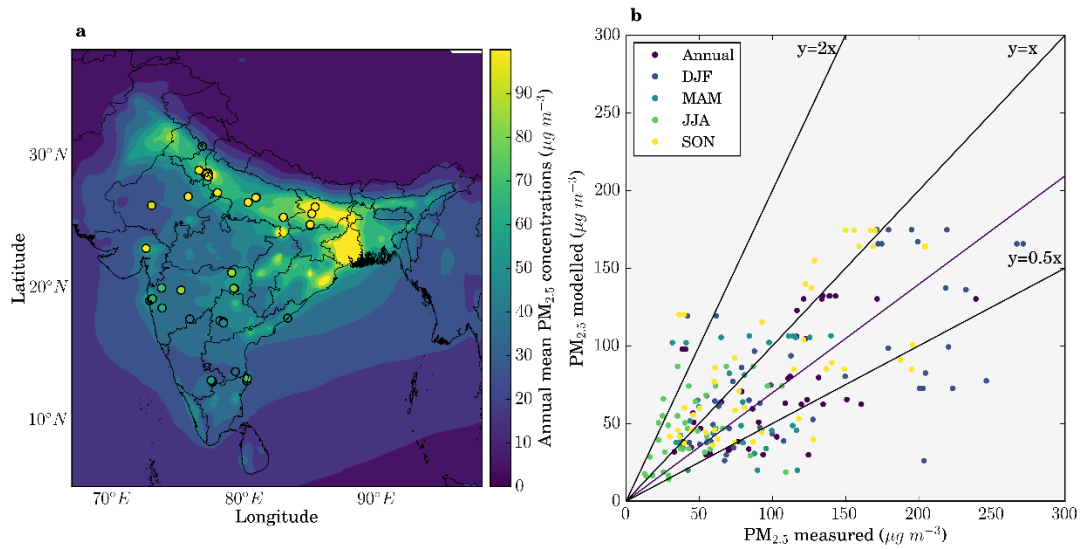


Figure 33: Comparison of observed and simulated $PM_{2.5}$ concentrations. (a) Annual-mean surface $PM_{2.5}$ concentrations. Model results for 2014 (background) are compared with surface measurements from 2016 (filled circles). (b) Comparison of annual and seasonal-mean surface $PM_{2.5}$ concentrations. The best-fit line (green), 1:1, 2:1, and 1:2 lines are shown (black). Annual, winter (DJF), spring (MAM), summer (JJA), and autumn (SON) NMB are -0.10, -0.24, -0.07, 0.69, and -0.10, respectively. The best-fit line for annual data has slope = 0.70 and Pearson's correlation coefficient (r) = 0.19.

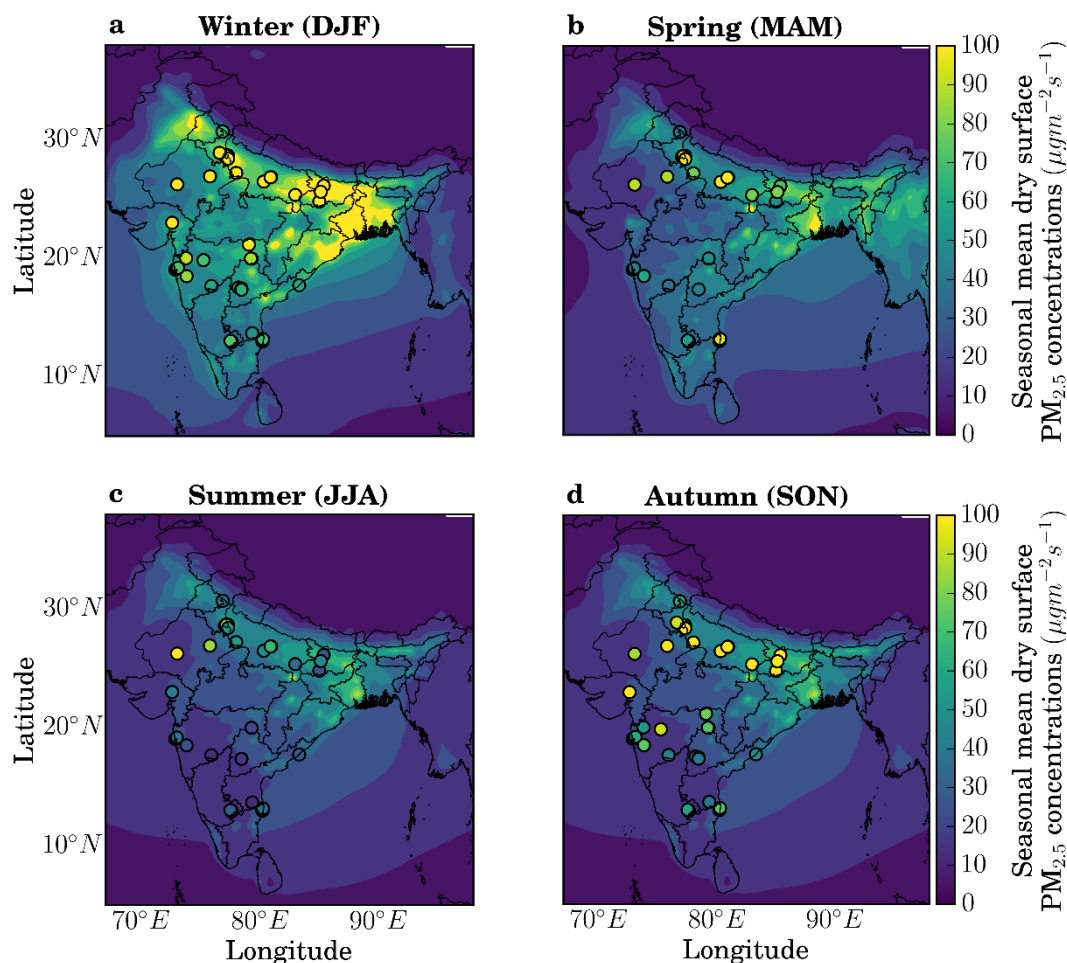


Figure 34: Seasonal-mean $PM_{2.5}$ concentrations for 2014. (a–d) model results (background) for 2014 for all sources are compared with ground-measurements (filled circles) from 2016, winter to autumn.

3.4. Aerosol optical depth

Aerosol optical depth (AOD) is the columnar aerosol estimated as the partial depletion of radiance per unit path length (km^{-1}) due to absorbing or scattering through the atmospheric column determined by aerosol loading, size distribution, and refractive index (Levy *et al* 2009, Remer *et al* 2008). An AOD of 0.01 corresponds to a clean atmosphere, 0.4 to a hazy atmosphere, and 1.0 means 37% of the sunlight is prevented from reaching the surface (Seinfeld 2004). Simulated AOD was evaluated against ground measurements (aerosol robotic network, AERONET) and satellite (MODIS). Level 2 (version 2) AERONET data was used, which are cloud-screened and quality assured with a low uncertainty of 0.01–0.02 at 500 nm. AERONET AOD was obtained at wavelengths between 340 nm and 1640 nm and was interpolated to obtain AOD at 550 nm from the closest neighbouring wavelengths. The model evaluation used AOD from the MODIS Aqua (MYD) satellite. Collection 6 (C6) level 2 (L2) AOD at 0.55 μm with the scientific data set *optical*

depth land and ocean mean, which produces AOD over land with the highest quality flag and has a spatial resolution of 10×10 km (at nadir) (Levy *et al* 2013). The error in MODIS derived AODs over land and ocean is $\pm 0.05 + (0.15 \times \text{AOD})$ and $\pm 0.03 + (0.05 \times \text{AOD})$, respectively. Data from MODIS Aqua was used due to Terra experiencing a calibration issue in global land AOD for collection 5 (Levy *et al* 2010). C6 was used for model evaluation as it is known to have statistically significant improvement in aerosol retrieval algorithms over some urban areas (Ford and Heald 2016), and non-linearities between the collections (6 and 5) arise due to pixel selection and calibration (Levy *et al* 2013). A spatial-then-temporal ordering of averaging was used to calculate daily-means, then equal-day-weighting was applied for seasonal- and annual-mean (Levy *et al* 2009, Gumley 2011). The evaluation used model data only when the satellite retrieved observations.

Figure 35 shows comparison of simulated AOD against ground observations and satellite. Comparison of simulated AOD against the AERONET shows similar good agreement (NMB = 0.09) as for $\text{PM}_{2.5}$, slightly underestimating in winter (NMB = -0.21) and slightly overestimating in summer (NMB = 0.34). Comparison of simulated AOD against MODIS shows a slight overestimation annually (NMB = 0.36), primarily due to overestimation in spring (NMB = 0.33) and summer (NMB = 0.41). MODIS AOD is likely to be biased high and over the IGP (Bibi *et al* 2015) and during the summer monsoon due to underestimated surface reflectance (Pan *et al* 2015, Seinfeld 2004).

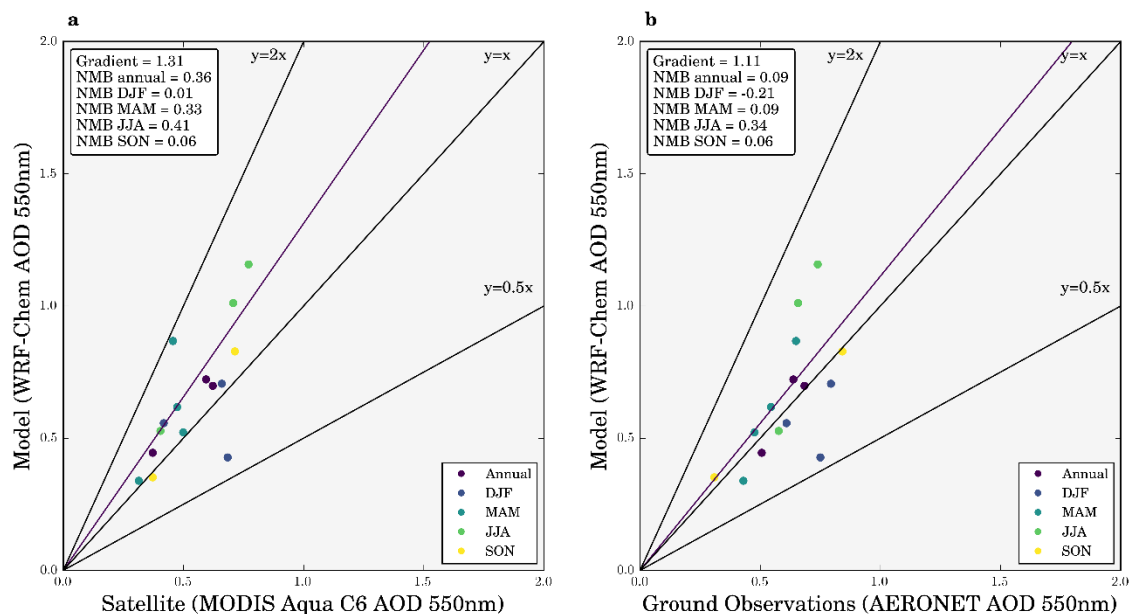


Figure 35: Evaluation of annual and seasonal-mean model AOD at 550 nm. (a) Comparison of model and satellite (MODIS Aqua C6) at AERONET locations. (b) Comparison of model and measured (AERONET). The best-fit line (green), 1:1, 2:1, and 1:2 lines are shown (black). NMB and slope of the best-fit line are given inset.

3.5. Ambient surface O₃ concentrations

Model evaluation for O₃ used ambient surface measurements from previous measurement studies over India representative of different chemical environments. Details of the monitoring sites are given in Table 14 (Appendix D). Surface O₃ observations used ultraviolet photometry online analysers with a 5% accuracy (Kleinman *et al* 1994). Similar to previous studies, the model evaluation used observational data of a different year to the simulation due to the paucity of O₃ observations over India (Kumar *et al* 2012b, 2015c, Ojha *et al* 2016, Sharma *et al* 2017a, Kumar *et al* 2018).

Figure 36 shows the comparison of observed and simulated O₃ concentrations. Simulated O₃ concentrations were highest in northern and eastern India. Simulated O₃ concentrations were lowest in summer (JJA), as seen in previous studies (Chatani *et al* 2014, Ojha *et al* 2016, Roy *et al* 2008, Lu *et al* 2018). The low O₃ concentrations in summer are likely due to the monsoon cloud cover reducing solar radiation and wet scavenging of O₃ precursors suppressing O₃ production (Lu *et al* 2018). Model simulations overestimated surface O₃ concentrations relative to observations with an overall NMB of 0.35. Previous modelling studies over India also mostly overestimated O₃ relative to observations (Kota *et al* 2018, Surendran *et al* 2015, Sharma *et al* 2017a, 2016, Marrapu *et al* 2014, Kumar *et al* 2012b, 2010a, Chatani *et al* 2014, Engardt 2008, Gupta and Mohan 2015, Lu *et al* 2018, Ojha *et al* 2012, 2016, Pommier *et al* 2018, Roy *et al* 2008, Karambelas *et al* 2018b).

Models have been found to have limited success in simulating local scale titration chemistry of O₃ with NO, causing O₃ concentrations to be overestimated (Chatani *et al* 2014, Sharma *et al* 2016, Engardt 2008, Sharma and Khare 2017, Pommier *et al* 2018). Urban observations close to large NO_x emission sources tend to have low O₃ concentrations due to this titration effect (Clapp and Jenkin 2001). To examine this effect, the model is separately evaluated against rural (including semi-rural, coastal, and high altitude) and urban (including semi-urban) observations (Figure 37). The model simulates O₃ concentrations closer to observations for rural sites (NMB = 0.28) than for urban sites (NMB = 0.41). This suggests that the titration of O₃ with large NO concentrations may be causing the model to overestimate O₃ where high NO concentrations are likely not captured by the model. Previous studies have found Indian O₃ concentrations to be larger downwind of heavily populated regions relative to urban areas (Lal *et al* 2008, Lawrence and Lelieveld 2010). The combination of EDGAR-HTAP with MOZART has also been found to enhance surface O₃ mixing ratios due to vertical mixing of enhanced O₃ that has been produced aloft (Sharma *et al* 2017a). The overestimation of O₃ could also be due to the underestimation of dust aerosols (Conibear *et al* 2018a). Heterogeneous reactions on dust surfaces have been found to reduce O₃ concentrations (Li *et al* 2017a, Kumar *et al* 2014a). Accurate simulation of dust emissions and the inclusion of these heterogeneous reactions reduced the difference between observed and simulated O₃ concentrations in India from 16 ppbv to 2 ppbv (Kumar *et al* 2014a).

Model overestimation of O_3 could also be due to uncertainties in emission inventories over India (Janssens-Maenhout *et al* 2015, Saikawa *et al* 2017, Monks *et al* 2015, Jena *et al* 2015a).

Overall, model simulation of O_3 concentrations is similar to previous studies (Kumar *et al* 2018, Kota *et al* 2018, Sharma *et al* 2017a, 2016, Kumar *et al* 2012b, Chatani *et al* 2014, Gupta and Mohan 2015, Pommier *et al* 2018, Karambelas *et al* 2018b).

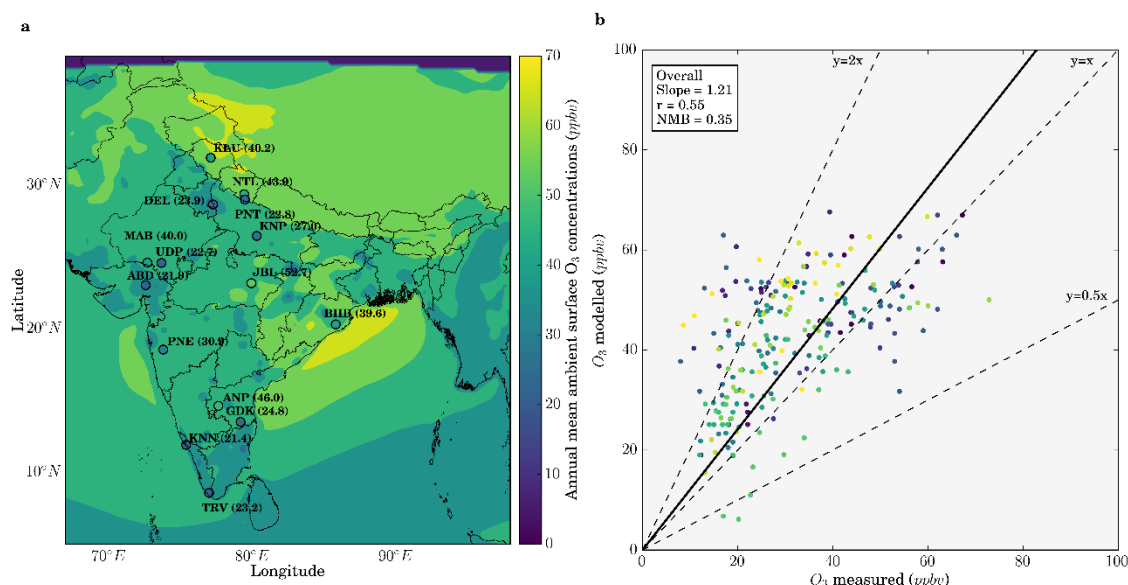


Figure 36: Comparison of observed and simulated O_3 concentrations. (a) Annual mean surface O_3 concentrations from the model for 2014 (background) compared with observations (filled circles, with text showing site abbreviation and measured annual mean). (b) Comparison of annual and monthly-mean surface O_3 concentrations (colours of filled circles are grouped per site for annual and monthly values). The overall best-fit line is solid, and the 1:1, 2:1, and 1:2 lines are dashed lines. Comparison of annual mean observed and simulated values: normalised mean bias (NMB) = 0.35; the best-fit line has slope = 1.21, and Pearson's correlation coefficient (r) = 0.55.

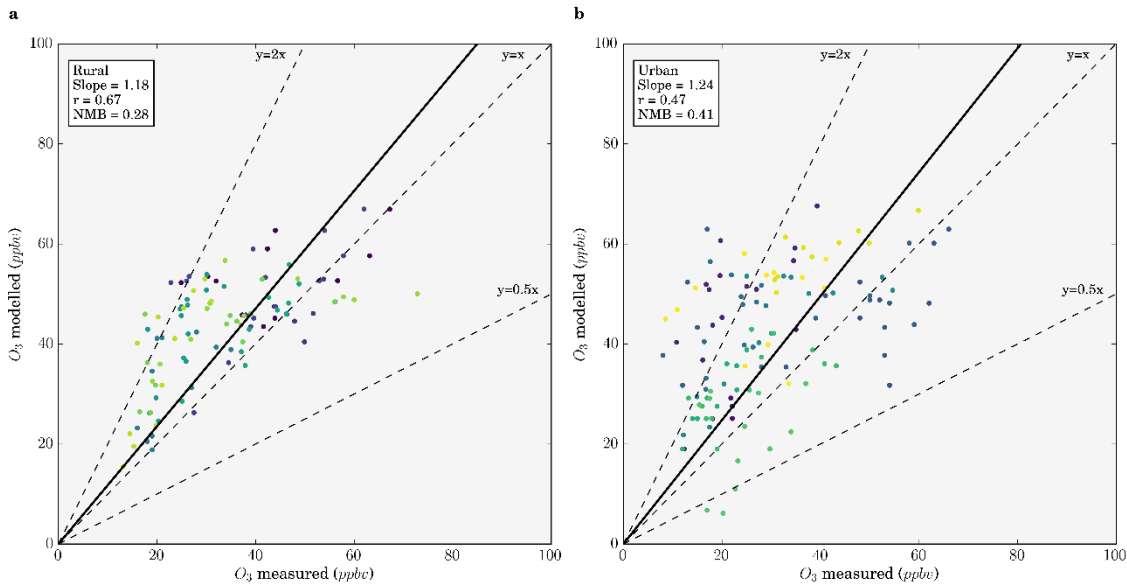


Figure 37: Comparison of rural and urban observed and simulated O_3 concentrations. (a) Comparison of annual and monthly-mean ambient surface O_3 concentrations from rural observation sites. The rural site best-fit line (solid), 1:1, 2:1, and 1:2 lines are shown (dashed). Rural site NMB is 0.28, the rural site best-fit line has slope = 1.18, and rural site $r = 0.67$. (b) Comparison of annual and monthly-mean ambient surface O_3 concentrations from urban observation sites. The urban site best-fit line (solid), 1:1, 2:1, and 1:2 lines are shown (dashed). Urban site NMB is 0.41, the urban site best-fit line has slope = 1.24, and urban site $r = 0.47$. Colours of filled circles grouped by site.

4. Residential energy use emissions dominate health impacts from exposure to ambient particulate matter in India

4.1. Abstract

Exposure to ambient PM_{2.5} is a leading contributor to disease in India. Previous studies analysing emission source attributions were restricted by coarse model resolution and limited PM_{2.5} observations. A regional model informed by new observations is used to make the first high-resolution study of the sector-specific disease burden from ambient PM_{2.5} exposure in India. Observed annual-mean PM_{2.5} concentrations exceed 100 µg m⁻³ and are well simulated by the model. Emissions from residential energy use dominate (52%) population-weighted annual-mean PM_{2.5} concentrations, and are attributed to 511,000 (95UI: 340,000–697,000) premature mortalities annually. However, removing residential energy use emissions would avert only 256,000 (95UI: 162,000–340,000), due to the non-linear exposure-response relationship causing health effects to saturate at high PM_{2.5} concentrations. Consequently, large reductions in emissions will be required to reduce the health burden from ambient PM_{2.5} exposure in India.

4.2. Introduction

Estimates of premature mortality from exposure to ambient PM_{2.5} in India vary by a factor of three, between 392,000 to 1,090,000 per year (GBD 2013 Risk Factors Collaborators 2015, Silva *et al* 2013, GBD 2016 Risk Factors Collaborators 2017, Cohen *et al* 2005, Apte *et al* 2015a, Ghude *et al* 2016, Giannadaki *et al* 2016, Chowdhury and Dey 2016, Lelieveld *et al* 2015, GBD 2010 Risk Factors Collaborators 2012, Silva *et al* 2016b, GBD 2015 Risk Factors Collaborators 2016a, World Health Organization 2016a, Lelieveld 2017), with differences due to variations in ambient PM_{2.5} estimates, health functions, population datasets, and methodological approaches. Previous global modelling studies find emissions from residential energy use dominate the contribution to PM_{2.5} exposure associated premature mortality in India (Lelieveld *et al* 2015, Lelieveld 2017, Silva *et al* 2016b), with estimates between 73,000 to 460,500 premature mortalities per year (Butt *et al* 2016, Chafe *et al* 2014a, Lelieveld *et al* 2015, Silva *et al* 2016b, Lelieveld 2017).

Previous studies used global models at relatively coarse resolution (Lelieveld *et al* 2015, Lelieveld 2017, Silva *et al* 2016b). Coarse resolution may underestimate PM_{2.5} concentrations over polluted areas and regional transport due to the short atmospheric lifetime of PM_{2.5} (Li *et al* 2016c, Pungler and West 2013, Thompson and Selin 2012, Thompson *et al* 2014). Underestimating PM_{2.5} concentrations will underestimate air pollution-related premature mortality (Pungler and West 2013). Model simulations using emissions at coarse spatial resolutions have been shown to have discrepancies relative to observations (Moorthy *et al* 2013b, Pan *et al* 2015, Pommier *et al* 2018, Karambelas *et al* 2018a), while higher resolution models

have been found to produce PM_{2.5} concentrations in closer agreement to observations (Kumar *et al* 2015c, Conibear *et al* 2018a, Saikawa *et al* 2017). Modelling air pollution at high spatial resolution is important as concentrations can vary substantially across small scales where population density and exposures are high (Punger and West 2013, Crippa *et al* 2017). Spatial variation differs with aerosol size (U.S. Environmental Protection Agency 2009b), where secondary PM_{2.5} generally has smaller spatial gradients than primary PM_{2.5} and is, therefore, less likely to be sensitive to spatial resolution (U.S. Environmental Protection Agency 2007). Resolution directly changes the resolved space, in addition to indirectly influencing parameterisation choices important for secondary pollutants (Wild and Prather 2006, Punger and West 2013).

This work is the first study to use high-resolution simulations to estimate the contribution of different emission sectors to ambient PM_{2.5} concentrations and the related disease burden from exposure across India. A regional numerical weather prediction model online-coupled with atmospheric chemistry at 30 km horizontal resolution is used to study the disease burden due to ambient PM_{2.5} exposure in India from seven emission sources. A control simulation is performed with all emission sources for the year of 2014. Then annual sensitivity simulations are performed removing the respective emissions from each source individually. The sources studied are agriculture (AGR), biomass burning (BBU), dust (DUS), power generation (ENE), industrial non-power (IND), residential energy use (RES) and land transport (TRA). The contribution of specific emission sources to PM_{2.5} concentrations is calculated by switching off the emission sources one at a time. The disease burden is then calculated using the exposure-response function from the GBD2015. Understanding the contribution of different emission sectors to ambient air pollution is essential to reduce the air pollution exposure associated disease burden.

4.3. Results

Annual mean PM_{2.5} concentrations were evaluated against observations (Section 3.3), where the model was found to be unbiased against observed annual-mean PM_{2.5} abundances (NMB = -0.10). Simulated population-weighted (country-scale exposure) annual-mean PM_{2.5} concentration across India was 57.2 µg m⁻³. Model simulations show that in 2014, 99% of the Indian population are exposed to annual-mean PM_{2.5} concentrations that exceeded the WHO AQG of 10 µg m⁻³ and 81% above the WHO Level 1 Interim Target (IT-1) of 35 µg m⁻³.

4.3.1. The contribution of emission sectors to ambient PM_{2.5} concentrations

To investigate the contribution of different emission sectors to ambient PM_{2.5} over India, emissions from different sectors are switched off one at a time in individual annual simulations. Table 5 shows the contribution of the different emission sectors to annual-mean PM_{2.5} concentrations across India.

Table 5: Reduction in population-weighted annual-mean $PM_{2.5}$ concentrations in India caused by removing different emission sectors. Sectors are agriculture (AGR), biomass burning (BBU), dust (DUS), power generation (ENE), industrial non-power (IND), residential energy use (RES), and land transport (TRA).

		AGR	BBU	DUS	ENE	IND	RES	TRA
Reduction	to	0.2	1.6	0.0	12.0	9.3	29.5	5.9
population	weighted							
$PM_{2.5}$	$\mu g m^{-3}$							
$(PM_{2.5_SECTOR_OFF})$	%	0	3	0	21	16	52	10

The largest reductions in population-weighted ambient $PM_{2.5}$ concentrations are achieved through the removal of emissions from residential energy use (52%) followed by power generation (21%), industry (16%), and land transport (10%). Removing emissions from residential energy use reduces ambient $PM_{2.5}$ concentrations by as much as 70% over the IGP, with reductions of 30–50% over southern India (Figure 38a). Figure 38b shows residential energy use contributes 67% of annual anthropogenic $PM_{2.5}$ emissions across India, with contributions as great as 90% over the IGP. Figure 39 shows that the contributions from residential energy use emissions to annual anthropogenic $PM_{2.5}$ emissions across India are 62% in summer and 70% in winter. The concentration and fractional contribution of residential emissions to $PM_{2.5}$ concentrations are largest in the winter (Figure 40). Emissions from residential energy use contribute a larger fraction of anthropogenic $PM_{2.5}$ emissions than to ambient $PM_{2.5}$ concentrations due to non-anthropogenic sources of $PM_{2.5}$, including dust and biomass burning, and due to the contribution of aerosol precursors such as SO_2 and NO_x , for which industry and power generation dominate emissions. Source apportionment suggests that 46–73% of BC concentrations in India are from non-fossil source (residential biofuel and biomass burning) (Butt *et al* 2016), which broadly matches this estimate of the contribution of residential emissions to $PM_{2.5}$ concentrations.

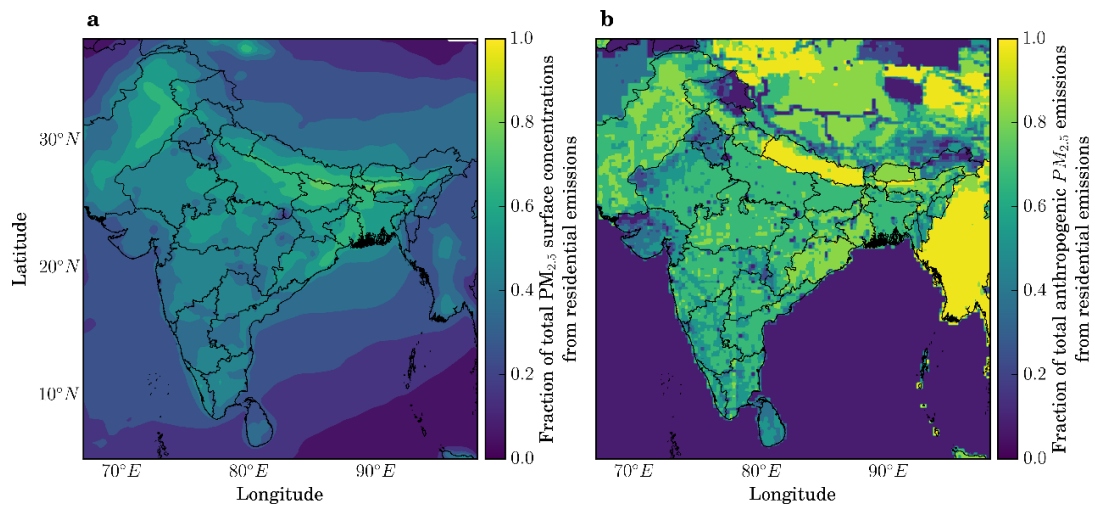


Figure 38: Fractional contribution of residential energy use to annual-mean $PM_{2.5}$. (a) Concentrations. (b) Anthropogenic emissions. Emissions are from EDGAR-HTAP v2.2 (Section 2.2.4).

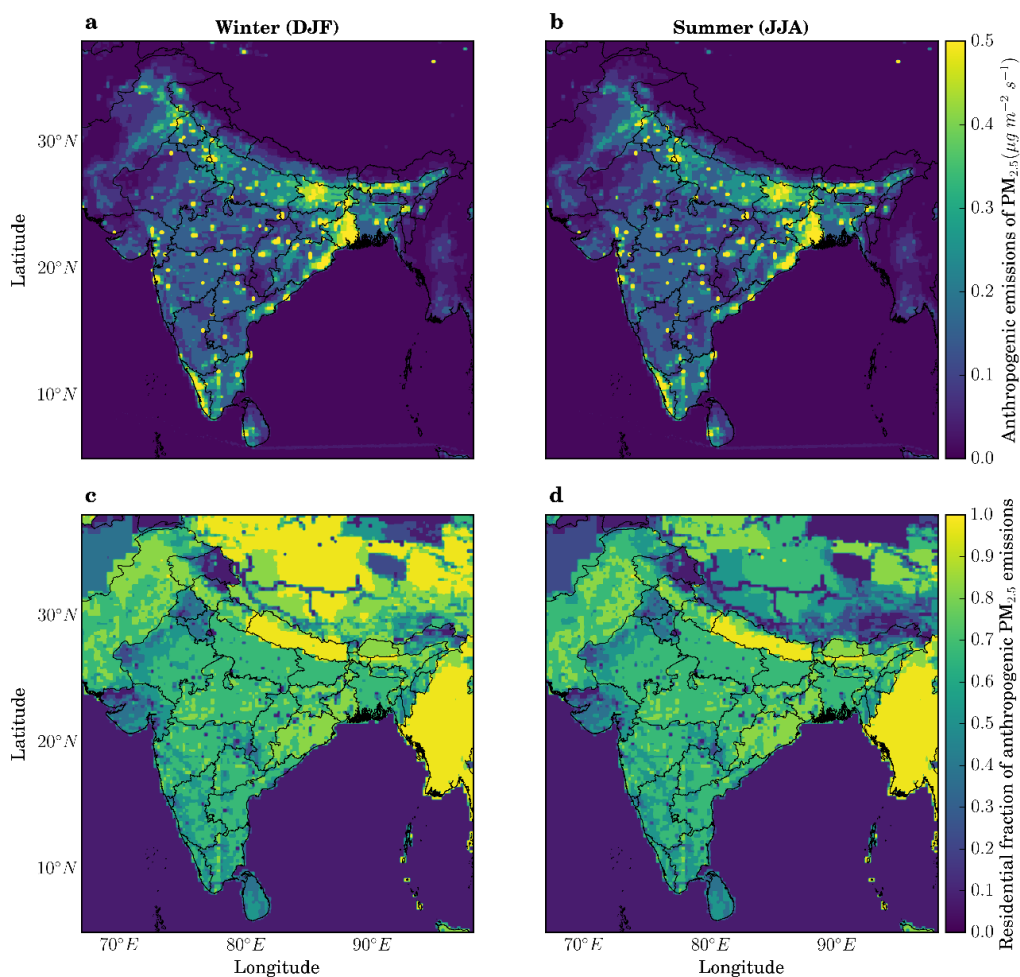


Figure 39: Seasonal-mean anthropogenic $PM_{2.5}$ emissions. Anthropogenic $PM_{2.5}$ emissions in (a) winter and (b) summer. Fractional contributions from the residential sector for (c) winter and (d) summer. Emissions are from EDGAR-HTAP v2.2 (Section 2.2.4).

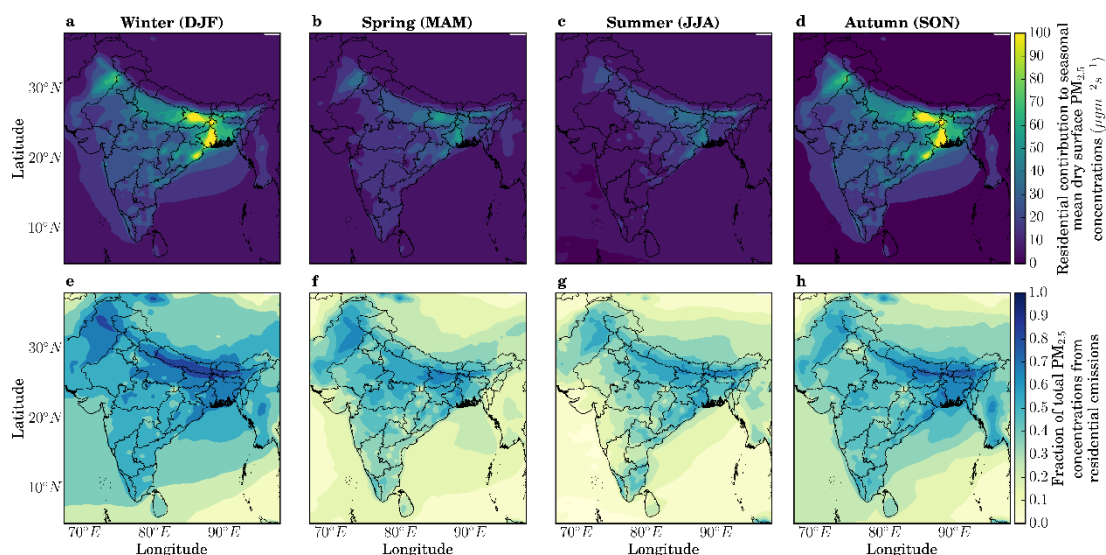


Figure 40: Seasonal-mean $PM_{2.5}$ concentrations for 2014. (a–d) Residential sector $PM_{2.5}$ concentrations, winter to summer. (e–h) The fraction from the residential sector, winter to summer.

4.3.2. Premature mortality due to ambient $PM_{2.5}$ exposure

Total premature mortality due to exposure to ambient $PM_{2.5}$ in India is estimated as 990,000 (95UI: 660,000–1,350,000) per year (Figure 41a), with 24,606,000 (95UI: 14,567,000–32,698,000) YLL. Most premature mortality due to exposure to ambient $PM_{2.5}$ occurs in urban areas (76%), defined by regions with population density larger than 400 persons’ km^{-2} . The IGP accounts for 71% of the premature mortalities associated with ambient $PM_{2.5}$ exposure with the dominant state (Uttar Pradesh) contributing 19%. The disease burden attributable to exposure to ambient $PM_{2.5}$ is dominated by IHD (35%) and COPD (31%).

Table 6: Estimated premature mortality associated with ambient $PM_{2.5}$ exposure in India. Results for different emission sectors (both absolute and fractional) for both subtraction and attribution methods. Values in parentheses represent the 95% uncertainty intervals (95UI). Sectors are agriculture (AGR), biomass burning (BBU), dust (DUS), power generation (ENE), industrial non-power (IND), residential energy use (RES), and land transport (TRA).

Premature mortalities per year (M_{SECTOR})		AGR	BBU	DUS	ENE	IND	RES	TRA
Subtraction	$\times 10^3$	1 (1–1)	12 (8–16)	0 (0–0)	90 (60–122)	66 (45–90)	256 (162–340)	43 (29–8)
	%	0	1	0	9	7	26	4
Attribution	$\times 10^3$	3 (2–5)	28 (18–38)	0 (0–0)	208 (139–283)	161 (107–220)	511 (340–697)	102 (68–139)
	%	0	3	0	21	16	52	10

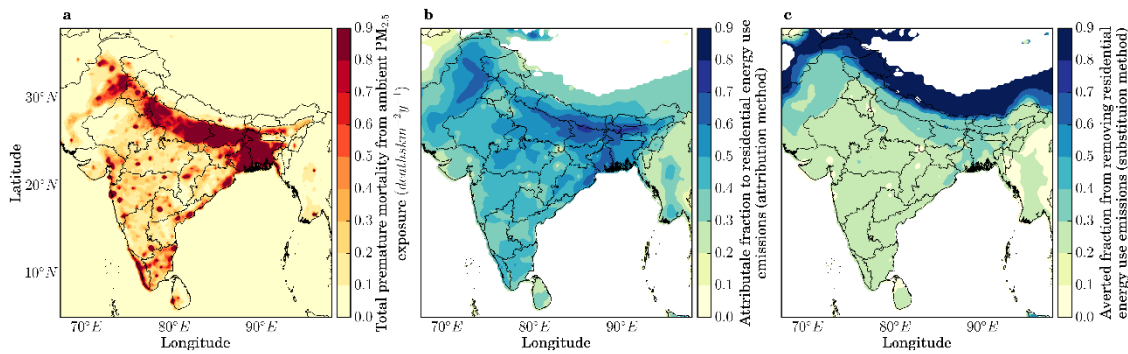


Figure 41: Disease burden due to exposure to ambient $PM_{2.5}$ across India. (a) Estimate of annual premature mortality due to exposure to $PM_{2.5}$ in India. (b) Attributable fraction of premature mortalities from residential energy use emissions (attribution method). (c) The averted fraction of premature mortalities from removing residential energy use emissions (subtraction method).

Figure 42 compares estimated premature mortality due to exposure to ambient $PM_{2.5}$ in India from this study with previous studies. The estimated premature mortality in India due to ambient $PM_{2.5}$ exposure estimated in this study agrees to within 4% with that from the GBD2015 (GBD 2015 Risk Factors Collaborators 2016a, Cohen *et al* 2017) and GBD2016 (GBD 2016 Risk Factors Collaborators 2017), which had similar $PM_{2.5}$ concentrations (Figure 61, Appendix B),

but is up to a factor of two greater than in many other studies. These previous studies applied different PM_{2.5} concentrations at a range of spatial resolutions (0.1° to 2.8°), as well as different population datasets, exposure-response functions, and baseline mortalities, all of which may play a role in the different premature mortality estimates. Likely reasons for lower premature mortality estimates in many previous studies are explored and summarised in Figure 42. Using lower resolution PM_{2.5} data (3° in place of 0.3°), reduced population-weighted PM_{2.5} concentrations by 20%, but reduced this study's premature mortality estimate by only 7%, due to the non-linear exposure-response relationship (Section 2.3). This approach does not account for the effect of resolution on the representation of atmospheric processes within the model (Punger and West 2013). Using population data for 2010 (SEDAC GPWv4 UN-adjusted), when the Indian population was 7% lower than in 2015, reduced this study's premature mortality estimates by 14%. Using the RR from the GBD2010 IER function (Apte *et al* 2015a, Burnett *et al* 2014) as in some previous studies (Giannadaki *et al* 2016, Apte *et al* 2015a, Ghude *et al* 2016, Lelieveld *et al* 2015, Silva *et al* 2016b, Chowdhury and Dey 2016), increased this study's premature mortality estimates by 22%. In contrast, applying RR from GBD2013 (GBD 2013 Risk Factors Collaborators 2015) reduced this study's mortality estimate by 31%. Using the GBD2015 baseline mortality estimates for 2010 (Institute for Health Metrics and Evaluation 2018), increased this study's premature mortality estimates by 7%. Applying state-specific baseline mortality values (Chowdhury and Dey 2016) (see Methods) reduced this study's estimate of premature mortality by 3%, while increasing impacts over the IGP due to the higher baseline mortality rates in this region (Figure 62, Appendix B). Many previous studies (Silva *et al* 2016b, 2016c, World Health Organization 2014a, Giannadaki *et al* 2016, Apte *et al* 2015a, GBD 2013 Risk Factors Collaborators 2015, Chafe *et al* 2014a, Brauer *et al* 2016) estimated maximum annual-mean PM_{2.5} concentrations across the IGP to be between 50–80 µg m⁻³, but lacked widespread measurements of PM_{2.5} for model evaluation. New observations suggest annual-mean PM_{2.5} concentrations of at least 120 µg m⁻³ across the IGP, which is well simulated by this study's model (Section 3.3). Scaling this study's PM_{2.5} concentrations so that annual-mean concentrations do not exceed 80 µg m⁻³ and 50 µg m⁻³ reduced this study's premature mortality estimates by 25% and 39%, respectively. Overall, this study suggests that different exposure-response relationships and different PM_{2.5} concentrations cause the largest differences in premature mortality estimates for India and are likely driving the majority of the difference between previous estimates.

4.3.3. The contribution of emission sectors to the disease burden

Table 6 shows the premature mortality estimates per emission sector for both the subtraction and attribution methods (Section 2.6), Table 9 (Appendix B) shows disease-specific results, and Table 10 (Appendix C) shows sector-specific YLL. The premature mortality estimates from the subtraction method (Figure 41c) are a factor of 2–2.5 smaller than the attribution method (Figure 41b). The difference is due to the non-linear exposure-response relationship, where health effects

saturate at high PM_{2.5} concentrations (Kodros *et al* 2016, Pope III *et al* 2015). The estimate of the reduction in premature mortality through removing an emission sector (subtraction method) is a factor 2–2.5 times less than the estimate of the premature mortality attributed to that sector (attribution method). Consequently, the summation of sector contributions from the subtraction method is 469,000 (95UI: 304,000–626,000) premature mortalities per year (47% of control), which is substantially lower than the sector summation from the attribution method of 1,012,000 (95UI: 675,000–1,381,000) premature mortalities per year (102% of control). Overall, this has implications for attempts to reduce air pollution mortality in regions with high PM_{2.5} concentrations.

For both methods, residential energy use is the dominant contributor to premature mortalities due to exposure to ambient PM_{2.5} across all states in India, except for Delhi where emissions from land transport are dominant. Emissions from residential energy use cause 511,000 (95UI: 340,000–697,000) premature mortalities per year, 52% of the total premature mortalities due to ambient PM_{2.5} exposure (attribution method). Removing emissions from residential energy use would prevent 256,000 (95UI: 162,000–340,000) premature mortalities per year, 26% of the total premature mortalities due to ambient PM_{2.5} exposure (subtraction method). After residential energy use, the next largest contributions are from power generation (9% of total premature mortalities for subtraction method and 21% for attribution method), industry (7% for subtraction and 16% for attribution), and land transport (4% for subtraction and 10% for attribution).

Figure 42 compares estimates of the source-specific premature mortality from ambient PM_{2.5} exposure in India. Previous studies also find emissions from residential energy use to dominate the contribution to PM_{2.5} exposure associated premature mortality in India (Lelieveld *et al* 2015, Lelieveld 2017, Silva *et al* 2016b). Power generation was the next largest contributor in all studies (Lelieveld *et al* 2015, Lelieveld 2017, Silva *et al* 2016b), while the percentage contribution in this study is approximately a factor of two larger. Industrial emissions are third largest in both this study and Silva *et al* (2016a) using the subtraction method, while dust was third for Lelieveld *et al* (2015, 2017) using the attribution method. The percentage contribution from land transport was double that of all previous studies (Lelieveld *et al* 2015, Lelieveld 2017, Silva *et al* 2016b). The two previous studies (Lelieveld *et al* 2015, Silva *et al* 2016b) that used the GBD2010 RR (which increased this study's estimates by 22%) obtained substantially lower total premature mortality than this study's estimates, likely due to lower PM_{2.5} concentrations. More recent previous studies (GBD 2015 Risk Factors Collaborators 2016a, Cohen *et al* 2017, GBD 2016 Risk Factors Collaborators 2017, Lelieveld 2017) using the GBD2015 RR, estimate similar total premature mortality to this study. Other studies estimating the contribution from residential energy use emissions to premature mortality are lower than this study due to a combination of using a log-linear exposure-response function with lower PM_{2.5} concentrations (Butt *et al* 2016) or only estimating the contribution from residential cooking (Chafe *et al* 2014a). This study's

estimate of the annual number of premature mortalities attributed to residential energy use (511,000; 95UI: 340,000–697,000) is at the upper end of the range (73,000–460,500) from previous work (Lelieveld *et al* 2015, Lelieveld 2017, Silva *et al* 2016b, Chafe *et al* 2014a, Butt *et al* 2016).

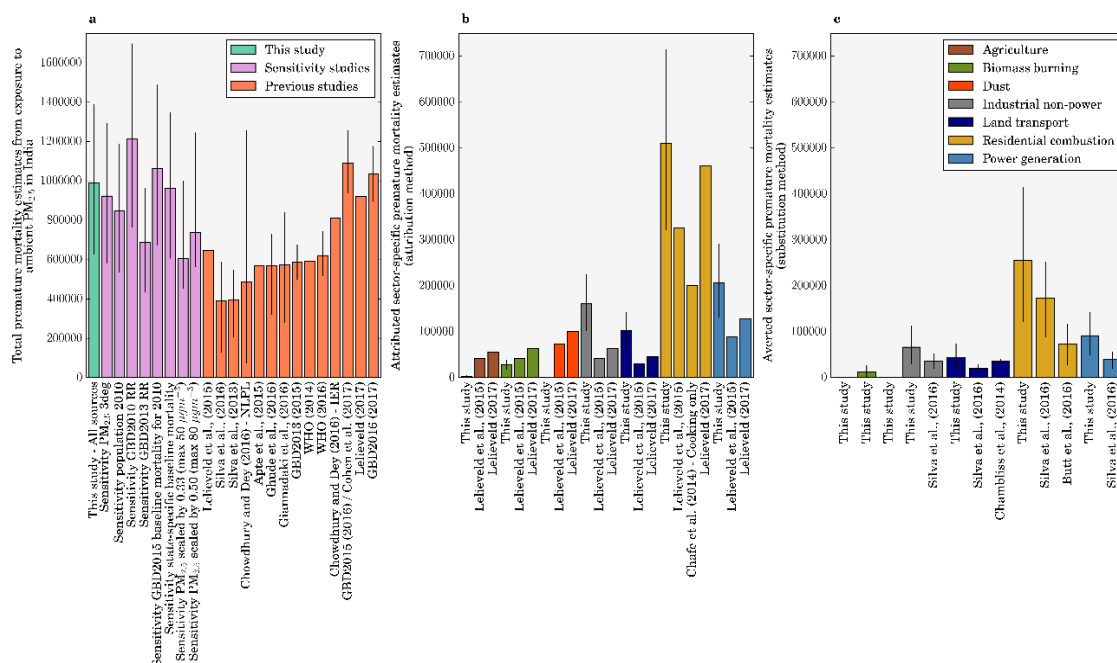


Figure 42: Comparison of annual premature mortality estimates for India due to exposure to ambient PM_{2.5}. (a) Total annual premature mortality from exposure to ambient PM_{2.5} from all emission sources. This study (green) and sensitivity studies (purple) comparing varying model spatial resolution, population year, exposure-response function, baseline mortality rates, and PM_{2.5} concentrations are compared with previous studies (orange). (b) Attributed sector-specific estimates from the attribution method from this study compared to previous studies. (c) Averted sector-specific estimates from the subtraction method from this study compared to previous studies. Error bars for this study and sensitivity analyses represent 95% uncertainty intervals (95UI) calculated by combining fractional errors in quadrature (see Methods). Error bars for previous studies given at the 95% uncertainty level where provided.

Since this study was published in Conibear *et al* (2018a), Upadhyay *et al* (2018) performed a similar study using the same model (WRF-Chem) and emission inventory (EDGAR-HTAP v2.2) at higher resolution (10 km) with a simpler aerosol scheme (GOCART bulk) to estimate the source contributions to the disease burden from ambient air pollution in India. Upadhyay *et al* (2018) found similar results to this study using the subtraction method, where residential energy use emissions dominated at the regional scale (48%, compared to 26% in this study), with localised contributions from transport (4%, compared to 7% in this study), industry (6%, compared to 4% in this study), and energy generation (2%, compared to 9% in this study). The total disease burden in Upadhyay *et al* (2018) was 20% lower than in this study, partially due to their study missing

agricultural burning emissions, increasing the relative contributions from other sources. Another study from Venkataraman *et al* (2018) was subsequently published detailing the emission inventories used in the GBD MAPS Working Group (2018) study of present and future ambient air pollution in India. They found solid fuel use (biomass and coal) combustion dominates the contributions to ambient PM_{2.5} concentrations and the associated disease burden, from residential use in the present day and industry and power generation in the future (GBD MAPS Working Group 2018, Venkataraman *et al* 2018). The key findings from Upadhyay *et al* (2018), Venkataraman *et al* (2018), and GBD MAPS Working Group (2018) are coherent with this study in that residential emissions from solid fuel use dominate the present day disease burden from ambient air pollution exposure.

4.4. Conclusion

In this study, a regional numerical weather prediction model online-coupled with chemistry is used to make the first high-resolution study of the contributions of seven emission sources to the disease burden associated with ambient PM_{2.5} exposure in India. New observations suggest annual-mean PM_{2.5} concentrations exceed 100 µg m⁻³ across northern India, matching concentrations simulated by the model and confirming the conclusions of recent studies with similar PM_{2.5} concentrations (Cohen *et al* 2017). Sensitivity studies suggest that different exposure-response relationships and PM_{2.5} concentrations drive the largest differences in estimates of premature mortality for previous studies. Residential energy use contributed 52% of population-weighted annual-mean PM_{2.5} concentrations resulting in an estimated 511,000 (95UI: 340,000–697,000) premature mortalities per year. Completely removing residential emissions would prevent 256,000 (95UI: 162,000–340,000) premature mortalities each year, 26% of the total premature mortalities due to exposure to ambient PM_{2.5}. The smaller relative reduction in premature mortality compared to the reduction in PM_{2.5} concentration is due to the non-linear exposure-response relationship, where the mortality response to PM_{2.5} concentrations is sub-linear at the high PM_{2.5} concentrations over India. Consequently, large reductions in emissions and PM_{2.5} concentrations will be required to reduce the substantial health burden. Information on the source contributions to the burden of disease attributable to ambient PM_{2.5} exposure is critical to support the national and sub-national control of air pollution.

5. Stringent emission control policies can provide large improvements in air quality and public health in India

5.1. Abstract

Exposure to high concentrations of ambient PM_{2.5} is a leading risk factor for public health in India causing a substantial burden of disease. Business-as-usual economic and industrial growth in India is predicted to increase emissions, worsen air quality, and increase the associated disease burden in future decades. A high-resolution online-coupled model is used to estimate the impacts of different air pollution control pathways on ambient PM_{2.5} concentrations and human health in India. With no change in emissions, the disease burden from exposure to ambient PM_{2.5} in 2050 will increase by 75% relative to 2015, due to population ageing and growth increasing the number of people susceptible to air pollution. The International Energy Agencies (IEA) New Policy Scenario (NPS) and Clean Air Scenario (CAS) in 2050 can reduce ambient PM_{2.5} concentrations below 2015 levels by 9% and 68%, respectively, offsetting 61,000 and 610,000 premature mortalities a year, which is 9% and 91% of the projected increase in premature mortalities due to population growth and ageing. Throughout India, the CAS stands out as the most effective scenario to reduce ambient PM_{2.5} concentrations and the associated disease burden, reducing the 2050 mortality rate per 100,000 below 2015 control levels by 15%. However, even under such stringent emission control policies, population growth and ageing results in premature mortality estimates from exposure to particulate air pollution to increase by 7% compared to 2015, highlighting the challenge facing efforts to improve public health in India.

5.2. Introduction

Emissions are predicted to substantially increase under a business-as-usual scenario relative to the present day (GBD MAPS Working Group 2018), with PM_{2.5}, SO₂, and NO_x emissions approximately doubling by 2050 relative to 2015 (Sharma and Kumar 2016, International Energy Agency 2016b), increasing PM_{2.5} concentrations by 67% (Pommier *et al* 2018). Climate change is also predicted to alter ambient PM_{2.5} concentrations in India; however, these changes are smaller relative to emission changes (Pommier *et al* 2018, Silva *et al* 2017, Fang *et al* 2013, Jacobson 2008, Kumar *et al* 2018). In addition to changing concentrations, the disease burden from air pollution exposure is affected by population growth, population ageing, and changes in baseline mortality rates (Lelieveld *et al* 2015, Hughes *et al* 2011). These other drivers vary the number of people susceptible to air pollution, and their effects can outweigh the impact from emission changes (GBD MAPS Working Group 2016, Chowdhury *et al* 2018, GBD MAPS Working Group 2018). The business-as-usual scenario in India is predicted to increase estimates of premature mortality from ambient PM_{2.5} exposure (Lelieveld *et al* 2015, Anenberg *et al* 2012, GBD MAPS Working Group 2018, International Energy Agency 2016a).

Alternative air pollution control pathways (scenarios) for India have been developed and evaluated in previous studies (Sharma and Kumar 2016, International Energy Agency 2016b, Pommier *et al* 2018, International Energy Agency 2016a, GBD MAPS Working Group 2018). The International Energy Agency (IEA) developed the New Policy Scenario (NPS) which considers all relevant existing and planned policies as of 2016 and the Clean Air Scenario (CAS) which represents aggressive policy action using proven energy policies and technologies tailored to national circumstances (International Energy Agency 2016b, 2016a). The NPS in 2040 was found to offset most of the growth in emissions of SO₂, NO_x, and PM_{2.5} relative to 2015 bringing the mean total growth per pollutant down to 9%, while under the CAS in 2040 emissions were reduced below 2015 levels by an average of 65% (International Energy Agency 2016b, 2016a). The IEA found the associated disease burden due to the NPS and the CAS scenarios changed by +53% and -5%, respectively, where population growth and ageing to 2040 substantially increased the number of people susceptible to air pollution (International Energy Agency 2016a).

The GBD MAPS Working Group studied a business-as-usual reference scenario, an ambitious scenario reflecting stringent emission standards, and an aspirational scenario all through to 2050 (Venkataraman *et al* 2018, GBD MAPS Working Group 2018). Population-weighted ambient PM_{2.5} concentrations across India in 2050 under the reference, ambitious, and aspirational scenarios will change by +43%, +10%, and -35%, respectively relative to the reference scenario in 2015 (Venkataraman *et al* 2018, GBD MAPS Working Group 2018). Total annual premature mortality from ambient PM_{2.5} exposure in 2050 relative to 2015 would increase under the reference, ambitious, and aspirational scenarios by 234%, 194%, and 125%, respectively, highlighting the substantial impact of the demographic transition in India (Venkataraman *et al* 2018, GBD MAPS Working Group 2018). The ambitious and aspirational scenarios reduced the 2050 reference population-weighted ambient PM_{2.5} concentrations by 23% and 54% in 2050, respectively in 2050, offsetting the increase in annual deaths by 0.34 and 1.2 million, respectively (Venkataraman *et al* 2018, GBD MAPS Working Group 2018).

Previous work using the ECLIPSE current legislation scenario found the estimate of premature mortalities from ambient PM_{2.5} exposure in India to increase by 125% in 2030 relative to 2010 for the reference case, and then increase again by 95% in 2050 relative to 2030 (Stohl *et al* 2015). The ECLIPSE short-lived climate pollutant mitigation scenario could offset 20% of the premature mortality from ambient PM_{2.5} exposure in India (Stohl *et al* 2015). CH₄ and BC mitigation measures have been found to lower future PM_{2.5} concentrations in India, reducing the exposure related associated disease burden (Anenberg *et al* 2012). Alternative scenarios for land transport has been studied in India, where air quality co-benefits are possible (Mittal *et al* 2015).

Previous studies that evaluated Indian scenarios (International Energy Agency 2016b, 2016a, Pommier *et al* 2018, GBD MAPS Working Group 2018) used relatively coarse spatial resolution (0.5° × 0.5° or 0.5° × 0.67°) chemical transport models to estimate the impacts on PM_{2.5}

concentrations per scenario, which may not resolve the high PM_{2.5} concentrations in India. The GBD MAPS Working Group then applied the fractional impacts on higher resolution ambient PM_{2.5} concentrations to estimate the impacts on health (GBD MAPS Working Group 2018). In this study, multiple air pollution control pathways (scenarios) in India are analysed using a higher resolution (30 km, 0.3° horizontal) regional numerical weather prediction model online-coupled with atmospheric chemistry, with the latest exposure-response functions (GBD2016), and disease-specific baseline mortality rates for 2015 and 2050. This study is the first high-resolution analysis of the impacts of scenarios on ambient PM_{2.5} concentrations and resulting disease burden in India. The impacts of both the NPS and CAS scenarios from the IEA are studied (International Energy Agency 2016a). Idealised simulations are performed applying individual emission changes to the four emission sectors that contribute most to ambient PM_{2.5} concentrations in India (RES, ENE, IND, and TRA) to help interpret the impacts of the scenarios. For each sector, simulations with small (-10% and +10%) emission changes are undertaken as well as simulations where the emission sector has been completely removed. It is assumed that both climate and emissions from countries outside India remain unchanged, allowing us to isolate the impacts of changing Indian emissions. Sensitivity studies are conducted to explore the impacts of the Indian demographic and epidemiologic transition through to 2050 on the public health burden associated with air pollution exposure. Conducting a large ensemble of simulations across sectors and scenarios, and estimating resulting ambient PM_{2.5} concentrations and human health impacts, produces a valuable resource to help inform environmental policy decisions at the state and national levels.

5.3. Specific methods

5.3.1. Air pollution control pathways

The NPS considers all relevant existing and planned policies as of 2016, including India's INDC to greenhouse gases under the United Nations Framework Convention on Climate Change. In the NPS SO₂, NO_x, and PM_{2.5} emissions increase overall by 10%, 10%, and 7% in 2040 relative to 2015, respectively. SO₂ emissions from the power sector are largely reduced by air quality policies, such as The New Environment Protection Amendment Rules (Ministry of Environment Forests and Climate Change 2015a). Transport NO_x emissions decrease due to the Bharat VI standards, due to be introduced in 2020, reducing emissions from buses and trucks (Ministry of Road Transport and Highways 2016a). Residential PM_{2.5} emissions decrease due to the expansion of LPG promotion policies, such as Ujjwala (Ministry of Petroleum and Natural Gas 2018a) and PAHAL (Ministry of Petroleum and Natural Gas 2018c). Substantial industrial growth offsets these reductions, mainly due to increases in iron and steel production using coal with low emission standards, despite Indian coal and imported Indonesian coal having low sulphur contents. The high growth rates from 2000 to 2015 in the number of household, electricity generation, cement production, land transport distance travelled are projected to continue between 2015 and 2030,

slowing after 2030 (Venkataraman *et al* 2018). Power generation is expected to increase by a factor of two over the next ten years, primarily fuelled by coal (Sahu *et al* 2017).

The CAS represents aggressive pollution abatement using proven energy policies and technologies. In the CAS SO₂, NO_x, and PM_{2.5} emissions decrease overall by 69%, 50%, and 76% in 2040 relative to 2015, respectively. SO₂ and NO_x emissions are lowered primarily due to industrial controls on iron, steel, and cement production and stricter standards for heavy-duty vehicles. PM_{2.5} emission reductions benefit from tight standards in iron and steel manufacturing, in addition to universal access to clean cooking facilities, such as modern fuels and clean cookstoves. Both the NPS and CAS suggest that the industrial sector will dominate anthropogenic emissions of SO₂, NO_x, and PM_{2.5} in the future.

The NPS and CAS are applied to anthropogenic emissions by scaling emissions by factors from the IEA (International Energy Agency 2016a), which are in Figure 43 and Table 13 (Appendix D). Sector-specific SO₂, NO_x, and PM_{2.5} emissions are scaled by factors from the IEA (International Energy Agency 2016a). Sector-specific BC and OC emissions are scaled by the same factor as PM_{2.5}, while CO and all VOCs are scaled by the mean of total factors across all sectors (1.09 and 0.35 for the NPS and CAS, respectively). NH₃ emissions are not scaled, consistent with the GBD MAPS Working Group (GBD MAPS Working Group 2018). This is due to the low contribution of NH₃ to ambient PM_{2.5} concentrations through the agricultural sector in India (Conibear *et al* 2018a, Pozzer *et al* 2017), that secondary nitrate contributes less than 5% of PM_{2.5} mass (Rastogi *et al* 2016, Kumar and Sunder Raman 2016, Ram and Sarin 2011), the low mortality response from NH₃ changes in India (Lee *et al* 2015, Pozzer *et al* 2017), that there are large uncertainties in future NH₃ emissions in India (Venkataraman *et al* 2018), and that the level of NH₃ emissions is relatively stable with no control measures applied (GBD MAPS Working Group 2018). Despite these reasons, fertiliser use is increasing across South Asia (Xu *et al* 2018). To help interpret the results for the CAS and NPS simulations, idealised simulations are performed where each of the leading four emission sources to ambient PM_{2.5} concentrations (RES, ENE, IND, and TRA) previously identified (Chapter 4) have emissions increased or decreased by 10% in addition to simulations where emissions from that sector are completely removed. All simulations are annual simulations using meteorology and boundary conditions for the year 2014.

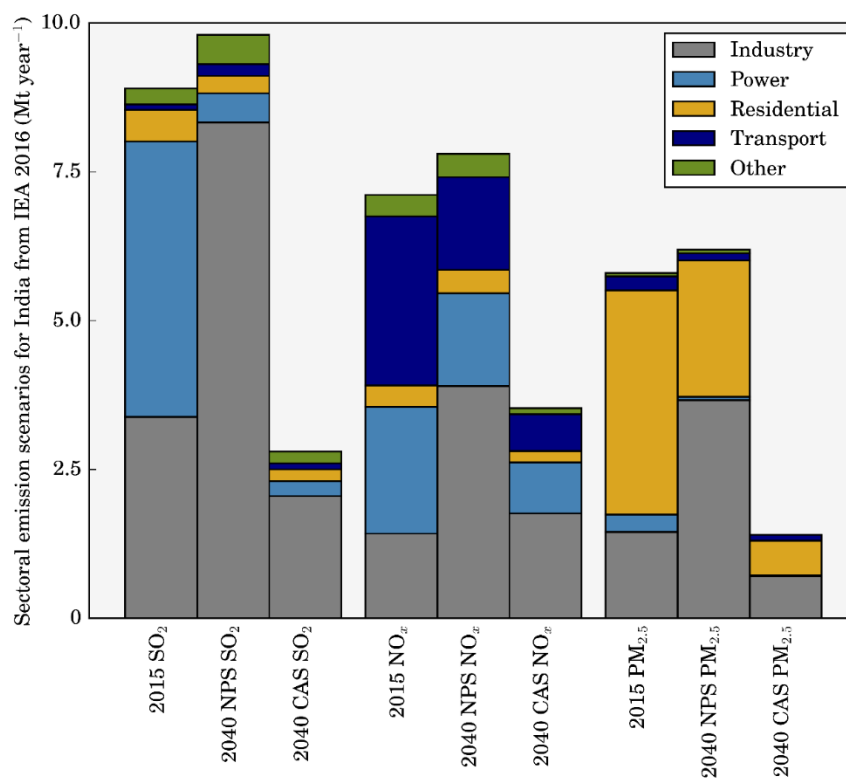


Figure 43: Cumulative emissions per source within India in 2015 and projected emissions in 2040 under the NPS and CAS (International Energy Agency 2016a).

5.3.2. Health impact estimates

Under the control scenario, total premature mortality due to exposure to ambient PM_{2.5} in India in 2015 is estimated as 900,000 (95UI: 683,000–1,252,000) per year, the mortality rate as 62 deaths per 100,000 population, with 21,528,000 (95UI: 15,997,000–30,268,000) YLL. This premature mortality estimate total is 9% lower than reported in Chapter 4 primarily due to the slightly lower risk estimates for cardiovascular diseases from the GBD2016 exposure-response function relative to the GBD2015. This study’s mortality estimate is 13% lower than the estimate from the GBD2016 (GBD 2016 Risk Factors Collaborators 2017), where the difference results from a combination of slightly lower population density from IFs, lower baseline mortality rates at higher ages for cardiovascular diseases, and this study’s slightly lower PM_{2.5} concentrations over the central and western IGP (Conibear *et al* 2018a, Shaddick *et al* 2018b).

5.4. Results

5.4.1. Impact of scenarios on ambient PM_{2.5} concentrations in India

Figure 44 shows the impacts of the scenarios on annual-mean PM_{2.5} concentrations across India. The NPS and CAS scenarios reduce population-weighted ambient PM_{2.5} concentrations by 9% and 68%, respectively, relative to the control scenario in 2015. In the CAS scenario, large reductions in ambient PM_{2.5} concentrations are simulated across the IGP, spatially matching the changes simulated by the scenario removing residential energy use emissions (RES 0%). The

reduction in ambient $PM_{2.5}$ concentrations achieved by the CAS scenario is greater than the reductions achieved in any of the simulations where emissions from one sector are completely removed.

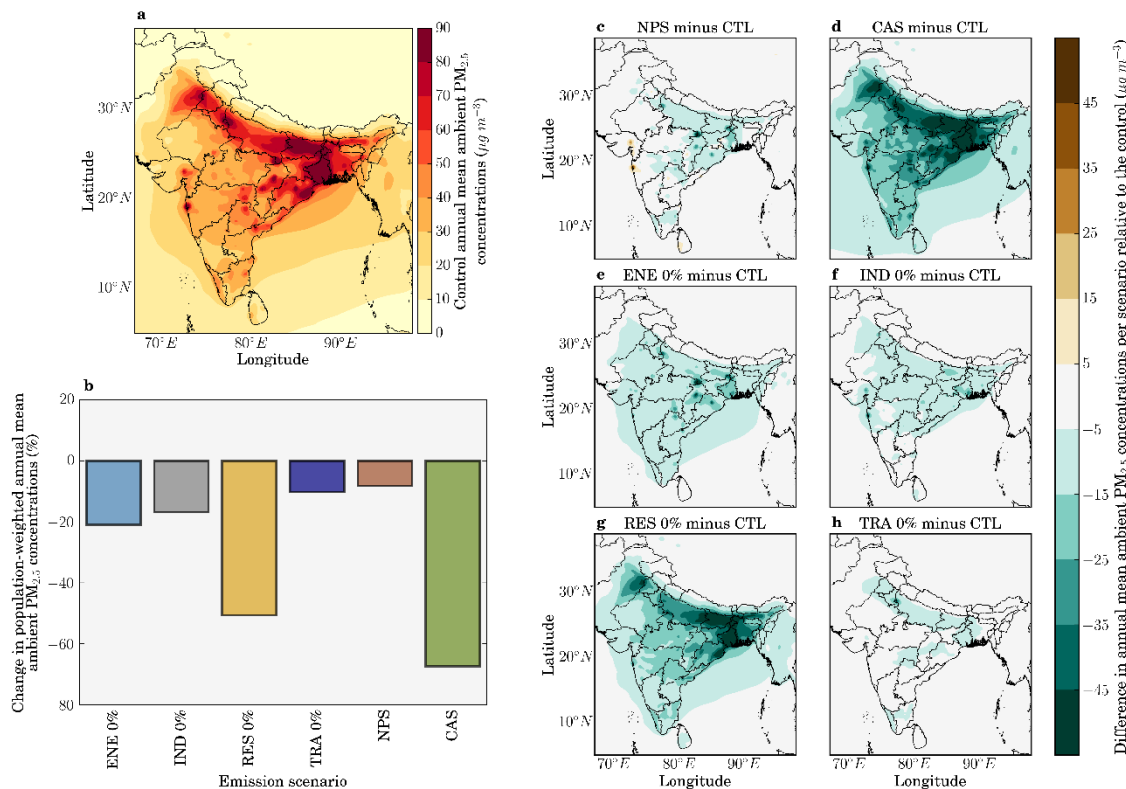


Figure 44: The impact of scenarios on annual-mean ambient $PM_{2.5}$ concentrations in India. (a) Annual-mean ambient $PM_{2.5}$ concentrations in India in 2015 from the control scenario. (b) National-mean changes in 2015 population-weighted annual-mean ambient $PM_{2.5}$ concentrations for each scenario. (c–h) Difference in annual-mean ambient $PM_{2.5}$ concentrations for IEA New Policy Scenario (NPS), IEA Clean Air Scenario (CAS), removal of power generation emissions (ENE 0%), removal of industry emissions (IND 0%), removal of residential energy use emissions (RES 0%), and removal of land transport emissions (TRA 0%) scenarios.

Figure 45 shows the population exposed to annual-mean $PM_{2.5}$ concentrations above the WHO AQG of $10 \mu\text{g m}^{-3}$, the WHO IT-1 of $35 \mu\text{g m}^{-3}$, and the Indian NAAQS of $40 \mu\text{g m}^{-3}$ released by the Government of India (World Health Organization 2006a, Ministry of Environment and Forests 2009). In all scenarios, with both 2015 and 2050 populations, more than 98% of the Indian population remains exposed to annual-mean $PM_{2.5}$ concentrations exceeding the WHO AQG. The emission reduction scenarios have a greater impact in bringing population exposure into line with the interim targets, where the percentage of the population in line with the WHO IT-1 ($35 \mu\text{g m}^{-3}$) is increased from 19% in the control scenario to 97% and 82% for the CAS and RES 0% scenarios, respectively. The increased adherence to these air quality metrics shows that improvements to air quality through emission reductions can provide important public health benefits, which is in agreement with the view from the WHO (World Health Organization 2006a).

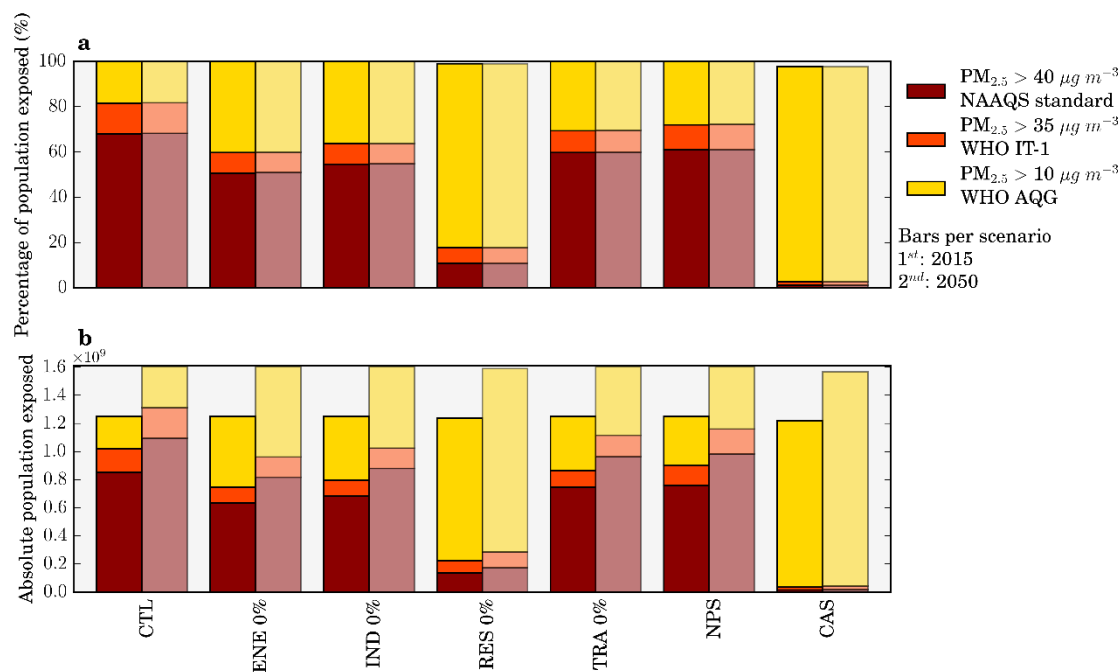


Figure 45: The impact of scenarios on air quality metrics in India. (a) Percentage of the population and (b) total population in 2015 (1st bar) and 2050 (2nd bar) exposed to annual-mean ambient $PM_{2.5}$ concentrations exceeding $10 \mu g m^{-3}$ (WHO AQG), $35 \mu g m^{-3}$ (WHO IT-1), and $40 \mu g m^{-3}$ (NAAQS) in each scenario.

5.4.2. Indian disease burden under air pollution control pathways

The impacts of the scenarios on premature mortality estimates from ambient $PM_{2.5}$ exposure across India is shown in Figure 46. Total premature mortality across India is shown assuming population and underlying health data appropriate for both 2015 and 2050 (Figure 46b). Reduced ambient $PM_{2.5}$ concentrations for the NPS and CAS reduce estimates of annual premature mortality for 2015 by 4% and 39%, respectively relative to the control scenario of 900,000 (95UI: 683,000–1,252,000) annual premature mortalities. Assuming no change in emissions, total annual premature mortality for the control scenario in 2050 is estimated to be 1,577,000 (95UI: 1,210,000–2,209,000). This estimate of premature mortality in 2050 is 75% greater than in 2015 due to population growth and ageing, partly offset by reducing baseline mortality rates. Under the NPS and CAS, total premature mortality in 2050 changes by +68% and +7%, respectively relative to the control scenario estimate for 2015. The NPS and CAS can therefore potentially reduce the annual premature mortality estimate in 2050 by 61,000 and 610,000 deaths relative to the 2015 control, equivalent to offsetting 9% and 91% of the increase in 2050 caused by population ageing and growth. Despite the small national increase in premature mortalities (7%), the disease burden is reduced in some states (Jammu and Kashmir, Himachal Pradesh, Uttaranchal, and Sikkim) (Figure 46d).

Figure 47 shows the impacts of the scenarios on the mortality rate per 100,000 population from exposure to ambient $PM_{2.5}$ across India. Under no change in emissions to 2050, the mortality rate

increases by 39% to 86 deaths per 100,000 population relative to 2015. The mortality rate is independent of population size, hence removing the changes from population growth. In 2050, the NPS and CAS change the mortality rate per 100,000 population by +31% and -15%, respectively. In summary, the CAS stands out as the most effective scenario to reduce ambient PM_{2.5} concentrations across India, reducing the mortality rate per 100,000 population in 2050 below 2015 control levels by 15%, while still increasing the total premature mortality estimate in 2050 above 2015 control levels by 7%. These results highlight the challenge facing efforts to improve air quality related public health in India.

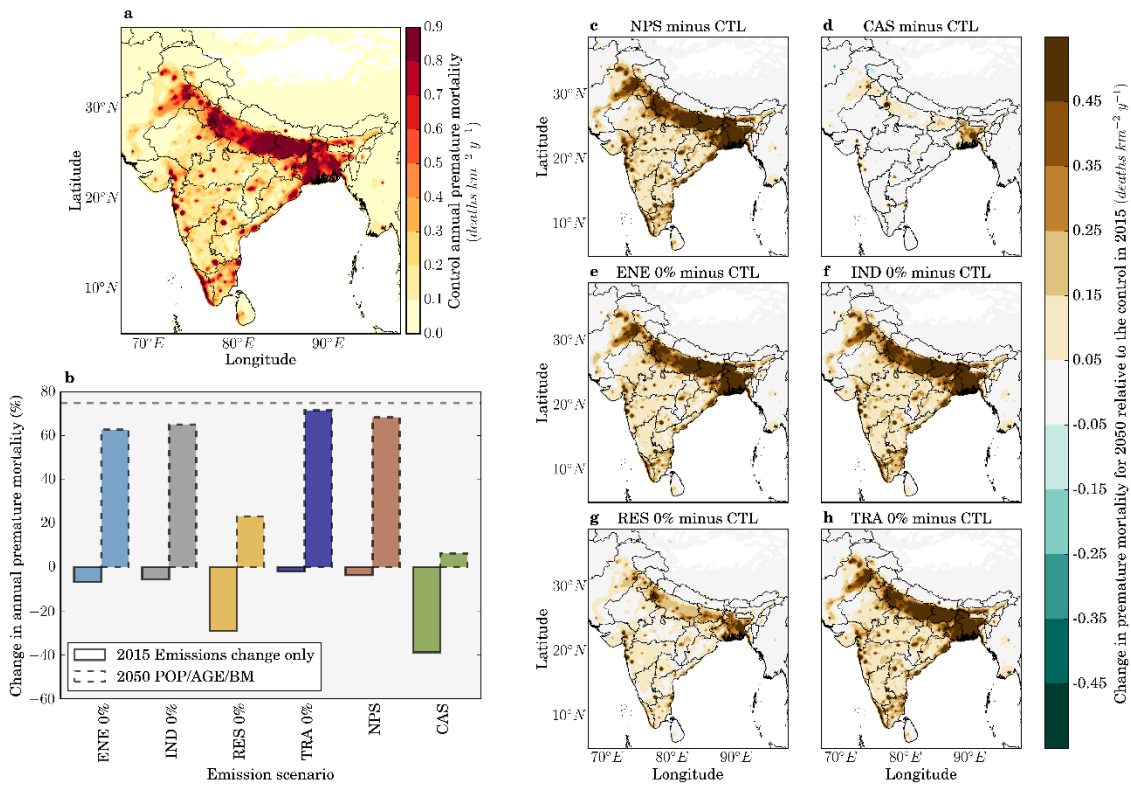


Figure 46: The impact of scenarios on annual premature mortality from exposure to ambient PM_{2.5} in India. (a) Annual premature mortality from exposure to ambient PM_{2.5} in India in 2015 from the control scenario. (b) National-mean changes in annual premature mortality estimates from ambient PM_{2.5} exposure per scenario, for both emissions only changes in 2015 and overall changes in 2050. The dashed horizontal line represents the change in annual premature mortality in 2050 if emissions remain at 2015 levels. (c–h) Difference in the annual premature mortality from ambient PM_{2.5} exposure in 2050 for IEA New Policy Scenario (NPS), IEA Clean Air Scenario (CAS), removal of power generation emissions (ENE 0%), removal of industry emissions (IND 0%), removal of residential energy use emissions (RES 0%), and removal of land transport emissions (TRA 0%) scenarios relative to the control scenario in 2015.

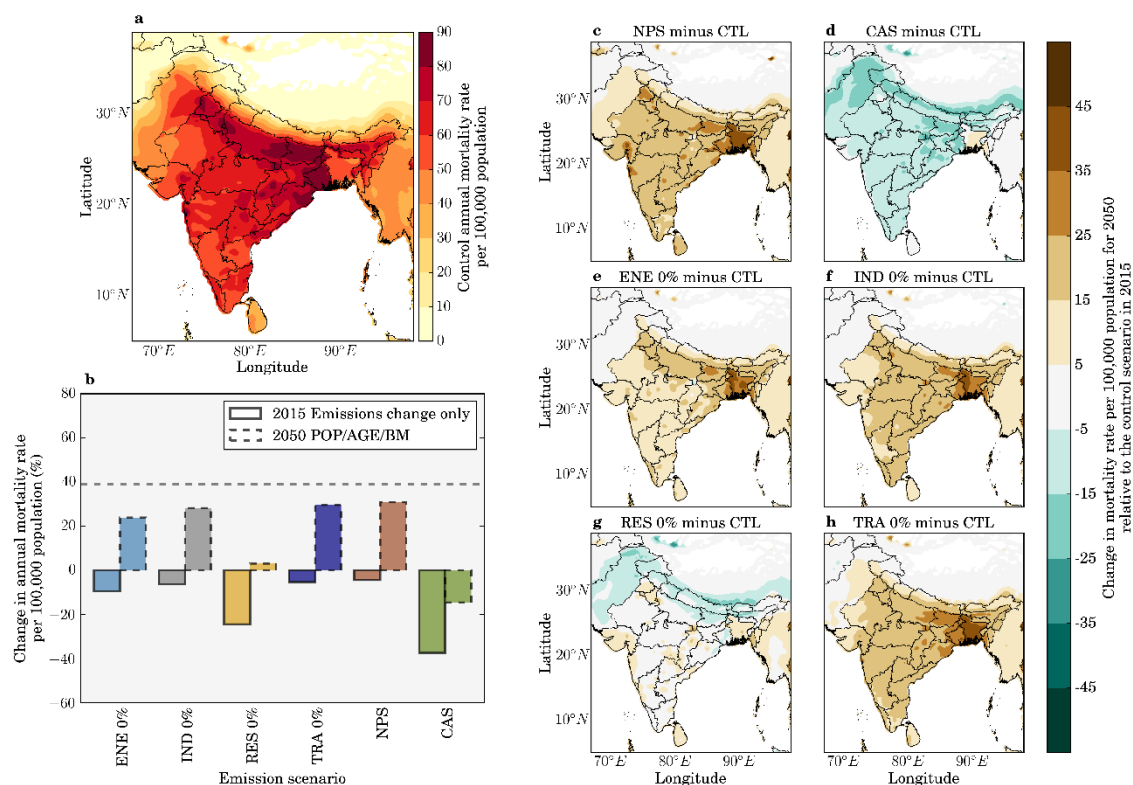


Figure 47: The impact of scenarios on annual mortality rate per 100,000 population from exposure to ambient $PM_{2.5}$ in India. (a) Annual mortality rate per 100,000 population from exposure to ambient $PM_{2.5}$ in India in 2015 from the control scenario. (b) National-mean changes in annual mortality rate per 100,000 population estimates from ambient $PM_{2.5}$ exposure per scenario, for both emissions only changes in 2015 and overall changes in 2050. The dashed horizontal line represents the change in annual mortality rate per 100,000 population in 2050 if emissions remain at 2015 levels. (c–h) Difference in the annual mortality rate per 100,000 population from ambient $PM_{2.5}$ exposure in 2050 for IEA New Policy Scenario (NPS), IEA Clean Air Scenario (CAS), removal of power generation emissions (ENE 0%), removal of industry emissions (IND 0%), removal of residential energy use emissions (RES 0%), and removal of land transport emissions (TRA 0%) scenarios relative to the control scenario in 2015.

In all states except Delhi, residential energy use is the dominant sectoral contributor to ambient $PM_{2.5}$ concentrations in the 2015 control scenario. In simulations where emissions from RES, ENE, IND, and TRA sectors are removed in 2050, the total premature mortality increases by 30%, 59%, 64%, and 68%, respectively relative to the control scenario estimate for 2015 (Figure 46b). The increase in the total premature mortality estimate in 2050 due to population ageing and growth can be offset by 407,000 (60%), 142,000 (21%), 105,000 (16%), and 68,000 (10%) premature mortalities by removing RES, ENE, IND, and TRA, respectively. The mean mortality rate per 100,000 population across India in 2050 relative to 2015 increases by 3%, 24%, 29%, and 31% by removing RES, ENE, IND, and TRA, respectively (Figure 47b). In Delhi, multiple emission sources contribute strongly to the very high annual-mean ambient $PM_{2.5}$ concentrations of $122 \mu g m^{-3}$ in the 2015 control scenario. Emissions from TRA dominate (36%), and emissions

from RES (27%), ENE (26%), and IND (13%) also contribute substantially. In West Bengal annual-mean ambient PM_{2.5} concentrations are also very high at 94 µg m⁻³, however RES emissions heavily dominate the source contribution (62%), and the scenario removing these is equivalent to 75% of the potential health benefits from the CAS. In West Bengal, annual premature mortality for the NPS and CAS in 2050 relative to the control scenario for 2015 are increased in line with the national averages of 68% and 7%, respectively. While for Delhi, both scenarios are less effective at reducing the disease burden where there is a 70% increase for the NPS and 22% increase for the CAS.

Figure 48 shows the impact of emission scaling from the idealised simulations (0%, -10%, and +10%) on population-weighted annual-mean ambient PM_{2.5} concentrations and the associated disease burden. There is an approximately linear reduction in population-weighted ambient PM_{2.5} concentrations relative to individual source emission changes. However, there is a non-linear reduction in premature mortality from the individual source change scenarios, due to the non-linear exposure-response function. Reductions in population-weighted ambient PM_{2.5} concentrations are relatively larger than reductions in the associated disease burden.

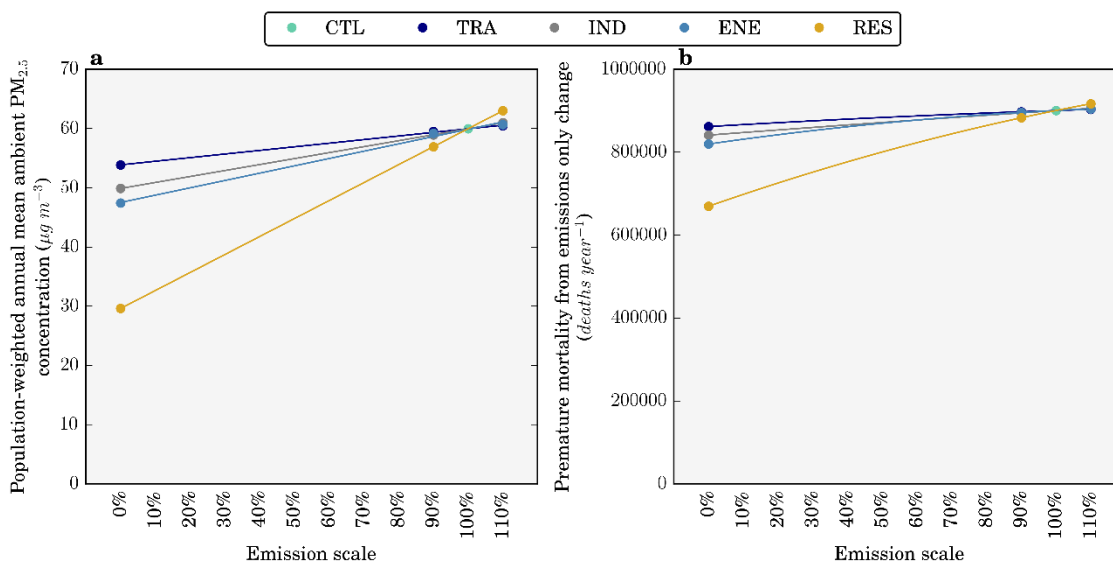


Figure 48: (a) The impact of emission scaling on population-weighted annual-mean ambient PM_{2.5} concentrations. (b) The impact of emission scaling on total annual premature mortality from exposure to ambient PM_{2.5} concentrations in India.

5.4.3. Sensitivities to demography and baseline mortality rates

Sensitivity studies are performed estimating the disease burden from emission only changes in 2015, and then for 2050 individually using population density from 2015 (POP2015), population age groupings from 2015 (AGE2015), or baseline mortality rates from 2015 (BM2015) to explore the impact of each variable in turn. Figure 49a shows the change in the national-mean premature mortality rate per 100,000 population in India due to ambient PM_{2.5} exposure from each scenario. Figure 49b shows the disease breakdown of the total premature

mortality estimates per scenario. Figure 49a and 49b do not show results from the -10% and +10% emission change scenarios as premature mortality estimates and mortality rates only change by $\pm 2\%$ for these scenarios. For emission only changes in 2015, the NPS and CAS reduced premature mortality estimates by 4% and 39%, respectively, while the individual removal of RES, ENE, IND, and TRA emissions reduced premature mortality estimates by 26%, 9%, 7%, and 4%, respectively (Figure 49b). Emissions reductions have a larger impact through reducing respiratory diseases (LRI and COPD), which respond more linearly, rather than the cardiovascular diseases (IHD and CEV), which have a more non-linear response to changes in $PM_{2.5}$ concentrations. The non-linearity was also found in previous studies (Apte *et al* 2015a, Kodros *et al* 2016, Conibear *et al* 2018a). These scenarios in which only emissions are modified highlight the need for stringent air quality management to reduce the disease burden in the highly polluted country of India due to the non-linear exposure-response function.

Each sensitivity (POP2015, AGE2015, and BM2015) uses 2015 data for that specific variable with 2050 data for the other variables. Each sensitivity shows the influence of the other parameters in combination in 2050, compared with 2015. The difference between each sensitivity mortality estimate for 2050 and the control mortality estimate for 2015 is the impact of the temporal change (2050 minus 2015) in that specific variable. For the control scenario, premature mortality estimates in 2050 for POP2015, AGE2015, and BM2015 changed by -22%, -60%, and +74%, respectively, relative to control scenario estimates for 2050 (Figure 49). Consequently, population ageing and growth together through to 2050 in India increase the number of people susceptible to air pollution, while a decrease in baseline mortality rates offsets a large part of this increase. The considerable sensitivity of premature mortality estimates to population ageing and baseline mortality rates illustrates the importance of demographic and epidemiological transitions in the future disease burden from exposure to ambient $PM_{2.5}$, which was also found in recent previous studies (Chowdhury *et al* 2018, GBD MAPS Working Group 2018).

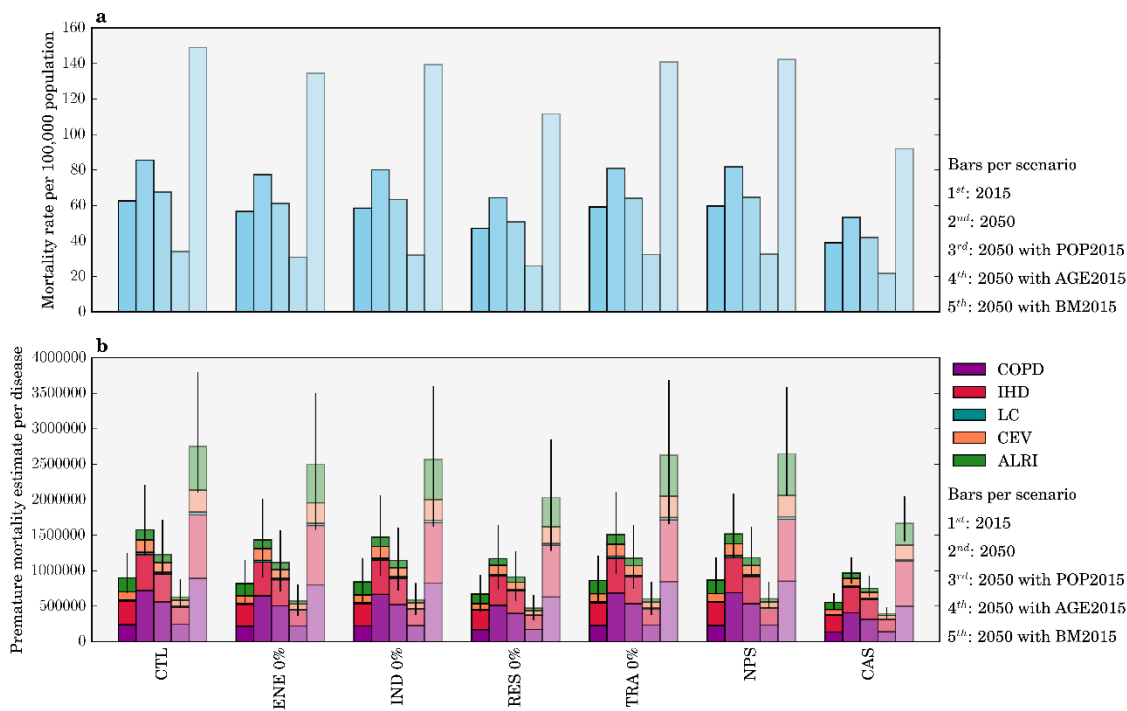


Figure 49: The impact of scenarios on the disease burden from exposure to ambient $PM_{2.5}$ in India. (a) National-mean annual premature mortality rate per 100,000 population due to ambient exposure to $PM_{2.5}$ in India. (b) Disease breakdown of health burden from ambient $PM_{2.5}$ exposure in India. For each panel, the bars show estimates for 2015, 2050, 2050 with population density from 2015, 2050 with population age grouping from 2015, and 2050 with baseline mortality rates from 2015 (1st to 5th bars per scenario). The vertical error bars show 95% uncertainty intervals (95UI) calculated by combining fractional errors in quadrature (see Methods).

5.4.4. Comparison to previous studies

Figure 50 compares this study's simulated impacts of the different scenarios on ambient $PM_{2.5}$ concentrations and the associated disease burden in India with previous studies (GBD MAPS Working Group 2018, International Energy Agency 2016a). This study estimates a larger percentage of the population exposed to ambient $PM_{2.5}$ concentrations exceeding the WHO IT-1 compared to the IEA study (International Energy Agency 2016a) (Figure 50b). This could potentially be a reflection of lower spatial resolution used in the IEA study underestimating the high ambient $PM_{2.5}$ concentrations in India, in addition to the different modelling choices. The IEA study used the Greenhouse gas–Air pollution Interactions and Synergies (GAINS) model (Amann *et al* 2011) driven by the European Monitoring and Evaluation Programme (EMEP) chemical transport model (Simpson *et al* 2012). The control scenario estimate of total premature mortality in 2015 from the IEA study was 34% smaller than this study (Figure 50c). This is likely due to the combination of lower ambient $PM_{2.5}$ concentrations, older baseline mortality rates (2011 versus 2016 in this study) corrected for risk but not cause of mortality, and the use of older exposure-response functions from the GBD2013 (GBD 2013 Risk Factors Collaborators 2015). The GBD2013 exposure-response functions have weaker relationships between risk and ambient

PM_{2.5} concentrations relative to the updated exposure-response functions from the GBD2016 (GBD 2016 Risk Factors Collaborators 2017, Cohen *et al* 2017) as used by this study and the GBD MAPS Working Group study. The IEA study estimated slightly smaller changes in premature mortality of +53% and -5% for the NPS and CAS, respectively relative to control scenario in 2015 compared to this study's estimates of +68% and +7%, primarily due to an earlier year of estimation (2040 versus 2050 in this study) reducing the impacts of population growth and ageing.

The control scenario population-weighted annual-mean ambient PM_{2.5} concentrations from the GBD MAPS Working Group study (GBD MAPS Working Group 2018) are 24% larger than those in this study (Figure 50a), potentially due to their use of higher resolution (0.1° × 0.1°) modelling and data assimilation within a Bayesian hierarchical model in the control scenario. The fractional impacts of the scenarios on ambient PM_{2.5} concentrations are then derived using the South Asia nested version of the GEOS-Chem chemical transport model at coarser resolution (0.5° × 0.67°) to scale the higher resolution ambient PM_{2.5} concentrations.

Present day emissions from this study are from EDGAR-HTAP v2.2 (Janssens-Maenhout *et al* 2015), and future emissions are scaled according to factors from the IEA NPS and CAS (International Energy Agency 2016a). Present day emissions of PM_{2.5}, BC, and OC from EDGAR-HTAP v2.2 (Janssens-Maenhout *et al* 2015) agree well with those from the GBD MAPS Working Group (Venkataraman *et al* 2018, GBD MAPS Working Group 2018). Present day emissions of SO₂, NO_x, and NMVOC from EDGAR-HTAP v2.2 (Janssens-Maenhout *et al* 2015) are a factor 1.5–2 larger than those from the GBD MAPS Working Group (Venkataraman *et al* 2018, GBD MAPS Working Group 2018), due largely to differences in the power sector.

The ambitious and aspirational scenarios analysed in the GBD MAPS Working Group study are different from the NPS and CAS scenarios analysed in this study. Both the IEA NPS and GBD MAPS Working Group ambitious scenarios are based on relevant existing and planned policies as of 2016 including India's INDCs. However, the technology shifts and sectoral growth rates vary between the different scenarios. In the NPS, SO₂, NO_x, and PM_{2.5} emissions increase by 10%, 10%, and 7% in 2040 relative to 2015, respectively, while in the GBD MAPS Working Group ambitious scenario SO₂, NO_x, and PM_{2.5} emissions increase by 156%, 96%, and 26% in 2050 relative to 2015, respectively. Similarly, while both the IEA CAS and the GBD MAPS Working Group aspirational scenario represent stringent air quality management, the specific realisations of these scenarios varies between the studies. In the CAS, SO₂, NO_x, and PM_{2.5} emissions change by -69%, -50%, and -76% in 2040 relative to 2015, respectively, while in the GBD MAPS Working Group aspirational scenario SO₂, NO_x, and PM_{2.5} emissions change by -6%, +13%, and -67% in 2050 relative to 2015, respectively. The GBD MAPS Working Group found larger resulting ambient PM_{2.5} concentrations from their scenarios (Figure 50a) and consequent increases in premature mortality in 2050 (Figure 50c). The NPS emissions of BC, OC,

SO₂, and NO_x are more similar to the GBD MAPS Working Group aspirational scenario (Venkataraman *et al* 2018, GBD MAPS Working Group 2018). NPS emissions of PM_{2.5} show a similar but lower (-30%) trend to the GBD MAPS Working Group ambitious scenario due to lower emissions from residential biomass and agricultural burning. NMVOC emissions are similar to the NPS and the GBD MAPS Working Group ambitious scenario (Venkataraman *et al* 2018, GBD MAPS Working Group 2018). This study, the GBD MAPS Working Group study, and the IEA study all find substantial potential public health benefits from stringent air quality management relative to a business-as-usual scenario.

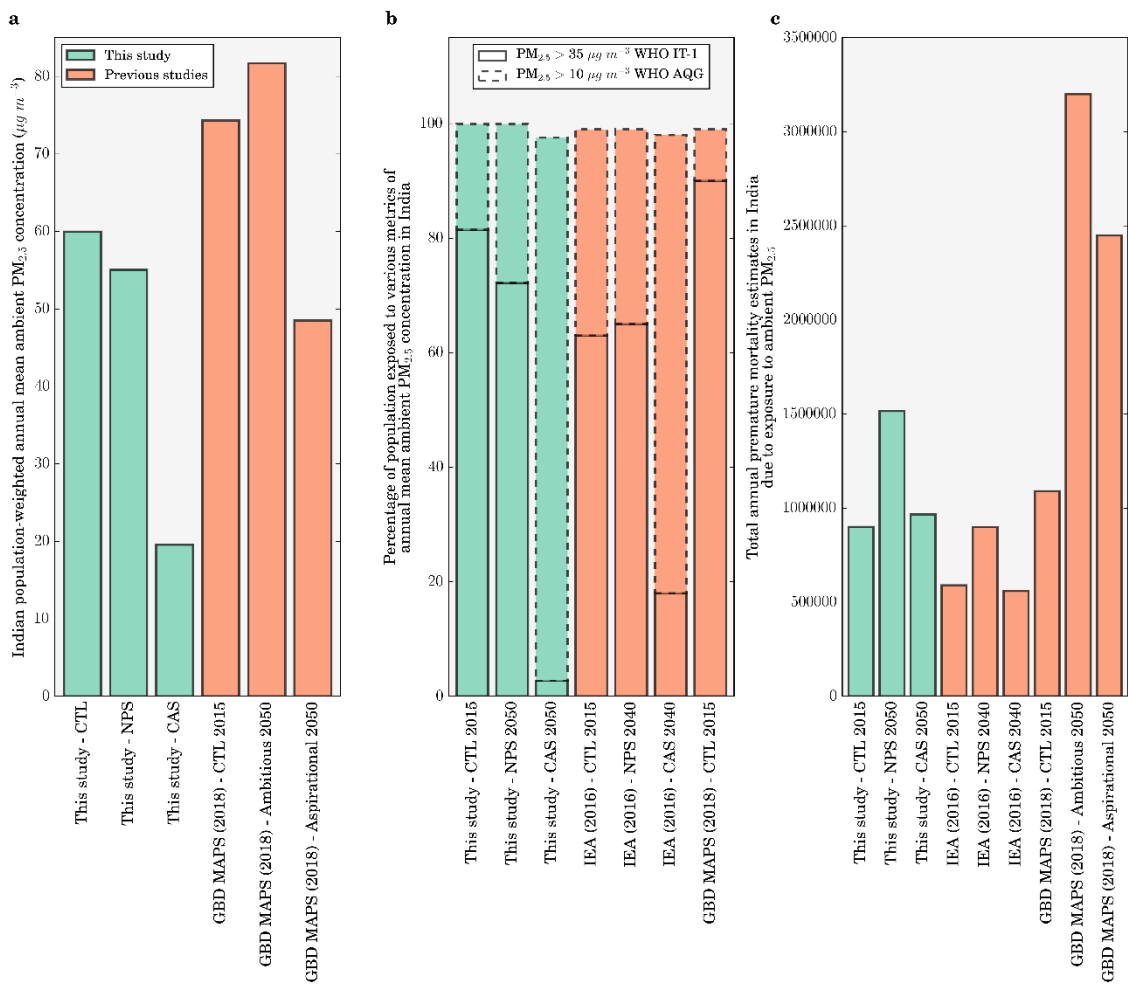


Figure 50: Comparison of the impacts of different scenarios on ambient PM_{2.5} concentrations and the associated disease burden in India from this study with previous studies. (a) Comparison of population-weighted annual-mean ambient PM_{2.5} concentrations. (b) Comparison of percentage of the population exposed to various metrics of annual-mean ambient PM_{2.5} concentrations in India. (c) Comparison of total premature mortality estimates due to exposure to ambient PM_{2.5} per year in India from different scenarios.

The influence of climate change on Indian PM_{2.5} concentrations is uncertain (Jacob and Winner 2009, Fiore *et al* 2012, Fang *et al* 2013). Climate changes are projected to be smaller than emission changes (Pommier *et al* 2018, Silva *et al* 2017, Fang *et al* 2013, Jacobson 2008, Kumar

et al 2018). Two recent studies analysed the combined impacts of climate change and emission scenarios on future air quality in South Asia by 2050 (Kumar *et al* 2018, Pommier *et al* 2018). The massive increase in anthropogenic emissions in India by 2050 has been found to have an order of magnitude larger impact on PM_{2.5} concentrations than climate change (Pommier *et al* 2018). Kumar *et al* (2018) found South Asian PM_{2.5} concentrations to change by +13 µg m⁻³ and +1 µg m⁻³ by 2050 relative to 2015 under Representative Concentration Pathways (RCP) 8.5 and RCP6.0, respectively. Kumar *et al* (2018) qualitatively related changes in meteorological variables with those in air quality, due to the limited number of simulations conducted relative to the large ensemble of simulations required to quantify the impacts of climate change. The health impacts of climate changes on PM_{2.5} concentrations in India were estimated to be 80,200 deaths per year by 2100 (Silva *et al* 2017). This is 3% of the increase in PM_{2.5} exposure associated mortality in India by 2050 due to emission changes under a reference scenario (GBD MAPS Working Group 2018). Both previous studies estimating the future health impacts of air pollution in India under different scenarios also used fixed meteorology to focus on the impacts of different air pollution control pathways (GBD MAPS Working Group 2018, International Energy Agency 2016a).

Regional transport of pollution from distant sources impacts local ambient PM_{2.5} concentrations (Task Force on Hemispheric Transport of Air Pollution 2010). In 2007, PM_{2.5} produced inside India was associated with 75,000 premature deaths outside of India, while PM_{2.5} produced outside India was associated with 67,000 premature deaths inside India (Zhang *et al* 2017). Aerosol transport from Africa and the Middle East is associated with 83,000 and 77,000 premature mortalities in India, respectively, primarily from dust (Liu *et al* 2009). Regional transport of PM_{2.5} into South Asia contributes 7% of the total mortality impact (Anenberg *et al* 2014).

This study, in agreement with previous studies (GBD MAPS Working Group 2018, International Energy Agency 2016a), finds substantial increases in the future disease burden associated with ambient PM_{2.5} exposure in India due to population growth and ageing. New policies as of 2016 or small (-10%) changes in emissions provide only small improvements in air quality and public health, with the impacts being heavily outweighed by the demographic transition. Stringent air quality management, such as under the IEA CAS, removing residential energy use emissions or the GBD MAPS Working Group aspirational scenario, will be required to provide vast improvements in air quality and essential public health benefits. The removal of residential energy use and land transport emissions might have further health benefits if exposures are studied at finer scales due to the collocation of emissions with exposures. The changes in disease burden estimates from ambient PM_{2.5} exposure do not consider that for some scenarios there is a sizeable accompanying reduction in the disease burden from reducing household air pollution from solid fuel use (e.g. the CAS and RES 0%).

5.5. Conclusion

Exposure to ambient particulate matter is a leading risk factor for public health in India. Business-as-usual economic and industrial growth in India in 2050 is predicted to increase emissions and further worsen ambient PM_{2.5} concentrations. Previous studies of alternative air pollution control scenarios in India have used relatively coarse spatial resolution models to estimate the impacts of the scenarios on ambient PM_{2.5} concentrations. In this study, a high-resolution online-coupled model was used with the latest exposure-response function to estimate the impacts of multiple Indian emission scenarios on ambient PM_{2.5} concentrations and human health in India. The impacts of climate change and the impacts of changing emissions from outside India are not included in this study. With no emissions growth in India, the disease burden from exposure to ambient PM_{2.5} in 2050 will increase by 75% relative to 2015, due to population ageing and growth increasing the number of people susceptible to air pollution, partly offset by decreasing baseline mortality rates. The IEA NPS and CAS in 2050 can reduce population-weighted ambient PM_{2.5} concentrations below 2015 levels by 9% and 68%, respectively. These reductions in ambient PM_{2.5} concentrations reduce the annual premature mortality estimate by 61,000 and 610,000 deaths, which is 9% and 91% of the projected increase in premature mortalities due to population growth and ageing, respectively. Throughout India, the CAS stands out as the most effective scenario to reduce ambient PM_{2.5} concentrations and the associated disease burden, reducing the 2050 mortality rate per 100,000 below 2015 control levels by 15%. However, even under the strong emission reductions in the CAS, population growth and ageing means that the annual premature mortality in 2050 will be 7% greater than in 2015. Small emission changes bring small improvements to air quality and human health, where the demographic transition to 2050 heavily outweighs the impacts. Strict implementation of air quality management, such as under the IEA CAS or removing residential energy use emissions from solid fuel use, can reduce the substantial and increasing health impacts of air pollution exposure in India bringing crucial public health benefits.

6. Current and future disease burden from ambient ozone exposure in India

6.1. Abstract

Long-term ambient O₃ exposure is a risk factor for human health. This study estimates the source-specific disease burden associated with long-term O₃ exposure in India at high spatial resolution using updated risk functions from the CPS-II. This study estimates 374,000 (95UI: 140,000–554,000) annual premature mortalities using the updated risk function in India in 2015, 200% larger than estimates using the earlier CPS-II risk function. This study finds land transport emissions dominate the source contribution to this disease burden (35%), followed by emissions from power generation (23%). With no change in emissions by 2050, this study estimates 1,126,000 (95UI: 421,000–1,667,000) annual premature mortalities, an increase of 200% relative to 2015 due to population ageing and growth increasing the number of people susceptible to air pollution. This study finds that the IEA NPS provides small changes (+1%) to this increasing disease burden from the demographic transition. Under the IEA CAS, this study estimates 791,000 (95UI: 202,000–1,336,000) annual premature mortalities in 2050, avoiding 335,000 annual premature mortalities (45% of the increase) compared to the scenario of no emission change. This study highlights that critical public health benefits are possible with stringent emission reductions, despite population growth and ageing increasing the attributable disease burden from O₃ exposure even under such strong emission reductions. The disease burden attributable to ambient PM_{2.5} exposure dominates that from ambient O₃ exposure in the present day, while in the future they may be similar in magnitude.

6.2. Introduction

The GBD2016 attributed 233,638 (95UI: 90,109–385,303) annual premature mortalities to ambient O₃ exposure globally, with 39% of the disease burden in India (GBD 2016 Risk Factors Collaborators 2017, Cohen *et al* 2017). The GBD2016 used the earlier CPS-II risk estimates (Jerrett *et al* 2009) for the cause of COPD only. These risk estimates have been updated for the same CPS-II cohort through an extended follow-up with an expanded study population (Turner *et al* 2016). Hazard ratios were found to increase (Turner *et al* 2016). The updated risks have been used to estimate global premature mortality from long-term ambient O₃ exposure, resulting in substantial mortality increases, including in India (Malley *et al* 2017). This increased public health burden due to O₃ exposure has implications for air quality management strategies.

Ambient surface O₃ concentrations have been increasing in India due to increasing emissions of O₃ precursors (Roy *et al* 2017, Ghude *et al* 2013). A business-as-usual scenario in India is projected to increase O₃ precursor emissions and future O₃ concentrations (Pommier *et al* 2018, Pozzer *et al* 2012, Chatani *et al* 2014, Fiore *et al* 2012, Wild *et al* 2012), with associated projections increasing the disease burden from O₃ exposure in India (Lelieveld *et al* 2015).

Previous studies have predicted an additional smaller increase due to climate change (Pommier *et al* 2018, Kumar *et al* 2018, Silva *et al* 2017). Pommier *et al* (2018) analysed the combined impacts of climate change and emission scenarios on future air quality in South Asia by 2050 and found the substantial increase in anthropogenic emissions in India to have at least a factor of three larger impact on O₃ concentrations than the impacts of climate change. Kumar *et al* (2018) studied RCPs in South Asia to 2050 and found South Asian daily average 8-hour O₃ concentrations changed by +11 ppbv and +2 ppbv by 2050 relative to 2015 under RCP8.5 and RCP6.0, respectively, due to the combined effects of a changing climate and air pollutant emissions. West *et al* (2007) found South Asian O₃ concentrations to increase by 15 ppbv under the Intergovernmental Panel on Climate Change (IPCC) Fourth Assessment Report A2 emission scenario by 2030, where 10% and 35% reductions were obtainable from the current legislation and maximum feasible reduction scenarios, respectively. Silva *et al* (2017) estimated the health impacts of climate changes on O₃ concentrations in India to be 16,000 premature mortalities per year by 2100. This estimate is 18% of the current disease burden in India attributable to ambient O₃ exposure estimated by the GBD2016 (GBD 2016 Risk Factors Collaborators 2017, Cohen *et al* 2017). The previous study estimating the future health impacts of air pollution in India under different scenarios used fixed meteorology to focus on the impacts of different air pollution control pathways (Silva *et al* 2016b).

Regional reductions in CH₄, an important O₃ precursor, have been found to lower future O₃ concentrations in India, reducing the exposure associated disease burden (Anenberg *et al* 2012). Reductions in non-methane VOCs and NO_x may have immediate air quality and health benefits near the emission reductions (West *et al* 2006, 2007, Anenberg *et al* 2012). NO_x reductions in Africa and North America impact Indian O₃ concentrations in spring, particularly in Delhi, while NO_x reductions in Southeast Asia and East Asia influence Indian O₃ concentrations in winter, specifically over Southern India (West *et al* 2009b, 2009a). Indian O₃ concentrations are mostly NO_x-sensitive, where NO_x emission reductions reduce the disease burden associated with O₃ exposure (West *et al* 2009a, Anenberg *et al* 2009). Regional transport contributes 10% to this reduction in the disease burden (Anenberg *et al* 2009).

The contribution of sources to the disease burden from ambient O₃ exposure in India were estimated in previous global studies (Silva *et al* 2016b, Lelieveld *et al* 2015) using the earlier CPS-II risk estimates, which found substantial contributions from precursor emissions from energy, land transport, and residential sources. Previous studies of the total or source-specific disease burden associated with O₃ exposure have used global, offline chemical transport models at relatively coarse spatial resolution (between 0.5° × 0.67° and 2.0° × 2.5°) (Malley *et al* 2017, Silva *et al* 2016b, Lelieveld *et al* 2015). Tropospheric O₃ has a non-linear dependence on precursors concentrations, with production on short timescales (Liang and Jacobson 2000, Carey Jang *et al* 1995, Wild and Prather 2006, Sharma *et al* 2017b). Coarse spatial resolution models dilute O₃ precursors, causing simulated concentrations to diverge from observations (Liang and

Jacobson 2000, Carey Jang *et al* 1995, Wild and Prather 2006, Sharma *et al* 2017b, Li *et al* 2016c, Pungler and West 2013, Thompson and Selin 2012, Thompson *et al* 2014). Resolution directly changes the resolved space, in addition to indirectly influencing parameterisation choices important for secondary pollutants (Wild and Prather 2006, Pungler and West 2013). The model resolution also affects estimates of the O₃ exposure related disease burden (Pungler and West 2013, Thompson *et al* 2014, Thompson and Selin 2012). O₃ has greater regional transport efficiency relative to PM_{2.5}, and studies focusing on both O₃ and PM_{2.5} found health impacts of PM_{2.5} to be more localised (Anenberg *et al* 2010, Ghude *et al* 2016, Anenberg *et al* 2014, 2009). Online-coupled modelling explicitly accounts for feedbacks between chemistry and meteorology (Grell *et al* 2004, Baklanov *et al* 2014), which can be important to consider when emissions are changing.

This study makes the first estimate of the source-specific disease burden due to O₃ exposure at high spatial resolution, using the updated CPS-II risk functions from Turner *et al* (2016), in addition to analysing the impacts of future air pollution control pathways. High-resolution (30km, 0.3° spatial resolution) numerical weather prediction, online-coupled with chemistry, model simulations are used to estimate the present-day reductions in surface O₃ concentrations in India resulting from the removal of different O₃ precursor source sectors. An annual control simulation was performed for the year 2014 and evaluated against surface observations; then annual sensitivity simulations are performed individually removing biomass burning (BBU), power generation (ENE), industrial non-power (IND), residential energy use (RES), and land transport (TRA). The impact of scenarios is conducted in line with the IEA NPS and CAS (International Energy Agency 2016a). To help interpret the impacts of these emission scenarios, idealised simulations individually changing emissions (-10% and +10%) are conducted for the four anthropogenic emission sectors (ENE, IND, RES, and TRA). The associated disease burden per risk estimate, per simulation, is estimated. Further sensitivity studies are performed to explore the impacts of the Indian demographic and epidemiologic transition through to 2050 on the public health burden associated with O₃ exposure. It is assumed that both climate and emissions from countries outside India remain unchanged, allowing the isolation of the impacts of changing Indian emissions. The aim is to produce a valuable resource to help inform environmental policy decisions at the state and national levels regarding O₃ precursor emission controls.

6.3. Precursor emissions

Figure 51 shows the spatial contributions of land transport, power generation, residential energy use, and industry to total annual anthropogenic emissions of NO_x, NMVOC, and CO. Land transport dominates anthropogenic emissions of NO_x, while residential energy use is the leading contributor to anthropogenic emissions of CO and NMVOC. Figure 52 shows the fractional contribution of each season (winter DJF, spring MAM, summer JJA, and autumn SON) to total anthropogenic emissions of NO_x, NMVOC, and CO. Anthropogenic emissions of NO_x, NMVOC,

and CO are all highest during the winter (DJF) and lowest in the summer (JJA). CO and VOC are more spatially dispersed in rural areas in contrast to NO_x (Kumar *et al* 2012b).

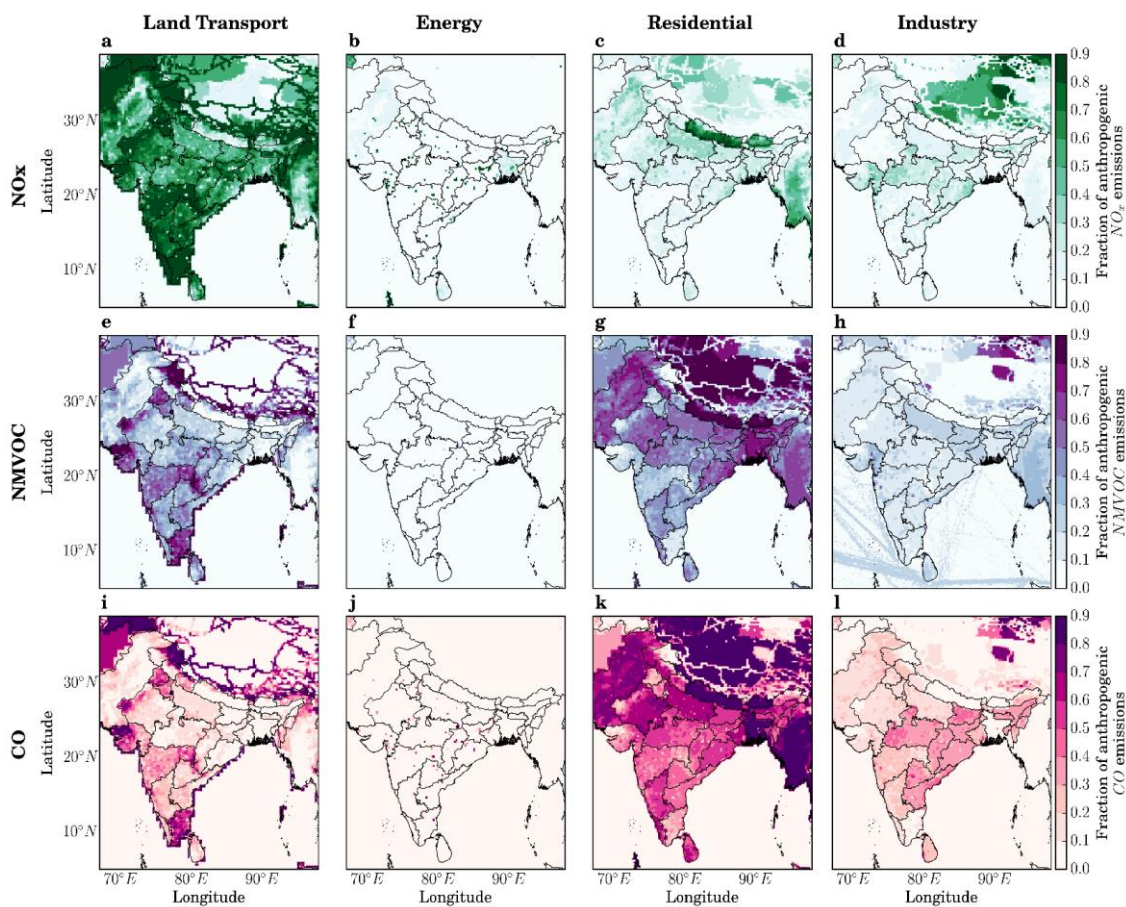


Figure 51: Fractional contribution per sector to total annual anthropogenic emissions. The fractional contribution of land transport (TRA), power generation (ENE), residential energy use (RES), and industry (IND) to anthropogenic emissions of (a–d) nitrogen oxides (NO_x), (e–h) non-methane volatile organic compounds (NMVOC), and (i–l) carbon monoxide (CO).

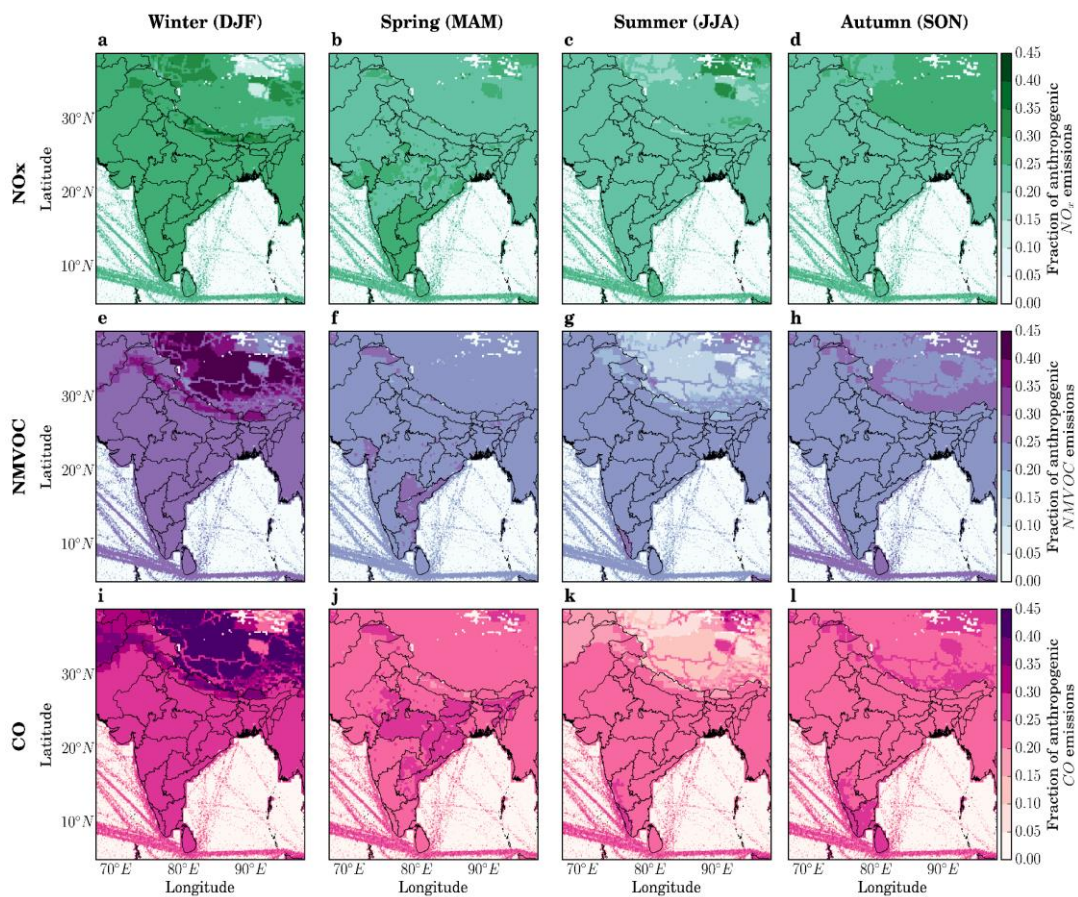


Figure 52: Fractional contribution per season to total anthropogenic emissions. The fractional contribution to total anthropogenic emissions of NO_x from winter (DJF), spring (MAM), summer (JJA), and autumn (SON) to anthropogenic emissions of (a–d) nitrogen oxides (NO_x), (e–h) non-methane volatile organic compounds (NMVOC), and (i–l) carbon monoxide (CO).

6.4. Results

6.4.1. Comparison of disease burden using earlier and updated risks

Figure 53 compares the estimates of premature mortality, mortality rate per 100,000 population, and YLL in 2015 from ambient O_3 exposure in India using model simulated surface O_3 , and risk estimates from both the earlier CPS-II study from Jerrett *et al* (2009) and the updated CPS-II study from Turner *et al* (2016). The disease burden estimates (premature mortality, YLL, and mortality rate) using the updated CPS-II risks from Turner *et al* (2016) are approximately 200% larger than the disease burden estimates using the earlier CPS-II risks from Jerrett *et al* (2009). This is primarily due to the larger hazard risk ratios (HR = 1.14 compared to HR = 1.04). Using earlier CPS-II risks, this study estimates 124,000 (95UI: 57,000–203,000) and 107,000 (95UI: 42,000–185,000) annual premature mortalities from COPD due to O_3 exposure in India for 2015 using LCC_{\min} and $\text{LCC}_{\text{fifth}}$, respectively. Using updated CPS-II risks, these increase to 374,000 (95UI: 140,000–554,000) and 336,000 (95UI: 128,000–501,000) annual premature mortalities from COPD due to O_3 exposure in India for 2015 using LCC_{\min} and $\text{LCC}_{\text{fifth}}$,

respectively. The annual premature mortality estimates using updated CPS-II risks are 202% and 214% larger than mortality estimates using earlier CPS-II risks for LCC_{min} and LCC_{fifth} , respectively. This study quantifies 1,899,000 (95UI: 875,000–3,111,000) and 1,639,000 (95UI: 650,000–2,834,000) annual YLL from COPD due to O_3 exposure in India for 2015 for earlier CPS-II risks using LCC_{min} and LCC_{fifth} , respectively. These increase to 5,729,000 (95UI: 2,138,000–8,482,000) and 5,148,000 (95UI: 1,963,000–7,679,000) annual YLL from COPD due to O_3 exposure in India for 2015 for updated CPS-II risks using LCC_{min} and LCC_{fifth} , respectively. The annual YLL estimates using updated CPS-II risks are 217% and 214% larger than estimates using earlier CPS-II risks for LCC_{min} and LCC_{fifth} , respectively. This study estimates the annual mean mortality rate per 100,000 population for India from O_3 exposure is 10 (95UI: 4–16) and 8 (95UI: 3–14) for the earlier CPS-II risks for LCC_{min} and LCC_{fifth} , respectively. The mortality rate is 28 (95UI: 11–43) and 25 (95UI: 10–39) per 100,000 population for the updated CPS-II risks for LCC_{min} and LCC_{fifth} , respectively. The annual mortality rates per 100,000 population are 180% and 213% larger for the updated CPS-II risks relative to the earlier CPS-II risks for LCC_{min} and LCC_{fifth} , respectively.

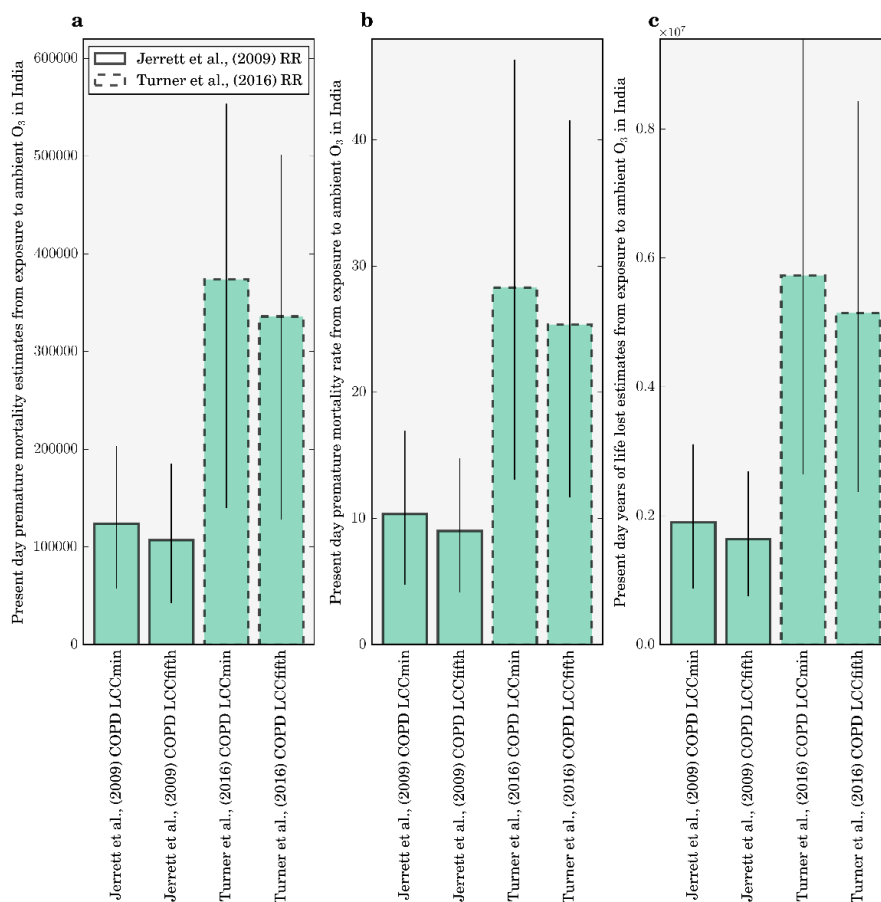


Figure 53: Estimates of (a) premature mortality, (b) mortality rate per 100,000 population, and (c) years of life lost (YLL) in 2015 from ambient O_3 exposure in India using the earlier CPS-II study risks from Jerrett et al (2009) (solid bars) and the updated CPS-II study risks from Turner et al (2016) (dashed bars). Error bars represent 95% uncertainty intervals.

Figure 54 shows the 3mDMA1 and ADM8h O₃ concentrations across India with the associated respective premature mortality estimates and mortality rate per 100,000 population. The population-weighted surface O₃ concentrations for the 3mDMA1 metric is 94.5 ppbv and for the ADM8h metric is 77.2 ppbv. Surface O₃ concentrations are larger over northern and eastern India. The overall disease burden is highly concentrated in the IGP, with hotspots across India relating to population density. The mortality rate is less spatially variable, though highest in northeastern India, with values of 13 per 100,000 population for the Jerrett *et al* (2009) risks and 34 per 100,000 population for the updated risks from Turner *et al* (2016).

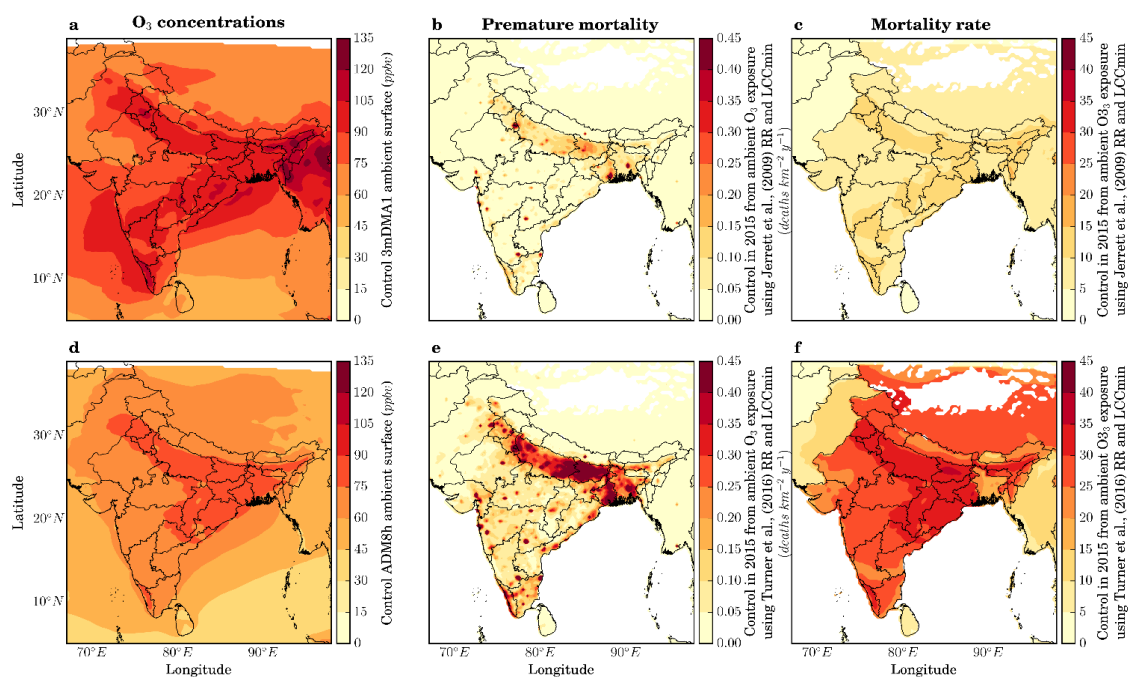


Figure 54: Premature mortality estimates due to O₃ exposure across India in 2015. All calculations for the control scenario. (a, d) Annual mean surface O₃ concentrations. (b, e) Annual premature mortality. (c, f) Annual mortality rate per 100,000 population. (a–c) Calculated following Jerrett *et al* (2009). (d–f) Calculated following Turner *et al* (2016). (a) Shows the 3mDMA1 O₃ metric. (d) Shows the ADM8h O₃ metric. See text for details.

6.4.2. Reduction in O₃ concentrations and disease burden per source removal

Table 7 shows the reduction in population-weighted 3mDMA1 and ADM8h O₃ concentrations across India associated with the removal of different emission sectors. The spatial change in annual-mean surface O₃ concentrations of these source removals are in Figure 63 (Appendix D). This study finds emissions from land transport dominate (28% of 3mDMA1 and 35% of ADM8h) the reduction in O₃ concentrations from all individual source removals, with substantial reductions from energy (14% of 3mDMA1 and 23% of ADM8h) and residential energy use emissions (9% of 3mDMA1 and 11% of ADM8h). The summation of these source reductions is 60% from 3mDMA1 and 76% from ADM8h. The summation of source reductions is less than 100% due to sources not investigated in this study (e.g. aircraft NO_x, biogenic VOCs), sources outside of the domain, natural sources (e.g. stratospheric O₃ transport, lightning NO_x, soil NO_x), and due to the

non-linear response of O₃ to precursor emission changes. The source summation less than 100% has been seen in a previous study over India by Silva *et al* (2016a) and Sharma *et al* (2016), and Fiore *et al* (2004) demonstrated the influence of additional sources to O₃ concentrations in the United States.

Table 7: Reduction in population-weighted surface O₃ concentrations in India associated with removing different sources. Two different O₃ metrics (3mDMA1 and ADM8h) are shown. Sources are biomass burning (BBU), power generation (ENE), industrial non-power (IND), residential energy use (RES), and land transport (TRA). Absolute (ppbv) and relative (%) reductions are shown.

Reduction to population-weighted surface O ₃ concentration		BBU	ENE	IND	RES	TRA	TOTAL
3mDMA1 O ₃	ppbv	4.0	13.5	4.5	8.1	26.4	56.5
	%	4	14	5	9	28	60
ADM8h O ₃	ppbv	1.7	17.4	3.9	8.1	27.0	58.1
	%	2	23	5	11	35	75

Table 8 shows the source contributions to the annual premature mortality estimate associated with O₃ exposure in India in 2015 using Turner *et al* (2016) risks and LCC_{min}. This study calculates the source contributions using two different methods: the attribution and subtraction methods (Section 2.6) (Conibear *et al* 2018a, Kodros *et al* 2016). The estimates from the attribution and subtraction method are expected to produce different results due to the shape of the exposure-response function, despite both methods using the same O₃ concentrations from each emission removal simulation.

At the national level, the contribution from land transport emissions to the disease burden calculated using Turner *et al* (2016) risks is 35% for the attribution method and 46% for the subtraction method. For energy emissions, the contribution to the total disease burden is 23% and 28% for the attribution and subtraction methods, respectively. The spatial distributions of the dominant contributing sources (land transport and energy emissions) to the disease burden associated with O₃ exposure in India are shown in Figure 64 (Appendix D). The summation of the source contributions to mortality from the attribution method is 284,000 (95UI: 106,000–421,000) annual premature mortalities (76% of control simulation), while for the subtraction method it is 355,000 (95UI: 133,000–526,000) annual premature mortalities (95% of control simulation). The source contributions to the O₃ burden from the attribution method are smaller than source contributions from the subtraction method, due to the present day O₃ concentrations experienced in India being in the linear section of the exposure-response function, and to the high minimum pollutant threshold (26.7 ppb for Turner *et al* (2016) risks and LCC_{min}).

Table 8: Source contributions to the annual premature mortalities associated with ambient O₃ exposure in India in 2015 calculated using Turner et al (2016) risks and LCC_{min}, including source contributions to the annual premature mortalities associated with ambient PM_{2.5} exposure from Conibear et al (2018a) (Chapter 4). The absolute number and percentage of total premature mortalities associated with O₃ exposure in India are shown for two different methods (attribution and subtraction), and for the subtraction method for PM_{2.5} exposure. Sources are biomass burning (BBU), power generation (ENE), industrial non-power (IND), residential energy use (RES), and land transport (TRA). Values in parentheses represent the 95% uncertainty intervals (95UI).

Source contribution to annual premature mortalities		BBU	ENE	IND	RES	TRA	TOTAL
O ₃ , attribution	×10 ³	7 (3–11)	86 (32–127)	19 (7–28)	41 (15–61)	131 (49–194)	284 (106–421)
	%	2	23	5	11	35	76
O ₃ , subtraction	×10 ³	10 (4–15)	105 (39–156)	22 (8–33)	45 (17–67)	173 (65–256)	355 (133–527)
	%	3	28	6	12	46	95
PM _{2.5} , subtraction (Chapter 4)	×10 ³	12 (8–16)	90 (60–122)	66 (45–90)	256 (162–340)	43 (29–58)	467 (304–626)
	%	1	9	7	26	4	47

6.4.3. Impact of emission mitigation scenarios on O₃ and the disease burden

Figure 55 shows the impact of different emission scenarios on surface O₃ concentrations. The NPS increased the population-weighted ADM8h O₃ concentrations by 1%, while the CAS reduced them by 24%. The removal of land transport emissions reduces population-weighted ADM8h O₃ concentrations by 35%, and the removal of energy emissions reduces them by 23%. These results show that the removal of land transport emissions produces greater reductions in O₃ concentrations than the CAS. The larger reduction of O₃ via removing land transport emissions may be due to land transport emissions heavily dominating contributions to anthropogenic NO_x emissions, coupled to many population regions of India being NO_x limited. O₃ production in India

has been found to be mostly NO_x -limited where O_3 reductions are more sensitive to the emission control of NO_x than VOC, while some studies find urban areas are VOC-limited (Mahajan *et al* 2015, Kumar *et al* 2012a, Sharma *et al* 2016, 2017a, Saikawa *et al* 2017, Ojha *et al* 2012, Pommier *et al* 2018, Lu *et al* 2018). The complex emission changes within the CAS combine a 24% increase in industrial NO_x emissions and a 78% reduction in land transport NO_x emissions, with substantial reductions in residential VOC emissions, which can potentially alter the O_3 sensitivity to NO_x changes. In the NPS where land transport NO_x emissions decrease by 45%, O_3 concentrations increase over Delhi. This increase is possibly due to the urban VOC limited regime where O_3 production is inversely proportional to NO_x . When designing air pollution control pathways to reduce the health impacts of O_3 exposure, care is required to consider how changing anthropogenic emissions will affect O_3 production, and specifically sensitivities to NO_x and VOC emissions under different regimes.

This study estimates the percentage of the population exposed to different concentration levels according to the WHO 8-hour daily maximum O_3 concentration of 50 ppb, which is the same as the Indian NAAQS (World Health Organization 2006a, Ministry of Environment and Forests 2009). For all scenarios except ENE 0%, CAS, and TRA 0%, all of the Indian populations in both 2015 and 2050 remain exposed to O_3 concentrations above WHO and NAAQS O_3 metrics. For the ENE 0%, CAS, and TRA 0% scenarios, 13%, 14%, and 52% of the populations, respectively had their exposures brought into line with the WHO and NAAQS O_3 metrics (Figure 65, Appendix D).

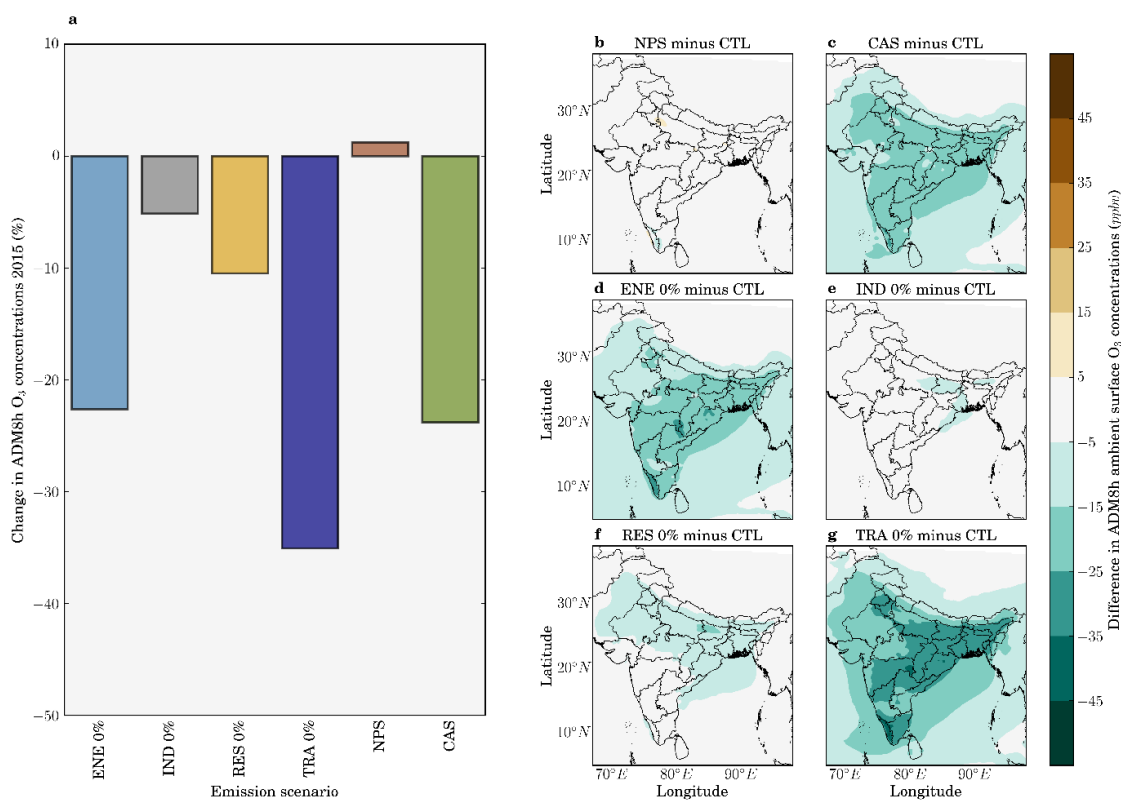


Figure 55: Impacts of air pollution control pathways on surface O_3 concentrations in India. (a) National-mean relative changes in population-weighted ADM8h surface O_3 concentrations

for different emission scenarios relative to the control scenario in 2015. (b–g) Absolute change in ADM8h O₃ concentrations for different emission scenarios relative to the control (CTL) scenario. Emission scenarios are New Policy Scenario (NPS), Clean Air Scenario (CAS), and when individual emission sectors are switched off: power generation (ENE 0%), industrial non-power (IND 0%), residential energy use (RES 0%), and land transport (TRA 0%).

Figure 56 shows the impacts of different emission scenarios on total premature mortality associated with O₃ exposure. Figure 57 shows the corresponding results for the mortality rate per 100,000 population. For emission change only in 2015 (i.e. population, age structure, and background mortality are unchanged), the NPS has small impacts (+1%) on annual premature mortality relative to the control in 2015 due to small change (+1%) in O₃ in this scenario. In contrast, the CAS reduces annual premature mortality by 30% relative to the control due to the 24% reduction in O₃ under this scenario. The greater relative reduction in premature mortality compared to O₃ is due to the strong sensitivity of risk to O₃ (Figure 24, Section 2.4) at the concentrations currently experienced across India (population-weighted ADM8h estimated to be 77.2 ppbv). The TRA 0% scenario results in a 46% reduction in premature mortality (due to a 35% reduction in O₃), and the ENE 0% results in a 28% reduction in premature mortality (due to a 23% reduction in O₃).

The impact of the demographic transition through to 2050 on the premature mortality estimates heavily outweighs the impacts of emission changes. If emissions remain at 2015 levels, this study estimates the annual premature mortality will increase by 200% to 1,126,000 (95UI: 421,000–1,667,000) due to population ageing and growth increasing the number of people susceptible to air pollution. The impact of the NPS is similar to changes to those from no emission change (+205%). The IND 0% and RES 0% scenarios offset part of the increase in the annual premature mortality estimate due to the demographic transition, avoiding 65,000 (9%) and 136,000 (18%) premature mortalities, respectively. The TRA 0%, CAS, and ENE 0% scenarios offset a substantial amount of the increasing disease burden from the demographic transition, avoiding 520,000 (69%), 335,000 (45%), and 316,000 (42%) premature mortalities per year. This means that even under the stringent emission controls implemented in the CAS, annual premature mortality from ambient O₃ exposure will increase in 2050 by 111% above the 2015 control scenario to 791,000 (95UI: 202,000–1,336,000) premature deaths.

For no change in emissions through to 2050, the mortality rate per 100,000 population will increase by 139% to 67 (95UI: 24–104) due to the demographic transition. The impact of the NPS by 2050 on mortality rate per 100,000 population is similar to changes to those from no emission change (+139%). The IND 0% and RES 0% scenarios offset part of the increase in the annual mortality rate estimate due to the demographic transition, avoiding 3 (4%) and 7 (10%) annual deaths per 100,000 population, respectively. The TRA 0%, CAS, and ENE 0% scenarios offset 32 (48%), 19 (28%), and 21 (31%) annual deaths per 100,000 population, respectively, from the demographic transition in 2050. Under the stringent emission control scenario of CAS, the annual

mortality rate from exposure to O₃ in 2050 will increase by 71% above the 2015 control scenario to 48 (95UI: 13–86) deaths per 100,000 population.

These results highlight the dominant role of the demographic transition by 2050 in controlling the susceptibility of the Indian population to air pollution, leading to a substantial mortality increase. Stringent air pollution control pathways can provide essential public health benefits offsetting part of the disease burden from O₃ exposure.

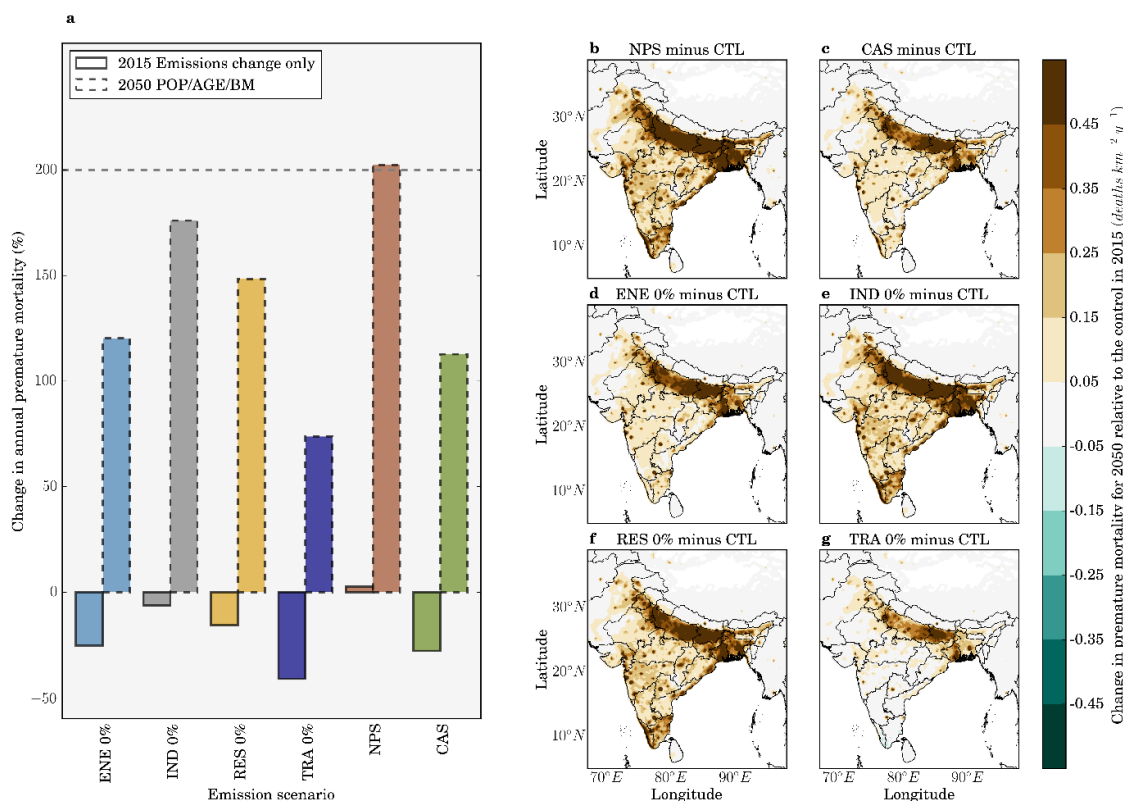


Figure 56: Impacts of air pollution control pathways on annual premature mortality from ambient O₃ exposure in India. (a) National-mean changes in annual premature mortality estimates from ambient O₃ exposure per scenario, for both emissions only changes between 2015 and 2050 (solid bars) and overall changes in 2050 including 2015 to 2050 changes in emissions as well as population growth, population ageing, and baseline mortality rates (POP/AGE/BM, dashed bars). The dashed horizontal line represents the change in annual premature mortality in 2050 if emissions remain at 2015 levels. (b–g) Change in annual premature mortality from ambient O₃ exposure in 2050 from different emission scenarios (see Figure 55) relative to the control scenario in 2015 accounting for emission changes and POP/AGE/BM changes. All health impacts are calculated using Turner et al (2016) RR and LCC_{min}.

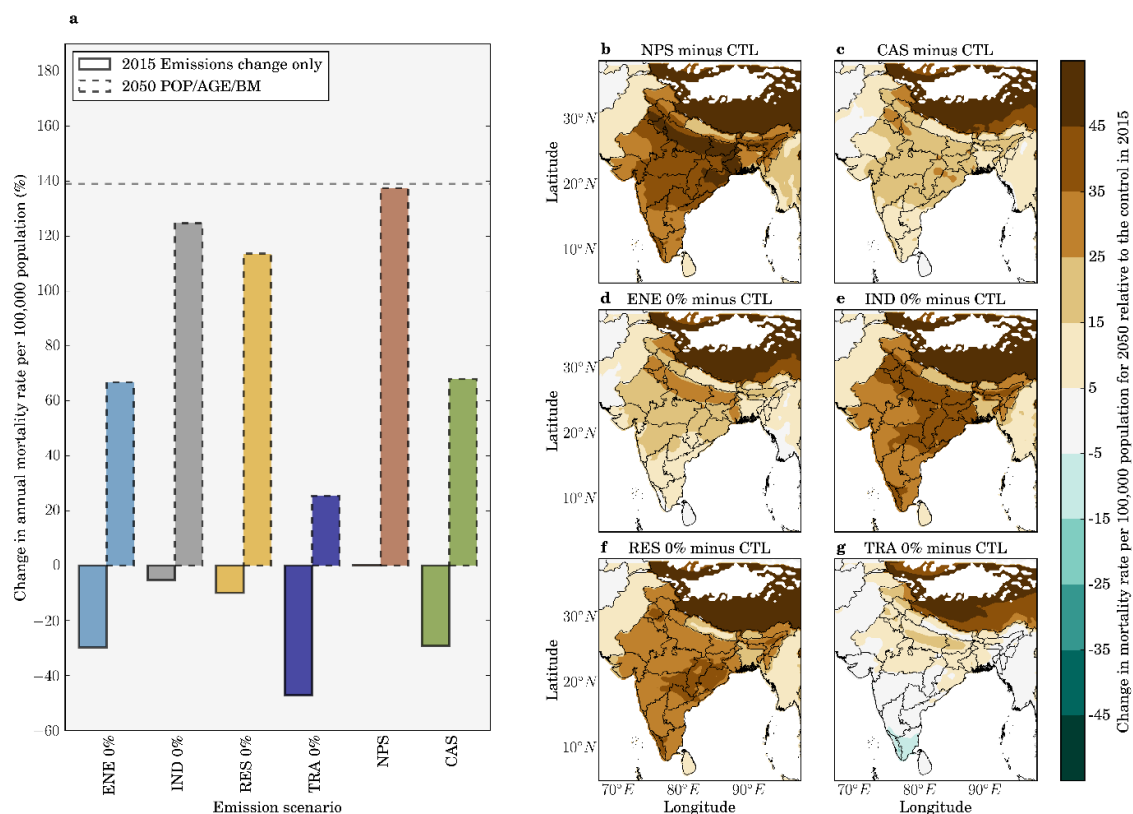


Figure 57: Impacts of air pollution control pathways on annual mortality rate per 100,000 population from ambient O_3 exposure in India. (a) National-mean changes in annual mortality rate per 100,000 population estimates from ambient O_3 exposure per scenario, for both emissions only changes between 2015 and 2050 (solid bars) and overall changes in 2050 including 2015 to 2050 changes in emissions as well as population ageing and baseline mortality rates (POP/AGE/BM, dashed bars). The dashed horizontal line represents the change in annual mortality rate per 100,000 population in 2050 if emissions remain at 2015 levels. (b–g) Annual change in mortality rate per 100,000 population from ambient O_3 exposure in 2050 from different emission scenarios (see Figure 55) relative to the control scenario in 2015 accounting for emission changes and POP/AGE/BM changes. All health impacts are calculated using Turner *et al* (2016) RR and LCC_{min} .

Figure 58 shows the impact of emission scaling from the idealised simulations (0%, -10%, and +10%) on surface O_3 concentrations and the associated disease burden. This study applied linear scaling to illustrate the influence of the non-linear response of O_3 concentrations to changes in O_3 precursors. Wild *et al* (2012), later developed by Turnock *et al* (2018), used simulations from 20% emission reductions of O_3 precursors to scale surface O_3 changes and found this parameterised approach worked well for small emission perturbations. The parameterised approach also works well for CO and NMVOC, while the O_3 response to NO_x was more non-linear (Wu *et al* 2009). The parameterisation was not expected to perform well for large emission perturbations ($> \pm 60\%$) or source regions under titration regimes (emission reductions may lead to O_3 increases) (Wild *et al* 2012, Turnock *et al* 2018). This study used a similar approach here.

However, the scaling was applied to a -10% emission change, per sector instead of per precursor, up to complete removal to illustrate the difference of the non-linear O₃ response.

This study estimates the non-linear O₃ response ($O_{3,non-linear}$) as a function of the O₃ from the control simulation ($O_{3,CTL}$), the 0% idealised simulation ($O_{3,sim0\%}$), and the -10% idealised simulation ($O_{3,sim-10\%}$) following Equation 14. The percentage contribution of non-linear O₃ response ($O_{3,non-linear,\%}$) is then estimated relative to the change in O₃ from the 0% idealised simulation following Equation 15. Calculations are performed for both population-weighted ADM8h O₃ concentrations and the premature mortality estimates from O₃ exposure following Turner *et al* (2016) risks and LCC_{min}.

$$O_{3,non-linear} = (O_{3,CTL} - O_{3,sim0\%}) - 10 \times (O_{3,CTL} - O_{3,sim-10\%})$$

Equation 14: *The non-linear O₃ response.*

$$O_{3,non-linear,\%} = 100 \times O_{3,non-linear} / (O_{3,CTL} - O_{3,sim0\%})$$

Equation 15: *The percentage contribution of the non-linear O₃ response.*

For population-weighted ADM8h O₃ concentrations, this study finds that the non-linear O₃ response accounts for 69%, 61%, 104%, and 43% of the change from the 0% idealised simulations for TRA, IND, ENE, and RES, respectively (Figure 58a). This means that the non-linear O₃ response plays a strong role for O₃ changes from TRA, IND, and ENE emission removal, although the absolute change for the IND simulations is small. The strong non-linear O₃ response for TRA and ENE may be due to the large, heterogeneous NO_x emissions across India (Figure 51, Section 6.3), and other precursors co-emitted with these sectors. For premature mortality estimates from O₃ exposure following Turner *et al* (2016) risks and LCC_{min}, this study finds that the non-linear O₃ response accounts for 73%, 65%, 103%, and 48% of the change from the 0% idealised simulations for TRA, IND, ENE, and RES, respectively (Figure 58b). The similar contributions of the non-linear O₃ response to O₃ concentrations and the associated premature mortality estimates suggest that the changes in O₃ concentrations are in the linear section of the exposure-response function (i.e. below approximately 100 ppb). Although these estimates are illustrative, they suggest a strongly non-linear chemical regime over India under large emission changes, which was also found in Turnock *et al* (2018), where the non-linear response of O₃ concentrations to changes in O₃ precursors plays a large role on surface O₃ concentrations and the exposure associated disease burden.

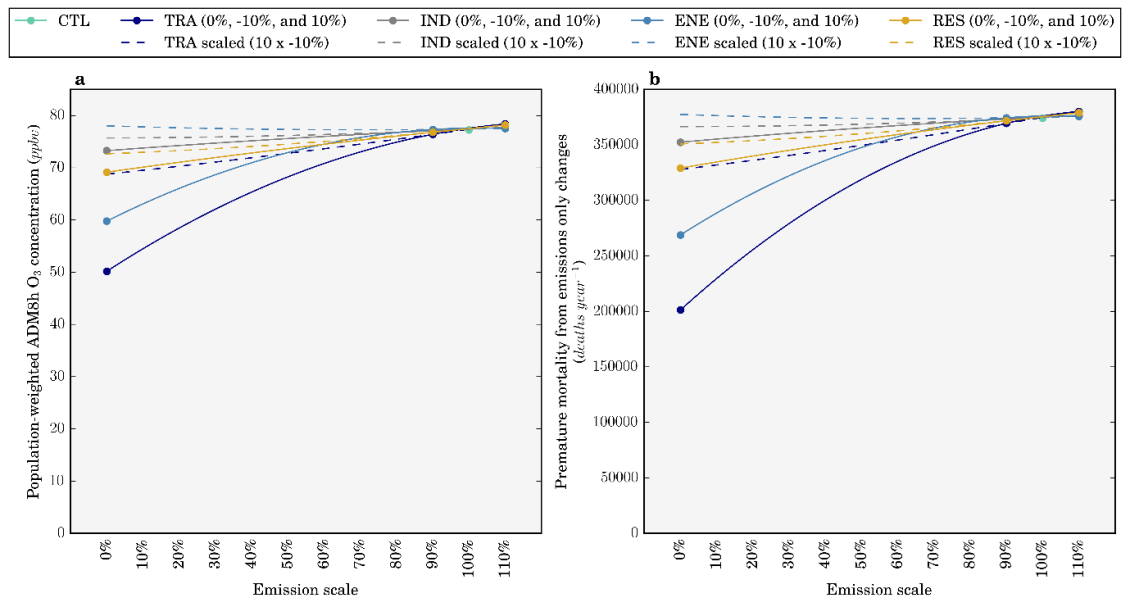


Figure 58: The impact of emission scaling on (a) population-weighted ADM8h surface O₃ concentrations, and (b) annual premature mortality estimates from O₃ exposure using Turner et al (2016) risks and LCC_{min} for emissions only changes between 2015 and 2050. For each source sector, a control scenario (CTL, 100%) is compared against scenarios where emission sectors are individually increased by 10% (110% of emissions), decreased by 10% (90% of emissions), and completely removed (0% of emissions). A solid line joins the data points from the idealised simulations (0%, -10%, and +10%) and is added to guide the eye. Linear scaling was applied to the 10% emission reduction scenarios per sector (10 × -10%, dashed lines) following a similar approach to Wild et al (2012) and Turnock et al (2018).

6.4.4. Sensitivities to demography and baseline mortality rates

To explore the sensitivity of calculated disease burden to different parameters in the methodology, this study applies population density from 2015 (POP2015), population age groupings from 2015 (AGE2015), or baseline mortality rates from 2015 (BM2015) individually. Each sensitivity study shows the influence of the other parameters in combination in 2050, highlighting the temporal impact in that specific variable (Figure 66, Appendix D). For the control scenario, the 2015 mortality rate changed by +139% in 2050 due to changes in demography and baseline mortality. In comparison, the mortality rate changed by +96% for POP2015, -21% for AGE2015, and +196% for BM2015. For the control scenario, the 2015 annual premature mortality estimate changed by +201% in 2050 due to changes in demography and baseline mortality. In comparison, premature mortality changed by +134% for POP2015, +2% for AGE2015, and +271% for BM2015. These sensitivity studies highlight the strong dependence of the future disease burden from O₃ exposure in India to an ageing population, where there is a large transition to increased susceptibility.

6.5. Discussion

Figure 59 compares this study's total and source-specific premature mortality estimates for India from O₃ exposure with previous studies (GBD 2016 Risk Factors Collaborators 2017, Cohen *et al* 2017, GBD 2010 Risk Factors Collaborators 2012, GBD 2013 Risk Factors Collaborators 2015, GBD 2015 Risk Factors Collaborators 2016a, Ghude *et al* 2016, Lelieveld *et al* 2015, Malley *et al* 2017, Silva *et al* 2016b, 2013).

For calculations using Jerrett *et al* (2009) risks, estimates of the total annual premature mortality from O₃ exposure in India in the present day vary from 78,000 to 190,000 (GBD 2015 Risk Factors Collaborators 2016a, GBD 2016 Risk Factors Collaborators 2017, Silva *et al* 2013, Lelieveld *et al* 2015, Silva *et al* 2016b, Malley *et al* 2017), between -36% smaller and +55% larger than this study's estimates. This study's estimates of premature mortality are +15% (LCC_{min}) and -1% (LCC_{fifth}) of the estimate from GBD2015 (GBD 2015 Risk Factors Collaborators 2016a) and +38% (LCC_{min}) and +19% (LCC_{fifth}) of the estimate from GBD2016 (GBD 2016 Risk Factors Collaborators 2017). The slightly larger estimates in this study are primarily due to higher estimates of O₃ concentrations combined with higher (lower) COPD baseline mortality rates from the IFs model relative to GBD2016 (GBD2015). For calculations using Turner *et al* (2016) risks, this study estimates annual premature mortality to be 12% higher than Malley *et al* (2017), the only other study that has applied these risks, due to higher O₃ concentrations across India in this study. Turner *et al* (2016) found significant positive associations between O₃ and all-cause, circulatory, and respiratory mortality, suggesting that our estimates from COPD only may be conservative. Overall, this study's estimates of annual premature mortality in India for the present day from O₃ exposure are in general agreement with previous key studies.

In terms of source contributions, Silva *et al* (2016a) calculated the disease burden from O₃ exposure in India for 2005 using Jerrett *et al* (2009) risks and the subtraction method. For seasonal O₃ concentrations, they found approximately equal leading contributions from energy (9%), land transport (9%), and residential (9%) emissions. They found premature mortality fractional contributions were approximately double the fractional contributions to O₃ concentrations, with 17% from energy, 16% from land transport, and 16% from residential emissions. In contrast, this study finds land transport to dominate the fractional source contributions to seasonal O₃ concentrations (28%) over energy (14%) and residential (9%) emissions (Table 7, 3mDMA1 metric). Our larger contribution from land transport may be due to the growth in land transport emissions between 2005 and 2010, where Indian passenger and freight kilometres increased by 6.54% and 3.61% per year, respectively (Venkataraman *et al* 2018). In agreement with Silva *et al* (2016a), this study finds the fractional source contributions to premature mortality were approximately double the fractional contributions to O₃ concentrations due to the low concentration cutoffs, with land transport again dominating (46%) over energy (28%) and residential (12%) emissions (Table 8, subtraction method).

Figure 59: Comparison of premature mortality estimates for India due to ambient O₃ exposure. Estimates are shown using relative risks from either the earlier CPS-II study from Jerrett *et al* (2009) (solid bars) or the updated CPS-II study from Turner *et al* (2016) (dashed bars). (a) Total premature mortality from O₃ exposure from all sources. Estimates are shown for both lower concentration cut-offs (LCC_{min} and LCC_{fifth}). This study (green) is compared with previous studies (orange). (b) Estimates of premature mortality from different emission sectors (see key) using either the attribution or the subtraction method. Estimates are shown for LCC_{min} . Error bars represent 95% uncertainty intervals.

This study shows that for the disease burden from ambient O₃ exposure in India, contributions from the subtraction method are up to 43% larger than the attribution method. However, in Chapter 4 estimating the disease burden from PM_{2.5} exposure in India, the source contributions from the subtraction method are 2–2.5 times smaller than those from the attribution method (Conibear *et al* 2018a). In this study for emissions only changes in 2015 for O₃, the CAS reduces annual premature mortality by 30% relative to the control, due to the 24% reduction in O₃ under this scenario. In Chapter 5 for emissions only changes in 2015 for PM_{2.5}, the CAS reduces annual premature mortality by 39% relative to the control, due to the 67% reduction in PM_{2.5} under this scenario (Conibear *et al* 2018b). The relative reduction in premature mortality from O₃ exposure is larger than the relative reduction in O₃ concentrations. In contrast, the relative reduction in premature mortality from PM_{2.5} exposure is smaller than the relative reduction in PM_{2.5} concentrations. The exposure-response functions for both O₃ and PM_{2.5} are non-linear. The differences in the relative reductions in concentration and mortality for both PM_{2.5} and O₃ are due to the position of present-day pollutant concentrations on the non-linear health functions, and also due to the different minimum pollutant thresholds assumed, below which there is no health impact.

The O₃ concentrations currently experienced across India (population-weighted ADM8h of 77.2 ppbv, Table 7) are in the steeper part of the exposure-response function, where the health effects are sensitive to changes in pollutant concentrations (Figure 24, Section 2.4). In contrast, the PM_{2.5} concentrations currently experienced across India (population-weighted annual mean of 57.2 µg m⁻³) are in the flatter part of the exposure-response functions, where the health effects are less sensitive to changing PM_{2.5} concentrations (Figure 22, Section 2.3). The O₃ exposure-response function assumes that there is no health impact below 26.7 ppbv, the LCC_{min} from Turner *et al* (2016). Reducing O₃ concentrations from the present day value (77.2 ppbv) to the LCC_{min} , a reduction of 65%, would, therefore, reduce premature mortality by 100%. The exposure-response function for PM_{2.5} assumes a theoretical minimum risk exposure level of 2.4 µg m⁻³, meaning that concentrations across India would need to be reduced by 96% (from 57.2 µg m⁻³) to reduce premature mortality from exposure to PM_{2.5} by 100% (Conibear *et al* 2018a). This difference results in larger relative reductions in health impacts for the same relative reduction in O₃, compared to PM_{2.5}. If subsequent exposure-response functions assume different minimum

pollutant thresholds (or lower concentration cut-offs, LCC), the calculated sensitivity of health impacts to changes in O₃ concentrations will also change.

This study finds that with no emissions change to 2050, the demographic and epidemiological transitions increase the annual premature mortality due to O₃ exposure by 200% and the mortality rate per 100,000 population by 139%, while the corresponding impacts of PM_{2.5} exposure in India are 75% and 39%, respectively (Conibear *et al* 2018b). The larger increase for the O₃ burden under constant emissions is due to the limited improvement in baseline mortality rate for COPD, while for the PM_{2.5} exposure burden there are substantial reductions in baseline mortality rates for LRI, IHD, and CEV.

Figure 60 compares the disease burden from PM_{2.5} and O₃ exposure in India in 2015 and 2050 due to changes in emissions, demography, and baseline mortality. Chapter 5 estimated the present day disease burden from ambient PM_{2.5} exposure in India to be 900,000 (95UI: 683,000–1,252,000) premature mortalities per year, increasing to 967,000 (95UI: 820,000–1,194,000) under the CAS in 2050, for a 67% reduction in population-weighted annual mean PM_{2.5} concentrations (Conibear *et al* 2018b). This study estimates the present day disease burden from ambient O₃ exposure in India to be 374,000 (95UI: 140,000–554,000) premature mortalities per year, increasing to 791,000 (95UI: 202,000–1,336,000) under the CAS in 2050, for a 24% reduction in population-weighted annual mean O₃ concentrations. This suggests that the future disease burden from PM_{2.5} and O₃ exposures in India may be similar in magnitude, in contrast to the present day where the disease burden from PM_{2.5} dominates that from O₃ exposure. This is due to the combination of the smaller reduction in O₃ (24%) compared to PM_{2.5} (67%) under the CAS and because the COPD baseline mortality rates are predicted to remain high through to 2050, whereas there are substantial reductions in the baseline mortality rates for other diseases that are related to PM_{2.5} exposure (LRI, IHD, and CEV). The predicted increase in health affects both from PM_{2.5} and O₃ exposure due to the demographic and epidemiologic changes highlight the challenge facing Indian efforts to reduce the public health risks from exposure to poor air quality in India.

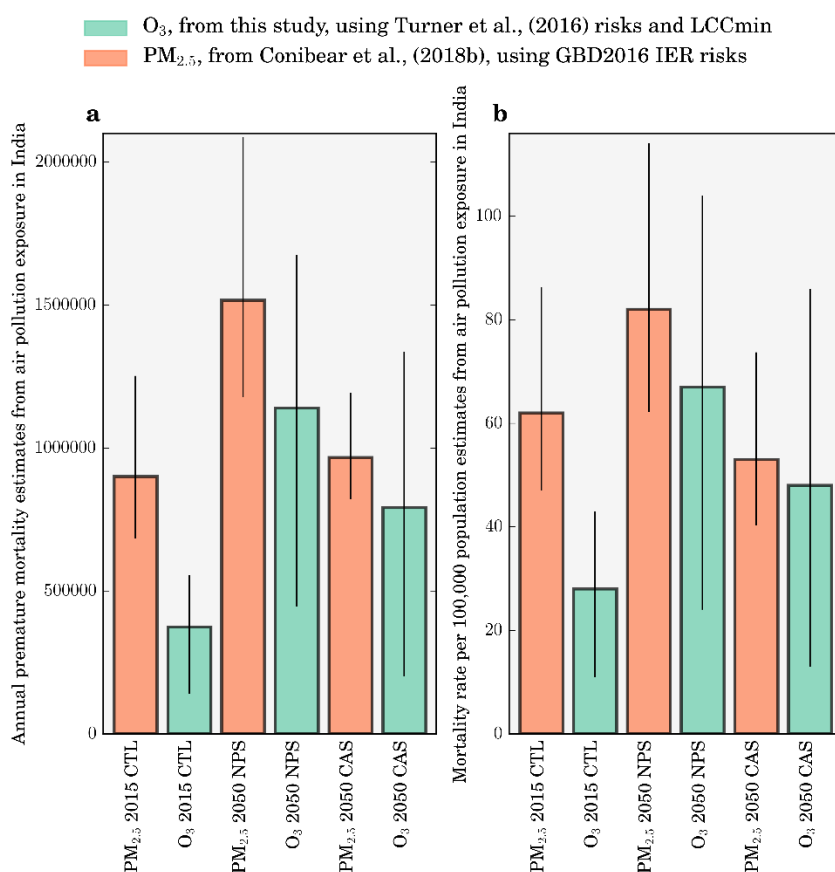


Figure 60: Comparison of (a) premature mortality and (b) mortality rate estimates for India due to PM_{2.5} and O₃ exposure. Estimates are shown for the 2015 control (CTL) scenario, the New Policy Scenario (NPS) in 2050, and the Clean Air Scenario (CAS) in 2050. Estimates of the disease burden for O₃ exposure (green) are from this study using relative risks from the updated CPS-II study from Turner et al (2016) and LCC_{min}. Estimates of the disease burden for PM_{2.5} exposure (orange) are from Conibear et al (2018b) (Chapter 5) using the IER function (Burnett et al 2014) updated for GBD2016 (GBD 2016 Risk Factors Collaborators 2017). Estimates for O₃ exposure are from COPD only. Estimates for PM_{2.5} exposure are from COPD, LRI, CEV, LC, and IHD combined. Error bars represent 95% uncertainty intervals.

6.6. Conclusion

Long-term exposure to surface O₃ is a risk factor for human health in India. This study is the first to estimate the source-specific disease burden associated with long-term O₃ exposure in India at high spatial resolution, using the updated risk functions from the CPS-II. This study estimates using the updated CPS-II risk function that in 2015 there were 374,000 (95UI: 140,000–554,000) annual premature mortalities from long-term O₃ exposure in India, 200% larger than the disease burden estimates using the older CPS-II risk function. This study finds land transport emissions dominate the source contribution to this disease burden (35%), followed by emissions from power generation (23%). The source contributions to the O₃ disease burden in India from the subtraction method are up to 43% larger than the attribution method due to the position of present day O₃

concentrations on the steeper part of the non-linear health function and the relatively high minimum pollutant threshold. This is in contrast to the PM_{2.5} disease burden in India where the source contributions from the subtraction method are 2–2.5 times smaller than those from the attribution method due to the position of present day PM_{2.5} concentrations on the flatter part of the non-linear health function and the relatively low minimum pollutant threshold.

With no change in emissions by 2050, this study estimates 1,126,000 (95UI: 421,000–1,667,000) annual premature mortalities, an increase of 200% relative to the control in 2015 due to population ageing and growth increasing the number of people susceptible to air pollution. This study finds the IEA New Policy Scenario provides small changes (+1%) to this increasing disease burden from the demographic transition. Under a stringent air pollution control pathway, the IEA Clean Air Scenario, this study estimates 791,000 (95UI: 202,000–1,336,000) annual premature mortalities in 2050. This represents an avoidance of 335,000 premature mortalities a year compared to the scenario of no emission change, offsetting 45% of the increase in premature mortalities due to the demographic transition. However, this shows that even under a scenario of strong emission reductions leading to a 24% reduction in O₃ concentrations across India, population growth and ageing are likely to lead to increasing premature mortality from O₃ exposure. This study does not include impacts of climate change or the impacts of changing emissions from outside India on O₃ concentrations or the disease burden. This study finds that the future disease burden from PM_{2.5} and O₃ exposures in India may be similar in magnitude, in contrast to the present day where the disease burden from PM_{2.5} dominates that from O₃ exposure. This study highlights the challenge facing efforts to improve air quality related public health in India, but that critical public health benefits are possible with stringent emission reductions.

7. Discussion and Conclusion

7.1. Summary of work

700 million Indians have used solid fuels in their homes for the last 30 years, contributing substantially to air pollutant emissions (Smith and Sagar 2014). India experienced large growth in its economy, industry, power generation, and transport sectors over the last decade leading to a large growth in emissions of air pollutants. Emissions of air pollutants are predicted to grow substantially over the coming years in India. These air pollutant emissions have caused present-day concentrations of ambient $PM_{2.5}$ and O_3 in India to be amongst the highest in the world (World Health Organization 2018a). Exposure to this air pollution is the second leading risk factor in India, contributing one-quarter of the global disease burden attributable to air pollution exposure (GBD 2016 Risk Factors Collaborators 2017, India State-Level Disease Burden Initiative Collaborators 2017).

Despite the importance of air quality in India, it remains relatively understudied, and knowledge of the sources and processes causing air pollution is limited. It is critical to understand the contribution of different emission sources to ambient air pollution to design effective policies to reduce this substantial disease burden. This thesis aimed to understand the present day contribution of different pollution sources to the ambient air pollution associated disease burden in India and the effects of future air pollution control pathways.

The thesis had three main objectives. The first objective was to quantify the contribution of different emission sources to ambient $PM_{2.5}$ concentrations and the related disease burden across India in the present day. This study combined high-resolution computer simulations with new observations, as previous studies used coarse model resolution with limited observations. The second objective studied different future air pollution control pathways in India, estimating the impacts on ambient $PM_{2.5}$ concentrations and human health. Poor air quality in India is predicted to worsen in the future, and limited air pollution control pathways have been studied at high resolution. Thirdly, the current and future disease burden from ambient O_3 exposure in India was studied, identifying critical contributing emission sources and the impacts of future policy scenarios. This study combined high-resolution computer simulations with the latest exposure-response relationships.

This thesis found ambient $PM_{2.5}$ and O_3 concentrations were high across India, especially in the IGP. Almost everyone in India is exposed to ambient $PM_{2.5}$ and O_3 concentrations above the WHO recommended guidelines. This thesis estimated that present-day exposure to ambient $PM_{2.5}$ in India caused 990,000 (95UI: 660,000–1,350,000) premature mortalities per year. Present day exposure to ambient O_3 in India caused 124,000 (95UI: 57,000–203,000) premature mortalities per year using old risk functions, increasing by 200% to 374,000 (95UI: 140,000–554,000) premature mortalities per year using updated risk functions. This suggests that the present-day

attributable disease burden from ambient PM_{2.5} exposure dominates that from ambient O₃ exposure in India.

Emissions from residential energy use contributed 52% of the population-weighted annual-mean PM_{2.5} concentrations, attributed to 511,000 (95UI: 340,000–697,000) premature mortalities each year. Removing residential energy use emissions would avert only 256,000 (95UI: 162,000–340,000) premature mortalities annually, due to the non-linear exposure-response relationship causing health effects to saturate at high PM_{2.5} concentrations. For ambient O₃ exposure, land transport emissions dominated the source contribution to the disease burden (35% attribution and 46% subtraction), followed by emissions from power generation (23% attribution and 28% subtraction). For ambient PM_{2.5} exposure, the summation of source contributions from the attribution method was 1,012,000 (95UI: 675,000–1,381,000) premature mortalities per year (102% of control), which is substantially higher than the sector summation from the subtraction method of 469,000 (95UI: 304,000–626,000) premature mortalities per year (47% of control). For ambient O₃ exposure, the summation of source contributions from the attribution method was 284,000 (95UI: 106,000–421,000) annual premature mortalities (76% of control), while for the subtraction method was 355,000 (95UI: 133,000–526,000) annual premature mortalities (95% of control). This difference of the attribution method estimates being larger than those from the subtraction method for PM_{2.5}, and smaller for O₃, is due to the shape of the exposure-response functions and the present day concentrations experienced. The exposure-response functions for both O₃ and PM_{2.5} are non-linear. However, the present day O₃ concentrations experienced in India are in the linear section (steeper) of the exposure-response function and the minimum pollutant threshold is relatively high (below which there is no health impact). The present-day PM_{2.5} concentrations experienced in India are in the non-linear section (flatter) of the exposure-response function and the minimum pollutant threshold is relatively low. This difference suggests that there are larger relative reductions in health impacts for the same relative reduction in O₃ compared to PM_{2.5}. This implication is dependent on the shape of the exposure-response function and the assumed minimum pollutant threshold.

This study avoided summing the disease burden from ambient O₃ and PM_{2.5} exposure in the main results as similar diseases (e.g. COPD) cause them both, although the risk estimates account for confounding. However, for illustrative purposes, the combined annual disease burden contributions from ambient PM_{2.5} and O₃ exposure for the subtraction method suggest that residential emissions dominate with 301,000 (95UI: 179,000–407,000) premature mortalities, followed by land transport emissions with 216,000 (95UI: 94,000–314,000) premature mortalities, then energy emissions with 195,000 (95UI: 99,000–278,000) premature mortalities. Overall, this highlights the need to control emissions from the residential sector.

With emissions remaining at 2015 levels, premature mortality from exposure to ambient PM_{2.5} in 2050 will increase by 75% relative to 2015, and the mortality rate will increase by 39%. For

ambient O₃ exposure under constant emissions from 2015, the number of premature mortalities in 2050 will increase by 201% relative to 2015, and the mortality rate will increase by 140%. The increase in disease burden from exposure to ambient PM_{2.5} and O₃ in 2050 relative to 2015 under constant emissions is due to population ageing and growth increasing the number of people susceptible to air pollution. The larger increase for the O₃ burden under constant emissions is due to the limited improvement in baseline mortality rate for COPD, while for the PM_{2.5} exposure burden there are substantial reductions in baseline mortality rates for LRI, IHD, and CEV.

This thesis also explored the impact of different future emission scenarios. In particular, two scenarios were compared, the NPS considering all relevant existing and planned policies as of 2016, and the CAS representing aggressive policy action using proven energy policies and technologies tailored to national circumstances. The IEA NPS in 2050 reduces population-weighted annual-mean ambient PM_{2.5} concentrations below 2015 levels by 9%, while population-weighted ADM8h O₃ concentrations increase by 1%. The IEA CAS in 2050 reduces population-weighted annual-mean ambient PM_{2.5} concentrations below 2015 levels by 68% and reduces population-weighted ADM8h O₃ concentrations by 24%. Under both the NPS and the CAS, the total number of premature mortalities in 2050 still increases relative to 2015 due to the strong drivers from population ageing and growth. The NPS offsets the rising number of premature mortalities from population ageing and growth by 9% (61,000 deaths) for PM_{2.5} exposure, while increasing the number of premature mortalities by 1% (13,000 deaths) for O₃ exposure. The CAS offsets the rising number of premature mortalities from population ageing and growth by 91% (610,000 deaths) for PM_{2.5} and 45% (335,000 deaths) for O₃. The CAS can reduce the mortality rate by 15% for PM_{2.5} in 2050 relative to 2015, while for O₃ the CAS in 2050 can offset 28% of the increase from population ageing and growth.

In the present day, the annual disease burden in India from ambient PM_{2.5} exposure (900,000 premature mortalities and mortality rate of 62 per 100,000) dominates that from O₃ exposure (374,000 premature mortalities and mortality rate of 28 per 100,000). In contrast, the future disease burden from ambient exposure to PM_{2.5} (under the CAS, 967,000 premature mortalities and mortality rate of 53 per 100,000) and O₃ (under the CAS, 791,000 premature mortalities and mortality rate of 48 per 100,000) may be similar in magnitude.

In summary, this thesis aimed to understand the source contributions to the ambient air pollution associated disease burden in India and the effects of future air pollution control pathways. The attributable disease burden from ambient PM_{2.5} exposure in India is substantial, where large reductions in emissions will be required to reduce the health burden due to the non-linear exposure-response relationship. The attributable disease burden from ambient O₃ exposure is larger than previously thought. Key sources contributing to the present day disease burden from ambient PM_{2.5} and O₃ exposure are the emissions from the residential combustion of solid fuels, land transport, and coal combustion in power plants. The attributable disease burden is estimated

to increase in the future due to population ageing and growth. Stringent air pollution control pathways are required to provide critical public health benefits in India. A key focus should be to reduce the burning of solid fuels. The attributable disease burden to ambient PM_{2.5} exposure dominates ambient O₃ exposure in the present day, while in the future they are of similar magnitudes. This thesis highlights the challenge facing efforts to improve air quality related public health in India.

7.2. Critical discussion of work

All health effects in this thesis were estimated as attributable burdens from associational epidemiology, rather than causations from mechanistic toxicology. A key criticism here is that the exposure-response functions used to estimate the attributable burdens are causal and reversible based on the *classic approach* to causal inference, using historical exposure-response functions to predict future changes in pollution and health (Dominici and Zigler 2017). The *potential outcomes* approach addresses this critique, where *causal effects* are explicitly defined as consequences of specific actions, as oppose to *inferring causality* (Zigler and Dominici 2014). However, the potential outcomes causal effect can be complicated by interference, for example from the regional transport of pollution, other policies, air quality trends, and meteorology (Tchetgen and Vanderweele 2012). Potential outcomes studies require prospective planning regarding what to measure, what control to use, and how to consider intended effects versus actual effects, so maybe more suitable for specific policy changes rather than source contributions (Hubbell and Greenbaum 2014).

The current standard in the literature is to use concentrations as surrogates for exposures. Recent advances in exposure assessment include the estimation of individual exposures based on household addresses (Beckerman *et al* 2013), the integration of personal exposure assessments between models and measurements (Shaddick *et al* 2018a), including household air pollution and second hand smoking (Kodros *et al* 2018, Hill *et al* 2017), and including time-activity data between household and ambient pollution (Hill *et al* 2017). This additional complexity in future work will improve the accuracy of health impact estimates.

The horizontal spatial resolution (30 km) used in this thesis was unable to resolve the very fine concentration gradients in different microenvironments (Beelen *et al* 2008). Risk assessments resolving microenvironments may capture the collocation of emissions and exposures, e.g. populations are nearer emissions from residential solid fuel use, land transport, and diesel generators, as opposed to larger stationary sources (GBD MAPS Working Group 2018).

The work in Chapter 4 found that ambient PM_{2.5} concentrations (influenced by model spatial resolution) and the exposure-response function were both strong drivers of the differences between disease burden estimates attributable to air pollution in India. Similar, recent work by Kushta *et al* (2018) over Europe found that in this domain, the exposure-response function is the

main source of uncertainty in the health impact assessments. This difference may be due to the use of the 95% uncertainty levels within a specific exposure-response function for the sensitivity estimates, rather than between different realisations of the exposure-response functions, and to the lower PM_{2.5} concentrations found over Europe (maximum of 40 µg m⁻³, compared to 120 µg m⁻³ over India). This difference for Europe suggests that uncertainty is driven by different causes in different countries, as found by Kodros *et al* (2018).

The source contribution estimates were for one model setup, not accounting for interannual variations in emissions and meteorology or sensitivity to model choices. There were additional emission sources not included, such as emissions from waste burning (Kodros *et al* 2016), bagasse combustion (Sahu *et al* 2015), and anthropogenic dust (GBD MAPS Working Group 2018). Different emission inventories would produce different results, for example, the Regional Emission inventory in Asia (REAS) more closely matched South Asian AOD from satellite relative to EDGAR, likely due to EDGAR underestimating SO₂, NO_x, and NH₃ emissions and hence producing less secondary aerosol (Saikawa *et al* 2017). Previous studies have highlighted the importance of using an ensemble of estimates (Post *et al* 2012, Silva *et al* 2016c), as variability among models is large for O₃ (Silva *et al* 2013, Post *et al* 2012). To account for these variabilities and limitations, an ensemble of model simulations would be suitable, changing emission inventories, year of simulation, and model parameterisations. However, this was beyond the time and computational constraints of this work.

The urban and rural splits were based on population density (400 persons' km⁻²), which did not capture the type of work undertaken. A recent study included the type of work (e.g. agricultural) undertaken and estimated larger rural contributions to the disease burden in India, relative to Chapter 4 (Karambelas *et al* 2018b).

The response of O₃ concentrations to changes in emissions is non-linear, meaning an emission removal approach to quantify attributions can differ from a source tracking approach (Silva *et al* 2016b, Grewe *et al* 2010, 2012, Mertens *et al* 2018, Koo *et al* 2009, Clappier *et al* 2017). The response of PM_{2.5} concentrations to changes in emissions is largely linear, which was also found in previous work (Dedoussi and Barrett 2014). Source tracking within chemical transport models also find residential emissions to dominate PM_{2.5} concentrations in North India, followed by industrial emissions (Guo *et al* 2017). The source tracking approach had not yet been used for health impact assessments at the time of these studies. Since the publication of this work, Guo *et al* (2018) used the source tracking approach to estimate the source-specific disease burden from ambient PM_{2.5} exposure in India and found similar results to this work where residential emissions contributed 56% to the 1 million premature mortalities per year. Source apportionment analyses of PM into source categories based on chemical composition are mixed in India, with widely varying results even for the same city (Pant and Harrison 2012). Source apportionment analyses

are limited by the availability of locally derived emissions source profiles (Pant and Harrison 2012).

Dust emissions were found to be low in Chapter 4 using the GOCART dust scheme with AFWA modifications. Previous studies have also found WRF-Chem to underestimate dust emissions in India (Dipu *et al* 2013, Kumar *et al* 2014b). This finding has led WRF-Chem studies over India to increase the dimensional proportionality constant within the GOCART AFWA dust emission online flux calculation. The dimensional proportionality constant was initially $1 \times 10^{-9} \text{ kg m}^{-5} \text{ s}^2$ (Legrand *et al* 2018). Previous studies increased this constant by a factor of 22 to $2.2 \times 10^{-8} \text{ kg m}^{-5} \text{ s}^2$ when using FDDA and by a factor of 9 to $9 \times 10^{-9} \text{ kg m}^{-5} \text{ s}^2$ when not using FDDA, based on most closely matching observed and simulated AOD and Angström exponent (Kumar *et al* 2014b). After correcting the underestimation of dust emissions in WRF-Chem, Kumar *et al* (2014a) added heterogeneous chemical reactions between dust and O_3 photochemistry and found these heterogeneous reactions reduced the difference between observed and simulated O_3 concentrations in India from 16 ppbv to 2 ppbv.

The simulation of meteorology could be improved, especially the summer monsoon precipitation dry bias and the winter boundary layer height overestimation. The Indian monsoon is better simulated at resolutions that explicitly resolve convection (Chen *et al* 2018, Chang *et al* 2009, Srinivas *et al* 2018), however, this requires substantial computational resources. Recent air quality studies over India using WRF found improved meteorological simulation of precipitation and relative humidity using ECMWF, rather than NCEP, initial and boundary conditions (Kumar *et al* 2017, Chatani and Sharma 2018). There are mixed results for different convection parameterisation schemes over India using WRF (Mukhopadhyay *et al* 2010, Srinivas *et al* 2013, Rotach and Zardi 2007, Chang *et al* 2009). Mukhopadhyay *et al* (2010) and Srinivas *et al* (2013) both found the Betts-Miller-Janjic convection parameterisation scheme simulated Indian monsoon precipitation with the lowest bias, while Rotach and Zardi (2007) and Chang *et al* (2009) found the best performance for the Grell-Devenyi scheme. Previous studies evaluating different boundary layer schemes (with tied land surface schemes) using WRF over India have found performance varies widely where the best choices may be application specific (Mohan and Gupta 2018, Gunwani and Mohan 2017, Hari Prasad *et al* 2016, Sonia *et al* 2014, Mohan and Bhati 2011, Panda and Sharan 2012, Madala *et al* 2014, Hari Prasad *et al* 2014). Srinivas *et al* (2018) recently found the Mellor-Yamada Nakanishi and Niino 2.5 boundary layer scheme performed better than alternative schemes, while still underestimating heavy rainfall. The meteorological evaluation could have used data from the India Meteorological Department, as opposed to ECMWF reanalysis products.

The part of the IER functions with the largest uncertainty ($30\text{--}100 \mu\text{g m}^{-3}$) coincides with $\text{PM}_{2.5}$ concentrations often found in India and China. Despite this, a recent study of long-term $\text{PM}_{2.5}$ exposures in China found the health response to be similar to the IER functions (Zheng *et*

al 2017). The exposure-response functions did not include epidemiological studies from long-term ambient air pollution studies in India, as they do not exist. The exposure estimates focused on single pollutants individually, rather than multipollutant approaches combining effects from PM_{2.5} and O₃ (Greenbaum and Shaikh 2010).

Future air pollution control pathways were applied through scaling factors to the anthropogenic emission inventory, which assumes changes are homogeneous across the model domain and do not consider changes in other countries over the same timeframe. The future scenarios did not include changes in land use or land cover. The future scenarios had a timing mismatch between emissions (2040) and demographic and epidemiological changes (2050).

These studies did not estimate DALYs (which account for YLD), economic costs, the impacts of Indian emissions on the disease burden in other countries (Zhang *et al* 2017), population effect modifiers (e.g. gender, socioeconomics, genes), crop impacts of O₃ (Ghude *et al* 2014, 2016, Sinha *et al* 2015), or the climate impacts (Shindell *et al* 2012).

7.3. Future work

Future estimates of the disease burden from ambient air pollution exposure can be more accurately estimated when epidemiological evidence resolves the specific characteristics, components, and sources of air pollution that cause the specific health effects (West *et al* 2016). The IERs are based on assumptions of equal toxicity and include data from household air pollution, second hand smoking, and active smoking. Recent work by Burnett *et al* (2018) relaxed these assumptions to develop the Global Exposure Mortality Model (GEMM), covering almost all of the global PM_{2.5} concentration range (2.5–84 µgm⁻³) from cohort studies of ambient air pollution only. GEMM hazard ratios are larger than those from the GBD2015 IER and are closer to linear, especially for high PM_{2.5} concentrations (Burnett *et al* 2018). The attributable disease burden from ambient PM_{2.5} exposure in India using the GEMM for the five causes of deaths used in this study (COPD, IHD, CEV, LC, and LRI) is 1,867,342 (95UI: 1,355,715–2,240,783) premature mortalities per year, approximately 70% larger than the GBD2015 estimates using the IER functions of 1,090,391 (95UI: 936,588–1,254,784) premature mortalities per year (Burnett *et al* 2018). Burnett *et al* (2018) also found that the disease burden from all NCD and LRI were 20% larger than those based on the five causes of death (COPD, IHD, CEV, LC, and LRI), suggesting that other diseases also contribute beyond the five causes studied here and in the GBD (Grandjean and Landrigan 2006, Landrigan *et al* 2017). These findings suggests the health impact from ambient PM_{2.5} exposure could be substantially larger than previously thought, the non-linear implications of emission changes would alter, and the future balance of disease burdens from PM_{2.5} and O₃ would change. The GEMM exposure-response function would be further suitable for India when it includes cohort studies of ambient air pollution from India, as only one study is available from a country with similar air pollution concentrations (China). The simulated

components of PM_{2.5} concentrations in India can be evaluated against measurements when they become publically available.

The total exposure to air pollution from ambient, household, and smoking sources could be investigated, as performed by Hill *et al* (2017) for Mongolia. This could include multiple air pollutants together, rather than the single pollutant approach, although the implementation challenge is vast (Dominici *et al* 2010). Risk assessments could also include DALYs and the economic costs from the health impacts attributable to air pollution.

Short-term drivers to pollution episodes could be explored in terms of the impact on human health. For example, in November 2016, daily-mean PM_{2.5} concentrations in Delhi were over 900 µg m⁻³, many times higher than the WHO AQG of 25 µg m⁻³. This pollution episode coincided with large agricultural burning of rice residues across northwest India, though the impact on PM_{2.5} concentrations and human health has not been quantified. Another study could analyse the impacts of the Indian solid fuel intervention to promote LPG to over 90% of households by early 2020's (Section 1.1.3.2) on air quality and human health, considering stove stacking and stove usage patterns.

The emission inventories used in this thesis could be improved by including additional emission sources, such as anthropogenic dust (Venkataraman *et al* 2018, GBD MAPS Working Group 2018), waste burning (Kodros *et al* 2016), and bagasse combustion (Sahu *et al* 2015). The emissions inventories from Venkataraman *et al* (2018) for 2015, 2030, and 2050 are now available upon request and would improve future scenario estimates of air pollution relative to using scaling factors (Chapters 5 and 6). Upcoming emission inventories plan to split residential emissions into cooking, heating, and lighting and by fuel, which will provide insights into the drivers behind this sectors large contributing disease burden. Sensitivity simulations could be conducted by applying an Indian-specific diurnal cycle to the anthropogenic emissions when data becomes available. The air pollution estimates could be improved by changing the dimensional proportionality constant for dust emissions and adding the heterogeneous chemical reactions between dust and O₃ photochemistry (Section 7.2). These changes were implemented into WRF-Chem for the GOCART bulk aerosol scheme and work is currently being undertaken to accommodate for these changes within the MOSAIC sectional scheme.

Simulations could be performed using WRF-Chem with chemical data assimilation, especially for AOD and PM_{2.5}, to improve the accuracy of simulated particulate air quality. Previous studies have developed and explored the use of chemical data assimilation in WRF-Chem (Li *et al* 2013, Peng *et al* 2017, Liu *et al* 2011, Saide *et al* 2013, Pagowski and Grell 2012, Bocquet *et al* 2015, Liu *et al* 2017, Mizzi *et al* 2016).

7.4. Conclusion

Since 1980, 700 million Indians have used solid fuels in their homes in poor quality stoves that produce substantial emissions of air pollutants (Smith and Sagar 2014). The Indian economy and industrial, power generation, and transport sectors have grown considerably over the last decade. These increasing emissions of air pollutants have caused present-day concentrations of ambient PM_{2.5} and O₃ in India to be amongst the highest in the world (World Health Organization 2018a). Exposure to this air pollution is the second leading risk factor in India, contributing one-quarter of the global disease burden attributable to air pollution exposure (GBD 2016 Risk Factors Collaborators 2017, India State-Level Disease Burden Initiative Collaborators 2017). Air pollutant emissions are predicted to grow extensively over the coming years in India.

Despite the importance of air quality in India, it remains relatively understudied, and knowledge of the sources and processes causing air pollution is limited. It is critical to understand the contribution of different emission sources to ambient air pollution to design effective policies to reduce this substantial disease burden. This thesis aimed to understand the contribution of different pollution sources to the ambient air pollution associated disease burden in India and the effects of future air pollution control pathways.

The thesis had three main objectives. Firstly, the contribution of different emission sources to ambient PM_{2.5} concentrations and the related disease burden across India in the present day was studied. Secondly, different future air pollution control pathways in India were analysed, estimating the impacts on ambient PM_{2.5} concentrations and human health. Thirdly, the current and future disease burden from ambient O₃ exposure in India was studied, identifying critical contributing emission sources and the impacts of future policy scenarios. This thesis combined high-resolution computer simulations with new observations and the latest exposure-response relationships.

The attributable disease burden from ambient PM_{2.5} exposure in India is substantial, where large reductions in emissions will be required to reduce the health burden due to the non-linear exposure-response relationship. The attributable disease burden from ambient O₃ exposure is larger than previously thought. Key sources contributing to the present day disease burden from ambient PM_{2.5} and O₃ exposure are the emissions from the residential combustion of solid fuels, land transport, and coal combustion in power plants. The attributable disease burden is estimated to increase in the future due to population ageing and growth. Stringent air pollution control pathways are required to provide critical public health benefits in India in a challenging environment. A key focus should be to reduce the burning of solid fuels. The attributable disease burden to ambient PM_{2.5} exposure dominates ambient O₃ exposure in the present day, while in the future they are of similar magnitudes. This thesis highlights the challenge facing efforts to improve air quality related public health in India.

References

- Achilleos S, Kioumourtzoglou M A, Wu C Da, Schwartz J D, Koutrakis P and Papatheodorou S I 2017 Acute effects of fine particulate matter constituents on mortality: A systematic review and meta-regression analysis *Environ. Int.* **109** 89–100
- Ackermann I J, Hass H, Memmesheimer M, Ebel A, Binkowski F S and Shankar U 1998 Modal Aerosol Dynamics model for Europe: Development and first applications *Atmos. Environ.* **32** 2981–99
- Adhikary B, Carmichael G R, Tang Y, Leung L R, Qian Y, Schauer J J, Stone E A, Ramanathan V and Ramana M V. 2007 Characterization of the seasonal cycle of south Asian aerosols: A regional-scale modeling analysis *J. Geophys. Res. Atmos.* **112** 1–22
- Akagi S K, Yokelson R J, Wiedinmyer C, Alvarado M J, Reid J S, Karl T, Crouse J D and Wennberg P O 2011 Emission factors for open and domestic biomass burning for use in atmospheric models *Atmos. Chem. Phys.* **11** 4039–72
- Alexander D, Northcross A, Wilson N, Dutta A, Pandya R, Ibigbami T, Adu D, Olamijulo J, Morhason-Bello O, Karrison T, Ojengbede O and Olopade C O 2017 Randomized controlled ethanol cookstove intervention and blood pressure in pregnant nigerian women *Am. J. Respir. Crit. Care Med.* **195** 1629–39
- Amann M, Bertok I, Borcken-Kleefeld J, Cofala J, Heyes C, Höglund-Isaksson L, Klimont Z, Nguyen B, Posch M, Rafaj P, Sandler R, Schöpp W, Wagner F and Winiwarter W 2011 Cost-effective control of air quality and greenhouse gases in Europe: Modeling and policy applications *Environ. Model. Softw.* **26** 1489–501
- Anderson G B, Krall J R, Peng R D and Bell M L 2012 Is the relation between ozone and mortality confounded by chemical components of particulate matter? Analysis of 7 components in 57 US communities *Am. J. Epidemiol.* **176** 726–32
- Anenberg S C, Horowitz L W, Tong D Q and West J J 2010 An estimate of the global burden of anthropogenic ozone and fine particulate matter on premature human mortality using atmospheric modeling *Environ. Health Perspect.* **118** 1189–95
- Anenberg S C, Schwartz J, Shindell D, Amann M, Faluvegi G, Klimont Z, Janssens-maenhout G, Pozzoli L, Dingenen R Van, Vignati E, Emberson L, Muller N Z, West J J, Williams M, Demkine V, Hicks W K, Kuylentierna J, Raes F and Ramanathan V 2012 Global Air Quality and Health Co-benefits of Mitigation Near-Term Climate Change through Methane and Black Carbon Emissions Controls *Environ. Heal. Perspect.* **120** 831–9
- Anenberg S C, Talgo K, Arunachalam S, Dolwick P, Jang C and West J J 2011 Impacts of global, regional, and sectoral black carbon emission reductions on surface air quality and human mortality *Atmos. Chem. Phys.* **11** 7253–67
- Anenberg S C, West J J, Fiore A M, Jaffe D A, Prather M J, Bergmann D, Cuvelier K, Dentener F J, Duncan B N, Gauss M, Hess P, Jonson J E, Lupu A, MacKenzie I A, Marmer E, Park R J, Sanderson M G, Schultz M, Shindell D T, Szopa S, Vivanco M G, Wild O and Zeng G 2009 Intercontinental Impacts of Ozone Pollution on Human Mortality *Environ. Sci. Technol.* **43** 6482–7
- Anenberg S C, West J J, Yu H, Chin M, Schulz M, Bergmann D, Bey I, Bian H, Diehl T, Fiore A, Hess P, Marmer E, Montanaro V, Park R, Shindell D, Takemura T and Dentener F 2014 Impacts of intercontinental transport of anthropogenic fine particulate matter on human mortality *Air Qual. Atmos. Heal.* **7** 369–79
- Apte J S, Bombrun E, Marshall J D and Nazaroff W W 2012 Global intraurban intake fractions for primary air pollutants from vehicles and other distributed sources *Environ. Sci. Technol.* **46** 3415–23
- Apte J S, Brauer M, Cohen A J, Ezzati M and Pope C A 2018 Ambient PM_{2.5} Reduces Global

and Regional Life Expectancy *Environ. Sci. Technol. Lett.* **5** 546–51

- Apte J S, Kirchstetter T W, Reich A H, Deshpande S J, Kaushik G, Chel A, Marshall J D and Nazaroff W W 2011 Concentrations of fine, ultrafine, and black carbon particles in auto-rickshaws in New Delhi, India *Atmos. Environ.* **45** 4470–80
- Apte J S, Marshall J D, Cohen A J and Brauer M 2015a Addressing Global Mortality from Ambient PM_{2.5} *Environ. Sci. Technol.* **49** 8057–66
- Apte J S, Marshall J D, Cohen A J and Brauer M 2015b Addressing Global Mortality from Ambient PM_{2.5} - Supplementary Information *Environ. Sci. Technol.* **49** 8057–66
- Archer-Nicholls S, Carter E, Kumar R, Xiao Q, Baumgartner J, Wiedinmyer C, Liu Y, Frostad J, Forouzanfar M H, Cohen A, Brauer M, Baumgartner J and Wiedinmyer C 2016 The Regional Impacts of Cooking and Heating Emissions on Air Quality and Disease Burden in China *Environ. Sci. Technol.* **50** 9416–23
- Arze del Granado F J, Coady D and Gillingham R 2012 The Unequal Benefits of Fuel Subsidies: A Review of Evidence for Developing Countries *Int. Monet. Fund* **10** 1–24
- Atkinson R W, Butland B K, Dimitroulopoulou C, Heal M R, Stedman J R, Carslaw N, Jarvis D, Heaviside C, Vardoulakis S, Walton H and Anderson H R 2016 Long-term exposure to ambient ozone and mortality: a quantitative systematic review and meta-analysis of evidence from cohort studies. *BMJ Open* **6** e009493
- Atkinson R W, Cohen A, Mehta S and Anderson H R 2012 Systematic review and meta-analysis of epidemiological time-series studies on outdoor air pollution and health in Asia *Air Qual. Atmos. Heal.* **5** 383–91
- Atkinson R W, Kang S, Anderson H R, Mills I C and Walton H A 2014 Epidemiological time series studies of PM_{2.5} and daily mortality and hospital admissions: a systematic review and meta-analysis. *Thorax* **69** 660–5
- Atkinson R W, Mills I C, Walton H A and Anderson H R 2015 Fine particle components and health—a systematic review and meta-analysis of epidemiological time series studies of daily mortality and hospital admissions *J. Expo. Sci. Environ. Epidemiol.* **25** 208–14
- Aunan K, Berntsen T K, Myhre G, Rypdal K, Streets D G, Woo J H and Smith K R 2009 Radiative forcing from household fuel burning in Asia *Atmos. Environ.* **43** 5674–81
- Aung T, Baumgartner J, Jain G, Sethuraman K, Reynolds C, Marshall J and Brauer M 2018 Blood pressure and eye health symptoms from a randomized cookstove intervention in rural India *Environ. Res.* **166** 658–67
- Aung T W, Jain G, Sethuraman K, Baumgartner J, Reynolds C C O, Grieshop A P, Marshall J D and Brauer M 2016 Health and Climate-relevant Pollutant Concentrations from a Carbon-finance Approved Cookstove Intervention in Rural India *Environ. Sci. Technol.* **50** 7228–38
- Badarinath K V S, Kumar Kharol S and Rani Sharma A 2009 Long-range transport of aerosols from agriculture crop residue burning in Indo-Gangetic Plains-A study using LIDAR, ground measurements and satellite data *J. Atmos. Solar-Terrestrial Phys.* **71** 112–20
- Bailis R, Drigo R, Ghilardi A and Masera O 2015 The carbon footprint of traditional woodfuels *Nat. Clim. Chang.* **5** 266–72
- Baklanov A, Schlünzen K, Suppan P, Baldasano J, Brunner D, Aksoyoglu S, Carmichael G, Douros J, Flemming J, Forkel R, Galmarini S, Gauss M, Grell G, Hirtl M, Joffre S, Jorba O, Kaas E, Kaasik M, Kallos G, Kong X, Korsholm U, Kurganskiy A, Kushta J, Lohmann U, Mahura A, Manders-Groot A, Maurizi A, Moussiopoulos N, Rao S T, Savage N, Seigneur C, Sokhi R S, Solazzo E, Solomos S, Sørensen B, Tsegas G, Vignati E, Vogel B and Zhang Y 2014 Online coupled regional meteorology chemistry models in Europe: Current status and prospects *Atmos. Chem. Phys.* **14** 317–98

- Balakrishnan K, Cohen A and Kirk R. Smith 2014a Addressing the Burden of Disease Attributable to Air Pollution in India: The Need to Integrate across Household and Ambient Air Pollution Exposures *Environ. Health Perspect.* **122** 6–7
- Balakrishnan K, Dhaliwal R S and Shah B 2011 Integrated Urban–Rural Frameworks for Air Pollution and Health-Related Research in India: The Way Forward *Environ. Health Perspect.* **119** a12–3
- Balakrishnan K, Ghosh S, Ganguli B, Sambandam S, Bruce N, Barnes D F and Smith K R 2013 State and national household concentrations of PM_{2.5} from solid cookfuel use: results from measurements and modeling in India for estimation of the global burden of disease. *Environ. Heal.* **12** 1–14
- Balakrishnan K, Ghosh S, Thangavel G, Sambandam S, Mukhopadhyay K, Puttaswamy N, Sadasivam A, Ramaswamy P, Johnson P, Kuppaswamy R, Natesan D, Maheshwari U, Natarajan A, Rajendran G, Ramasami R, Madhav S, Manivannan S, Nargunanadan S, Natarajan S, Saidam S, Chakraborty M, Balakrishnan L and Thanasekaraan V 2018 Exposures to fine particulate matter (PM_{2.5}) and birthweight in a rural-urban, mother-child cohort in Tamil Nadu, India *Environ. Res.* **161** 524–31
- Balakrishnan K, Mehta S, Ghosh S, Johnson M, Brauer M, Zhang J, Naeher L and Smith K R 2014b WHO Indoor Air Quality Guidelines: Household Fuel Combustion - Review 5: Population levels of household air pollution and exposures
- Balakrishnan K, Sambandam S, Ramaswamy P, Ghosh S, Venkatesan V, Thangavel G, Mukhopadhyay K, Johnson P, Paul S, Puttaswamy N, Dhaliwal R S and Shukla D K 2015 Establishing integrated rural-urban cohorts to assess air pollution-related health effects in pregnant women, children and adults in Southern India: an overview of objectives, design and methods in the Tamil Nadu Air Pollution and Health Effects (TAPHE) s *BMJ Open* **5** e008090
- Barnard J C, Fast J D, Paredes-Miranda G, Arnott W P and Laskin A 2010 Technical note: Evaluation of the WRF-Chem “Aerosol chemical to aerosol optical properties” module using data from the MILAGRO campaign *Atmos. Chem. Phys.* **10** 7325–40
- Bates M N and Bruce N 2014 WHO Indoor Air Quality Guidelines: Household Fuel Combustion - Review 9: Summary of systematic review of household kerosene use 1–13
- Bauer S E, Menon S, Koch D, Bond T C and Tsigaridis K 2010 A global modeling study on carbonaceous aerosol microphysical characteristics and radiative effects *Atmos. Chem. Phys.* **10** 7439–56
- Baumgartner J, Zhang Y, Schauer J J, Huang W, Wang Y and Ezzati M 2014 Highway proximity and black carbon from cookstoves as a risk factor for higher blood pressure in rural China *Proc. Natl. Acad. Sci.* **111** 13229–34
- Beckerman B S, Jerrett M, Serre M, Martin R V, Lee S-J, van Donkelaar A, Ross ev Z, Su J and Burnett R T 2013 A Hybrid Approach to Estimating National Scale Spatiotemporal Variability of PM_{2.5} in the Contiguous United States *Environ. Sci. Technol.* **47** 7233–41
- Beelen R, Hoek G, Brandt P A Van Den, Goldbohm R A, Fischer P, Schouten L J, Jerrett M, Hughes E, Armstrong B and Brunekreef B 2008 Long-Term Effects of Traffic-Related Air Pollution on Mortality in a Dutch Cohort (NLCS-AIR Study) *Environ. Health Perspect.* **116** 196–202
- Beig G, Gunthe S and Jadhav D B 2007 Simultaneous measurements of ozone and its precursors on a diurnal scale at a semi urban site in India *J. Atmos. Chem.* **57** 239–53
- Bell M L, Samet J M and Dominici F 2004 Time-Series Studies of Particulate Matter *Annu. Rev. Public Health* **25** 247–80
- Bell M L, Zanobetti A and Dominici F 2013 Evidence on Vulnerability and Susceptibility to Health Risks Associated With Short-Term Exposure to Particulate Matter: A Systematic

- Bennett D H, McKone T E, Evans J S, William W N, Margni M D, Jolliet O and Smith K R 2002 Defining Intake Fraction *Environ. Sci. Technol.* 206–11
- Berge E, Huang H-C, Chang J and Liu T-H 2001 A study of the importance of initial conditions for photochemical oxidant modeling *J. Geophys. Res.* **106** 1347
- Bibi H, Alam K, Chishtie F, Bibi S, Shahid I and Blaschke T 2015 Intercomparison of MODIS, MISR, OMI, and CALIPSO aerosol optical depth retrievals for four locations on the Indo-Gangetic plains and validation against AERONET data *Atmos. Environ.* **111** 113–26
- Bocquet M, Elbern H, Eskes H, Hirtl M, Aabkar R, Carmichael G R, Flemming J, Inness A, Pagowski M, Pérez Camaño J L, Saide P E, San Jose R, Sofiev M, Vira J, Baklanov A, Carnevale C, Grell G and Seigneur C 2015 Data assimilation in atmospheric chemistry models: Current status and future prospects for coupled chemistry meteorology models *Atmos. Chem. Phys.* **15** 5325–58
- Bollasina M A, Ming Y and Ramaswamy V 2011 Anthropogenic Aerosols and the Summer Monsoon *Science* **334** 502–5
- Bond T C, S. J. Doherty, Fahey D W, Forster P M, Berntsen T, DeAngelo B J, Flanner M G, Ghan S, Kärcher B, Koch D, Kinne S, Kondo Y, Quinn P K, Sarofim M C, Schultz M G, Schulz M, Venkataraman C, Zhang H, Zhang S, Bellouin N, Guttikunda S K, Hopke P K, Jacobson M Z, Kaiser J W, Klimont Z, Lohmann U, Schwarz J P, Shindell D, Storelvmo T, Warren S G and Zender C S 2013 Bounding the role of black carbon in the climate system: A scientific assessment *J. Geophys. Res. Atmos.* **118** 5380–552
- Bond T, Venkataraman C and Masera O 2004 Global atmospheric impacts of residential fuels *Energy Sustain. Dev.* **8** 20–32
- Bonjour S, Adair-Rohani H, Wolf J, Bruce N G, Mehta S, Pruss-Usten A, Lahiff M, Rehfuess E A, Mishra V and Smith K R 2013 Solid Fuel Use for Household Cooking: Country and Regional Estimates for 1980–2010 *Environ. Health Perspect.* **121** 784–90
- Brasseur G P and Jacob D J 2016 *Modeling of Atmospheric Chemistry* (Cambridge University Press)
- Brauer M, Amann M, Burnett R T, Cohen A, Dentener F, Ezzati M, Henderson S B, Krzyzanowski M, Martin R V, Van Dingenen R, van Donkelaar A and Thurston G D 2012 Exposure assessment for estimation of the global burden of disease attributable to outdoor air pollution. *Environ. Sci. Technol.* **46** 652–60
- Brauer M, Freedman G, Frostad J, van Donkelaar A, Martin R V., Dentener F, Dingenen R van, Estep K, Amini H, Apte J S, Balakrishnan K, Barregard L, Broday D, Feigin V, Ghosh S, Hopke P K, Knibbs L D, Kokubo Y, Liu Y, Ma S, Morawska L, Sangrador J L T, Shaddick G, Anderson H R, Vos T, Forouzanfar M H, Burnett R T and Cohen A 2016 Ambient Air Pollution Exposure Estimation for the Global Burden of Disease 2013 *Environ. Sci. Technol.* **50** 79–88
- Bromberg P A 2016 Mechanisms of the acute effects of inhaled ozone in humans *Biochim. Biophys. Acta* **1860** 2771–81
- Brook R D, Rajagopalan S, Pope C A, Brook J R, Bhatnagar A, Diez-Roux A V., Holguin F, Hong Y, Luepker R V., Mittleman M A, Peters A, Siscovick D, Smith S C, Whitsel L and Kaufman J D 2010 Particulate matter air pollution and cardiovascular disease: An update to the scientific statement from the American heart association *Circulation* **121** 2331–78
- Bruce N, Dherani M, Liu R, Hosgood H D, Sapkota A, Smith K R, Straif K, Lan Q and Pope D 2015a Does household use of biomass fuel cause lung cancer? A systematic review and evaluation of the evidence for the GBD 2010 study. *Thorax* **70** 433–41
- Bruce N, Pope D, Rehfuess E, Balakrishnan K, Adair-Rohani H and Dora C 2015b WHO indoor air quality guidelines on household fuel combustion: Strategy implications of new evidence

on interventions and exposure–risk functions *Atmos. Environ.* **106** 451–7

- Bruce N, Smith K R, Balmes J, Pope D, Dherani M, Zhang J, Duan X, Bates M, Lin W, Adair-Rohani H, Mehta S and Cohen A 2014 WHO Indoor Air Quality Guidelines: Household Fuel Combustion - Review 4: Health effects of household air pollution (HAP) exposure
- Brunekreef B, Miller B G and Hurley J F 2007 The brave new world of lives sacrificed and saved, deaths attributed and avoided *Epidemiol. Soc.* **18** 785–8
- Burnett R, Chen H, Szyszkowicz M, Fann N, Hubbell B, Pope C A, Apte J S, Brauer M, Cohen A, Weichenthal S, Coggins J, Di Q, Brunekreef B, Frostad J, Lim S S, Kan H, Walker K D, Thurston G D, Hayes R B, Lim C C, Turner M C, Jerrett M, Krewski D, Gapstur S M, Diver W R, Ostro B, Goldberg D, Crouse D L, Martin R V., Peters P, Pinault L, Tjepkema M, van Donkelaar A, Villeneuve P J, Miller A B, Yin P, Zhou M, Wang L, Janssen N A H, Marra M, Atkinson R W, Tsang H, Quoc Thach T, Cannon J B, Allen R T, Hart J E, Laden F, Cesaroni G, Forastiere F, Weinmayr G, Jaensch A, Nagel G, Concin H and Spadaro J V. 2018 Global estimates of mortality associated with long-term exposure to outdoor fine particulate matter *Proc. Natl. Acad. Sci.* 1–6
- Burnett R T, Arden Pope C, Ezzati M, Olives C, Lim S S, Mehta S, Shin H H, Singh G, Hubbell B, Brauer M, Ross Anderson H, Smith K R, Balmes J R, Bruce N G, Kan H, Laden F, Prüss-Ustün A, Turner M C, Gapstur S M, Diver W R and Cohen A 2014 An integrated risk function for estimating the global burden of disease attributable to ambient fine particulate matter exposure *Environ. Health Perspect.* **122** 397–403
- Butt E W, Rap A, Schmidt A, Scott C, Pringle K, Reddington C, Richards N, Woodhouse M, Ramirez-villegas J, Yang H, Vakkari V, Stone E A, Rupakheti M, Praveen P S, Zyl P G Van, Beukes J P, Josipovic M, Mitchell E J S, Sallu S, Forster P and Spracklen D V 2016 The impact of emissions from residential combustion on atmospheric aerosol, human health and climate *Atmos. Chem. Phys.* **16** 873–905
- Campbell P, Zhang Y, Yahya K, Wang K, Hogrefe C, Pouliot G, Knote C, Hodzic A, San Jose R, Perez J L, Jimenez Guerrero P, Baro R and Makar P 2015 A multi-model assessment for the 2006 and 2010 simulations under the Air Quality Model Evaluation International Initiative (AQMEII) phase 2 over North America: Part I. Indicators of the sensitivity of O₃ and PM_{2.5} formation regimes *Atmos. Environ.* **115** 569–86
- Carey Jang J C, Jeffries H E, Byun D and Pleim J E 1995 Sensitivity of ozone to model grid resolution-I. Application of high-resolution regional acid deposition model *Atmos. Environ.* **29** 3085–100
- Center for International Earth Science Information Network and NASA Socioeconomic Data and Applications Center 2016a *Gridded Population of the World, Version 4 (GPWv4): National Identifier Grid* (Palisades, NY)
- Center for International Earth Science Information Network and NASA Socioeconomic Data and Applications Center 2016b *Gridded Population of the World, Version 4 (GPWv4): Population Density* *Columbia Univ.*
- Chafe Z A, Brauer M, Klimont Z, Dingenen R Van, Mehta S and Rao S 2014a Household Cooking with Solid Fuels Contributes to Ambient PM_{2.5} Air Pollution and the Burden of Disease *Environ. Health Perspect.* **122** 1314–20
- Chafe Z a, Brauer M, Klimont Z, Van Dingenen R, Mehta S, Rao S, Riahi K, Dentener F and Smith K R 2014b Household Cooking with Solid Fuels Contributes to Ambient PM_{2.5} Air Pollution and the Burden of Disease - Supplementary Material *Environ. Health Perspect.* **122** 1314–20
- Chakraborty T, Beig G, Dentener F J and Wild O 2015 Atmospheric transport of ozone between Southern and Eastern Asia *Sci. Total Environ.* **523** 28–39
- Chambliss S E, Silva R, West J J, Zeinali M and Minjares R 2014 Estimating source-attributable health impacts of ambient fine particulate matter exposure: global premature mortality from

surface transportation emissions in 2005 *Environ. Res. Lett.* **9** 104009, 1–10

- Chang H I, Kumar A, Niyogi D, Mohanty U C, Chen F and Dudhia J 2009 The role of land surface processes on the mesoscale simulation of the July 26, 2005 heavy rain event over Mumbai, India *Glob. Planet. Change* **67** 87–103
- Chapman E G, Gustafson, W I, Easter R C, Barnard J C, Ghan S J, Pekour M S and Fast J D 2009 Coupling aerosol-cloud-radiative processes in the WRF-Chem model: investigating the radiative impact of elevated point sources *Atmos. Chem. Phys.* **9** 945–64
- Chatani S, Amann M, Goel A, Hao J, Klimont Z, Kumar A, Mishra A, Sharma S, Wang S X, Wang Y X and Zhao B 2014 Photochemical roles of rapid economic growth and potential abatement strategies on tropospheric ozone over South and East Asia in 2030 *Atmos. Chem. Phys.* **14** 9259–77
- Chatani S and Sharma S 2018 Uncertainties Caused by Major Meteorological Analysis Data Sets in Simulating Air Quality Over India *J. Geophys. Res. Atmos.* **123** 1–18
- Chate D, Beig G, Satpute T, Sahu S K, Ali K, Parkhi N and Ghude S 2013 Assessments of population exposure to environmental pollutants using air quality measurements during Commonwealth Games-2010. *Inhal. Toxicol.* **25** 333–40
- Chauhan A and Singh R P 2017 POOR AIR QUALITY AND DENSE HAZE/SMOG DURING 2016 IN THE INDO-GANGETIC PLAINS ASSOCIATED WITH THE CROP RESIDUE BURNING AND DIWALI FESTIVAL *Geosci. Remote Sens. Symp.* 6048–51
- Chen C, Zeger S, Breyse P, Katz J, Checkley W, Curriero F C and Tielsch J M 2016 Estimating indoor PM_{2.5} and CO concentrations in households in southern Nepal: The Nepal cookstove intervention trials *PLoS One* **11** 1–17
- Chen D, Xie X, Zhou Y, Lang J, Xu T, Yang N, Zhao Y and Liu X 2017a Performance Evaluation of the WRF-Chem Model with Different Physical Parameterization Schemes during an Extremely High PM_{2.5} Pollution Episode in Beijing *Aerosol Air Qual. Res.* **7** 262–77
- Chen L, Shi M, Gao S, Li S, Mao J, Zhang H, Sun Y, Bai Z and Wang Z 2017b Assessment of population exposure to PM_{2.5} for mortality in China and its public health benefit based on BenMAP *Environ. Pollut.* **221** 311–7
- Chen X, Pauluis O and Zhang F 2018 Regional simulation of Indian summer monsoon intraseasonal oscillations at gray-zone resolution *Atmos. Chem. Phys.* **18** 1003–22
- Cherian R, Venkataraman C, Quaas J and Ramachandran S 2013 GCM simulations of anthropogenic aerosol-induced changes in aerosol extinction, atmospheric heating and precipitation over India *J. Geophys. Res. Atmos.* **118** 2938–55
- Chin M, Diehl T, Dubovik O, Eck T F, Holben B N, Sinyuk A and Streets D G 2009 Light absorption by pollution, dust, and biomass burning aerosols: A global model study and evaluation with AERONET measurements *Ann. Geophys.* **27** 3439–64
- Chin M, Ginoux P, Kinne S, Torres O, Holben B N, Duncan B N, Martin R V., Logan J a., Higurashi A and Nakajima T 2002 Tropospheric Aerosol Optical Thickness from the GOCART Model and Comparisons with Satellite and Sun Photometer Measurements *J. Atmos. Sci.* **59** 461–83
- Chin M, Rood R B, Lin S-J, Müller J-F and Thompson A M 2000 Atmospheric sulfur cycle simulated in the global model GOCART: Model description and global properties *J. Geophys. Res.* **105** 24671–87
- Choudhry P, Misra A and Tripathi S N 2012 Study of MODIS derived AOD at three different locations in the Indo Gangetic Plain: Kanpur, Gandhi College and Nainital *Ann. Geophys.* **30** 1479–93
- Chowdhury S and Dey S 2016 Cause-specific premature death from ambient PM_{2.5} exposure in India: Estimate adjusted for baseline mortality *Environ. Int.* **91** 283–90

- Chowdhury S, Dey S and Smith K R 2018 Ambient PM_{2.5} exposure and expected premature mortality to 2100 in India under climate change scenarios *Nat. Commun.* **9** 1–10
- Chum H, Faaij A, Moreira J, Berndes G, Dhamija P, Dong H, Gabrielle B, Goss Eng A, Lucht W, Mapako M, Masera Cerutti O, McIntyre T, Minowa T, Pingoud K, Edenhofer O, Pichs-Madruga R, Sokona Y, Seyboth K, Matschoss P, Kadner S, Zwickel T, Eickemeier P, Hansen G, Schlömer S and von Stechow C 2011 Bioenergy *IPCC Spec. Rep. Renew. Energy Sources Clim. Chang. Mitig.* 332
- Clapp L J and Jenkin M E 2001 Analysis of the relationship between ambient levels of O₃, NO₂ and NO as a function of NO_x in the UK *Atmos. Environ.* **35** 6391–405
- Clappier A, Belis C A, Pernigotti D and Thunis P 2017 Source apportionment and sensitivity analysis: Two methodologies with two different purposes *Geosci. Model Dev.* **10** 4245–56
- Cohen A J, Anderson H R, Ostro B, Pandey K D, Krzyzanowski M, Künzli N, Gutschmidt K, Iii C A P, Romieu I, Samet J M and Smith K R 2004 Urban Air Pollution *Comp. Quantif. Heal. Risks Glob. Reg. Burd. Dis. Attrib. to Sel. Major Risk Factors.* **WHO** 1353–433
- Cohen A J, Brauer M, Burnett R, Anderson H R, Frostad J, Estep K, Balakrishnan K, Brunekreef B, Dandona L, Dandona R, Feigin V, Freedman G, Hubbell B, Jobling A, Kan H, Knibbs L, Liu Y, Martin R, Morawska L, III C A P, Shin H, Straif K, Shaddick G, Thomas M, Dingenen R van, Donkelaar A van, Vos T, Murray C J L and Forouzanfar M H 2017 Estimates and 25-year trends of the global burden of disease attributable to ambient air pollution: An analysis of data from the Global Burden of Diseases Study 2015 *Lancet* **389** 1907–18
- Cohen A J, Ross Anderson H, Ostro B, Pandey K D, Krzyzanowski M, Künzli N, Gutschmidt K, Pope A, Romieu I, Samet J M and Smith K 2005 The global burden of disease due to outdoor air pollution. *J. Toxicol. Environ. Health* **68** 1301–7
- Cole S R and Hernán M A 2008 Constructing inverse probability weights for marginal structural models *Am. J. Epidemiol.* **168** 656–64
- Committee on the Medical Effects of Air Pollutants 2015 Quantification of Mortality and Hospital Admissions Associated with Ground-level Ozone *A Rep. by Comm. Med. Eff. Air Pollut.* 132
- Conibear L, Butt E W, Knot C, Arnold S R and Spracklen D V. 2018a Residential energy use emissions dominate health impacts from exposure to ambient particulate matter in India *Nat. Commun.* **9** 1–9
- Conibear L, Butt E W, Knot C, Arnold S R and Spracklen D V. 2018b Stringent emission control policies can provide large improvements in air quality and public health in India *GeoHealth* **2** 196–211
- Courant R, Friedrichs K and H L 1928 Über die partiellen Differenzgleichungen der mathematischen Physik *Math. Ann.* **100** 32–74
- Cox L A T and Popken D A 2015 Has reducing fine particulate matter and ozone caused reduced mortality rates in the United States? *Ann. Epidemiol.* **25** 162–73
- Cox L J 2017 Do causal concentration–response functions exist? A critical review of associational and causal relations between fine particulate matter and mortality *Crit. Rev. Toxicol.* **47** 609–37
- Crippa P, Sullivan R C, Thota A and Pryor S C 2017 The impact of resolution on meteorological, chemical and aerosol properties in regional simulations with WRF-Chem *Atmos. Chem. Phys.* **17** 1511–28
- Cropper M L, Simon N B, Alberini A, Arora S and Sharma P K 1997 The Health Benefits of Air Pollution Control in Delhi *Am. J. Agric. Econ.* **79** 1625–9
- Crouse D L, Peters P A, Hystad P, Brook J R, van Donkelaar A, Martin R V., Villeneuve P J,

- Jerrett M, Goldberg M S, Arden Pope C, Brauer M, Brook R D, Robichaud A, Menard R and Burnett R T 2015 Ambient PM_{2.5}, O₃, and NO₂ exposures and associations with mortality over 16 years of follow-up in the Canadian census health and environment cohort (CanCHEC) *Environ. Health Perspect.* **123** 1180–6
- Cusworth D H, Mickley L J, Sulprizio M P, Liu T, Marlier M E, DeFries R S, Guttikunda S K and Gupta P 2018 Quantifying the influence of agricultural fires in northwest India on urban air pollution in Delhi, India *Environ. Res. Lett.* **13**
- Dabadge A, Sreenivas A and Josey A 2018 What Has the Pradhan Mantri Ujjwala Yojana Achieved So Far? *Econ. Polit. Wkly.* **LIII** 69–75
- Damian V, Sandu A, Damian M, Potra F and Carmichael G R 2002 The kinetic preprocessor KPP—a software environment for solving chemical kinetics *Comput. Chem. Eng.* **26** 1567–79
- Dash S K, Shekhar M S and Singh G P 2006 Simulation of Indian summer monsoon circulation and rainfall using RegCM3 *Theor. Appl. Climatol.* **86** 161–72
- Dave P, Bhushan M and Venkataraman C 2017 Aerosols cause intraseasonal short-term suppression of Indian monsoon rainfall *Sci. Rep.* **7** 17347
- David L M and Nair P R 2011 Diurnal and seasonal variability of surface ozone and NO_x at a tropical coastal site: Association with mesoscale and synoptic meteorological conditions *J. Geophys. Res.* **116** D10303
- David L M, Ravishankara A R, Kodros J K, Venkataraman C, Sadavarte P, Pierce J R, Chaliyakunnel S and Millet D B 2018 Aerosol Optical Depth Over India *J. Geophys. Res. Atmos.* **123** 3688–703
- Dedoussi I C and Barrett S R H 2014 Air pollution and early deaths in the United States. Part II: Attribution of PM_{2.5} exposure to emissions species, time, location and sector *Atmos. Environ.* **99** 610–7
- Dee D P, Uppala S M, Simmons A J, Berrisford P, Poli P, Kobayashi S, Andrae U, Balmaseda M A, Balsamo G, Bauer P, Bechtold P, Beljaars A C M, van de Berg L, Bidlot J, Bormann N, Delsol C, Dragani R, Fuentes M, Geer A J, Haimberger L, Healy S B, Hersbach H, Holm E V., Isaksen I, Kallberg P, Kohler M, Matricardi M, McNally A P, Monge-Sanz B M, Morcrette J J, Park B K, Peubey C, de Rosnay P, Tavolato C, Thapaut J N and Vitart F 2011 The ERA-Interim reanalysis: Configuration and performance of the data assimilation system *Q. J. R. Meteorol. Soc.* **137** 553–97
- Dey S and Di Girolamo L 2010 A climatology of aerosol optical and microphysical properties over the Indian subcontinent from 9 years (2000–2008) of Multiangle Imaging Spectroradiometer (MISR) data *J. Geophys. Res. Atmos.* **115** 1–22
- Dey S, Sarkar S and Singh R P 2004a Comparison of aerosol radiative forcing over the Arabian Sea and the Bay of Bengal *Adv. Sp. Res.* **33** 1104–8
- Dey S, Tripathi S N, Singh R P and Holben B N 2004b Influence of dust storms on the aerosol optical properties over the Indo-Gangetic basin *J. Geophys. Res.* **109** 1–13
- Dholakia H H, Bhadra D and Garg A 2014 Short term association between ambient air pollution and mortality and modification by temperature in five Indian cities *Atmos. Environ.* **99** 168–74
- Di Q, Wang Y, Zanobetti A, Wang Y, Koutrakis P, Choirat C, Dominici F and Schwartz J D 2017 Air Pollution and Mortality in the Medicare Population *N. Engl. J. Med.* **376** 2513–22
- Dipu S, Prabha T V., Pandithurai G, Dudhia J, Pfister G, Rajesh K and Goswami B N 2013 Impact of elevated aerosol layer on the cloud macrophysical properties prior to monsoon onset *Atmos. Environ.* **70** 454–67
- Dixit Y and Tandon S K 2016 Hydroclimatic variability on the Indian subcontinent in the past

- millennium: Review and assessment *Earth-Science Rev.* **161** 1–15
- Dockery D, Rich D, George P, Goodman P, Ohman-Strickland P, Clancy L and Kotlov T 2013 Effect of Air Pollution Control on Mortality and Hospital Admissions in Ireland *Heal. Eff. Institute, Res. Report. Boston, MA.* **176** 152
- Dominici F, Peng R D, Barr C D and Bell M L 2010 Protecting human health from air pollution: Shifting from a single-pollutant to a multipollutant approach *Epidemiology* **21** 187–94
- Dominici F and Zigler C 2017 Best practices for gauging evidence of causality in air pollution epidemiology *Am. J. Epidemiol.* **186** 1303–9
- van Donkelaar A, Martin R V., Brauer M and Boys B L 2015 Use of Satellite Observations for Long-Term Exposure Assessment of Global Concentrations of Fine Particulate Matter *Environ. Health Perspect.* **123** 135–43
- van Donkelaar A, Martin R V., Brauer M, Kahn R, Levy R, Verduzco C and Villeneuve P J 2010 Global estimates of ambient fine particulate matter concentrations from satellite-based aerosol optical depth: Development and application *Environ. Health Perspect.* **118** 847–55
- van Donkelaar A, Martin R V, Brauer M, Hsu N C, Kahn R A, Levy R C, Lyapustin A, Sayer A M and Winker D M 2016 Global Estimates of Fine Particulate Matter using a Combined Geophysical-Statistical Method with Information from Satellites, Models, and Monitors *Environ. Sci. Technol.* **50** 3762–72
- Easter R C, Ghan S J, Zhang Y, Saylor R D, Chapman E G, Laulainen N S, Abdul-Razzak H, Leung L R, Bian X and Zaveri R A 2004 MIRAGE: Model description and evaluation of aerosols and trace gases *J. Geophys. Res. Atmos.* **109** D20210
- Edwards R, Karnani S, Fisher E M, Johnson M, Naeher L, Smith K R and Morawska L 2014 WHO Indoor Air Quality Guidelines: Household fuel Combustion - Review 2: Emissions of Health-Damaging Pollutants from Household Stoves 1–42
- Ek M B, Mitchell K E, Lin Y, Rogers E, Grunmann P, Koren V, Gayno G and Tarpley J D 2003 Implementation of Noah land surface model advances in the National Centers for Environmental Prediction operational mesoscale Eta model *J. Geophys. Res. Atmos.* **108** 8851–67
- Emery C, Tai E and Yarwood G 2001 Enhanced Meteorological Modeling and Performance Evaluation for Two Texas Ozone Episodes *Air Sci.* 1–235
- Emmons L K, Walters S, Hess P G, Lamarque J-F, Pfister G G, Fillmore D, Granier C, Guenther A, Kinnison D, Laepple T, Orlando J, Tie X, Tyndall G, Wiedinmyer C, Baughcum S L and Kloster S 2010 Description and evaluation of the Model for Ozone and Related chemical Tracers, version 4 (MOZART-4) *Geosci. Model Dev.* **3** 43–67
- Energy Sector Management Assistance Program and Global Alliance for Clean Cookstoves 2015 The state of the global clean and improved cooking sector 179
- Engardt M 2008 Modelling of near-surface ozone over South Asia *J. Atmos. Chem.* **59** 61–80
- van Erp A M and Cohen A J 2009 HEI's Research Program on the Impact of Actions to Improve Air Quality: Interim Evaluation and Future Directions *Heal. Eff. Institute, Commun. Boston, MA.* **14** 34
- Evans J, van Donkelaar A, Martin R V., Burnett R, Rainham D G, Birkett N J and Krewski D 2013 Estimates of global mortality attributable to particulate air pollution using satellite imagery *Environ. Res.* **120** 33–42
- Ezzati M, Pearson-Stuttard J, Bennett J E and Mathers C D 2018 Acting on non-communicable diseases in low- and middle-income tropical countries *Nature* **559** 507–16
- Fang Y, Mauzerall D L, Liu J, Fiore A M and Horowitz L W 2013 Impacts of 21st-century climate change on global air pollution-related premature mortality *Clim. Change* **121** 239–53

- Fantke P, Jolliet O, Apte J S, Hodas N, Evans J S, Weschler C J, Stylianou K, Jantunen M and McKone T E 2017 Characterizing Aggregated Exposure to Primary Particulate Matter: Recommended Intake Fractions for Indoor and Outdoor Sources *Environ. Sci. Technol.* **51** 9089–100
- Fast J D, Gustafson W I, Chapman E G, Easter R C, Rishel J P, Zaveri R A, Grell G A and Barth M C 2011 The aerosol modeling testbed: A community tool to objectively evaluate aerosol process modules *Bull. Am. Meteorol. Soc.* **92** 343–60
- Fast J D, Gustafson W I, Easter R C, Zaveri R A, Barnard J C, Chapman E G, Grell G A and Peckham S E 2006 Evolution of ozone, particulates, and aerosol direct radiative forcing in the vicinity of Houston using a fully coupled meteorology-chemistry-aerosol model *J. Geophys. Res. Atmos.* **111** 1–29
- Fiore A, Jacob D J, Liu H, Yantosca R M, Fairlie T D and Li Q 2004 Variability in surface ozone background over the United States: Implications for air quality policy *J. Geophys. Res. Atmos.* **108** 4787
- Fiore A M, Naik V, Spracklen D V., Steiner A, Unger N, Prather M, Bergmann D, Cameron-Smith P J, Cionni I, Collins W J, Dalsøren S, Eyring V, Folberth G A, Ginoux P, Horowitz L W, Josse B, Lamarque J-F, MacKenzie I A, Nagashima T, O'Connor F M, Righi M, Rumbold S, Shindell D T, Skeie R B, Sudo K, Szopa S, Takemura T and Zeng G 2012 Global Air Quality and Climate *Chem. Soc. Rev.* **41** 6663–83
- Fleming L T, Weltman R, Yadav A, Edwards R D, Arora N K, Pillarisetti A, Meinardi S, Smith K R, Blake D R and Nizkorodov S A 2018a Emissions from village cookstoves in Haryana, India and their potential impacts on air quality *Atmos. Chem. Phys. Discuss.* 1–21
- Fleming Z L, Doherty R M, Von Schneidemesser E, Malley C S, Cooper O R, Pinto J P, Colette A, Xu X, Simpson D, Schultz M G, Lefohn A S, Hamad S, Moolla R, Solberg S and Feng Z 2018b Tropospheric ozone assessment report: Present-day ozone distribution and trends relevant to human health *Elem. Sci. Anthr.* **6** 41
- Food and Agriculture Organization of the United Nations 2012 *State of the World's Forests*
- Ford B and Heald C L 2016 Exploring the uncertainty associated with satellite-based estimates of premature mortality due to exposure to fine particulate matter *Atmos. Chem. Phys.* **156** 3499–523
- Forest Survey of India 2017 Forest Cover *State For. Rep. 2017. Minist. Environ. For. Gov. India.* 36
- Fosu B O, Wang S-Y S, Wang S-H, Gillies R R and Zhao L 2017 Greenhouse gases stabilizing winter atmosphere in the Indo-Gangetic plains may increase aerosol loading *Atmos. Sci. Lett.* **18** 168–74
- Fuzzi S, Baltensperger U, Carslaw K, Decesari S, Denier van der Gon H, Facchini M C, Fowler D, Koren I, Langford B, Lohmann U, Nemitz E, Pandis S, Riipinen I, Rudich Y, Schaap M, Slowik J G, Spracklen D V., Vignati E, Wild M, Williams M and Gilardoni S 2015 Particulate matter, air quality and climate: lessons learned and future needs *Atmos. Chem. Phys.* **15** 8217–99
- Gao M, Ji D, Liang F and Liu Y 2018 Attribution of aerosol direct radiative forcing in China and India to emitting sectors *Atmos. Environ.* **190** 35–42
- Gapminder 2018 Income Mountain. Version 2.
- Gaur A, Tripathi S N, Kanawade V P, Tare V and Shukla S P 2014 Four-year measurements of trace gases (SO₂, NO_x, CO, and O₃) at an urban location, Kanpur, in Northern India *J. Atmos. Chem.* **71** 283–301
- GBD 2010 Risk Factors Collaborators 2012 A comparative risk assessment of burden of disease and injury attributable to 67 risk factors and risk factor clusters in 21 regions, 1990–2010: a systematic analysis for the Global Burden of Disease Study 2010. *Lancet* **380** 2224–60

- GBD 2013 Risk Factors Collaborators 2015 Global, regional, and national comparative risk assessment of 79 behavioural, environmental and occupational, and metabolic risks or clusters of risks in 188 countries, 1990-2013: A systematic analysis for the Global Burden of Disease Study 2013 *Lancet* **386** 2287–323
- GBD 2015 Risk Factors Collaborators 2016a Global, regional, and national comparative risk assessment of 79 behavioural, environmental and occupational, and metabolic risks or clusters of risks, 1990-2015: a systematic analysis for the Global Burden of Disease Study 2015 *Lancet* **388** 1659–724
- GBD 2015 Risk Factors Collaborators 2016b Supplement to: GBD 2015 Risk Factors Collaborators. Global, regional, and national comparative risk assessment of 79 behavioural, environmental and occupational, and metabolic risks or clusters of risks, 1990–2015: a systematic analysis for the Global Bur *Lancet* **388** 1659–724
- GBD 2016 Risk Factors Collaborators 2017 Global, regional, and national comparative risk assessment of 84 behavioural, environmental and occupational, and metabolic risks or clusters of risks, 1990–2016: a systematic analysis for the Global Burden of Disease Study 2016 *Lancet* **390** 1345–422
- GBD MAPS Working Group 2016 *Burden of Disease Attributable to Coal-Burning and Other Air Pollution Sources in China*
- GBD MAPS Working Group 2018 *Burden of Disease Attributable to Major Air Pollution Sources in India*
- Ghude S D, Chate D M, Jena C, Beig G, Kumar R, Barth M C, Pfister G G, Fadnavis S and Pithani P 2016 Premature mortality in India due to PM_{2.5} and ozone exposure *Geophys. Res. Lett.* **43** 1–9
- Ghude S D, Jena C, Chate D M, Beig G, G. G. Pfister, Kumar R and Ramanathan V 2014 Reductions in India's crop yield due to ozone *Geophys. Res. Lett.* **41** 5685–91
- Ghude S D, Kulkarni S H, Jena C, Pfister G G, Beig G, Fadnavis S and Van Der R J 2013 Application of satellite observations for identifying regions of dominant sources of nitrogen oxides over the Indian subcontinent *J. Geophys. Res. Atmos.* **118** 1075–89
- Giannadaki D, Lelieveld J, Pozzer A, Lim S, Vos T, Flaxman A, Danaei G, Shibuya K, Cohen A, Anderson H, Ostra B, Pandey K, Krzyzanowski M, Künzli N, Gutschmidt K, Pope A, Romieu I, Samet J, Smith K, Ezzati M, Lopez A, Rodgers A, Hoorn S, Murray C, Laden F, Schwartz J, Speizer F, Dockery D, Pope C, Ezzati M, Dockery D, Lelieveld J, Evans J, Fnais M, Giannadaki D, Pozzer A, Pinault L, Tjepkema M, Crouse D, Weichenthal S, Donkelaar A, Martin R, Brauer M, Chen H, Burnett R, Bell M, Morgenstern R, Harrington W, Giannadaki D, Pozzer A, Lelieveld J, Anenberg S, Horowitz L, Tong D, West J, Jöckel P, Tost H, Pozzer A, Brühl C, Buchholz J, Ganzeveld L, Hoor P, Kerkweg A, Lawrence M, Sander R, Steil B, Stiller G, Tanarhte M, Taraborelli D, Aardenne J, Lelieveld J, Pozzer A, Meij A, Yoon J, Tost H, Georgoulias A, Astitha M, Lelieveld J, Barlas C, Giannadaki D, Pozzer A, Green J, Sánchez S, Zheng S, Pozzer A, Cao C, Lelieveld J, Krzyzanowski M, Cohen A, Cooke R, Wilson A, Tuomisto J, Morales O, Tainio M, Evans J, Kinney P, Roman H, Walker K, et al 2016 Implementing the US air quality standard for PM_{2.5} worldwide can prevent millions of premature deaths per year *Environ. Heal.* **15** 1–11
- Gifford M L 2010 A Global Review of Cookstove Programs 34
- Ginoux P, Chin M, Tegen I, Prospero J M, Holben B, Dubovik O and Lin S J 2001 Sources and distributions of dust aerosols simulated with the GOCART model *J. Geophys. Res.* **106** 20255–73
- Glass T A, Goodman S N, Hernán M A and Samet J M 2013 Causal Inference in Public Health *Annu. Rev. Public Health* **34** 61–75
- Global Alliance for Clean Cookstoves and Dalberg Global Development Advisors 2013 *India Cookstoves and Fuels Market Assessment*

- Global Burden of Disease Collaborative Network 2017 Global Burden of Disease Study 2016 (GBD 2016) Causes of Death and Nonfatal Causes Mapped to ICD Codes *Inst. Heal. Metrics Eval. (IHME). Seattle, United States*. Online: <http://ghdx.healthdata.org/record/global-burden-disease-study-2016-gbd-2016-causes-death-and-nonfatal-causes-mapped-icd-codes>
- Global Burden of Disease Study 2015 2016a Global Burden of Disease Study 2015 (GBD 2015) Population Estimates 1970–2015 *Seattle, United States Inst. Heal. Metrics Eval.* Online: <http://ghdx.healthdata.org/record/global-burden-disease-study-2015-gbd-2015-population-estimates-1970-2015>
- Global Burden of Disease Study 2015 2016b Global Burden of Disease Study 2015 (GBD 2015) Reference Life Table *Seattle, United States Inst. Heal. Metrics Eval.* Online: <http://ghdx.healthdata.org/record/global-burden-disease-study-2015-gbd-2015-reference-life-table>
- Global Burden of Disease Study 2016 2017a Global Burden of Disease Study 2016 (GBD 2016) Population Estimates 1950–2016 *Seattle, United States Inst. Heal. Metrics Eval.* Online: <http://ghdx.healthdata.org/record/global-burden-disease-study-2016-gbd-2016-population-estimates-1950-2016>
- Global Burden of Disease Study 2016 2017b Global Burden of Disease Study 2016 (GBD 2016) Reference Life Table *Seattle, United States Inst. Heal. Metrics Eval.* Online: <http://ghdx.healthdata.org/record/global-burden-disease-study-2016-gbd-2016-reference-life-table>
- Goldemberg J, Martinez-Gomez J, Sagar A and Smith K R 2018 Household air pollution, health, and climate change: cleaning the air *Environ. Res. Lett.* **13** 030201
- Goodman J E, Prueitt R L, Sax S N, Lynch H N, Zu K, Lemay J C, King J M and Venditti F J 2014 Weight-of-evidence evaluation of short-term ozone exposure and cardiovascular effects *Crit. Rev. Toxicol.* **44** 725–90
- Gordon S B, Bruce N G, Grigg J, Hibberd P L, Kurmi O P, Lam K H, Mortimer K, Asante K P, Balakrishnan K, Balmes J, Bar-Zeev N, Bates M N, Breysse P N, Buist S, Chen Z, Havens D, Jack D, Jindal S, Kan H, Mehta S, Moschovis P, Naeher L, Patel A, Perez-Padilla R, Pope D, Rylance J, Semple S and Martin W J 2014 Respiratory risks from household air pollution in low and middle income countries. *Lancet* **2** 823–60
- Gordon S, Mortimer K, Grigg J and Balmes J 2017 In control of ambient and household air pollution — how low should we go? *Lancet Respir. Med.* **5** 918–20
- Govardhan G R, Nanjundiah R S, Satheesh S K, Moorthy K K and Kotamarthi V R 2015 Performance of WRF-Chem over Indian region: Comparison with measurements. *J. Earth Syst. Sci.* **124** 875–96
- Government of India 2014 Auto Fuel Vision & Policy 2025 *Gov. India* 294
- Government of India 2011 Census of India 2011
- Government of India 2018 Give it Up LPG Scheme Online: <http://mylpg.in/index.aspx>
- Government of India 2015 *India's Intended Nationally Determined Contribution*
- Grandjean P and Landrigan P 2006 Developmental neurotoxicity of industrial chemicals *Lancet* **368** 2167–78
- Greenbaum D and Shaikh R 2010 First steps toward multipollutant science for air quality decisions *Epidemiology* **21** 195–7
- Gregersen H, El Lakany H, Bailey L and White A 2011 *The greener side of REDD+: Lessons for REDD+ from countries where forest area is increasing*
- Grell G A and Devenyi D 2002 A generalized approach to parameterizing convection combining ensemble and data assimilation techniques *Geophys. Res. Lett.* **29** 10–3

- Grell G A and Freitas S R 2014 A scale and aerosol aware stochastic convective parameterization for weather and air quality modeling *Atmos. Chem. Phys.* **14** 5233–50
- Grell G A, Knoche R, Peckham S E and McKeen S A 2004 Online versus offline air quality modeling on cloud-resolving scales *Geophys. Res. Lett.* **31** 6–9
- Grell G A, Peckham S E, Schmitz R, McKeen S A, Frost G, Skamarock W C and Eder B 2005 Fully coupled “online” chemistry within the WRF model *Atmos. Environ.* **39** 6957–75
- Grewe V, Dahlmann K, Matthes S and Steinbrecht W 2012 Attributing ozone to NO_x emissions: Implications for climate mitigation measures *Atmos. Environ.* **59** 102–7
- Grewe V, Tsati E and Hoor P 2010 On the attribution of contributions of atmospheric trace gases to emissions in atmospheric model applications *Geosci. Model Dev.* **3** 487–99
- Grieshop A P, Jain G, Sethuraman K and Marshall J D 2017 Emission factors of health- and climate-relevant pollutants measured in home during a carbon-finance-approved cookstove intervention in rural India *GeoHealth* **1** 222–36
- Grieshop A P, Marshall J D and Kandlikar M 2011 Health and climate benefits of cookstove replacement options *Energy Policy* **39** 7530–42
- Grosovsky A J, Sasaki J C, Arey J, Eastmond D A, Parks K K and Atkinson R 1999 Evaluation of the potential health effects of the atmospheric reaction products of polycyclic aromatic hydrocarbons *HEI Res. Rep. 84. Boston, MA Health Eff. Inst.* 40
- Guarnieri M and Balmes J R 2014 Outdoor air pollution and asthma *Lancet* **383** 1581–92
- Guenther A, Karl T, Harley P, Wiedinmyer C, Palmer P I and Geron C 2006 Estimates of global terrestrial isoprene emissions using MEGAN (Model of Emissions of Gases and Aerosols from Nature) *Atmos. Chem. Phys.* **6** 3181–210
- Gumley L 2011 ECNU IMAPP WORKSHOP LAB FIVE: MODIS AOD Analysis
- Gunwani P and Mohan M 2017 Sensitivity of WRF model estimates to various PBL parameterizations in different climatic zones over India *Atmos. Res.* **194** 43–65
- Guo H, Kota S H, Chen K, Sahu S K, Hu J and Ying Q 2018 Source contributions and potential reductions to health effects of particulate matter in India *Atmos. Chem. Phys.* **18** 15219–29
- Guo H, Kota S H, Sahu S K, Hu J, Ying Q, Gao A and Zhang H 2017 Source apportionment of PM_{2.5} in North India using source-oriented air quality models *Environ. Pollut.* **231** 426–36
- Gupta M and Mohan M 2015 Validation of WRF/Chem model and sensitivity of chemical mechanisms to ozone simulation over megacity Delhi *Atmos. Environ.* **122** 220–9
- Gustafsson Ö, Kruså M, Zencak Z, Sheesley R J, Granat L, Engström E, Praveen P S, Rao P S P, Leck C and Rodhe H 2009 Brown Clouds over South Asia: Biomass or Fossil Fuel Combustion? *Science* **323** 495–9
- Guttikunda S K and Goel R 2013 Health impacts of particulate pollution in a megacity - Delhi, India *Environ. Dev.* **6** 8–20
- Guttikunda S K and Gurjar B R 2012 Role of meteorology in seasonality of air pollution in megacity Delhi, India *Environ. Monit. Assess.* **184** 3199–211
- Guttikunda S K and Mohan D 2014 Re-fueling road transport for better air quality in India *Energy Policy* **68** 556–61
- Haines A, Amann M, Borgford-Parnell N, Leonard S, Kuylentierna J and Shindell D 2017 Short-lived climate pollutant mitigation and the Sustainable Development Goals *Nat. Clim. Chang.* **7** 863–9
- Han Y, Qi M, Chen Y, Shen H, Liu J, Huang Y, Chen H, Liu W, Wang X, Liu J, Xing B and Tao S 2015 Influences of ambient air PM_{2.5} concentration and meteorological condition on the indoor PM_{2.5} concentrations in a residential apartment in Beijing using a new approach

- Hanbar R D and Karve P 2002 National Programme on Improved Chulha (NPIC) of the Government of India: an overview *Energy Sustain. Dev.* **6** 49–55
- Hanna R, Duflo E and Greenstone M 2016 Up in Smoke: The Influence of Household Behavior on the Long-Run Impact of Improved Cooking Stoves *Am. Econ. J. Econ. Policy* **8** 80–114
- Hansen M C, Potapov P V., Moore R, Hancher M, Turubanova S A, Tyukavina A, Thau D, Stehman S V., Goetz S J, Loveland T R, Kommareddy A, Egorov A, Chini L, Justice C O and Townshend J R G 2013 High-Resolution Global Maps of 21st-Century Forest Cover Change *Science* **342** 850–3
- Hari Prasad K B R R, Venkata Srinivas C, Venkateswara Naidu C, Baskaran R and Venkatraman B 2016 Assessment of surface layer parameterizations in ARW using micro-meteorological observations from a tropical station *Meteorol. Appl.* **23** 191–208
- Hari Prasad K B R R, Srinivas C V., Singh A B, Vijaya Bhaskara Rao S, Baskaran R and Venkatraman B 2014 Numerical simulation and intercomparison of boundary layer structure with different PBL schemes in WRF using experimental observations at a tropical site *Atmos. Res.* **145–146** 27–44
- Haywood J and Boucher O 2000 Estimates of the direct and indirect radiative forcing due to tropospheric aerosols: A review *Rev. Geophys.* **38** 513–43
- Heald C L and Spracklen D V. 2015 Land Use Change Impacts on Air Quality and Climate *Chem. Rev.* **115** 4476–96
- Health Effects Institute 2018 State of Global Air 2018 *Heal. Eff. Institute, Spec. Report. Boston, MA.*
- Health Effects Institute Household Air Pollution Working Group 2018 Household Air Pollution and Noncommunicable Disease *Heal. Eff. Institute, Commun. Boston, MA.* **18** 86
- Health Effects Institute International Scientific Oversight Committee 2010 Outdoor Air Pollution and Health in the Developing Countries of Asia: A Comprehensive Review *Heal. Eff. Institute, Spec. Report. Boston, MA.* **18** 284
- Health Effects Institute Public Health and Air Pollution in Asia Program 2011 *Public Health and Air Pollution in Asia (PAPA): Coordinated Studies of Short-Term Exposure to Air Pollution and Daily Mortality in Two Indian Cities* vol 157
- Health Effects Institute Review Panel on Ultrafine Particles 2013 Understanding the Health Effects of Ambient Ultrafine Particles *Heal. Eff. Institute, Perspect. Boston, MA.* **3**
- Heft-Neal S, Burney J, Bendavid E and Burke M 2018 Robust relationship between air quality and infant mortality in Africa *Nature* **559** 254–8
- Henneman L R F, Liu C, Mulholland J A and Russell A G 2017 Evaluating the effectiveness of air quality regulations: A review of accountability studies and frameworks *J. Air Waste Manag. Assoc.* **67** 144–72
- Henriksson S V., Laaksonen A, Kerminen V M, Räisänen P, Järvinen H, Sundström A M and De Leeuw G 2011 Spatial distributions and seasonal cycles of aerosols in India and China seen in global climate-aerosol model *Atmos. Chem. Phys.* **11** 7975–90
- Héroux M E, Anderson H R, Atkinson R, Brunekreef B, Cohen A, Forastiere F, Hurley F, Katsouyanni K, Krewski D, Krzyzanowski M, Künzli N, Mills I, Querol X, Ostro B and Walton H 2015 Quantifying the health impacts of ambient air pollutants: recommendations of a WHO/Europe project *Int. J. Public Health* **60** 619–27
- Hijmans R, University of California, Berkeley Museum of Vertebrate Zoology, Kapoor J, Wieczorek J, International Rice Research Institute, Garcia N, Maunahan A, Rala A and Davis A M 2016 Global Administrative Areas (GADM): Boundaries without limits. Version 2.8.

- Hill L D, Edwards R, Turner J R, Argo Y D, Olkhanud P B, Odsuren M, Guttikunda S, Ochir C and Smith K R 2017 Health assessment of future PM_{2.5} exposures from indoor, outdoor, and secondhand tobacco smoke concentrations under alternative policy pathways in Ulaanbaatar, Mongolia *PLoS One* **12** 1–26
- Hodzic A, D. G and Cui Y Meteorological conditions, emissions and transport of anthropogenic pollutants over the Central Rocky Mountains during the 2011 BEACHON-RoMBAS field study *In prep.*
- Hodzic A and Jimenez J L 2011 Modeling anthropogenically controlled secondary organic aerosols in a megacity: a simplified framework for global and climate models *Geosci. Model Dev.* **4** 901–17
- Hodzic A and Knote C 2014 WRF-Chem 3.6.1: MOZART gas-phase chemistry with MOSAIC aerosols *Atmos. Chem. Div. (ACD), Natl. Cent. Atmos. Res.* **7**
- Huang Y, Shen H, Chen Y, Zhong Q, Chen H, Wang R, Shen G, Liu J, Li B and Tao S 2015 Global organic carbon emissions from primary sources from 1960 to 2009 *Atmos. Environ.* **122** 505–12
- Huang Y, Unger N, Storelvmo T, Harper K, Zheng Y and Heyes C 2018 Global radiative effects of solid fuel cookstove aerosol emissions *Atmos. Chem. Phys.* **18** 5219–33
- Hubbell B and Greenbaum D 2014 Counterpoint: Moving from potential-outcomes thinking to doing-changing research planning to enable successful health outcomes research *Am. J. Epidemiol.* **180** 1141–4
- Hughes B B, Irfan M T, Moyer J D, Rothman D S and Solórzano J R 2012 Exploring Future Impacts of Environmental Constraints on Human Development *Sustainability* **4** 958–94
- Hughes B B, Kuhn R, Peterson C M, Rothman D S, Solórzano J R, Mathers C D and Dickson J R 2011 Projections of global health outcomes from 2005 to 2060 using the International Futures integrated forecasting model *Bull. World Health Organ.* **89** 478–86
- Hutton G, Rehfuess E, Tedioso F and Weiss S 2006 Evaluation of the costs and benefits of household energy and health interventions at global and regional levels *World Heal. Organ.* **109**
- Iacono M J, Delamere J S, Mlawer E J, Shephard M W, Clough S A and Collins W D 2008 Radiative forcing by long-lived greenhouse gases: Calculations with the AER radiative transfer models *J. Geophys. Res. Atmos.* **113** 2–9
- ICF International Spatial Data Repository, The Demographic and Health Surveys Program Online: spatialdata.dhsprogram.com
- Im U, Bianconi R, Solazzo E, Kioutsioukis I, Badia A, Balzarini A, Baró R, Bellasio R, Brunner D, Chemel C, Curci G, Flemming J, Forkel R, Giordano L, Jiménez-Guerrero P, Hirtl M, Hodzic A, Honzak L, Jorba O, Knote C, Kuenen J J P, Makar P A, Manders-Groot A, Neal L, Pérez J L, Pirovano G, Pouliot G, San Jose R, Savage N, Schroder W, Sokhi R S, Syrakov D, Torian A, Tuccella P, Werhahn J, Wolke R, Yahya K, Zabkar R, Zhang Y, Zhang J, Hogrefe C and Galmarini S 2015 Evaluation of operational on-line-coupled regional air quality models over Europe and North America in the context of AQMEII phase 2. Part I: Ozone *Atmos. Environ.* **115** 404–20
- India State-Level Disease Burden Initiative Collaborators 2017 Nations within a nation: variations in epidemiological transition across the states of India, 1990–2016 in the Global Burden of Disease Study *Lancet* **390** 2437–60
- Indian Council of Medical Research, Public Health Foundation of India and Institute for Health Metrics and Evaluation 2017a GBD India Compare Data Visualization. *ICMR, PHFI, IHME* Online: vizhub.healthdata.org/gbd-compare/india
- Indian Council of Medical Research, Public Health Foundation of India and Institute for Health Metrics and Evaluation 2017b *India: Health of the Nation's States. The India State-Level*

- Indian Institute of Management 2010 *Evaluation of Central Pollution Control Board (CPCB)*
- Institute for Health Metrics and Evaluation 2018 GBD Compare Data Visualization. *Seattle, WA IHME, Univ. Washingt.* Online: vizhub.healthdata.org/gbd-compare
- Intergovernmental Panel on Climate Change 2013 Contribution of Working Group I to the Fifth Assessment Report of the Intergovernmental Panel on Climate Change - Summary for Policymakers in Climate Change 2013: the Physical Science Basis 27
- International Energy Agency 2016a *Energy and Air Pollution. World Energy Outlook Special Report* (Paris, France)
- International Energy Agency 2016b *World Energy Outlook 2016* (Paris, France)
- Jack D W, Asante K P, Wylie B J, Chillrud S N, Whyatt R M, Ae-Ngibise K A, Quinn A K, Yawson A K, Boamah E A, Agyei O, Mujtaba M, Kaali S, Kinney P and Owusu-Agyei S 2015 Ghana randomized air pollution and health study (GRAPHS): Study protocol for a randomized controlled trial *Trials* **16** 1–10
- Jacob D J and Winner D A 2009 Effect of climate change on air quality *Atmos. Environ.* **43** 51–63
- Jacobson M Z 2012 Investigating cloud absorption effects: Global absorption properties of black carbon, tar balls, and soil dust in clouds and aerosols *J. Geophys. Res. Atmos.* **117** 1–25
- Jacobson M Z 2008 On the causal link between carbon dioxide and air pollution mortality *Geophys. Res. Lett.* **35** 1–5
- Jacobson M Z 2010 Short-term effects of controlling fossil-fuel soot, biofuel soot and gases, and methane on climate, Arctic ice, and air pollution health *J. Geophys. Res. Atmos.* **115** D14209:1-24
- Jain A, Ray S, Ganesan K, Aklin M, Cheng C and Urpelainen J 2015 ACCESS TO CLEAN COOKING ENERGY AND ELECTRICITY: Survey of States *Columbia Univ. Counc. Energy, Environ. Water Shakti Sustain. Energy Found.* 98
- Jain S L, Arya B C, Kumar A, Ghude S D and Kulkarni P S 2005 Observational study of surface ozone at New Delhi, India *Int. J. Remote Sens.* **26** 3515–24
- Jain V, Dey S and Chowdhury S 2017 Ambient PM_{2.5} exposure and premature mortality burden in the holy city Varanasi, India *Environ. Pollut.* **226** 182–9
- Janssens-Maenhout G, Crippa M, Guizzardi D, Dentener F, Muntean M, Pouliot G, Keating T, Zhang Q, Kurokawa J, Wankmüller R, Denier Van Der Gon H, Kuenen J J P, Klimont Z, Frost G, Darras S, Koffi B and Li M 2015 HTAP-v2.2: A mosaic of regional and global emission grid maps for 2008 and 2010 to study hemispheric transport of air pollution *Atmos. Chem. Phys.* **15** 11411–32
- Jayarathne T, Stockwell C E, Bhawe P V., Praveen P S, Rathnayake C M, Md Islam R, Panday A K, Adhikari S, Maharjan R, Douglas Goetz J, Decarlo P F, Saikawa E, Yokelson R J and Stone E A 2018 Nepal Ambient Monitoring and Source Testing Experiment (NAMaSTE): Emissions of particulate matter from wood-and dung-fueled cooking fires, garbage and crop residue burning, brick kilns, and other sources *Atmos. Chem. Phys.* **18** 2259–86
- Jena C, Ghude S D, Beig G, Chate D M, Kumar R, Pfister G G, Lal D M, Surendran D E, Fadnavis S and van der A R J 2015a Inter-comparison of different NO_x emission inventories and associated variation in simulated surface ozone in Indian region *Atmos. Environ.* **117** 61–73
- Jena C, Ghude S D, Pfister G G, Chate D M, Kumar R, Beig G, Surendran D E, Fadnavis S and Lal D M 2015b Influence of springtime biomass burning in South Asia on regional ozone (O₃): A model based case study *Atmos. Environ.* **100** 37–47
- Jerrett M 2015 The death toll from air-pollution sources *Nature* **525** 330–1

- Jerrett M, Burnett R T, Pope C A, Ito K, Thurston G, Krewski D, Shi Y, Calle E and Thun M 2009 Long-Term Ozone Exposure and Mortality *N. Engl. J. Med.* **360** 1085–95
- Jethva H, Chand D, Torres O, Gupta P, Lyapustin A and Patadia F 2018 Agricultural Burning and Air Quality over Northern India: A Synergistic Analysis using NASA's A-train Satellite Data and Ground Measurements *Aerosol Air Qual. Res.*
- Jethva H, Satheesh S K and Srinivasan J 2007 Evaluation of Moderate-Resolution Imaging Spectroradiometer (MODIS) Collection 004 (C004) aerosol retrievals at Kanpur, Indo-Gangetic Basin *J. Geophys. Res. Atmos.* **112** 1–9
- Jetter J J and Kariher P 2009 Solid-fuel household cook stoves: Characterization of performance and emissions *Biomass and Bioenergy* **33** 294–305
- Jetter J, Zhao Y, Smith K R, Khan B, Yelverton T, Decarlo P and Hays M D 2012a Pollutant emissions and energy efficiency under controlled conditions for household biomass cookstoves and implications for metrics useful in setting international test standards *Environ. Sci. Technol.* **46** 10827–34
- Jetter J, Zhao Y, Smith K R, Khan B, Yelverton T, DeCarlo P and Hays M D 2012b Pollutant emissions and energy efficiency under controlled conditions for household biomass cookstoves and implications for metrics useful in setting international test standards *Environ. Sci. Technol.* **46** 10827–34
- Jones S L, Adams-Selin R, Hunt E D, Creighton G A and Cetola J D 2010 Adapting WRF-CHEM GOCART for Fine-Scale Dust Forecasting *AGU Fall Meet. Abstr. Vol. 1*
- Jones S L, Adams-Selin R, Hunt E D, Creighton G A and Cetola J D 2012 Update on modifications to WRF-CHEM GOCART for fine-scale dust forecasting at AFWA *Am. Geophys. Union, Fall Meet. 2012* **A33D–0188**
- Joshi H, Naja M, Singh K P, Kumar R, Bhardwaj P, Babu S S, Satheesh S K, Moorthy K K and Chandola H C 2016 Investigations of aerosol black carbon from a semi-urban site in the Indo-Gangetic Plain region *Atmos. Environ.* **125** 346–59
- Junker C and Liousse C 2008 A global emission inventory of carbonaceous aerosol from historic records of fossil fuel and biofuel consumption for the period 1860-1997 *Atmos. Chem. Phys.* **8** 1195–207
- Kar A, Rehman I H, Burney J, Puppala S P, Suresh R, Singh L, Singh V K, Ahmed T, Ramanathan N and Ramanathan V 2012 Real-time assessment of black carbon pollution in Indian households due to traditional and improved biomass cookstoves *Environ. Sci. Technol.* **46** 2993–3000
- Kar J, Deeter M N, Fishman J, Liu Z, Omar A, Creilson J K, Trepte C R, Vaughan M A and Winker D M 2010 Wintertime pollution over the Eastern Indo-Gangetic Plains as observed from MOPITT, CALIPSO and tropospheric ozone residual data *Atmos. Chem. Phys.* **10** 12273–83
- Karagulian F, Dora C F C, Prüss-Ustün A M, Bonjour S, Adair-Rohani H and Amann M 2015 Contributions to cities' ambient particulate matter (PM): a systematic review of local source contributions at global level *Atmos. Environ.* **120** 475–83
- Karambelas A, Holloway T, Kiesewetter G and Heyes C 2018a Constraining the uncertainty in emissions over India with a regional air quality model evaluation *Atmos. Environ.* **174** 194–203
- Karambelas A, Holloway T, Kinney P L, Fiore A M, Fries R De, Kiesewetter G and Heyes C 2018b Urban versus rural health impacts attributable to PM_{2.5} and O₃ in northern India *Environ. Res. Lett.* **13** 064010
- Karki R, Hasson S ul, Gerlitz L, Talchabhadel R, Schenk E, Schickhoff U, Scholten T and Böhner J 2018 WRF-based simulation of an extreme precipitation event over the Central Himalayas: Atmospheric mechanisms and their representation by microphysics parameterization

schemes *Atmos. Res.* **214** 21–35

- Kaskaoutis D G, Kumar S, Sharma D, Singh R P, Kharol S K, Sharma M, Singh A K, Singh S, Singh A and Singh D 2014 Effects of crop residue burning on aerosol properties, plume characteristics, and long-range transport over northern India *J. Geophys. Res. Atmos.* **119** 5424–44
- Kaufman Y J, Tanré D and Boucher O 2002 A satellite view of aerosols in the Climate System *Nature* **419** 215–23
- Kedia S, Cherian R, Islam S, Das S K and Kaginalkar A 2016 Regional simulation of aerosol radiative effects and their influence on rainfall over India using WRFChem model *Atmos. Res.* **182** 232–42
- Kedia S, Ramachandran S, Holben B N and Tripathi S N 2014 Quantification of aerosol type, and sources of aerosols over the Indo-Gangetic Plain *Atmos. Environ.* **98** 607–19
- Kedia S, Vellore R K, Islam S and Kaginalkar A 2018 A study of Himalayan extreme rainfall events using WRF-Chem *Meteorol. Atmos. Phys.* 1–11
- Kelly F, Armstrong B, Atkinson R, Anderson H R, Barratt B, Beevers S, Cook D, Green D, Derwent D, Mudway I and Wilkinson P 2011 The London low emission zone baseline study *Heal. Eff. Institute, Res. Report. Boston, MA.* **163** 116
- Kelly F J and Fussell J C 2012 Size, source and chemical composition as determinants of toxicity attributable to ambient particulate matter *Atmos. Environ.* **60** 504–26
- Kharol S K, Badarinath K V S, Sharma A R, Kaskaoutis D G and Kambezidis H D 2011 Multiyear analysis of Terra/Aqua MODIS aerosol optical depth and ground observations over tropical urban region of Hyderabad, India *Atmos. Environ.* **45** 1532–42
- Kishore R 2017 India's poor are not using LPG cylinders they got under Ujjwala scheme *LiveMint* Online: <https://www.livemint.com/Politics/oqLQDFKNUmdbmLEVL88krN/Indias-poor-are-not-using-LPG-cylinders-they-got-under-Ujjw.html>
- Kleinman L, Lee Y, Springston S R, Nunnermacker L, Zhou X, Brown R, Hallock K, Klotz P, Leahy D, Lee J H and Newman L 1994 Ozone formation at a rural site in the southeastern United States *J. Geophys. Res.* **99** 3469–82
- Klimont Z, Kupiainen K, Heyes C, Purohit P, Cofala J, Rafaj P, Borken-Kleefeld J and Schöpp W 2017 Global anthropogenic emissions of particulate matter including black carbon *Atmos. Chem. Phys.* **17** 8681–723
- Knote C, Hodzic A and Jimenez J L 2015 The effect of dry and wet deposition of condensable vapors on secondary organic aerosols concentrations over the continental US *Atmos. Chem. Phys.* **15** 1–18
- Knote C, Hodzic A, Jimenez J L, Volkamer R, Orlando J J, Baidar S, Brioude J, Fast J, Gentner D R, Goldstein A H, Hayes P L, Knighton W B, Oetjen H, Setyan A, Stark H, Thalman R, Tyndall G, Washenfelder R, Waxman E and Zhang Q 2014 Simulation of semi-explicit mechanisms of SOA formation from glyoxal in aerosol in a 3-D model *Atmos. Chem. Phys.* **14** 6213–39
- Koch D and Del Genio A D 2010 Black carbon semi-direct effects on cloud cover: Review and synthesis *Atmos. Chem. Phys.* **10** 7685–96
- Kodros J K, Carter E, Brauer M, Volckens J, Bilsback K R, L'Orange C, Johnson M and Pierce J R 2018 Quantifying the Contribution to Uncertainty in Mortality Attributed to Household, Ambient, and Joint Exposure to PM_{2.5} From Residential Solid Fuel Use *GeoHealth* **2** 1–15
- Kodros J K, Scott C E, Farina S C, Lee Y H, L'Orange C, Volckens J and Pierce J R 2015 Uncertainties in global aerosols and climate effects due to biofuel emissions *Atmos. Chem. Phys.* **15** 8577–96
- Kodros J K, Wiedinmyer C, Ford B, Cucinotta R, Gan R, Magzamen S and Pierce J R 2016 Global

burden of mortalities due to chronic exposure to ambient PM_{2.5} from open combustion of domestic waste *Environ. Res. Lett.* **11** 1–9

- Kok J F 2011 A scaling theory for the size distribution of emitted dust aerosols suggests climate models underestimate the size of the global dust cycle *Proc. Natl. Acad. Sci.* **108** 1016–21
- Koo B, Wilson G M, Morris R E, Dunker A M and Yarwood G 2009 Comparison of Source Apportionment and Sensitivity Analysis in a Particulate Matter Air Quality Model *Environ. Sci. Technol.* **43** 6669–75
- Kota S H, Guo H, Myllyvirta L, Hu J, Sahu S K, Garaga R, Ying Q, Gao A, Dahiya S, Wang Y and Zhang H 2018 Year-long simulation of gaseous and particulate air pollutants in India *Atmos. Environ.* **180** 244–55
- Kottek M, Grieser J, Beck C, Rudolf B and Rubel F 2006 World map of the Köppen-Geiger climate classification updated *Meteorol. Zeitschrift* **15** 259–63
- Krewski D, Jerrett M, Burnett R T, Ma R, Hughes E, Shi Y, Turner M C, Pope 3rd C A, Thurston G, Calle E E, Thun M J, Beckerman B, DeLuca P, Finkelstein N, Ito K, Moore D K, Newbold K B, Ramsay T, Ross Z, Shin H and Tempalski B 2009 Extended follow-up and spatial analysis of the American Cancer Society study linking particulate air pollution and mortality *HEI Res. Report. Boston, MA* **140**
- Kulkarni S, Sobhani N, Miller-Schulze J P, Shafer M M, Schauer J J, Solomon P a., Saide P E, Spak S N, Cheng Y F, Denier van der Gon H a. C, Lu Z, Streets D G, Janssens-Maenhout G, Wiedinmyer C, Lantz J, Artamonova M, Chen B, Imashev S, Sverdlik L, Deminter J T, Adhikary B, D’Allura A, Wei C and Carmichael G R 2015 Source sector and region contributions to BC and PM_{2.5} in Central Asia *Atmos. Chem. Phys.* **15** 1683–705
- Kumar M, Singh R K, Murari V, Singh A K, Singh R S and Banerjee T 2016 Fireworks induced particle pollution: A spatio-temporal analysis *Atmos. Res.* **180** 78–91
- Kumar P, Khare M, Harrison R M, Bloss W J, Lewis A C, Coe H and Morawska L 2015a New Directions: Air pollution challenges for developing megacities like Delhi *Atmos. Environ.* **122** 657–661
- Kumar P, Kishtawal C M and Pal P K 2017 Impact of ECMWF, NCEP, and NCMRWF global model analysis on the WRF model forecast over Indian Region *Theor. Appl. Climatol.* **127** 143–51
- Kumar R, Barth M C, Madronich S, Naja M, Carmichael G R, Pfister G G, Knote C, Brasseur G P, Ojha N and Sarangi T 2014a Effects of dust aerosols on tropospheric chemistry during a typical pre-monsoon season dust storm in northern India *Atmos. Chem. Phys.* **14** 6813–34
- Kumar R, Barth M C, Nair V S, Pfister G G, Suresh Babu S, Satheesh S K, Krishna Moorthy K, Carmichael G R, Lu Z and Streets D G 2015b Sources of black carbon aerosols in South Asia and surrounding regions during the Integrated Campaign for Aerosols, Gases and Radiation Budget (ICARB) *Atmos. Chem. Phys.* **15** 5415–28
- Kumar R, Barth M C, Pfister G G, Monache L D, Lamarque J F, Archer-Nicholls S, Tilmes S, Ghude S D, Wiedinmyer C, Naja M and Walters S 2018 How will air quality change in South Asia by 2050? *J. Geophys. Res. Atmos.* **123** 1–25
- Kumar R, Barth M C, Pfister G G, Nair V S, Ghude S D and Ojha N 2015c What controls the seasonal cycle of black carbon aerosols in India? *J. Geophys. Res. Atmos.* **120** 7788–812
- Kumar R, Barth M C, Pfister G G, Naja M and Brasseur G P 2014b WRF-Chem simulations of a typical pre-monsoon dust storm in northern India: Influences on aerosol optical properties and radiation budget *Atmos. Chem. Phys.* **14** 2431–46
- Kumar R, Naja M, Pfister G G, Barth M C and Brasseur G P 2012a Simulations over South Asia using the Weather Research and Forecasting model with Chemistry (WRF-Chem): Set-up and meteorological evaluation *Geosci. Model Dev.* **5** 321–43

- Kumar R, Naja M, Pfister G G, Barth M C, Wiedinmyer C and Brasseur G P 2012b Simulations over South Asia using the Weather Research and Forecasting model with Chemistry (WRF-Chem): chemistry evaluation and initial results *Geosci. Model Dev.* **5** 321–43
- Kumar R, Naja M, Venkataramani S and Wild O 2010a Variations in surface ozone at Nainital: A high-altitude site in the central Himalayas *J. Geophys. Res. Atmos.* **115** 1–12
- Kumar R, Sharma S K, Thakur J S, Lakshmi P V M, Sharma M K and Singh T 2010b Association of air pollution and mortality in the ludhiana city of India: A time-series study *Indian J. Public Health* **54** 98–103
- Kumar S and Sunder Raman R 2016 Inorganic ions in ambient fine particles over a National Park in central India: Seasonality, dependencies between SO₄²⁻, NO₃⁻, and NH₄⁺, and neutralization of aerosol acidity *Atmos. Environ.* **143** 152–63
- Kurokawa J, Ohara T, Morikawa T, Hanayama S, Janssens-Maenhout G, Fukui T, Kawashima K and Akimoto H 2013 Emissions of air pollutants and greenhouse gases over Asian regions during 2000–2008: Regional Emission inventory in ASia (REAS) version 2 *Atmos. Chem. Phys.* **13** 11019–58
- Kushta J, Pozzer A and Lelieveld J 2018 Uncertainties in estimates of mortality attributable to ambient PM_{2.5} in Europe. *Environ. Res. Lett.* **13** 064029
- L'Orange C, DeFoort M and Willson B 2012 Influence of testing parameters on biomass stove performance and development of an improved testing protocol *Energy Sustain. Dev.* **16** 3–12
- L'Orange C, Leith D, Volckens J and DeFoort M 2015 A quantitative model of cookstove variability and field performance: Implications for sample size *Biomass and Bioenergy* **72** 233–41
- Lal S, Naja M and Subbaraya B H 2000 Seasonal variations in surface ozone and its precursors over an urban site in India *Atmos. Environ.* **34** 2713–24
- Lal S, Sahu L K, Venkataramani S, Rajesh T A and Modh K S 2008 Distributions of O₃, CO and NMHCs over the rural sites in central India *J. Atmos. Chem.* **61** 73–84
- Lam N L, Chen Y, Weyant C, Venkataraman C, Sadavarte P, Johnson M a, Smith K R, Brem B T, Arineitwe J, Ellis J E and Bond T C 2012 Household light makes global heat: high black carbon emissions from kerosene wick lamps *Environ. Sci. Technol.* **46** 13531–8
- Landrigan P J, Fuller R, Acosta N J R, Adeyi O, Arnold R, Basu N (Nil), Baldé A B, Bertollini R, Bose-O'Reilly S, Boufford J I, Breyse P N, Chiles T, Mahidol C, Coll-Seck A M, Cropper M L, Fobil J, Fuster V, Greenstone M, Haines A, Hanrahan D, Hunter D, Khare M, Krupnick A, Lanphear B, Lohani B, Martin K, Mathiasen K V, McTeer M A, Murray C J L, Ndahimananjara J D, Perera F, Potočnik J, Preker A S, Ramesh J, Rockström J, Salinas C, Samson L D, Sandilya K, Sly P D, Smith K R, Steiner A, Stewart R B, Suk W A, van Schayck O C P, Yadama G N, Yumkella K and Zhong M 2017 The Lancet Commission on pollution and health *Lancet* **6736**
- Laprise R 1992 The Euler Equations of Motion with Hydrostatic Pressure as an Independent Variable *Mon. Weather Rev.* **120** 197–207
- Lau K M, Ramanathan V, Wu G X, Li Z, Tsay S C, Hsu C, Sikka R, Holben B, Lu D, Tartari G, Chin M, Koudelova P, Chen H, Ma Y, Huang J, Taniguchi K and Zhang R 2008 The joint aerosol-monsoon experiment: A new challenge for monsoon climate research *Bull. Am. Meteorol. Soc.* **89** 369–83
- Lawrence M G and Lelieveld J 2010 Atmospheric pollutant outflow from southern Asia: A review *Atmos. Chem. Phys.* **10** 11017–96
- Lee C J, Martin R V., Henze D K, Brauer M, Cohen A and Donkelaar A Van 2015 Response of global particulate-matter-related mortality to changes in local precursor emissions *Environ. Sci. Technol.* **49** 4335–44

- Legrand S L, Polashenski C, Letcher T W, Creighton G A, Peckham E and Cetola J D 2018 The AFWA Dust Emissions Scheme for the GOCART Aerosol Model in WRF-Chem *Geosci. Model Dev. Discuss.* 1–57
- Lelieveld J 2017 Clean air in the Anthropocene *Faraday Discuss.* **200** 693–703
- Lelieveld J, Barlas C, Giannadaki D and Pozzer A 2013 Model calculated global, regional and megacity premature mortality due to air pollution *Atmos. Chem. Phys.* **13** 7023–37
- Lelieveld J, Evans J S, Fnais M, Giannadaki D and Pozzer A 2015 The contribution of outdoor air pollution sources to premature mortality on a global scale *Nature* **525** 367–71
- Lelieveld J, Haines A and Pozzer A 2018 Age-dependent health risk from ambient air pollution: a modelling and data analysis of childhood mortality in middle-income and low-income countries *Lancet Planet. Heal.* **2** e292–300
- Leon J-F, Chazette P, Dulac F, Pelon J, Flamant C, Bonazzola M, Foret G, Alfaro S C, Cachier H, Cautenet S, Hamonou E, Gaudichet A, Gomes L, Rajot J-L, Lavenu F, Inamdar R, Sarode P R and Kadadevarmath J S 2001 Large-scale advection of continental aerosols during INDOEX *J. Geophys. Res.* **106** 28427–39
- Levy J I, Diez D, Dou Y, Barr C D and Dominici F 2012 A meta-analysis and multisite time-series analysis of the differential toxicity of major fine particulate matter constituents *Am. J. Epidemiol.* **175** 1091–9
- Levy R C, Leptoukh G G, Kahn R, Zubko V, Gopalan A and Remer L A 2009 A Critical Look at Deriving Monthly Aerosol Optical Depth From Satellite Data *IEEE Trans. Geosci. Remote Sens.* **47** 2942–56
- Levy R C, Mattoo S, Munchak L A, Remer L A, Sayer A M, Patadia F and Hsu N C 2013 The Collection 6 MODIS aerosol products over land and ocean *Atmos. Meas. Tech.* **6** 2989–3034
- Levy R C, Remer L A, Kleidman R G, Mattoo S, Ichoku C, Kahn R and Eck T F 2010 Global evaluation of the Collection 5 MODIS dark-target aerosol products over land *Atmos. Chem. Phys.* **10** 10399–420
- Lewis J J, Hollingsworth J W, Chartier R T, Cooper E M, Foster W M, Gomes G L, Kussin P S, MacInnis J J, Padhi B K, Panigrahi P, Rodes C E, Ryde I T, Singha A K, Stapleton H M, Thornburg J, Young C J, Meyer J N and Pattanayak S K 2017 Biogas Stoves Reduce Firewood Use, Household Air Pollution, and Hospital Visits in Odisha, India *Environ. Sci. Technol.* **51** 560–9
- Li K, Liao H, Mao Y and Ridley D A 2016a Source sector and region contributions to concentration and direct radiative forcing of black carbon in China *Atmos. Environ.* **124** 351–66
- Li M H, Fan L C, Mao B, Yang J W, Choi A M K, Cao W J and Xu J F 2016b Short-term exposure to ambient fine particulate matter increases hospitalizations and mortality in COPD: A systematic review and meta-analysis *Chest* **149** 447–58
- Li M, Wang T, Han Y, Xie M, Li S, Zhuang B and Chen P 2017a Modeling of a severe dust event and its impacts on ozone photochemistry over the downstream Nanjing megacity of eastern China *Atmos. Environ.* **160** 107–23
- Li M, Zhang Q, Kurokawa J, Woo J-H, He K, Lu Z, Ohara T, Song Y, Streets D G, Carmichael G R, Cheng Y, Hong C, Huo H, Jiang X, Kang S, Liu F, Su H and Zheng B 2017b MIX: a mosaic Asian anthropogenic emission inventory under the international collaboration framework of the MICS-Asia and HTAP *Atmos. Chem. Phys.* **17** 935–63
- Li X, Wang S, Duan L, Hao J and Nie Y 2009 Carbonaceous aerosol emissions from household biofuel combustion in China *Environ. Sci. Technol.* **43** 6076–81
- Li Y, Henze D K, Jack D and Kinney P L 2016c The influence of air quality model resolution on health impact assessment for fine particulate matter and its components *Air Qual. Atmos.*

- Li Z, Zang Z, Li Q B, Chao Y, Chen D, Ye Z, Liu Y and Liou K N 2013 A three-dimensional variational data assimilation system for multiple aerosol species with WRF/Chem and an application to PM_{2.5} prediction *Atmos. Chem. Phys.* **13** 4265–78
- Liang J and Jacobson M Z 2000 Effects of subgrid segregation on ozone production efficiency in a chemical model *Atmos. Environ.* **34** 2975–82
- Liu J, Mauzerall D L and Horowitz L W 2009 Evaluating inter-continental transport of fine aerosols:(2) Global health impact *Atmos. Environ.* **43** 4339–47
- Liu T, Marlier M E, DeFries R S, Westervelt D M, Xia K R, Fiore A M, Mickley L J, Cusworth D H and Milly G 2018 Seasonal impact of regional outdoor biomass burning on air pollution in three Indian cities: Delhi, Bengaluru, and Pune *Atmos. Environ.* **172** 83–92
- Liu X, Mizzi A P, Anderson J L, Fung I Y and Cohen R C 2017 Assimilation of satellite NO₂ observations at high spatial resolution using OSSEs *Atmos. Chem. Phys.* **17** 7067–81
- Liu Y, Bourgeois A, Warner T, Swerdlin S and Hacker J 2005 Implementation of observation-nudging based on FDDA into WRF for supporting AFEC test operations *WRF Users Work.*
- Liu Y, Bourgeois A, Warner T, Swerdlin S and Yu W 2006 An update on “observation nudging”-based FDDA for WRF-ARW: Verification using OSSE and performance of real-time forecasts *WRF Users Work.*
- Liu Z, Liu Q, Lin H C, Schwartz C S, Lee Y H and Wang T 2011 Three-dimensional variational assimilation of MODIS aerosol optical depth: Implementation and application to a dust storm over East Asia *J. Geophys. Res.* **116** 1–19
- Lodhi N K, Beegum S N, Singh S and Kumar K 2013 Aerosol climatology at Delhi in the western Indo-Gangetic Plain: Microphysics, long-term trends, and source strengths *J. Geophys. Res. Atmos.* **118** 1361–75
- Lohmann U and Feichter J 2005 Global indirect aerosol effects: a review *Atmos. Chem. Phys.* **5** 715–37
- Loomis D, Grosse Y, Lauby-Secretan B, Ghissassi F El, Bouvard V, Benbrahim-Tallaa L, Guha N, Baan R, Mattock H, Straif K and International Agency for Research on Cancer Monograph Working Group IARC 2013 The carcinogenicity of outdoor air pollution *Lancet Oncol.* **14** 1262–3
- Lopez A D, Mathers C D, Ezzati M, Jamison D T and Murray C J L 2006 *Global Burden of Disease and Risk Factors* ed Disease Control Priorities Project (The World Bank and Oxford University Press)
- Lu X, Zhang L, Liu X, Gao M, Zhao Y and Shao J 2018 Lower tropospheric ozone over India and its linkage to the South Asian monsoon *Atmos. Chem. Phys.* **18** 3101–18
- Lu Z and Streets D G 2012 Increase in NO_x Emissions from Indian Thermal Power Plants during 1996–2010: Unit-Based Inventories and Multisatellite Observations *Environ. Sci. Technol.* **46** 7463–70
- Lu Z, Zhang Q and Streets D G 2011 Sulfur dioxide and primary carbonaceous aerosol emissions in China and India, 1996–2010 *Atmos. Chem. Phys.* **11** 9839–64
- Madala S, Satyanarayana A N V and Rao T N 2014 Performance evaluation of PBL and cumulus parameterization schemes of WRF ARW model in simulating severe thunderstorm events over Gadanki MST radar facility - Case study *Atmos. Res.* **139** 1–17
- Madronich S and Weller G 1990 Numerical integration errors in calculated tropospheric photodissociation rate coefficients *J. Atmos. Chem.* **10** 289–300
- Mahajan A S, De Smedt I, Biswas M S, Ghude S, Fadnavis S, Roy C and van Roozendaal M 2015 Inter-annual variations in satellite observations of nitrogen dioxide and formaldehyde over

India *Atmos. Environ.* **116** 194–201

- Mahapatra P S, Panda S, Walvekar P P, Kumar R, Das T and Gurjar B R 2014 Seasonal trends, meteorological impacts, and associated health risks with atmospheric concentrations of gaseous pollutants at an Indian coastal city *Environ. Sci. Pollut. Res.* **21** 11418–32
- Maji S, Ahmed S, Siddiqui W A and Ghosh S 2017 Short term effects of criteria air pollutants on daily mortality in Delhi, India *Atmos. Environ.* **150** 210–9
- Maji S, Ghosh S and Ahmed S 2018 Association of air quality with respiratory and cardiovascular morbidity rate in Delhi, India *Int. J. Environ. Health Res.* **00** 1–20
- Malley C S, Henze D K, Kuylenstierna J C I, Vallack H W, Davila Y, Anenberg S C, Turner M C and Ashmore M R 2017 Updated Global Estimates of Respiratory Mortality in Adults ≥ 30 Years of Age Attributable to Long-Term Ozone Exposure *Environ. Health Perspect.* **125** 1–9
- Mallik C, Lal S and Venkataramani S 2015 Trace gases at a semi-arid urban site in western India: Variability and inter-correlations *J. Atmos. Chem.* **72** 143–64
- Marrapu P, Cheng Y, Beig G, Sahu S, Srinivas R and Carmichael G R 2014 Air quality in Delhi during the Commonwealth Games *Atmos. Chem. Phys.* **14** 10619–30
- Martcorena B and Bergametti G 1995 Modeling the atmospheric dust cycle: 1. Design of a soil-derived dust emission scheme *J. Geophys. Res.* **100** 16415–30
- Martin W J, Glass R I, Araj H, Balbus J, Collins F S, Curtis S, Diette G B, Elwood W N, Falk H, Hibberd P L, Keown S E J, Mehta S, Patrick E, Rosenbaum J, Sapkota A, Tolunay H E and Bruce N G 2013 Household air pollution in low- and middle-income countries: health risks and research priorities *PLoS Med.* **10** e1001455
- Martinsson J, Eriksson A C, Nielsen I E, Malmberg V B, Ahlberg E, Andersen C, Lindgren R, Nyström R, Nordin E Z, Brune W H, Svenningsson B, Swietlicki E, Boman C and Pagels J H 2015 Impacts of Combustion Conditions and Photochemical Processing on the Light Absorption of Biomass Combustion Aerosol *Environ. Sci. Technol.* **49** 14663–71
- Masera O, Edwards R, Arnez C A, Berrueta V, Johnson M, Bracho L R, Riojas-Rodríguez H and Smith K R 2007 Impact of Patsari improved cookstoves on indoor air quality in Michoacán, Mexico *Energy Sustain. Dev.* **11** 45–56
- Masera O R, Saatkamp B D and Kammen D M 2000 From linear fuel switching to multiple cooking strategies: A critique and alternative to the energy ladder model *World Dev.* **28** 2083–103
- Matawle J L, Pervez S, Shrivastava A, Tiwari S, Pant P, Deb M K, Bisht D S and Pervez Y F 2017 PM_{2.5} pollution from household solid fuel burning practices in central India: 1. Impact on indoor air quality and associated health risks *Environ. Geochem. Health* **39** 1045–1058
- Maynard A D and Maynard R L 2002 A derived association between ambient aerosol surface area and excess mortality using historic time series data *Atmos. Environ.* **36** 5561–7
- McGranahan G and Murray F 2003 *Air Pollution and Health in Developing Countries* vol 41, ed Stockholm Environment Institute (London, Sterling VA: Earthscan Publications Ltd)
- Mertens M, Grewe V, Rieger V S and Jöckel P 2018 Revisiting the contribution of land transport and shipping emissions to tropospheric ozone *Atmos. Chem. Phys.* **18** 5567–88
- Ministry of Environment and Forests 2018 Continuous Ambient Air Quality Monitoring (CAAQM). Central Pollution Control Board (CPCB). Government of India. *Gov. India* Online: <http://www.cpcb.gov.in/CAAQM/>
- Ministry of Environment and Forests 2013 *Guidelines for Manual Sampling & Analyses. National Ambient Air Quality Standards (NAAQS) Guidelines for the Measurement of Ambient Air Pollutants - Volume II*

- Ministry of Environment and Forests 2009 *National Ambient Air Quality Standards*
- Ministry of Environment Forests and Climate Change 2015a *Environment (Protection) Amendment Rules*
- Ministry of Environment Forests and Climate Change 2018 National Clean Air Programme (NCAP) India Gov. India Online: http://www.moef.gov.in/sites/default/files/NCAP_with_annex-ilovepdf-compressed.pdf
- Ministry of Environment Forests and Climate Change 2015b Press Information Bureau: Environment Ministry Notifies Stricter Standards for Coal Based Thermal Power Plants to Minimise Pollution Gov. India Online: <http://pib.nic.in/newsite/PrintRelease.aspx?relid=133726>
- Ministry of Finance 2016 Union Budget 2016–2017 Gov. India
- Ministry of Health and Family Welfare 2015a Report of the Steering Committee on Air Pollution and Health-Related Issues. Gov. India **New Delhi**
- Ministry of Health and Family Welfare 2015b *Report of the Steering Committee on Air Pollution and Health Related Issues*
- Ministry of New and Renewable Energy 2010 *National Solar Mission: Jawaharlal Nehru National Solar Mission. Towards Building SOLAR INDIA.*
- Ministry of Petroleum and Natural Gas 2018a Pradhan Mantri Ujjwala Yojana (PMUY). Government of India. Gov. India Online: <http://www.pmujjwalayojana.com/>
- Ministry of Petroleum and Natural Gas 2018b Pradhan Mantri Ujjwala Yojana achieves 5 core mark *Press Inf. Bur. Gov. India* Online: pib.nic.in/Pressreleaseshare.aspx?PRID=1541545
- Ministry of Petroleum and Natural Gas 2018c Pratyaksh Hanstantrit Labh (PAHAL) - Direct Benefits Transfer for LPG (DBTL) Consumers Scheme. Government of India. Gov. India Online: <http://petroleum.nic.in/dbt/index.php>
- Ministry of Power 2015 Press Information Bureau: Energy Efficient Norms For Power Plants Gov. India Online: <http://pib.nic.in/newsite/PrintRelease.aspx?relid=117384>
- Ministry of Road Transport and Highways 2016a *Central Motor Vehicles (Amendment) Rules*
- Ministry of Road Transport and Highways 2016b Press Information Bureau: Government decides to directly shift from BS-IV to BS-VI Emission norms Gov. India Online: <http://pib.nic.in/newsite/PrintRelease.aspx?relid=134232>
- Ministry of Statistics and Programme Implementation 2016 *Life expectancy at birth - 2014*
- Mishra A K and Shibata T 2012 Synergistic analyses of optical and microphysical properties of agricultural crop residue burning aerosols over the Indo-Gangetic Basin (IGB) *Atmos. Environ.* **57** 205–18
- Mittal N, Mukherjee A and Gelb A 2017 *Fuel Subsidy Reform in Developing Countries: Direct Benefit Transfer of LPG Cooking Gas Subsidy in India*
- Mittal S, Hanaoka T, Shukla P R and Masui T 2015 Air pollution co-benefits of low carbon policies in road transport: A sub-national assessment for India *Environ. Res. Lett.* **10** 1–10
- Mittal S K, Singh N, Agarwal R, Awasthi A and Gupta P K 2009 Ambient air quality during wheat and rice crop stubble burning episodes in Patiala *Atmos. Environ.* **43** 238–44
- Mizzi A P, Arellano A F, Edwards D P, Anderson J L and Pfister G G 2016 Assimilating compact phase space retrievals of atmospheric composition with WRF-Chem/DART: A regional chemical transport/ensemble Kalman filter data assimilation system *Geosci. Model Dev.* **9** 965–78
- Mlawer E J, Taubman S J, Brown P D, Iacono M J and Clough S A 1997 Radiative transfer for inhomogeneous atmospheres: RRTM, a validated correlated-k model for the longwave *J.*

- Mohan M and Bhati S 2011 Analysis of WRF Model Performance over Subtropical Region of Delhi, India *Adv. Meteorol.* **2011** 1–13
- Mohan M and Gupta M 2018 Sensitivity of PBL parameterizations on PM10 and ozone simulation using chemical transport model WRF-Chem over a sub-tropical urban airshed in India *Atmos. Environ.* **185** 53–63
- Monks P S, Archibald A T, Colette A, Cooper O, Coyle M, Derwent R, Fowler D, Granier C, Law K S, Mills G E, Stevenson D S, Tarasova O, Thouret V, von Schneidmesser E, Sommariva R, Wild O and Williams M L 2015 Tropospheric ozone and its precursors from the urban to the global scale from air quality to short-lived climate forcer *Atmos. Chem. Phys.* **15** 8889–973
- Moolgavkar S H 2016 Fine Particulate Matter Pollution and Mortality *Risk Anal.* **36** 1766–9
- Moorthy K K 2016 South Asian aerosols in perspective: Preface to the special issue *Atmos. Environ.* **125** 307–11
- Moorthy K K, Babu S, Manoj M R and Satheesh S K 2013a Buildup of aerosols over the Indian Region *Geophys. Res. Lett.* **40** 1011–4
- Moorthy K K, Beegum S N, Srivastava N, Satheesh S K, Chin M, Blond N, Babu S S and Singh S 2013b Performance evaluation of chemistry transport models over India *Atmos. Environ.* **71** 210–25
- Moorthy K K, Saha A, Prasad B S N, Niranjana K, Jhurry D and Pillai P S 2001 Aerosol optical depths over peninsular India and adjoining oceans during the INDOEX campaigns: Spatial, temporal, and spectral characteristics *J. Geophys. Res.* **106** 28539–54
- Moorthy K K, Sunilkumar S V., Pillai P S, Parameswaran K, Nair P R, Ahmed Y N, Ramgopal K, Narasimhulu K, Reddy R R, Vinoj V, Satheesh S K, Niranjana K, Rao B M, Brahmanandam P S, Saha A, Badarinath K V S, Kiranchand T R and Latha K M 2005 Wintertime spatial characteristics of boundary layer aerosols over peninsular India *J. Geophys. Res. Atmos.* **110** 1–11
- Mortimer K, Ndamala C B, Naunje A W, Malava J, Katundu C, Weston W, Havens D, Pope D, Bruce N G, Nyirenda M, Wang D, Crampin A, Grigg J, Balmes J and Gordon S B 2017 A cleaner burning biomass-fuelled cookstove intervention to prevent pneumonia in children under 5 years old in rural Malawi (the Cooking and Pneumonia Study): a cluster randomised controlled trial *Lancet* **389** 167–75
- Mukhopadhyay P, Taraphdar S, Goswami B N and Krishnakumar K 2010 Indian Summer Monsoon Precipitation Climatology in a High-Resolution Regional Climate Model: Impacts of Convective Parameterization on Systematic Biases *Weather Forecast.* **25** 369–87
- Muralidharan V, Sussan T E, Limaye S, Koehler K, Williams D L, Rule A M, Juvekar S, Breyse P N, Salvi S and Biswal S 2015 Field testing of alternative cookstove performance in a rural setting of Western India *Int. J. Environ. Res. Public Health* **12** 1773–87
- Murray C J L, Ezzati M, Flaxman A D, Lim S, Lozano R, Michaud C, Naghavi M, Salomon J A, Shibuya K, Vos T, Wikler D and Lopez A D 2012 GBD 2010: Design, definitions, and metrics *Lancet* **380** 2063–6
- Mwampamba T H 2007 Has the woodfuel crisis returned? Urban charcoal consumption in Tanzania and its implications to present and future forest availability *Energy Policy* **35** 4221–34
- Naeher L P, Brauer M, Lipsett M, Zelikoff J T, Simpson C D, Koenig J Q and Smith K R 2007 Woodsmoke health effects: a review. *Inhal. Toxicol.* **19** 67–106
- Nagpure A S, Gurjar B R and Martel C J 2014 Human health risks in national capital territory of Delhi due to air pollution *Atmos. Pollut. Res.* **5** 371–80

- Nain Gill G 2010 A green tribunal for India *J. Environ. Law* **22** 461–74
- Nair V S, Moorthy K K, Alappattu D P, Kunhikrishnan P K, George S, Nair P R, Babu S S, Abish B, Satheesh S K, Tripathi S N, Niranjana K, Madhavan B L, Srikant V, Dutt C B S, Badarinath K V S and Reddy R R 2007 Wintertime aerosol characteristics over the Indo-Gangetic Plain (IGP): Impacts of local boundary layer processes and long-range transport *J. Geophys. Res. Atmos.* **112** 1–15
- Naja M and Lal S 2002 Surface ozone and precursor gases at Gadanki (13.5°N, 79.2°E), a tropical rural site in India *J. Geophys. Res. Atmos.* **107**
- Naja M, Lal S and Chand D 2003 Diurnal and seasonal variabilities in surface ozone at a high altitude site Mt Abu (24.6°N, 72.7°E, 1680 m asl) in India *Atmos. Environ.* **37** 4205–15
- Nakanishi M and Niino H 2006 An improved Mellor-Yamada Level-3 model: Its numerical stability and application to a regional prediction of advection fog *Boundary-Layer Meteorol.* **119** 397–407
- Nasir U P and Brahmaiah D 2015 Impact of fireworks on ambient air quality: a case study *Int. J. Environ. Sci. Technol.* **12** 1379–86
- National Center for Atmospheric Research 2016 ACOM MOZART-4/GEOS-5 global model output UCAR
- National Centers for Environmental Prediction, National Weather Service, National Oceanic and Atmospheric Administration and U.S. Department of Commerce 2000 NCEP Final (FNL) Operational Model Global Tropospheric Analyses, continuing from July 1999. Research Data Archive at the National Center for Atmospheric Research, Computational and Information Systems Laboratory.
- National Centers for Environmental Prediction, National Weather Service, National Oceanic and Atmospheric Administration and U.S. Department of Commerce 2007 NCEP Global Forecast System (GFS) Analyses and Forecasts. Research Data Archive at the National Center for Atmospheric Research, Computational and Information Systems Laboratory.
- National Institution for Transforming India 2015 India Energy Security Scenarios (IESS) 2047 *Gov. India* Online: <http://indiaenergy.gov.in/>
- National Institution for Transforming India 2017 *Three-year action agenda, 2017–18 to 2019–20*
- National Transport Development Policy Committee 2014 *India Transport Report: Moving India to 2032* vol I (New Delhi, India)
- Neu J L and Prather M J 2012 Toward a more physical representation of precipitation scavenging in global chemistry models: Cloud overlap and ice physics and their impact on tropospheric ozone *Atmos. Chem. Phys.* **12** 3289–310
- Newby D E, Mannucci P M, Tell G S, Baccarelli A A, Brook R D, Donaldson K, Forastiere F, Franchini M, Franco O H, Graham I, Hoek G, Hoffmann B, Hoylaerts M F, Künzli N, Mills N, Pekkanen J, Peters A, Piepoli M F, Rajagopalan S and Storey R F 2015 Expert position paper on air pollution and cardiovascular disease *Eur. Heart J.* **36** 83–93
- Nidhi J G 2008 Air pollution and associated respiratory morbidity in Delhi *Health Care Manag. Sci.* **11** 132–8
- Nishanth T, Satheesh Kumar M K and Valsaraj K T 2012 Variations in surface ozone and NO_x at Kannur: a tropical, coastal site in India *J. Atmos. Chem.* **69** 101–26
- Oberdörster G, Oberdörster E and Oberdörster J 2005 Nanotoxicology: An Emerging Discipline Evolving from Studies of Ultrafine Particles *Environ. Health Perspect.* **113** 823–39
- Odum J R, Jungkamp T P W, Griffin R J, Forstner H J L, Flagan R C and Seinfeld J H 1997 Aromatics, reformulated gasoline, and atmospheric organic aerosol formation *Environ. Sci. Technol.* **31** 1890–7

- Odum Jay R, Hoffmann T, Bowman F, Collins D, Flagan Richard C and Seinfeld John H 1996 Gas particle partitioning and secondary organic aerosol yields *Environ. Sci. Technol.* **30** 2580–5
- Ojha N, Naja M, Singh K P, Sarangi T, Kumar R, Lal S, Lawrence M G, Butler T M and Chandola H C 2012 Variabilities in ozone at a semi-urban site in the Indo-Gangetic Plain region: Association with the meteorology and regional processes *J. Geophys. Res. Atmos.* **117** 1–19
- Ojha N, Pozzer A, Rauthe-Schöch A, Baker A K, Yoon J, Brenninkmeijer C A M and Lelieveld J 2016 Ozone and carbon monoxide over India during the summer monsoon: Regional emissions and transport *Atmos. Chem. Phys.* **16** 3013–32
- Ostro B D and Chestnut L G 1999 Letters to the Editor *Int. Epidemiol. Assoc.* **28** 990–2
- Ostro B, Spadaro J V., Gumy S, Mudu P, Awe Y, Forastiere F and Peters A 2018 Assessing the recent estimates of the global burden of disease for ambient air pollution: Methodological changes and implications for low- and middle-income countries *Environ. Res.* 1–13
- Pachauri S, van Ruijven B J, Nagai Y, Riahi K, van Vuuren D P, Brew-Hammond A and Nakicenovic N 2013 Pathways to achieve universal household access to modern energy by 2030 *Environ. Res. Lett.* **8** 8
- Pagowski M and Grell G A 2012 Experiments with the assimilation of fine aerosols using an ensemble Kalman filter *J. Geophys. Res.* **117** 1–15
- Pal R, Mahima G, Singh C, Tripathi A and Singh R 2014 The effects of fireworks on ambient air and possible impact on cardiac health, during Deepawali festival in north India *World Heart J.* **5** 21–32
- Paliwal U, Sharma M and Burkhart J F 2016 Monthly and Spatially Resolved Black Carbon Emission Inventory of India: Uncertainty Analyses *Atmos. Chem. Phys.* **16** 12457–76
- Palmer T and Williams P 2010 *Stochastic Physics and Climate Modelling* (Cambridge University Press)
- Pan X, Chin M, Gautam R, Bian H, Kim D, Colarco P R, Diehl T L, Takemura T, Pozzoli L, Tsigaridis K, Bauer S and Bellouin N 2015 A multi-model evaluation of aerosols over South Asia: common problems and possible causes *Atmos. Chem. Phys.* **15** 5903–28
- Panda J and Sharan M 2012 Influence of land-surface and turbulent parameterization schemes on regional-scale boundary layer characteristics over northern India *Atmos. Res.* **112** 89–111
- Pande P, Dey S, Chowdhury S, Choudhary P, Ghosh S, Srivastava P and Sengupta B 2018 Seasonal transition in PM10 exposure and associated all-cause mortality risks in India *Environ. Sci. Technol.* **52** 8756–63
- Pandey A, Sadavarte P, Rao A B and Venkataraman C 2014 Trends in multi-pollutant emissions from a technology-linked inventory for India: II. Residential, agricultural and informal industry sectors *Atmos. Environ.* **99** 341–52
- Pandey A and Venkataraman C 2014 Estimating emissions from the Indian transport sector with on-road fleet composition and traffic volume *Atmos. Environ.* **98** 123–33
- Pandey K 2000 Ambient particulate matter concentrations in residential areas of world cities: new estimates based on global model of ambient particulates (GMAPS) *Dev. Res. Gr. Environ. Dep. World Bank, Washington, DC*
- Pang X, Mu Y, Lee X, Zhang Y and Xu Z 2009 Influences of characteristic meteorological conditions on atmospheric carbonyls in Beijing, China *Atmos. Res.* **93** 913–9
- Pant P, Guttikunda S K and Peltier R E 2016 Exposure to particulate matter in India: A synthesis of findings and future directions *Environ. Res.* **147** 480–96
- Pant P and Harrison R M 2012 Critical review of receptor modelling for particulate matter: A case study of India *Atmos. Environ.* **49** 1–12

- Pant P, Lal R M, Guttikunda S K, Russell A G, Nagpure A S, Ramaswami A and Peltier R E 2018 Monitoring particulate matter in India: recent trends and future outlook *Air Qual. Atmos. Heal.*
- Pant P, Shukla A, Kohl S D, Chow J C, Watson J G and Harrison R M 2015 Characterization of ambient PM_{2.5} at a pollution hotspot in New Delhi, India and inference of sources *Atmos. Environ.* **109** 178–89
- Patange O S, Ramanathan N, Rehman I H, Tripathi S N, Misra A, Kar A, Graham E, Singh L, Bahadur R and Ramanathan V 2015 Reductions in indoor black carbon concentrations from improved biomass stoves in rural India *Environ. Sci. Technol.* **49** 4749–56
- Pattenden S, Armstrong B, Milojevic A, Heal M R, Chalabi Z, Doherty R, Barratt B, Kovats R S and Wilkinson P 2010 Ozone, heat and mortality: Acute effects in 15 British conurbations *Occup. Environ. Med.* **67** 699–707
- Peel J L, Klein M, Flanders W D, Mulholland J A and Tolbert P E 2010 Impact of improved air quality during the 1996 Summer Olympic Games in Atlanta on multiple cardiovascular and respiratory outcomes *Heal. Eff. Institute, Res. Report. Boston, MA.* **148** 56
- Peng Z, Liu Z, Chen D and Ban J 2017 Improving PM_{2.5} forecast over China by the joint adjustment of initial conditions and source emissions with an ensemble Kalman filter *Atmos. Chem. Phys.* **17** 4837–55
- Pillarisetti A, Vaswani M, Jack D, Balakrishnan K, Bates M N, Arora N K and Smith K R 2014 Patterns of stove usage after introduction of an advanced cookstove: the long-term application of household sensors. *Environ. Sci. Technol.* **48** 14525–33
- Pincus R, Barker H W and Morcrette J-J 2003 A fast, flexible, approximate technique for computing radiative transfer in inhomogeneous cloud fields *J. Geophys. Res.* **108** 1–5
- Pine K, Edwards R, Masera O, Schilman A, Marren-Mares A and Riojas-Rodriguez H 2011 Adoption and use of improved biomass stoves in Rural Mexico *Energy Sustain. Dev.* **15** 176–83
- Pommier M, Fagerli H, Gauss M, Simpson D, Sharma S, Sinha V, Ghude S D, Landgren O, Nyiri A and Wind P 2018 Impact of regional climate change and future emission scenarios on surface O₃ and PM_{2.5} over India *Atmos. Chem. Phys.* **18** 103–27
- Pope D, Bruce N, Dherani M, Jagoe K and Rehfuess E 2017 Real-life effectiveness of ‘improved’ stoves and clean fuels in reducing PM_{2.5} and CO: Systematic review and meta-analysis *Environ. Int.* **101** 7–18
- Pope III C A 2007 Mortality effects of longer term exposures to fine particulate air pollution: review of recent epidemiological evidence *Inhal. Toxicol.* **19** 33–8
- Pope III C A, Burnett R T, Krewski D, Jerrett M, Shi Y, Calle E E and Thun M J 2009 Cardiovascular mortality and exposure to airborne fine particulate matter and cigarette smoke: Shape of the exposure-response relationship *Circulation* **120** 941–8
- Pope III C A, Burnett R T, Turner M C, Cohen A, Krewski D, Jerrett M, Gapstur S M and Thun M J 2011 Lung Cancer and Cardiovascular Disease Mortality Associated with Ambient Air Pollution and Cigarette Smoke: Shape of the Exposure – Response Relationships *Environ. Health Perspect.* **119** 1616–21
- Pope III C A, Cohen A J and Burnett R T 2018 Cardiovascular Disease and Fine Particulate Matter. Lessons and Limitations of an Integrated Exposure–Response Approach *Circ. Res.* **122** 1645–7
- Pope III C A, Cropper M, Coggins J and Cohen A 2015 Health Benefits of Air Pollution Abatement Policy: Role of the Shape of the Concentration-Response Function *J. Air Waste Manage. Assoc.* **65** 516–22
- Pope III C A and Dockery D W 2006 Health Effects of Fine Particulate Air Pollution: Lines that

Connect *J. Air Waste Manage. Assoc.* **56** 709–42

- Post E S, Grambsch A, Weaver C, Morefield P, Huang J, Leung L Y, Nolte C G, Adams P, Liang X Z, Zhu J H and Mahoney H 2012 Variation in estimated ozone-related health impacts of climate change due to modeling choices and assumptions *Environ. Health Perspect.* **120** 1559–64
- Postma D S, Bush A and Van Den Berge M 2015 Risk factors and early origins of chronic obstructive pulmonary disease *Lancet* **385** 899–909
- Powers J G, Klemp J B, Skamarock W C, Davis C A, Dudhia J, Gill D O, Coen J L, Gochis D J, Ahmadov R, Peckham S E, Grell G A, Michalakes J, Trahan S, Benjamin S G, Alexander C R, Dimego G J, Wang W, Schwartz C S, Romine G S, Liu Z, Snyder C, Chen F, Barlage M J, Yu W and Duda M G 2017 The weather research and forecasting model: Overview, system efforts, and future directions *Bull. Am. Meteorol. Soc.* **98** 1717–37
- Pozzer A, Tsimpidi A P, Karydis V A, Meij A De and Lelieveld J 2017 Impact of agricultural emission reductions on fine-particulate matter and public health *Atmos. Chem. Phys.* **17** 12813–26
- Pozzer A, Zimmermann P, Doering U M, Van Aardenne J, Tost H, Dentener F, Janssens-Maenhout G and Lelieveld J 2012 Effects of business-as-usual anthropogenic emissions on air quality *Atmos. Chem. Phys.* **12** 6915–37
- Prasad A K and Singh R P 2007a Changes in aerosol parameters during major dust storm events (2001-2005) over the Indo-Gangetic Plains using AERONET and MODIS data *J. Geophys. Res.* **112** 1–18
- Prasad A K and Singh R P 2007b Comparison of MISR-MODIS aerosol optical depth over the Indo-Gangetic basin during the winter and summer seasons (2000-2005) *Remote Sens. Environ.* **107** 109–19
- Punger E M and West J J 2013 The effect of grid resolution on estimates of the burden of ozone and fine particulate matter on premature mortality in the United States *Air Qual. Atmos. Heal.* **6** 1–22
- Puyravaud J P, Davidar P and Laurance W F 2010 Cryptic Loss of India's Native Forests *Science* **329** 32
- Rajeevan M, Kesarkar A, Thampi S B, Rao T N, Radhakrishna B and Rajasekhar M 2010 Sensitivity of WRF cloud microphysics to simulations of a severe thunderstorm event over Southeast India *Ann. Geophys.* **28** 603–19
- Rajput P, Sarin M, Sharma D and Singh D 2014 Characteristics and emission budget of carbonaceous species from post-harvest agricultural-waste burning in source region of the Indo-Gangetic plain *Tellus, Ser. B Chem. Phys. Meteorol.* **66**
- Ram K and Sarin M M 2011 Day-night variability of EC, OC, WSOC and inorganic ions in urban environment of Indo-Gangetic Plain: Implications to secondary aerosol formation *Atmos. Environ.* **45** 460–8
- Ram K and Sarin M M 2010 Spatio-temporal variability in atmospheric abundances of EC, OC and WSOC over Northern India *J. Aerosol Sci.* **41** 88–98
- Ramachandran S and Cherian R 2008 Regional and seasonal variations in aerosol optical characteristics and their frequency distributions over India during 2001–2005 *J. Geophys. Res.* **113** D08207
- Ramachandran S, Kedia S and Sheel V 2015 Spatiotemporal characteristics of aerosols in India: Observations and model simulations *Atmos. Environ.* **116** 225–44
- Ramanathan V and Carmichael G 2008 Global and regional climate changes due to black carbon *Nat. Geosci.* **1** 221–7
- Ramanathan V, Chung C, Kim D, Bettge T, Buja L, Kiehl J T, Washington W M, Fu Q, Sikka D

- R and Wild M 2005 Atmospheric brown clouds: impacts on South Asian climate and hydrological cycle. *Proc. Natl. Acad. Sci.* **102** 5326–33
- Ramanathan V, Crutzen P J, Lelieveld J, Mitra a. P, Althausen D, Anderson J, Andreae M O, Cantrell W, Cass G R, Chung C E, Clarke a. D, Coakley J a., Collins W D, Conant W C, Dulac F, Heintzenberg J, Heymsfield a. J, Holben B, Howell S, Hudson J, Jayaraman A, Kiehl J T, Krishnamurti T N, Lubin D, McFarquhar G, Novakov T, Ogren J a., Podgorny I a., Prather K, Priestley K, Prospero J M, Quinn P K, Rajeev K, Rasch P, Rupert S, Sadourny R, Satheesh S K, Shaw G E, Sheridan P and Valero F P J 2001 Indian Ocean Experiment: An integrated analysis of the climate forcing and effects of the great Indo-Asian haze *J. Geophys. Res.* **106** 28371
- Randerson J T, Chen Y, Van Der Werf G R, Rogers B M and Morton D C 2012 Global burned area and biomass burning emissions from small fires *J. Geophys. Res. G Biogeosciences* **117**
- Rastogi N, Singh A, Sarin M M and Singh D 2016 Temporal variability of primary and secondary aerosols over northern India: Impact of biomass burning emissions *Atmos. Environ.* **125** 396–403
- Ravindranath N, Srivastava N, Murthy I K, Malaviya S, Munsri M and Sharma N 2012 Deforestation and Forest Degradation in India: Implications for REDD+ *Curr. Sci.* **102** 1117–25
- Reddington C L, Butt E W, Ridley D a., Artaxo P, Morgan W T, Coe H and Spracklen D V. 2015 Air quality and human health improvements from reductions in deforestation-related fire in Brazil *Nat. Geosci.* **8** 768–71
- Reddington C L, Spracklen D V, Artaxo P, Ridley D and Rizzo L V 2016 Analysis of particulate emissions from tropical biomass burning using a global aerosol model and long-term surface observations *Atmos. Chem. Phys.* **16** 11083–106
- Reddy B S K, Kumar K R, Balakrishnaiah G, Gopal K R, Reddy R R, Ahammed Y N, Narasimhulu K, Reddy L S S and Lal S 2010 Observational studies on the variations in surface ozone concentration at Anantapur in southern India *Atmos. Res.* **98** 125–39
- Reddy M S and Venkataraman C 2002 Inventory of aerosol and sulphur dioxide emissions from India. Part II—biomass combustion *Atmos. Environ.* **36** 699–712
- Reddy R R, Gopal K R, Reddy L S S, Narasimhulu K, Kumar K R, Ahammed Y N and Reddy C V K 2008 Measurements of surface ozone at semi-arid site Anantapur (14.62 degrees N, 77.65 degrees E, 331 m asl) in India *J. Atmos. Chem.* **59** 47–59
- Rehman I H, Ahmed T, Praveen P S, Kar A and Ramanathan V 2011 Black carbon emissions from biomass and fossil fuels in rural India *Atmos. Chem. Phys.* **11** 7289–99
- Remer L a., Kleidman R G, Levy R C, Kaufman Y J, Tanré D, Mattoo S, Martins J V, Ichoku C, Koren I, Yu H and Holben B N 2008 Global aerosol climatology from the MODIS satellite sensors *J. Geophys. Res.* **113** 1–18
- Reshmi Mohan P, Srinivas C V., Yesubabu V, Baskaran R and Venkatraman B 2018 Simulation of a heavy rainfall event over Chennai in Southeast India using WRF: Sensitivity to microphysics parameterization *Atmos. Res.* **210** 83–99
- Robinson A L, Donahue N M, Shrivastava M K, Weitkamp E a, Sage A M, Grieshop A P, Lane T E, Pierce J R and Pandis S N 2007 Rethinking Organic Aerosols: Semivolatile Emissions and Photochemical Aging *Science* **315** 1259–62
- Roden C A, Bond T C, Conway S and Osorto Pinel A B 2006 Emission factors and real-time optical properties of particles emitted from traditional wood burning cookstoves *Environ. Sci. Technol.* **40** 6750–7
- Roden C A, Bond T C, Conway S, Osorto Pinel A B, MacCarty N and Still D 2009 Laboratory and field investigations of particulate and carbon monoxide emissions from traditional and

- improved cookstoves *Atmos. Environ.* **43** 1170–81
- Rosenthal J, Quinn A, Grieshop A P, Pillarisetti A and Glass R I 2018 Clean cooking and the SDGs: Integrated analytical approaches to guide energy interventions for health and environment goals *Energy Sustain. Dev.* **42** 152–9
- Rotach M W and Zardi D 2007 On the boundary-layer structure over highly complex terrain: Key findings from MAP *Q. J. R. Meteorol. Soc.* **133** 937–48
- Roy C, Fadnavis S, Müller R, Chaudhary A D, Ploeger F and Rap A 2017 Influence of enhanced Asian NO_x emissions on ozone in the Upper Troposphere and Lower Stratosphere (UTLS) in chemistry climate model simulations *Atmos. Chem. Phys.* **17** 1279–311
- Roy S, Beig G and Jacob D 2008 Seasonal distribution of ozone and its precursors over the tropical Indian region using regional chemistry-transport model *J. Geophys. Res. Atmos.* **113** 1–15
- Ruiz-Mercado I, Masera O, Zamora H and Smith K R 2011 Adoption and sustained use of improved cookstoves *Energy Policy* **39** 7557–66
- Ryu C, Yang Y Bin, Khor A, Yates N E, Sharifi V N and Swithenbank J 2006 Effect of fuel properties on biomass combustion: Part I. Experiments—fuel type, equivalence ratio and particle size *Fuel* **85** 1039–46
- S. Mehta 2003 Characterizing exposures to indoor air pollution from household solid fuel use
- Sadavarte P and Venkataraman C 2014 Trends in multi-pollutant emissions from a technology-linked inventory for India: I. Industry and transport sectors *Atmos. Environ.* **99** 353–64
- Sadavarte P, Venkataraman C, Cherian R, Patil N, Madhavan B L, Gupta T, Kulkarni S, Carmichael G R and Adhikary B 2016 Seasonal differences in aerosol abundance and radiative forcing in months of contrasting emissions and rainfall over northern South Asia *Atmos. Environ.* **125** 512–23
- Sagar A, Balakrishnan K, Guttikunda S, Roychowdhury A and Smith K R 2016 India leads the way: A health-centered strategy for air pollution *Environ. Health Perspect.* **124** 116–7
- Sahu L K and Lal S 2006 Distributions of C₂–C₅ NMHCs and related trace gases at a tropical urban site in India *Atmos. Environ.* **40** 880–91
- Sahu S K, Ohara T and Beig G 2017 The role of coal technology in redefining India's climate change agents and other pollutants *Environ. Res. Lett.* **12** 1–10
- Sahu S K, Ohara T, Beig G, Kurokawa J and Nagashima T 2015 Rising critical emission of air pollutants from renewable biomass based cogeneration from the sugar industry in India *Environ. Res. Lett.* **10** 1–8
- Saide P E, Carmichael G R, Liu Z, Schwartz C S, Lin H C, Da Silva A M and Hyer E 2013 Aerosol optical depth assimilation for a size-resolved sectional model: Impacts of observationally constrained, multi-wavelength and fine mode retrievals on regional scale analyses and forecasts *Atmos. Chem. Phys.* **13** 10425–44
- Saikawa E, Trail M, Zhong M, Wu Q, Young C L, Janssens-Maenhout G, Klimont Z, Wagner F, Kurokawa J, Nagpure A S, Ram B and Gurjar 2017 Uncertainties in emissions estimates of greenhouse gases and air pollutants in India and their impacts on regional air quality *Environ. Res. Lett.* **12**
- Sambandam S, Balakrishnan K, Ghosh S, Sadasivam A, Madhav S, Ramasamy R, Samanta M, Mukhopadhyay K, Rehman H and Ramanathan V 2015 Can currently available advanced combustion biomass cook-stoves provide health relevant exposure reductions? Results from initial assessment of select commercial models in India. *Ecohealth* **12** 25–41
- Sarangi C, Tripathi S N, Tripathi S and Barth M C 2015 Aerosol-cloud associations over Gangetic Basin during a typical monsoon depression event using WRF-Chem simulation *J. Geophys. Res. Atmos.* **120** 10,974–10,995

- Sarangi T, Naja M, Ojha N, Kumar R, Lal S, Venkataramani S, Kumar A, Sagar R and Chandola H C 2014 First simultaneous measurements of ozone, CO, and NO_y at a high-altitude regional representative site in the central Himalayas *J. Geophys. Res. Atmos.* **19** 1592–611
- Sarkar S, Chokngamwong R, Cervone G, Singh R P and Kafatos M 2006 Variability of aerosol optical depth and aerosol forcing over India *Adv. Sp. Res.* **37** 2153–9
- Sarkar S, Srivastava R K and Sagar K 2015 Diurnal Monitoring Of Surface Ozone And PM_{2.5} Concentration And Its Correlation With Temperature *Int. J. Technol. Enhanc. Emerg. Eng. Res.* **3** 121–9
- Satheesh S K, Krishna Moorthy K, Suresh Babu S, Vinoj V and Dutt C B S 2008 Climate implications of large warming by elevated aerosol over India *Geophys. Res. Lett.* **35** 1–6
- Satheesh S K, Ramanathan V, Holben B N, Krishna Moorthy K, Loeb N G, Mating H, Prospero J M and Savoie D 2002 Chemical, microphysical, and radiative effects of Indian Ocean aerosols *J. Geophys. Res. Atmos.* **107**
- Schilmann A, Riojas-Rodriguez H, Ramirez-Sedeno K, Berrueta V M, Perez-Padilla R and Romieu I 2015 Children's Respiratory Health After an Efficient Biomass Stove (Patsari) Intervention *Ecohealth* **12** 68–76
- Seaton A, MacNee W, Donaldson K and Godden D 1995 Particulate air pollution and acute health effects. *Lancet* **345** 176–8
- Seaton A, Soutar A, Crawford V, Elton R, McNerlan S, Cherie J, Watt M, Agius R and Stout R 1999 Particulate air pollution and the blood *Thorax* **54** 1027–32
- Seinfeld J H 2004 Black carbon and brown clouds *Geochemistry, Geophys. Geosystems* **1** 15–6
- Seinfeld J H and Pandis S N 2016 *Atmospheric Chemistry and Physics. From Air Pollution to Climate Change.* (John Wiley & Sons, Inc.)
- Shaddick G, Thomas M, Amini H, Broday D M, Cohen A, Frostad J, Green A, Gumy S, Liu Y, Martin R V, Prüss-Üstün A, Simpson D, van Donkelaar A and Brauer M 2018a Data Integration for the Assessment of Population Exposure to Ambient Air Pollution for Global Burden of Disease Assessment *Environ. Sci. Technol.* **52** 9069–78
- Shaddick G, Thomas M L, Green A, Brauer M, Donkelaar A Van, Burnett R, Chang H H, Cohen A, Dingenen R Van, Dora C, Gumy S, Liu Y, Martin R, Waller L A, West J, Zidek J V and Pruss-Ustun A 2018b Data integration model for air quality: a hierarchical approach to the global estimation of exposures to ambient air pollution *J. R. Stat. Soc. Appl. Stat. Ser. C* **67** 231–53
- Sharma A, Ojha N, Pozzer A, Mar K A, Beig G, Lelieveld J and Gunthe S S 2017a WRF-Chem simulated surface ozone over South Asia during the pre-monsoon: Effects of emission inventories and chemical mechanisms *Atmos. Chem. Phys.* **17** 14393–413
- Sharma A R, Kharol S K, Badarinath K V S and Singh D 2010 Impact of agriculture crop residue burning on atmospheric aerosol loading - A study over Punjab State, India *Ann. Geophys.* **28** 367–79
- Sharma M and Dikshit O 2016 Comprehensive Study on Air Pollution and Green House Gases (GHGs) in Delhi *Indian Inst. Technol. Kanpur* 334
- Sharma P, Kuniyal J C, Chand K, Guleria R P, Dhyani P P and Chauhan C 2013 Surface ozone concentration and its behaviour with aerosols in the northwestern Himalaya, India *Atmos. Environ.* **71** 44–53
- Sharma S, Chatani S, Mahtta R, Goel A and Kumar A 2016 Sensitivity analysis of ground level ozone in India using WRF-CMAQ models *Atmos. Environ.* **131** 29–40
- Sharma S and Khare M 2017 Simulating ozone concentrations using precursor emission inventories in Delhi – National Capital Region of India *Atmos. Environ.* **151** 117–32

- Sharma S and Kumar A 2016 *Air pollutant emissions scenario for India - Version 1*
- Sharma S, Sharma P and Khare M 2017b Photo-chemical transport modelling of tropospheric ozone: A review *Atmos. Environ.* **159** 34–54
- Shen G, Yang Y, Wang B I N, Wang R and Russell A G 2010 Emission Factors of Particulate Matter and Elemental Carbon for Crop Residues and Coals Burned in Typical Household Stoves in China *Environ. Sci. Technol.* **44** 7157–62
- Shindell D, Kuylensstierna J C I, Vignati E, Dingenen R Van, Amann M, Klimont Z, Anenberg S C, Muller N, Janssens-Maenhout G, Raes F, Schwartz J, Faluvegi G, Pozzoli L, Kupiainen K, Höglund-isaksson L, Emberson L, Streets D, Ramanathan V, Hicks K, Oanh N T K, Milly G, Williams M, van Dingenen R, Amann M, Klimont Z, Anenberg S C, Muller N, Janssens-Maenhout G, Raes F, Schwartz J, Faluvegi G, Pozzoli L, Kupiainen K, Höglund-Isaksson L, Emberson L, Streets D, Ramanathan V, Hicks K, Oanh N T K, Milly G, Williams M, Demkine V and Fowler D 2012 Simultaneously Mitigating Near-Term Climate Change and Improving Human Health and Food Security *Science* **335** 183–90
- Silva R A, Adelman Z, Fry M M and West J J 2016a The Impact of Individual Anthropogenic Emissions Sectors on the Global Burden of Human Mortality due to Ambient Air Pollution. Supplementary Information. *Environ. Health Perspect.* **124** 1776–84
- Silva R A, Adelman Z, Fry M M and West J J 2016b The Impact of Individual Anthropogenic Emissions Sectors on the Global Burden of Human Mortality due to Ambient Air Pollution *Environ. Health Perspect.* **124** 1776–84
- Silva R A, West J J, Lamarque J-F, Shindell D T, Collins W J, Dalsoren S, Faluvegi G, Folberth G, Horowitz L W, Nagashima T, Naik V, Rumbold S T, Sudo K, Takemura T, Bergmann D, Cameron-Smith P, Cionni I, Doherty R M, Eyring V, Josse B, MacKenzie I A, Plummer D S, Righi M, Stevenson D S, Strode S, Szopa S and Zengast G 2016c The effect of future ambient air pollution on human premature mortality to 2100 using output from the ACCMIP model ensemble *Atmos. Chem. Phys.* **16** 9847–62
- Silva R A, West J J, Lamarque J-F, Shindell D T, Collins W J, Faluvegi G, Folberth G A, Horowitz L W, Nagashima T, Naik V, Rumbold S T, Sudo K, Takemura T, Bergmann D, Cameron-Smith P, Doherty R M, Josse B, Mackenzie I A, Stevenson D S and Zeng G 2017 Future global mortality from changes in air pollution attributable to climate change *Nat. Clim. Chang.* **7** 647–651
- Silva R A, West J J, Zhang Y, Anenberg S C, Lamarque J-F, Shindell D T, Collins W J, Dalsoren S, Faluvegi G, Folberth G, Horowitz L W, Nagashima T, Naik V, Rumbold S, Skeie R, Sudo K, Takemura T, Bergmann D, Cameron-Smith P, Cionni I, Doherty R M, Eyring V, Josse B, MacKenzie I a, Plummer D, Righi M, Stevenson D S, Strode S, Szopa S and Zeng G 2013 Global premature mortality due to anthropogenic outdoor air pollution and the contribution of past climate change *Environ. Res. Lett.* **8** 1–11
- Simpson D, Benedictow A, Berge H, Bergström R, Emberson L D, Fagerli H, Flechard C R, Hayman G D, Gauss M, Jonson J E, Jenkin M E, Nyúri A, Richter C, Semeena V S, Tsyro S, Tuovinen J P, Valdebenito A and Wind P 2012 The EMEP MSC-W chemical transport model - technical description *Atmos. Chem. Phys.* **12** 7825–65
- Singh R P, Dey S, Tripathi S N, Tare V and Holben B 2004 Variability of aerosol parameters over Kanpur, northern India *J. Geophys. Res. Atmos.* **109** 1–14
- Singh R P and Kaskaoutis D G 2014 Crop residue burning: A threat to South Asian air quality *Eos (Washington, DC).* **95** 333–4
- Sinha B, Singh Sangwan K, Maurya Y, Kumar V, Sarkar C, Chandra B P and Sinha V 2015 Assessment of crop yield losses in Punjab and Haryana using 2 years of continuous in situ ozone measurements *Atmos. Chem. Phys.* **15** 9555–76
- Sinton J E, Smith K R, Peabody J W, Yaping L, Xiliang Z, Edwards R and Quan G 2004 An assessment of programs to promote improved household stoves in China *Energy Sustain.*

- Skamarock W C and Klemp J B 2008 A time-split nonhydrostatic atmospheric model for weather research and forecasting applications *J. Comput. Phys.* **227** 3465–85
- Skamarock W C, Klemp J B, Dudhi J, Gill D O, Barker D M, Duda M G, Huang X-Y, Wang W and Powers J G 2008 A Description of the Advanced Research WRF Version 3 *NCAR Tech. Rep.* **June** 1–113
- Smith K R 1987 Biofuels, Air Pollution, and Health: A Global Review 480
- Smith K R 2015 Changing paradigms in clean cooking. *Ecohealth* **12** 196–9
- Smith K R 1989 Dialectics of Improved Stoves *Econ. Polit. Wkly.* **24** 517–22
- Smith K R 1995 Environmental hazards during economic development: the risk transition and overlap *Assess. Manag. Heal. Risks from Drink. Water Contam. Approaches Appl. (Proceedings Rome Symp.* 3–13
- Smith K R 1993 Fuel Combustion, Air Pollution Exposure, and Health: The Situation In Developing Countries *Annu. Rev. Energy Environ.* **18** 529–66
- Smith K R 2014 In praise of power *Science* **345** 603
- Smith K R 2013 One million premature deaths from cooking fuels in India: How estimated and what does it mean? *First VPCI Honour Lect. Vallabhbai Patel Chest Institute, Delhi* 47
- Smith K R 2017a *The Indian LPG programmes: globally pioneering initiatives*
- Smith K R 2017b Why both gas and biomass are needed today to address the solid fuel cooking problem in India: A challenge to the biomass stove community *Energy Sustain. Dev.* **38** 102–3
- Smith K R, Aggarwal A L and Dave R M 1983 Air pollution and rural biomass fuels in developing countries: A pilot village study in India and implications for research and policy *Atmos. Environ.* **17** 2343–62
- Smith K R, Bruce N, Balakrishnan K, Adair-Rohani H, Balmes J, Chafe Z, Dherani M, Hosgood H D, Mehta S, Pope D and Rehfuess E 2014a Millions dead: how do we know and what does it mean? Methods used in the comparative risk assessment of household air pollution. *Annu. Rev. Public Health* **35** 185–206
- Smith K R, Dutta K, Chengappa C, Gusain P P S, Berrueta O M and V, Edwards R, Bailis R and Shields K N 2007 Monitoring and evaluation of improved biomass cookstove programs for indoor air quality and stove performance: conclusions from the Household Energy and Health Project *Energy Sustain. Dev.* **11** 5–18
- Smith K R and Ezzati M 2005 HOW ENVIRONMENTAL HEALTH RISKS CHANGE WITH DEVELOPMENT: The Epidemiologic and Environmental Risk Transitions Revisited *Annu. Rev. Environ. Resour.* **30** 291–333
- Smith K R and Haigler E 2008 Co-benefits of climate mitigation and health protection in energy systems: scoping methods *Annu. Rev. Public Health* **29** 11–25
- Smith K R, Jerrett M, Anderson H R, Burnett R T, Stone V, Derwent R, Atkinson R W, Cohen A, Shonkoff S B, Krewski D, Pope C A, Thun M J and Thurston G 2009a Public health benefits of strategies to reduce greenhouse-gas emissions: health implications of short-lived greenhouse pollutants *Lancet* **374** 2091–103
- Smith K R, McCracken J P, Weber M W, Hubbard A, Jenny A, Thompson L M, Balmes J, Diaz A, Arana B and Bruce N 2011 Effect of reduction in household air pollution on childhood pneumonia in Guatemala (RESPIRE): A randomised controlled trial *Lancet* **378** 1717–26
- Smith K R, Mehta S and Maeusezahl-Feuz M 2004 Chapter 18 - Indoor air pollution from household use of solid fuels *Comp. Quantif. Heal. Risks Glob. Reg. Burd. Dis. due to Sel. Major Risk Factors* 1435–94

- Smith K R and Peel J L 2010 Mind the Gap *Environ. Health Perspect.* **118** 1643–5
- Smith K R and Sagar A 2015 Fossil fuel subsidies and health. *Lancet* **3** e674
- Smith K R and Sagar A 2014 Making the clean available: Escaping India's Chulha Trap *Energy Policy* **75** 410–4
- Smith K R, Shuhua G, Kun H and Daxiong Q 1993 One hundred million improved cookstoves in China: How was it done? *World Dev.* **21** 941–61
- Smith K R, Uma R, Kishore V V N, Lata K, Joshi V, Zhang J, Rasmussen R A and Khalil M A . 2000a GREENHOUSE GASES FROM SMALL-SCALE COMBUSTION DEVICES IN DEVELOPING COUNTRIES: PHASE IIA Household Stoves in India *U.S. Environ. Prot. Agency R-00-052* 98
- Smith K R, Uma R, Kishore V V N, Zhang J, Joshi V and Khalil M A K 2000b GREENHOUSE IMPLICATIONS OF HOUSEHOLD STOVES: An Analysis for India *Annu. Rev. Energy Environ.* **25** 741–63
- Smith K R, Woodward A, Campbell-Lendrum D, Chadee D, Honda Y, Liu Q, Olwoch J, Revich B and Sauerborn R 2014b Human Health: Impacts, Adaptation, and Co-Benefit. *Clim. Chang. 2014 Impacts, Adapt. Vulnerability. Part A Glob. Sect. Asp. Contrib. Work. Gr. II to Fifth Assess. Rep. Intergov. Panel Clim. Chang.* 709–54
- Smith R L, Xu B and Switzer P 2009b Reassessing the relationship between ozone and short-term mortality in U.S. urban communities *Inhal. Toxicol.* **21** 37–61
- Sonia M, Payraa S, Sinhab P and Vermaa S 2014 A Performance Evaluation of WRF Model Using Different Physical Parameterization Scheme during Winter Season over a Semi-Arid Region, India *Int. J.* **1** 104–14
- Sovacool B K 2012 The political economy of energy poverty: A review of key challenges *Energy Sustain. Dev.* **16** 272–82
- Spracklen D V, Pringle K J, Carslaw K S, Chipperfield M P and Mann G W 2005 A global off-line model of size-resolved aerosol microphysics: I. Model development and prediction of aerosol properties *Atmos. Chem. Phys.* **5** 2227–52
- Srinivas C V., Hariprasad D, Bhaskar Rao D V., Anjaneyulu Y, Baskaran R and Venkatraman B 2013 Simulation of the Indian summer monsoon regional climate using advanced research WRF model *Int. J. Climatol.* **33** 1195–210
- Srinivas C V., Yesubabu V, Hari Prasad D, Hari Prasad K B R R, Greeshma M M, Baskaran R and Venkatraman B 2018 Simulation of an extreme heavy rainfall event over Chennai, India using WRF: Sensitivity to grid resolution and boundary layer physics *Atmos. Res.* **210** 66–82
- Stieb D M, Judek S and Burnett R T 2003 Meta-Analysis of Time-Series Studies of Air Pollution and Mortality: Update in Relation to the Use of Generalized Additive Models *J. Air Waste Manage. Assoc.* **53** 258–61
- Stohl A, Aamaas B, Amann M, Baker L H, Bellouin N, Berntsen T K, Boucher O, Cherian R, Collins W, Daskalakis N, Dusinska M, Eckhardt S, Fuglestedt J S, Harju M, Heyes C, Hodnebrog, Hao J, Im U, Kanakidou M, Klimont Z, Kupiainen K, Law K S, Lund M T, Maas R, MacIntosh C R, Myhre G, Myriokefalitakis S, Olivie D, Quaas J, Quennehen B, Raut J C, Rumbold S T, Samset B H, Schulz M, Seland, Shine K P, Skeie R B, Wang S, Yttri K E and Zhu T 2015 Evaluating the climate and air quality impacts of short-lived pollutants *Atmos. Chem. Phys.* **15** 10529–66
- Streets D G, Yan F, Chin M, Diehl T, Mahowald N, Schultz M, Wild M, Wu Y and Yu C 2009 Anthropogenic and natural contributions to regional trends in aerosol optical depth, 1980–2006 *J. Geophys. Res. Atmos.* **114** 1–16
- Su L and Fung J C H 2015 Sensitivities of WRF-chem to dust emission schemes and land surface

properties in simulating dust cycles during springtime over East Asia *J. Geophys. Res. Atmos.* **120** 11,215–11,230

Subramanian B Y M 2016 Can Delhi save itself from its toxic air? *Nature* **534** 166–9

Sudhakar Reddy C, Jha C S, Dadhwal V K, Hari Krishna P, Vazeed Pasha S, Satish K V., Dutta K, Saranya K R L, Rakesh F, Rajashekar G and Diwakar P G 2016 Quantification and monitoring of deforestation in India over eight decades (1930–2013) *Biodivers. Conserv.* **25** 93–116

Sukhsohale N D, Narlawar U W, Phatak M S, Agrawal S B and Ughade S N 2013 Effect of indoor air pollution during cooking on peak expiratory flow rate and its association with exposure index in rural women *Indian J. Physiol. Pharmacol.* **57** 184–8

Surendran D E, Ghude S D, Beig G, Emmons L K, Jena C, Kumar R, Pfister G G and Chate D M 2015 Air quality simulation over South Asia using Hemispheric Transport of Air Pollution version-2 (HTAP-v2) emission inventory and Model for Ozone and Related chemical Tracers (MOZART-4) *Atmos. Environ.* **122** 357–72

Tao S, Ru M Y, Du W, Zhu X, Zhong Q R, Li B G, Shen G F, Pan X L, Meng W J, Chen Y L, Shen H Z, Lin N, Su S, Zhuo S J, Huang T B, Xu Y, Yun X, Liu J F, Wang X L, Liu W X, Cheng H F and Zhu D Q 2018 Quantifying the rural residential energy transition in China from 1992 to 2012 through a representative national survey *Nat. Energy* **3** 567–73

Task Force on Hemispheric Transport of Air Pollution 2010 Hemispheric Transport of Air Pollution 2010. Part A: Ozone and Particulate Matter. Air Pollution Studies No. 17 *United Nations Econ. Comm. Eur.*

Tchetgen E J T and Vanderweele T J 2012 On causal inference in the presence of interference *Stat. Methods Med. Res.* **21** 55–75

The World Bank 1995 *Annual World Bank Conference on Development Economics*

The World Bank 1993 *World Development Report 1993: Investing in Health* vol June

The World Bank and Institute for Health Metrics and Evaluation 2016 *The Cost of Air Pollution: Strengthening the Economic Case for Action.* (Washington, DC)

Thompson G, Rasmussen R M and Manning K 2008 Explicit Forecasts of Winter Precipitation Using an Improved Bulk Microphysics Scheme. Part II: Implementation of a New Snow Parameterization *Am. Meteorol. Soc.* **136** 5095–115

Thompson T M, Saari R K and Selin N E 2014 Air quality resolution for health impact assessment: Influence of regional characteristics *Atmos. Chem. Phys.* **14** 969–78

Thompson T M and Selin N E 2012 Influence of air quality model resolution on uncertainty associated with health impacts *Atmos. Chem. Phys.* **12** 9753–62

Thurston G D, Burnett R T, Turner M C, Shi Y, Krewski D, Lall R, Ito K, Jerrett M, Gapstur S M, Ryan Diver W and Arden Pope C 2016 Ischemic heart disease mortality and long-term exposure to source-related components of U.S. fine particle air pollution *Environ. Health Perspect.* **124** 785–94

Thurston G D, Kipen H, Annesi-Maesano I, Balmes J, Brook R D, Cromar K, De Matteis S, Forastiere F, Forsberg B, Frampton M W, Grigg J, Heederik D, Kelly F J, Kuenzli N, Laumbach R, Peters A, Rajagopalan S T, Rich D, Ritz B, Samet J M, Sandstrom T, Sigsgaard T, Sunyer J and Brunekreef B 2017 A joint ERS/ATS policy statement: what constitutes an adverse health effect of air pollution? An analytical framework *Eur. Respir. J.* **49** 1600419

Tie X, Madronich S, Walters S, Edwards D P, Ginoux P, Mahowald N, Zhang R Y, Lou C and Brasseur G 2005 Assessment of the global impact of aerosols on tropospheric oxidants *J. Geophys. Res. Atmos.* **110** 1–32

Tie X, Madronich S, Walters S, Zhang R, Rasch P and Collins W 2003 Effect of clouds on

- photolysis and oxidants in the troposphere *J. Geophys. Res.* **108** 4642, 1–11
- Tielsch J M, Katz J, Khattry S K, Shrestha L, Breyse P, Zeger S, Checkley W, Mullany L C, Kozuki N, LeClerq S C and Adhikari R 2016 Effect of an improved biomass stove on acute lower respiratory infections in young children in rural Nepal: a cluster-randomised, step-wedge trial *Lancet Glob. Heal.* **4**
- Tiwari S, Tiwari S, Hopke P K, Attri S D, Soni V K and Singh A K 2016 Variability in optical properties of atmospheric aerosols and their frequency distribution over a mega city New Delhi, India *Environ. Sci. Pollut. Res.* **23** 8781–93
- Tonne C, Salmon M, Sanchez M, Sreekanth V, Bhogadi S, Sambandam S, Balakrishnan K, Kinra S and Marshall J D 2017 Integrated assessment of exposure to PM_{2.5} in South India and its relation with cardiovascular risk: Design of the CHAI observational cohort study *Int. J. Hyg. Environ. Health* **220** 1081–8
- Tripathi A, Sagar A D and Smith K R 2015 PROMOTING CLEAN AND AFFORDABLE COOKING: SMARTER SUBSIDIES FOR LPG *Work. Pap.* **July** 1–10
- Tuomisto J T, Wilson A, Evans J S and Tainio M 2008 Uncertainty in mortality response to airborne fine particulate matter: Combining European air pollution experts *Reliab. Eng. Syst. Saf.* **93** 732–44
- Turner M C, Jerrett M, Pope III C A, Krewski D, Gapstur S M, Diver R W, Beckerman B S, Marshall J D, Su J G, Crouse D L and Burnett R T 2016 Long-Term Ozone Exposure and Mortality in a Large Prospective Study *Am. J. Respir. Crit. Care Med.* **193** 1134–42
- Turnock S, Wild O, Dentener F, Davila Y, Emmons L, Flemming J, Folberth G, Henze D, Jonson J, Keating T, Kengo S, Lin M, Lund M, Tilmes S and O'Connor F 2018 The Impact of Future Emission Policies on Tropospheric Ozone using a Parameterised Approach *Atmos. Chem. Phys.* **18** 8952–78
- U.S. Environmental Protection Agency 2009a A Conceptual Framework for U.S. EPA's National Exposure Research Laboratory *Washington, DC. EPA/600/R-09/003. Final Report.* 52
- U.S. Environmental Protection Agency 2007 Guidance on the Use of Models and Other Analyses for Demonstrating Attainment of Air Quality Goals for Guidance on the Use of Models and Other Air Quality Goals for Ozone, PM_{2.5}, and Regional Haze *Washington, DC. EPA - 454/B-07-002* 262
- U.S. Environmental Protection Agency 2010 Integrated Science Assessment for Carbon Monoxide *Washington, DC. EPA/600/R-09/019F. Final Report.* 593
- U.S. Environmental Protection Agency 2013a Integrated Science Assessment for Lead *Washington, DC. EPA/600/R-10/075F. Final Report.* 1886
- U.S. Environmental Protection Agency 2016 Integrated Science Assessment for Oxides of Nitrogen – Health Criteria *Washington, DC. EPA/600/R-15/068.* 1148
- U.S. Environmental Protection Agency 2013b Integrated Science Assessment for Ozone and Related Photochemical Oxidants *Washington, DC. EPA/600/R-10/076F. Final Report.* 1251
- U.S. Environmental Protection Agency 2009b Integrated Science Assessment for Particulate Matter *Washington, DC. EPA/600/R-08/139F. Final Report.* 1071
- U.S. Environmental Protection Agency 2017 Integrated Science Assessment for Sulfur Oxides – Health Criteria *Washington, DC. EPA/600/R-17/451.*
- U.S. Environmental Protection Agency 2012 Provisional Assessment of Recent Studies on Health Effects of Particulate Matter Exposure *Washington, DC. EPA/600/R-12/056F. Final Report.* 75
- U.S. National Research Council 2012 *Exposure Science in the 21st Century: A Vision and a Strategy* (Washington DC: National Academy of Sciences)

- Unger N, Bond T C, Wang J S, Koch D M, Menon S, Shindell D T and Bauer S 2010 Attribution of climate forcing to economic sectors. *Proc. Natl. Acad. Sci.* **107** 3382–7
- United Nations 2015 *Transforming our world: the 2030 Agenda for Sustainable Development*
- Upadhyay A, Dey S, Chowdhury S and Goyal P 2018 Expected health benefits from mitigation of emissions from major anthropogenic PM_{2.5} sources in India: Statistics at state level *Environ. Pollut.* **242** 1817–26
- Vadrevu K, Ohara T and Justice C 2017 Land cover, land use changes and air pollution in Asia: A synthesis *Environ. Res. Lett.* **12** 1–18
- Vadrevu K P, Ellicott E, Badarinath K V S and Vermote E 2011 MODIS derived fire characteristics and aerosol optical depth variations during the agricultural residue burning season, north India *Environ. Pollut.* **159** 1560–9
- Vadrevu K P, Giglio L and Justice C 2013 Satellite based analysis of fire-carbon monoxide relationships from forest and agricultural residue burning (2003-2011) *Atmos. Environ.* **64** 179–91
- Venkataraman C, Brauer M, Tibrewal K, Sadavarte P, Ma Q, Cohen A, Chaliyakunnel S, Frostad J, Klimont Z, Martin R V., Millet D B, Philip S, Walker K and Wang S 2018 Source influence on emission pathways and ambient PM_{2.5} pollution over India (2015–2050) *Atmos. Chem. Phys.* **18** 8017–39
- Venkataraman C, Sagar A D, Habib G, Lam N and Smith K R 2010 The Indian National Initiative for Advanced Biomass Cookstoves: The benefits of clean combustion *Energy Sustain. Dev.* **14** 63–72
- Verma S 2015 A New Classification of Aerosol Sources and Types as Measured over Jaipur, India *Aerosol Air Qual. Res.* **2015** 985–93
- Villalobos A M, Amonov M O, Shafer M M, Devi J J, Gupta T, Tripathi S N, Rana K S, Mckenzie M, Bergin M H and Schauer J J 2015 Source apportionment of carbonaceous fine particulate matter (PM_{2.5}) in two contrasting cities across the Indo–Gangetic Plain *Atmos. Pollut. Res.* **6** 398–405
- Walcek C J, Brost R A, Chang J S and Wesely M L 1986 SO₂, sulfate and HNO₃ deposition velocities computed using regional landuse and meteorological data *Atmos. Environ.* **20** 949–64
- Wang K, Yahya K, Zhang Y, Hogrefe C, Pouliot G, Knote C, Hodzic A, San Jose R, Perez J L, Jimenez-Guerrero P, Baro R, Makar P and Bennartz R 2015 A multi-model assessment for the 2006 and 2010 simulations under the Air Quality Model Evaluation International Initiative (AQMEII) Phase 2 over North America: Part II. Evaluation of column variable predictions using satellite data *Atmos. Environ.* **115** 587–603
- Wang R, Tao S, Wang W, Liu J, Shen H, Shen G, Wang B, Liu X, Li W, Huang Y, Zhang Y, Lu Y, Chen H, Chen Y, Wang C, Zhu D, Wang X, Li B, Liu W and Ma J 2012 Black carbon emissions in China from 1949 to 2050 *Environ. Sci. Technol.* **46** 7595–603
- Wesely M L 1989 PARAMETERIZATION OF SURFACE RESISTANCES TO GASEOUS DRY DEPOSITION IN REGIONAL-SCALE NUMERICAL MODELS *Atmos. Environ.* **23** 1293–304
- West J, Cohen A, Dentener F, Brunekreef B, Zhu T, Armstrong B, Bell M, Brauer M, Carmichael G R, Costa D, Dockery D, Kleeman M J, Krzyzanowski M, Kunzli N, Liousse C, Lung S-C, Martin R V, Pöschl U, Pope C A, Roberts J M, Russell A G and Wiedinmyer C 2016 What we breathe impacts our health: improving understanding of the link between air pollution and health *Environ. Sci. Technol.* **50** 4895–904
- West J J, Fiore A M, Horowitz L W and Mauzerall D L 2006 Global health benefits of mitigating ozone pollution with methane emission controls. *Proc. Natl. Acad. Sci. U. S. A.* **103** 3988–93

- West J J, Naik V, Horowitz L W and Fiore A M 2009a Effect of regional precursor emission controls on long-range ozone transport - Part 2: Steady-state changes in ozone air quality and impacts on human mortality *Atmos. Chem. Phys.* **9** 6095–107
- West J J, Naik V, Horowitz L W and Fiore A M 2009b Effect of regional precursor emission controls on long-range ozone transport – Part 1: Short-term changes in ozone air quality *Atmos. Chem. Phys.* **9** 6077–93
- West J J, Szopa S and Hauglustaine D A 2007 Human mortality effects of future concentrations of tropospheric ozone *Comptes Rendus - Geosci.* **339** 775–83
- Wiedinmyer C, Akagi S K, Yokelson R J, Emmons L K, Al-Saadi J A, Orlando J J and Soja A J 2011 The Fire INventory from NCAR (FINN) – a high resolution global model to estimate the emissions from open burning *Geosci. Model Dev.* **4** 624–41
- Wild O, Fiore A M, Shindell D T, Doherty R M, Collins W J, Dentener F J, Schultz M G, Gong S, Mackenzie I A, Zeng G, Hess P, Duncan B N, Bergmann D J, Szopa S, Jonson J E, Keating T J and Zuber A 2012 Modelling future changes in surface ozone: A parameterized approach *Atmos. Chem. Phys.* **12** 2037–54
- Wild O and Prather M J 2006 Global tropospheric ozone modeling: Quantifying errors due to grid resolution *J. Geophys. Res. Atmos.* **111** 1–14
- Wilkinson P, Smith K R, Davies M, Adair H, Armstrong B G, Barrett M, Bruce N, Haines A, Hamilton I, Oreszczyn T, Ridley I, Tonne C and Chalabi Z 2009 Public health benefits of strategies to reduce greenhouse-gas emissions: household energy *Lancet* **374** 1917–29
- Williams K N, Northcross L and Graham J P 2015 Health impacts of household energy use: indicators of exposure to air pollution and other risks *Bull. World Health Organ.* **93** 507–8
- Wilson A, Rappold A G, Neas L M and Reich B J 2014 Modeling the effect of temperature on ozone-related mortality *Ann. Appl. Stat.* **8** 1728–49
- Winijkul E, Fierce L and Bond T C 2016 Emissions from Residential Combustion Considering End-Uses and Spatial Constraints: Part I, Methods and Spatial Distribution *Atmos. Environ.* **125** 126–39
- World Health Organization 2006a Air Quality Guidelines for Particulate Matter, Ozone, Nitrogen Dioxide and Sulfur Dioxide: Global Update 2005. 22
- World Health Organization 2016a Ambient air pollution: A global assessment of exposure and burden of disease 121
- World Health Organization 2014a Burden of disease from Ambient Air Pollution for 2012 - Results 2014
- World Health Organization 2016b Burning Opportunity: Clean Household Energy for Health, Sustainable Development, and Wellbeing of Women and Children 129
- World Health Organization 2006b Fuel for Life: Household Energy and Health
- World Health Organization 2018a Global Ambient Air Quality Database (update 2018) [website] Online: www.who.int/airpollution/data/cities/en/
- World Health Organization 2018b Global Health Estimates 2016: Deaths by Cause, Age, Sex, by Country and by Region, 2000-2016 Online: http://www.who.int/healthinfo/global_burden_disease/en/
- World Health Organization 2009 *Global Health Risks: Mortality and burden of disease attributable to selected major risks*
- World Health Organization 2003 *Guide to Cost-Effectiveness Analysis* ed and C J L M Tan-Torres Edejer, T., R. Baltussem, T. Adam, R. Hutubessy, A. Acharya, D.B. Evans (Geneva, Switzerland)
- World Health Organization 2016c *Health and the environment. Draft road map for an enhanced*

global response to the adverse health effects of air pollution. A69/18. Provisional agenda item 13.5.

- World Health Organization 2018c ICD-11 (International Statistical Classification of Diseases and Related Health Problems) for Mortality and Morbidity Statistics (ICD-11 MMS). 2018 version. *Geneva, Switz.* Online: <https://icd.who.int>
- World Health Organization 2015 Population using solid fuels (%), 2013 *Public Heal. Environ. Househ. air Pollut.*
- World Health Organization 2013 *Review of evidence on health aspects of air pollution – REVIHAAP Project. Technical Report.*
- World Health Organization 2014b WHO Guidelines for Indoor Air Quality: Household Fuel Combustion 172
- World Health Organization 2011 World Health Statistics 174
- World Health Organization Regional Office for Europe 2013 Health risks of air pollution in Europe – HRAPIE project: Recommendations for concentration–response functions for cost–benefit analysis of particulate matter, ozone and nitrogen dioxide. 60
- World Health Organization South East Asia Region 2013 *Action Plan for The Prevention and Control of Noncommunicable Diseases in South-East Asia, 2013–2020. SEA-NCD-89.*
- Wrangham R 2010 *Catching Fire: How Cooking Made Us Human*
- Wu S, Duncan B N, Jacob D J, Fiore A M and Wild O 2009 Chemical nonlinearities in relating intercontinental ozone pollution to anthropogenic emissions *Geophys. Res. Lett.* **36** 1–5
- Xu R T, Pan S F, Chen J, Chen G S, Yang J, Dangal S R S, Shepard J P and Tian H Q 2018 Half-Century Ammonia Emissions From Agricultural Systems in Southern Asia: Magnitude, Spatiotemporal Patterns, and Implications for Human Health *GeoHealth* **2** 40–53
- Yadav R, Sahu L K, Jaaffrey S N A and Beig G 2014 Distributions of ozone and related trace gases at an urban site in western India *J. Atmos. Chem.* **71** 125–44
- Yin P, Brauer M, Cohen A, Burnett R T, Liu J, Liu Y, Liang R, Wang W, Qi J, Wang L and Zhou M 2017 Long-term Fine Particulate Matter Exposure and Nonaccidental and Cause-specific Mortality in a Large National Cohort of Chinese Men *Environ. Health Perspect.* **125** 117002:1-11
- Yu E, Wang H, Gao Y and Sun J 2011 Impacts of cumulus convective parameterization schemes on summer monsoon precipitation simulation over China *Acta Meteorol. Sin.* **25** 581–92
- Yu S, Eder B, Dennis R, Chu S-H and Schwartz S E 2006 New unbiased symmetric metrics for evaluation of air quality models *Atmos. Sci. Lett.* **7** 26–34
- Zanobetti A and Schwartz J 2011 Ozone and survival in four cohorts with potentially predisposing diseases *Am. J. Respir. Crit. Care Med.* **184** 836–41
- Zaveri R A, Easter R C, Fast J D and Peters L K 2008 Model for Simulating Aerosol Interactions and Chemistry (MOSAIC) *J. Geophys. Res.* **113** 1–29
- Zhang M, Uno I, Zhang R, Han Z, Wang Z and Pu Y 2006 Evaluation of the Models-3 Community Multi-scale Air Quality (CMAQ) modeling system with observations obtained during the TRACE-P experiment: Comparison of ozone and its related species *Atmos. Environ.* **40** 4874–82
- Zhang Q, Jiang X, Tong D, Davis S J, Zhao H, Geng G, Feng T, Zheng B, Lu Z, Streets D G, Ni R, Brauer M, van Donkelaar A, Martin R V., Huo H, Liu Z, Pan D, Kan H, Yan Y, Lin J, He K and Guan D 2017 Transboundary health impacts of transported global air pollution and international trade *Nature* **543** 705–9
- Zhang X Y, Wang J Z, Wang Y Q, Liu H L, Sun J Y and Zhang Y M 2015 Changes in chemical components of aerosol particles in different haze regions in China from 2006 to 2013 and

- contribution of meteorological factors *Atmos. Chem. Phys.* **15** 12935–52
- Zheng Y, Xue T, Zhang Q, Geng G, Tong D, Li X and He K 2017 Air quality improvements and health benefits from China's clean air action since 2013 *Environ. Res.* **12** 114020
- Zhong M, Saikawa E, Liu Y, Naik V, Horowitz L W, Takigawa M, Zhao Y, Lin N-H and Stone E A 2016a Air Quality Modeling with WRF-Chem v3.5 in East and South Asia: sensitivity to emissions and evaluation of simulated air quality *Geosci. Model Dev.* **9** 1201–18
- Zhong M, Saikawa E, Liu Y, Naik V, Horowitz L W, Takigawa M, Zhao Y, Lin N-H and Stone E A 2016b Air Quality Modeling with WRF-Chem v3.5 in East and South Asia: sensitivity to emissions and evaluation of simulated air quality *Geosci. Model Dev.* **9** 1201–18
- Zhou B, Shen H, Huang Y, Li W, Chen H, Zhang Y, Su S, Chen Y, Lin N, Zhuo S, Zhong Q, Liu J, Li B and Tao S 2015 Daily variations of size-segregated ambient particulate matter in Beijing *Environ. Pollut.* **197** 36–42
- Zigler C M and Dominici F 2014 Point: Clarifying policy evidence with potential-outcomes thinking-beyond exposure-response estimation in air pollution epidemiology *Am. J. Epidemiol.* **180** 1133–40

Appendix A: Acronyms and Abbreviations

3mDMA1	3-month average daily maximum 1-hour O ₃ concentrations
95UI	95 th uncertainty interval
ACI	Aerosol-Cloud Interaction
ACOM	Atmospheric Chemistry Observations and Modelling Lab
ADM8h	Annual average daily maximum 8-hour O ₃ concentrations
AERONET	Aerosol Robotic Network
AGE2015	Population age groupings from 2015
AGR	Agriculture
AOD	Aerosol Optical Depth
AQG	Air Quality Guideline
ARI	Aerosol Radiation Interaction
ARW	Advanced Research WRF
BBU	Biomass Burning
BC	Black Carbon
BM2015	Baseline mortality rates from 2015
Ca	Calcium
CanCHEC	Canadian Census Health and Environment Cohort
CAS	Clean Air Scenario
CEV	Cerebrovascular Disease
CFL	Courant-Friedrichs-Levy
CH ₃ SO ₃	Methanesulfonate
CH ₄	Methane
CIESIN	Centre for International Earth Science Information Network
CMNND	Communicable, Maternal, Neonatal, and Nutritional Diseases
CO	Carbon Monoxide
CO ₂	Carbon Dioxide

CO ₃	Carbonate
COPD	Chronic Obstructive Pulmonary Disease
CPS-II	American Cancer Society Cancer Prevention Study II
CTM	Chemical Transport Model
DALYs	Disability-Adjusted Life Years
DBTL	Direct Benefit Transfer of LPG
DDUGJY	Deen Dayal Upadhyaya Gram Jyoti Yojana
DIMAQ	Data Integration Model for Air Quality
DUS	Dust
ECLIPSE	Evaluating the Climate and Air Quality Impacts of Short-Lived Pollutants
ECMWF	European Centre for Medium-range Weather Forecasts
EF	Emission Factor
EDGAR	Emissions Database for Global Atmospheric Research
EMEP	European Monitoring and Evaluation Programme
ENE	Energy
EPSRC	Engineering and Physical Sciences Research Council
ERA	ECMWF Re-Analysis
EPA	Environmental Protection Agency
FDDA	Four-Dimensional Data Assimilation
FINN	Fire Inventory from NCAR
FNL	Final
ftUV	Fast Tropospheric Ultraviolet-Visible photolysis scheme
GACC	Global Alliance for Clean Cookstoves
GAINS	Greenhouse gas–Air pollution Interactions and Synergies
GBD	Global Burden of Disease
GDP	Gross Domestic Product
GEMM	Global Exposure Mortality Model

GFS	Global Forecast System
GOCART	Global Ozone Chemistry Aerosol Radiation and Transport
GPWv4	Gridded Population of the World, Version 4
H ₂ O	Water
H ₂ SO ₄	Sulphuric acid
HO ₂	Hydro-peroxy radical
HEI	Health Effects Institute
HPC	High Performance Computing
HR	Hazard Ratios
HTAP	Task Force on Hemispheric Transport of Air Pollution
HWRF	Hurricane WRF
IARC	International Agency for Research on Cancer
ICMR	Indian Council of Medical Research
ICS	Improved Cookstoves
IEA	International Energy Agency
IER	Integrated Exposure-Response
IGBP	International Geosphere-Biosphere Programme
IGP	Indo-Gangetic Plain
IHD	Ischaemic Heart Disease
IHME	Institute for Health Metrics and Evaluation
IND	Industry
INDC	Intended Nationally Defined Contribution
IPCC	Intergovernmental Panel on Climate Change
IT-1	Interim Target 1
IT-2	Interim Target 2
IT-3	Interim Target 3
KPP	Kinetic PreProcessor
LC	Lung Cancer

LCC	Low-Concentration Cut-off
LPG	Liquefied Petroleum Gas
LRI	Lower Respiratory Infections
MADE	Modal Aerosol Dynamics Model for Europe
MBE	Mean Bias Error
MIX	Model Intercomparison Study for Asia Phase III
MODIS	Moderate Resolution Imaging Spectroradiometer
MOSAIC	Model for Simulating Aerosol Interactions and Chemistry
MOZART-4	Model for Ozone and Related chemical Tracers, version 4
N	Nitrogen
NAAQS	National Ambient Air Quality Standards
NAQI	National Air Quality Index
NaCl	Sea salt
NAMP	National Air Quality Monitoring Program
NASA	National Aeronautics and Space Administration
NBCI	National Biomass Cookstove Initiative
NCAP	National Clean Air Programme
NCAR	National Centre for Atmospheric Research
NCD	Non-Communicable Diseases
NCEP	National Centres for Environmental Prediction
NH ₃	Ammonia
NH ₄	Ammonium
NH ₄ NO ₃	Ammonium nitrate
(NH ₄) ₂ SO ₄	Ammonium sulphate
NITI Aayog	National Institution for Transforming India
NMBF	Normalised Mean Bias Factor
NMVOC	Non-Methane Volatile Organic Compound
NO	Nitric oxide

NO ₂	Nitrogen dioxide
NO ₃	Nitrate
NO _x	Nitrogen oxides
NOAA	National Oceanic and Atmospheric Administration
NPS	New Policy Scenario
NWP	Numerical Weather Prediction
O(³ P)	Ground-state oxygen atom
O ₂	Oxygen
O ₃	Ozone
OA	Organic Aerosol
OC	Organic Carbon
OM	Primary Organic Mass
PAHAL	Pratyaksh Hanstantrit Labh
PAPA	Public Health and Air Pollution in Asia
PM	Particulate Matter
PM _{2.5}	Fine particulate matter, under 2.5 μm in size
PM ₁₀	Coarse and fine particulate matter, under 10 μm in size
PNG	Piped Natural Gas
POA	Primary Organic Aerosol
POP2015	Population density from 2015
r	Pearson's' Correlation Coefficient
RCP	Representative Concentration Pathways
RCT	Randomised Control Trial
REAS	Regional Emission inventory in Asia
RES	Residential
RGGLVY	Rajiv Gandhi Gramin LPG Vitran Yojana
RMSE	Root Mean Square Error
RO ₂	Organic-peroxy radical

RR	Relative Risk
RRTM	Rapid Radiative Transfer Model
SAFAR	System of Air Quality and Weather Forecasting and Research
SDG	Sustainable Development Goals
SEDAC	Socioeconomic Data and Applications Centre
SIA	Secondary Inorganic Aerosol
SFU	Solid Fuel Use
SO ₂	Sulphur dioxide
SO ₄	Sulphate
SO _x	Sulphur oxides
SOA	Secondary Organic Aerosol
SORGAM	Secondary Organic Aerosol Model
SVOC	Semi-Volatile Organic Compounds
S/IVOC	Semi- and Intermediate-Volatility Organic Compounds
TF HTAP	Task Force Hemispheric Transport of Air Pollution
TMREL	Theoretical Minimum-Risk Exposure Level
TRA	Land transport
TUV	Tropospheric Ultraviolet-Visible
Ujjwala	Pradhan Mantri Ujjwala Yojana
UTC	Coordinated Universal Time
UV	Ultra-Violet
VBS	Volatility Basis Set
VOC	Volatile Organic Compounds
VOC _A	Volatile Organic Compounds from anthropogenic origin
VOC _{BB}	Volatile Organic Compounds from biomass burning origin
WEO	World Energy Outlook
WHA	World Health Assembly
WHO	World Health Organization

WRF	Weather Research and Forecasting Model
WRF-Chem	WRF with Chemistry
WRF-Fire	Fire WRF
WRF-Hydro	WRF with hydrology
WRF-LES	WRF with turbulence
WRF-POLAR	WRF with polar environments
WRF-Solar	WRF with solar and wind energy
WRF-Urban	WRF with urban meteorology
WPS	WRF preprocessing system
YLL	Years of Life Lost
YLD	Years Lost due to Disability

Appendix B: Supplementary information for “Residential energy use emissions dominate health impacts from exposure to ambient particulate matter in India”

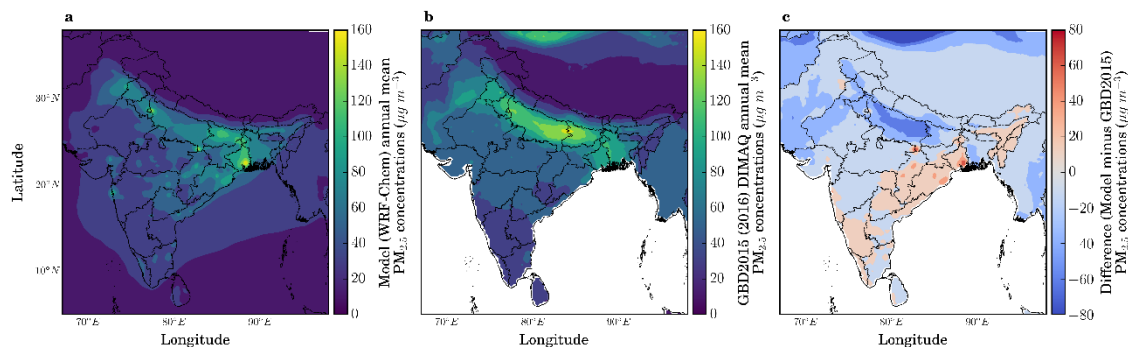


Figure 61: Comparison of annual-mean PM_{2.5} concentrations. (a) Model (WRF-Chem). (b) GBD2015 (2016) (Shaddick et al 2018b) DIMAQ. (c) Model minus GBD2015.

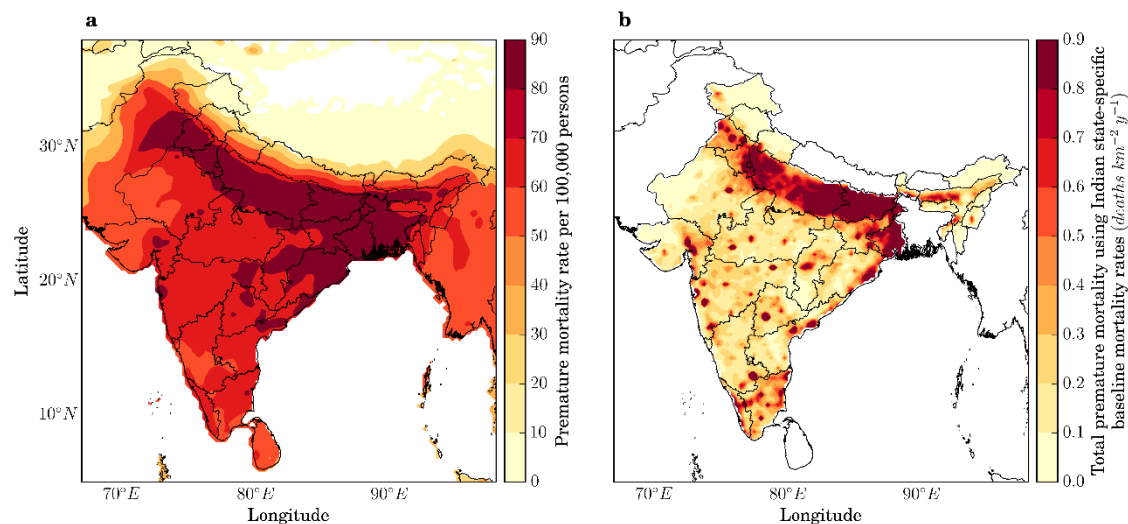


Figure 62: Premature mortality estimates from exposure to ambient PM_{2.5} in India. (a) Premature mortality rate per 100,000 population. (b) Premature mortality estimate using Indian state-specific baseline mortality rates (Chowdhury and Dey 2016), where white space represents where there was no state-specific baseline mortality rate data available.

Table 9: Estimated premature mortality associated with ambient PM_{2.5} exposure in India per disease from both subtraction and attribution methods. Values in parentheses represent the 95% uncertainty intervals (95UI). Sectors are agriculture (AGR), biomass burning (BBU), dust (DUS), power generation (ENE), industrial non-power (IND), residential energy use (RES), and land transport (TRA).

		AGR	BBU	DUS	ENE	IND	RES	TRA
Premature mortality per year, subtraction method	COPD	0	4	0	33	24	92	16
	($\times 10^3$)	(0–1)	(3–7)	(0–0)	(21–49)	(16–36)	(56–135)	(10–24)
	IHD	0	3	0	22	16	64	11
	($\times 10^3$)	(0–0)	(3–4)	(0–0)	(19–28)	(14–20)	(53–79)	(9–13)
	LC	0	0	0	3	2	8	1
($\times 10^3$)	(0–0)	(0–0)	(0–0)	(2–4)	(1–3)	(5–10)	(1–2)	
	CEV	0	2	0	12	9	34	6
	($\times 10^3$)	(0–0)	(1–2)	(0–0)	(9–15)	(7–11)	(25–42)	(4–7)
	LRI	0	3	0	21	15	58	10
	($\times 10^3$)	(0–0)	(1–4)	(0–0)	(9–26)	(7–19)	(23–74)	(4–12)
Premature mortality per year, attribution method	COPD	1	9	0	65	51	161	32
	($\times 10^3$)	(1–2)	(6–13)	(0–0)	(43–97)	(33–75)	(105–238)	(21–48)
	IHD	1	10	0	73	57	180	36
	($\times 10^3$)	(1–2)	(7–13)	(0–0)	(55–96)	(43–74)	(135–236)	(27–47)
	LC	0	1	0	4	3	10	2
($\times 10^3$)	(0–0)	(0–1)	(0–0)	(3–6)	(2–4)	(7–14)	(1–3)	
	CEV	0	4	0	30	23	73	15
	($\times 10^3$)	(0–1)	(3–5)	(0–0)	(22–38)	(17–30)	(55–94)	(11–19)
	LRI	1	5	0	35	27	87	17
	($\times 10^3$)	(0–1)	(2–6)	(0–0)	(15–47)	(12–36)	(38–12)	(8–23)

Table 10: Estimated years of life lost (YLL) associated with ambient PM_{2.5} exposure in India per sector from both subtraction and attribution methods. Values in parentheses represent the 95% uncertainty intervals (95UI). Sectors are agriculture (AGR), biomass burning (BBU), dust (DUS), power generation (ENE), industrial non-power (IND), residential energy use (RES), and land transport (TRA).

	AGR	BBU	DUS	ENE	IND	RES	TRA
YLL, subtraction, ×10³	26 (17–34)	316 (188–401)	-8 (-4–10)	2,313 (1,324– 2,956)	1,699 (997– 2,177)	6,553 (3,573– 8,296)	1,100 (645– 1,408)
YLL, attribution, ×10³	86 (51–114)	688 (407–915)	-16 (-10–22)	5,162 (3,056– 6,860)	4,001 (2,368– 5,316)	12,690 (7,513– 16,864)	2,538 (1,503– 3,373)

Table 11: Ground measurement air quality stations.

State	City	Station	Code	Lat	Lon
Andhra	Tirupati	Tirumala	APT	79.35	13.68
Pradesh	Visakhapatnam	GVMC Ram Nagar	APN	83.31	17.72
	Gaya	Gaya Collectorate	BGA	85.01	24.79
Bihar	Muzaffarpur	Muzaffarpur Collectorate	BMZ	85.38	26.12
	Patna	IGSC Planetarium Complex	BPT	85.13	25.61
		Anand Vihar	DAV	77.30	28.65
		Dwarka	DDW	77.05	28.59
		IHBAS	DIH	77.31	28.68
Delhi	Delhi	Income Tax Office	DIT	77.25	28.63
		Mandir Marg	DMM	77.28	28.66
		Punjabi Bagh	DPB	77.13	28.67
		R K Puram	DPR	77.18	28.57
		Shadipur	DSP	77.16	28.65
Gurjarat	Ahmedabad	Manianagar	GMG	72.60	23.00
	Faridabad	Sector16A Faridabad	HFB	77.32	28.41
Haryana	Gurgaon	HSPCB Gurgaon	HGG	76.85	30.71
	Panchkula	Panchkula	HPK	76.86	30.69
	Rohtak	Rohtak	HRT	76.61	28.90
		BTM	KBT	77.61	12.91
Karnataka	Bengaluru	BWSSB	KBW	77.62	12.97
		Peenya	KPY	77.52	13.03
	Aurangabad	More Chowk-Waluj	MWJ	75.25	19.84
	Chandrapur	Chandrapur	MCP	79.30	19.97
		MIDC Khutala	MKT	79.24	19.98
	Mumbai	MPCB Bandra	MBD	72.87	19.04
Maharashtra		NMMC Airoli	MAL	73.00	19.16
	Nagpur	Civil Lines	MNP	79.07	21.15
	Nashik	KTHM College	MKC	73.78	20.01
	Pune	Karve Road Pune	MPU	73.82	18.46
	Solapur	Solapur	MSP	75.91	17.66
	Thane	Pimpleshwar Mandir	MMD	73.09	19.19
Rajasthan	Jaipur	Jaipur	RJA	75.79	26.91
	Jodhpur	Jodhpur	RJO	73.02	26.24
Tamil Nadu	Chennai	Alandur	TNA	80.20	13.00
		IIT	TNI	80.23	12.99

Telangana	Hyderabad	Manali	TNM	80.26	13.16	
		IDA Pashamylaram	TPM	78.18	17.53	
		Sanathnagar	TSN	78.44	17.45	
		Zoo Park	TZP	78.45	17.35	
	Agra	Sanjay Palace	UPA	78.01	27.20	
Uttar Pradesh	Lucknow	Kanpur	Nehru Nagar	UPK	80.32	26.47
		Central School	UPS	80.90	26.83	
		Lalbagh	UPL	80.94	26.85	
	Varanasi	Talkatora	UPT	80.90	26.83	
		Ardhali Bazar	UPZ	82.98	25.35	

Table 12: AERONET stations.

State	City	Station	Code	Lat	Lon
Rajasthan	Jaipur	Jaipur	JAI	26.90	75.80
Uttar Pradesh	Kanpur	Kanpur	KPR	26.51	80.23
Maharashtra	Pune	Pune	PNE	18.52	73.85
Jharkhand	Bokaro	Gandhi College	GAN	25.87	84.13

Appendix C: Supplementary information for “Stringent emission control policies can provide large improvements in air quality and public health in India”

Table 13: Scaling factors per emission sector and air pollutant in India (International Energy Agency 2016a).

	New Policy Scenario (NPS)			Clean Air Scenario (CAS)		
	SO₂	NO_x	PM_{2.5}	SO₂	NO_x	PM_{2.5}
Industry (IND)	2.46	2.75	2.52	0.61	1.24	0.48
Power (ENE)	0.11	0.73	0.21	0.05	0.40	0.07
Residential (RES)	0.55	1.10	0.61	0.37	0.54	0.15
Transport (TRA)	2.20	0.55	0.53	1.12	0.22	0.43
Other	1.84	1.10	1.07	0.75	0.27	0.00
Total	1.10	1.10	1.07	0.31	0.50	0.24

Appendix D: Supplementary information for “Current and future disease burden from ambient ozone exposure in India”

Table 14: Ambient surface O₃ observation site details.

Site	Type	Lat. (°N)	Lon. (°E)	Alt. (m)	Data period	Ref.
Ahmedabad (ABD)	Semi-arid,	23.00	72.60	49	1993–1996	(Lal <i>et al</i> 2000)
	urban	23.03	72.58	53	2002–2003	(Sahu and Lal 2006)
					2011	(Mallik <i>et al</i> 2015)
Anantapur (ANP)	Semi-arid	14.62	77.65	331	2002–2003	(Reddy <i>et al</i> 2008)
	rural site				2008–2009	(Reddy <i>et al</i> 2010)
Bhubaneswar (BHB)	Coastal	20.30	85.83	45	2010–2012	(Mahapatra <i>et al</i> 2014)
Delhi (DEL)	Urban	28.65	77.27	220	1997–2004	(Jain <i>et al</i> 2005)
Gadanki (GDK)	Rural	13.50	79.20	375	1993–1996	(Naja and Lal 2002)
Jabalpur (JBL)	Semi-urban	23.17	79.92	411	2013–2014	(Sarkar <i>et al</i> 2015)
Kannur (KNN)	Semi-rural	11.90	75.40	5	2009–2010	(Nishanth <i>et al</i> 2012)
Kanpur (KNP)	Urban	26.46	80.33	125	2009–2013	(Gaur <i>et al</i> 2014)
Kullu (KLU)	Semi-urban	31.90	77.12	1154	2010	(Sharma <i>et al</i> 2013)
Mt. Abu (MAB)	High altitude	24.60	72.70	1680	1993–2000	(Naja <i>et al</i> 2003)
Nainital (NTL)	High altitude	29.37	79.45	1958	2006–2008	(Kumar <i>et al</i> 2010a)
					2009–2011	(Sarangi <i>et al</i> 2014)
Pune (PNE)	Semi-urban	18.54	73.81	600	2003–2004	(Beig <i>et al</i> 2007)
Pantnagar (PNT)	Semi-urban	29.00	79.50	231	2009–2011	(Ojha <i>et al</i> 2012)
Trivandrum (TRV)	Coastal	8.55	77.00	5	2007–2009	(David and Nair 2011)
Udaipur (UDP)	Urban	24.58	73.68	598	2010–2011	(Yadav <i>et al</i> 2014)

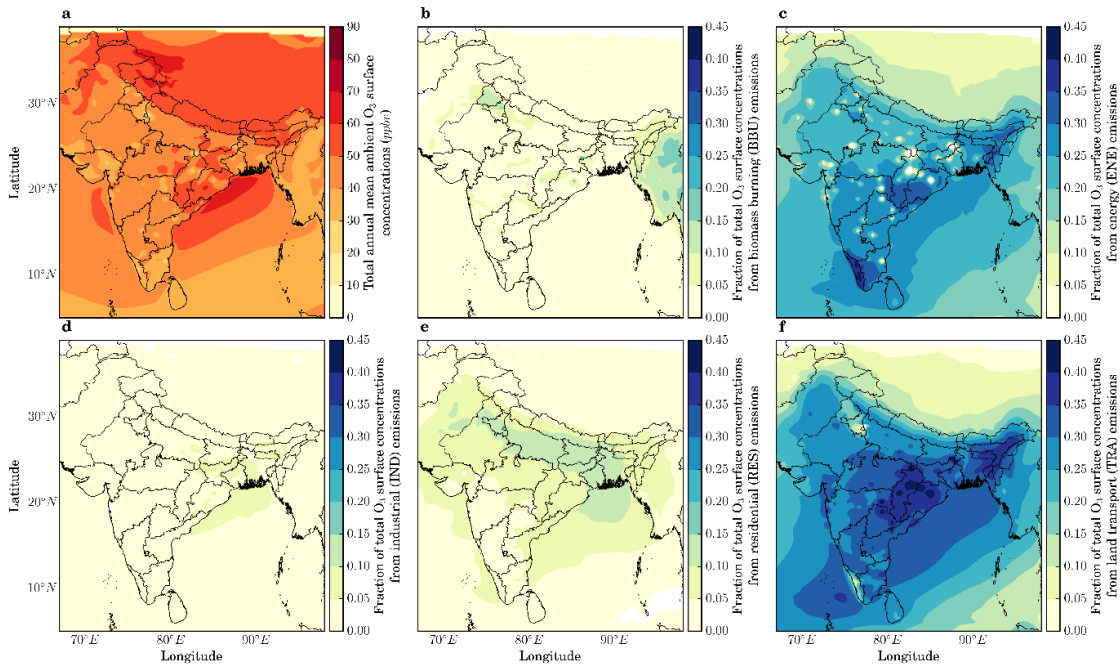


Figure 63: Fractional contribution per source to total annual-mean ambient O_3 surface concentrations. (a) Total annual-mean ambient O_3 surface concentrations. (b–f) Fractional contribution from biomass burning (BBU), power generation (ENE), industrial non-power (IND), residential energy use (RES), and land transport (TRA).

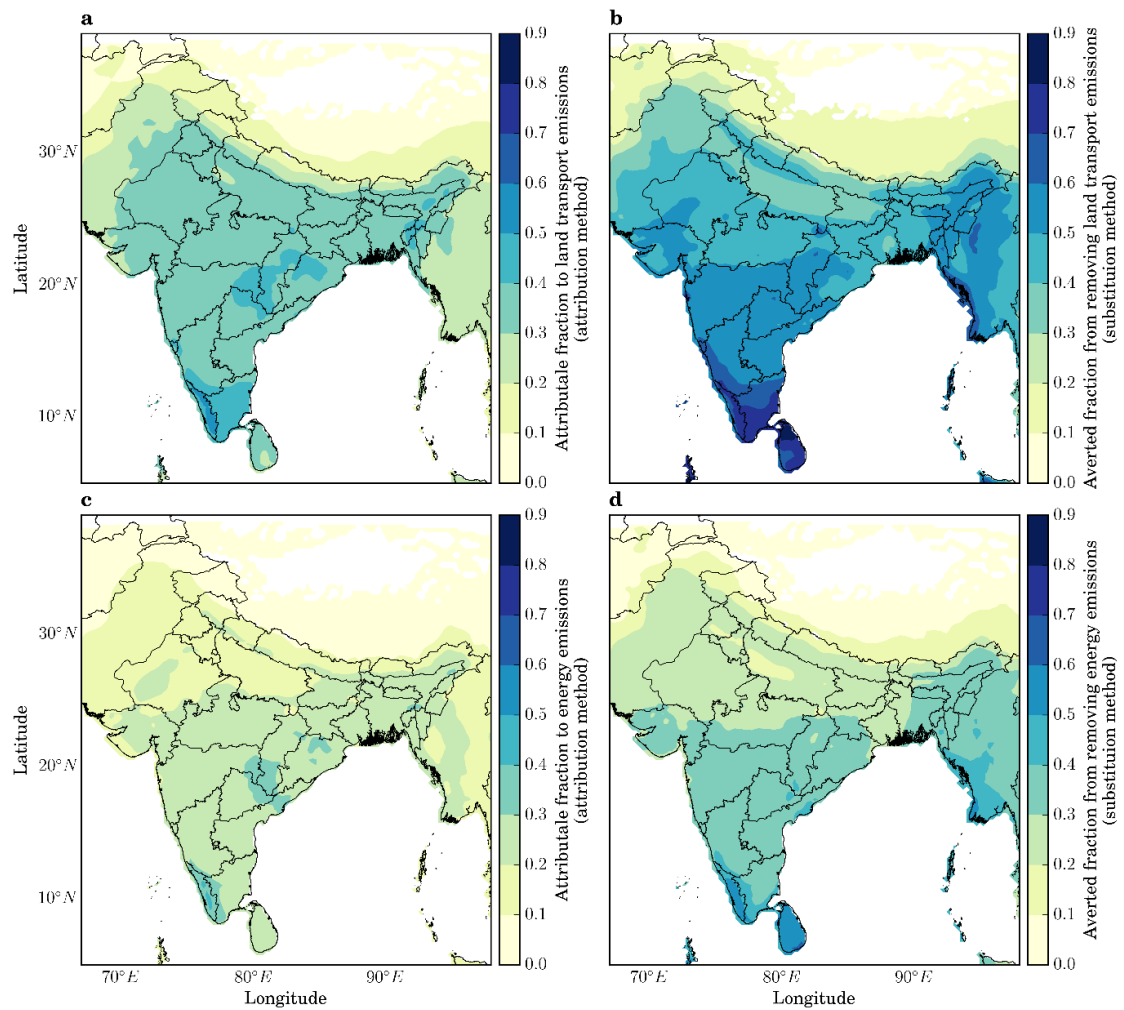


Figure 64: Dominant source contributions to premature mortality burden due to O_3 exposure across India in 2015. (a) Attributable fraction of premature mortalities from land transport emissions (attribution method). (b) Averted fraction of premature mortalities from removing land transport emissions (subtraction method). (c) Attributable fraction of premature mortalities from energy emissions (attribution method). (d) Averted fraction of premature mortalities from removing energy emissions (subtraction method). All health impacts are calculated using Turner et al (2016) RR and LCC_{min} .

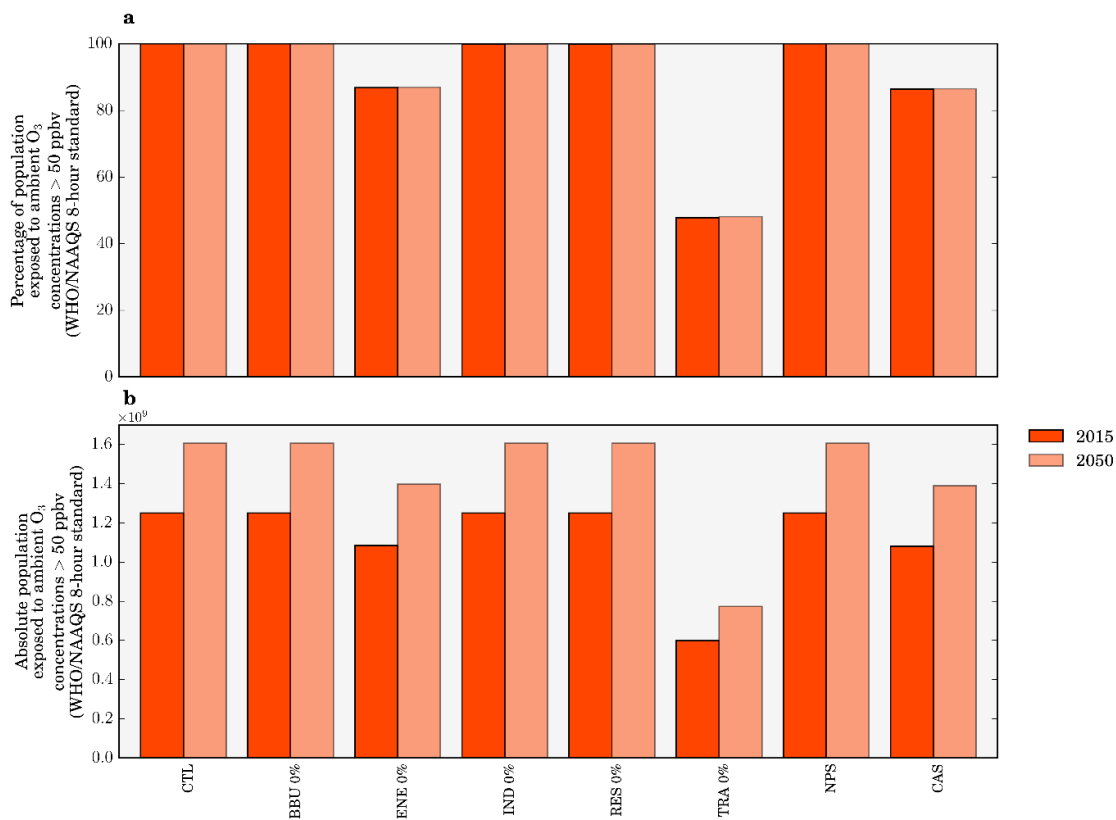


Figure 65: The impact of scenarios on O_3 metrics. (a) Percentage of population in 2015 (1st bar) and 2050 (2nd bar) exposed to population-weighted ambient surface O_3 concentrations above 50 ppb (WHO AQG, Indian NAAQS) in each scenario. (b) Absolute population in 2015 (1st bar) and 2050 (2nd bar) exposed to population-weighted ambient surface O_3 concentrations above 50 ppb (WHO AQG, Indian NAAQS) in each scenario.

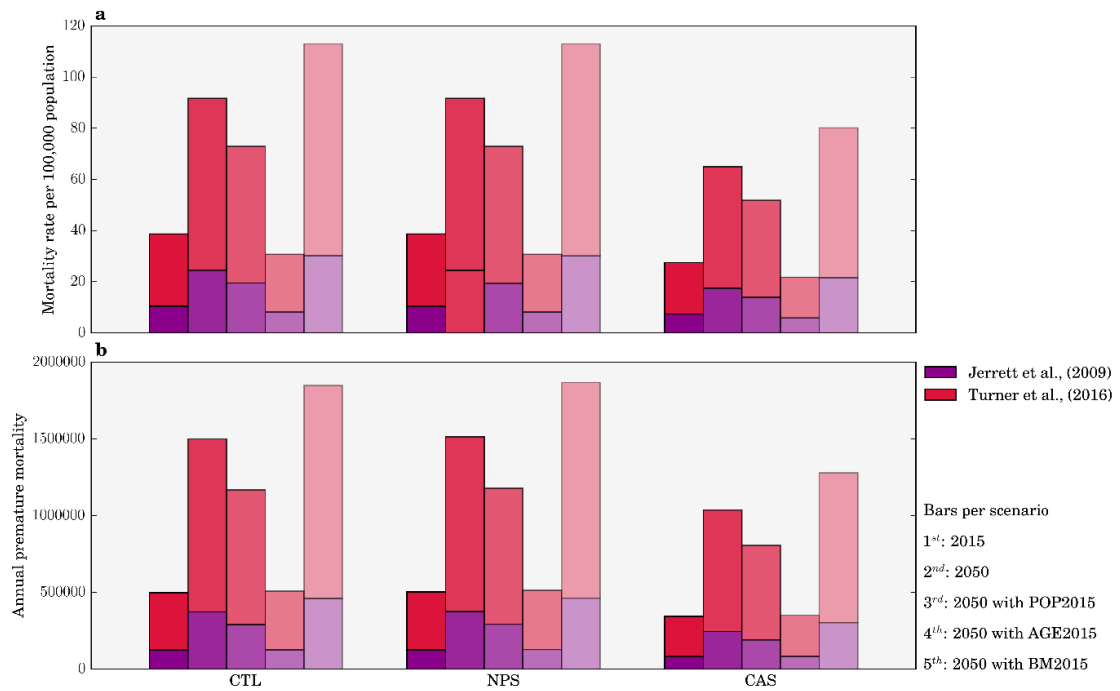


Figure 66: Sensitivities of health impacts due to O₃ exposure in India to demography and baseline mortality rates. (a) Mortality rate per 100,000 population. (b) Total annual premature mortality. Impacts are estimated using either Jerrett et al (2009) (red) and Turner et al (2016) (purple) relative risks with LCC_{min}. For each panel, the control (CTL) scenario is compared against the NPS and CAS scenarios. For each panel, the five bars (left to right) show estimates for 2015 with 2015 population, age, and baseline mortality, 2050 with 2050 population, age, and baseline mortality, and 2050 with population from 2015 (POP2015), population age grouping from 2015 (AGE2015), and baseline mortality rates from 2015 (BM2015).